

Functional Lipid Membranes: Bio-inspired Nanomaterials for Sensing and Catalysis

Dissertation

zur Erlangung

des Doktorgrades der Naturwissenschaften

(Dr. rer. nat.)

an der Fakultät für Chemie und Pharmazie

der Universität Regensburg



vorgelegt von

Benjamin Gruber

aus Berchtesgaden

Regensburg – 2012

The experimental part of this work was carried out between October 2008 and June 2012 at the Institute of Organic Chemistry at the University of Regensburg under the supervision of Prof. Dr. B. König.

Submission of thesis: 05 / 07 / 2012

Date of colloquium: 27 / 07 / 2012

Board of Examiners	Prof. Dr. Jörg Daub	(Chairman)
	Prof. Dr. Burkhard König	(1 st Referee)
	Prof. Dr. Kirsten Zeitler	(2 nd Referee)
	Prof. Dr. Henri Brunner	(Examiner)

I, Benjamin Gruber, solemnly declare to have completed this work without any aid or help of any kind not mentioned in this thesis.

Regensburg,.....

"Save a tree – don't publish..."

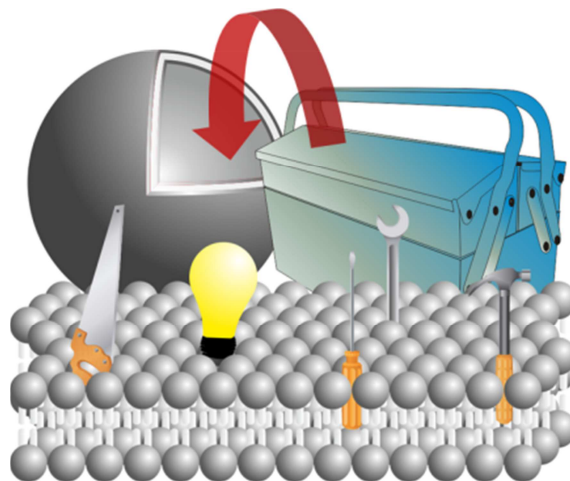
Reviewer comment

To Anna & my family

TABLE OF CONTENTS

CHAPTER 01 - CONCEPT: SELF-ASSEMBLED VESICLES WITH FUNCTIONALIZED MEMBRANES	1
INTRODUCTION.....	2
FUNCTIONALIZED VESICLE MEMBRANES.....	2
FROM BULK SOLUTION TO TWO-DIMENSIONAL SURFACE ARRAYS	5
LABELED MEMBRANES AS OPTICAL REPORTERS AND TRANSDUCERS	7
DYNAMIC FUNCTIONALIZED INTERFACES RESPONDING TO EXTERNAL STIMULI.....	11
SUMMARY AND OUTLOOK.....	16
REFERENCES.....	17
CHAPTER 02 - LUMINESCENT VESICULAR RECEPTORS FOR THE RECOGNITION OF BIOLOGICALLY IMPORTANT PHOSPHATE SPECIES	20
INTRODUCTION.....	21
RESULTS AND DISCUSSION.....	21
CONCLUSION.....	29
EXPERIMENTAL PART	29
SUPPORTING INFORMATION	41
REFERENCES.....	52
CHAPTER 03 - MODULAR CHEMOSENSORS FROM SELF-ASSEMBLED VESICLE MEMBRANES WITH AMPHIPHILIC BINDING SITES AND REPORTER DYES	56
INTRODUCTION.....	57
RESULTS AND DISCUSSION.....	57
CONCLUSION.....	62
EXPERIMENTAL PART AND SUPPORTING INFORMATION	62
REFERENCES.....	74
CHAPTER 04 - DYNAMIC INTERFACE IMPRINTING: HIGH AFFINITY PEPTIDE BINDING SITES ASSEMBLED BY ANALYTE-INDUCED RECRUITING OF MEMBRANE RECEPTORS..	77
INTRODUCTION.....	78
RESULTS AND DISCUSSION.....	79
CONCLUSION.....	83
EXPERIMENTAL PART AND SUPPORTING INFORMATION	83
REFERENCES.....	110

CHAPTER 05 - VESICLES AND MICELLES FROM AMPHIPHILIC ZN(II)-CYCLEN COMPLEXES AS HIGHLY POTENT PROMOTERS OF HYDROLYTIC DNA CLEAVAGE.....	113
INTRODUCTION.....	114
RESULTS AND DISCUSSION.....	114
CONCLUSION.....	119
EXPERIMENTAL PART AND SUPPORTING INFORMATION	120
REFERENCES.....	136
SUMMARY	138
ZUSAMMENFASSUNG	139
ABBREVIATIONS	140
CURRICULUM VITAE	143
ACKNOWLEDGEMENTS	146

CHAPTER 1**CONCEPT: SELF-ASSEMBLED VESICLES WITH FUNCTIONALIZED MEMBRANES**

Biological membranes play a key role for the function of living organisms. Thus many artificial systems have been designed to mimic natural cell membranes and their functions. A useful concept for the preparation of functional membranes is the embedding of synthetic amphiphiles into vesicular bilayers. The dynamic nature of such non-covalent assemblies allows the rapid and simple development of bio-inspired responsive nanomaterials, which find applications in molecular recognition, sensing or catalysis. However, the complexity that can be achieved in artificial functionalized membranes is still rather limited and the control of their dynamic properties and the analysis of membrane structures down to the molecular level remain challenging.

This chapter has been published:

B. Gruber and B. König, *Chem. Eur. J.* **2012**, DOI: 10.1002/chem.201202982 (Concept Article).

Author contributions:

BG wrote the manuscript; BK supervised the project and is corresponding author.

Introduction

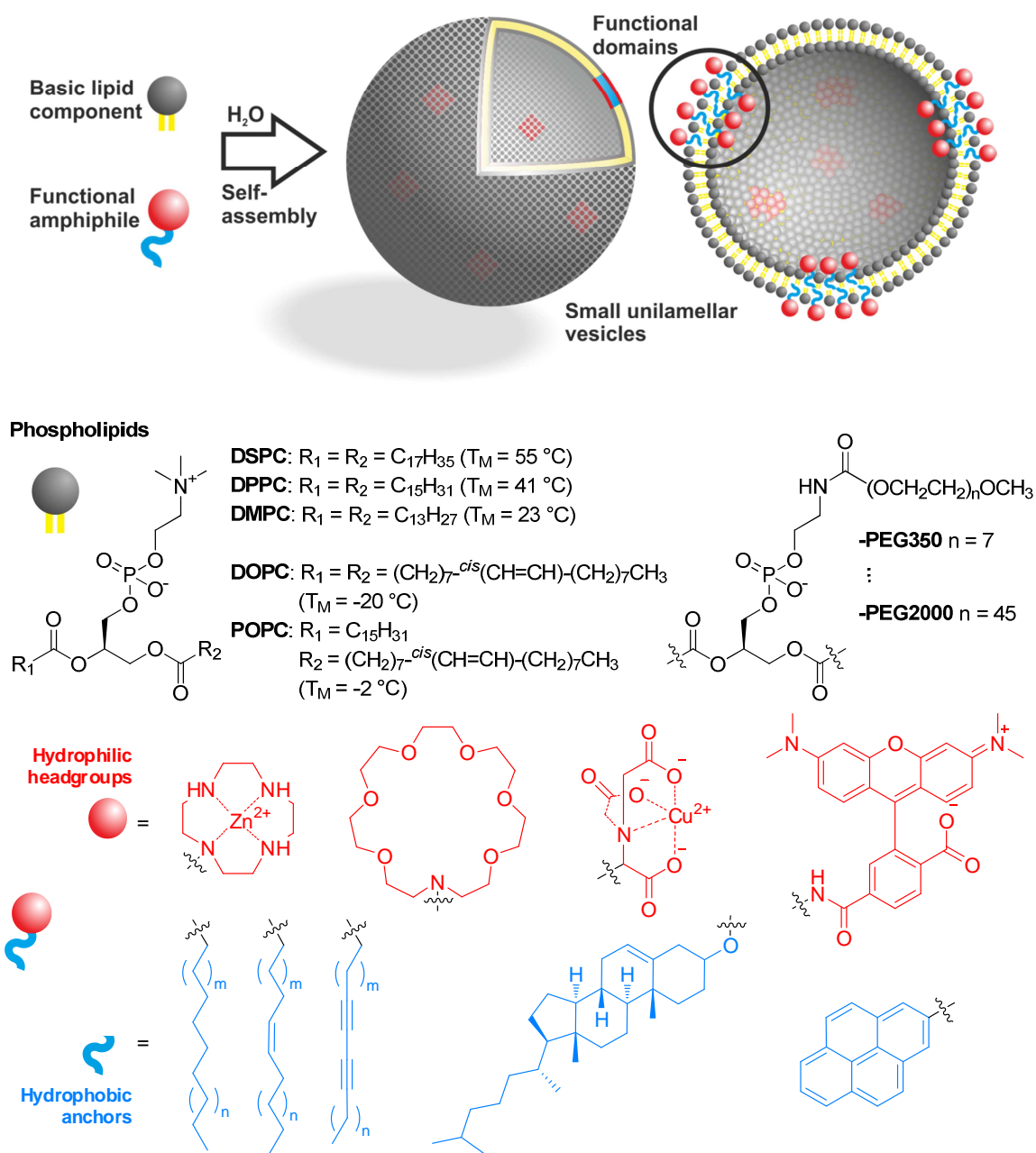
Many fundamental molecular processes in living organism are controlled by biological membranes. They play a key role in cell signalling transmitting the signal of external stimuli across cell membranes or between distinct cells. Molecular recognition processes of membrane embedded receptors and their dynamic ligand-induced assembly within the phospholipid bilayer sheets are essential for this function.^{1, 2} As a result it has become a wide, but still challenging field of research to mimic biological recognition and transport mechanisms and to derive and develop artificial systems – either to use them as models in order to gain a better understanding or as bio-inspired and biomimetic materials for completely different applications.³

Besides solid-supported mono- and bilayer systems, unilamellar vesicles are useful membrane models.⁴ On a lab scale these spherical shells encapsulating an aqueous core are easily prepared from natural or synthetic amphiphiles via self-assembly by established methods.⁵ Various reports of vesicular membranes as nanoscale carrier systems^{6, 7} and reaction containers⁸, switchable assemblies^{9, 10} and sensor materials¹¹⁻¹⁵ as well as supramolecular catalysts¹⁶ can be found in recent literature. In contrast to vesicles or liposomes, which are assembled from phospholipids, the so-called polymersomes¹⁷ are entirely built of one (or several) artificial functional amphiphile or block co-polymer.¹⁸ These compounds often require significant synthetic effort, but their vesicular aggregates can be employed as versatile stimuli-responsive nanomaterials. Such systems however are not within the scope of this brief concept article which is mainly focussed on biomimetic vesicles assembled from a (phospho)lipid scaffold and distinct embedded functional amphiphiles. Also the embedding of synthetic building blocks for artificial channels^{19, 20} or pores²¹ goes well beyond the scope of this article, thus transport processes²² across vesicle membranes as well as compartmentalization and triggered release of encapsulated compounds²³ shall not be discussed in more detail here. Instead we want to present the development of surface functionalized vesicles by modular co-embedding and strategies to exploit dynamic rearrangement processes within these bilayers, inspired by biological cell membranes, for sensing and transformation of biomolecules.

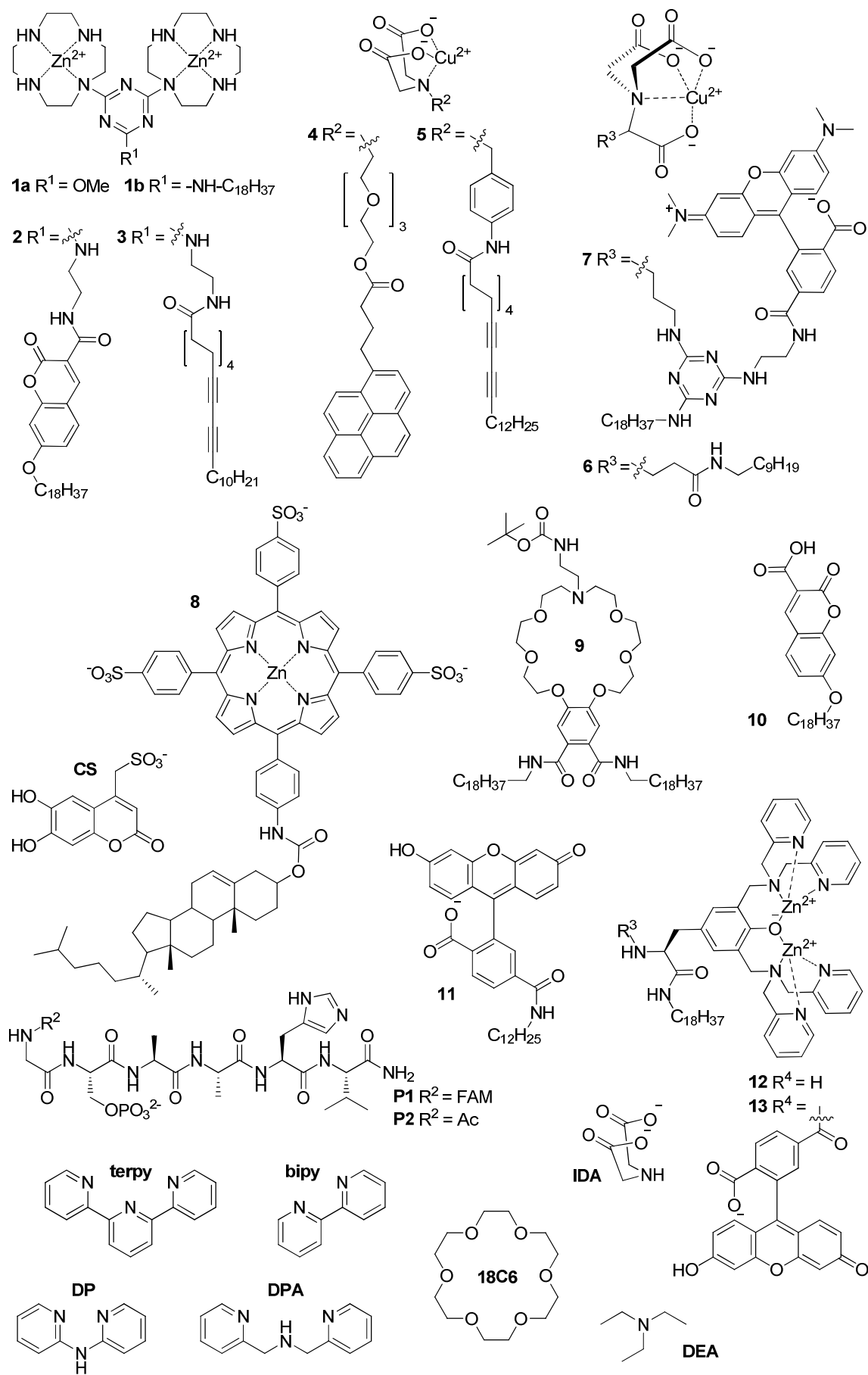
Functionalized vesicle membranes

With growing interest in the function and properties of natural lipid bilayers synthetic liposomes have been intensively studied for several decades.²⁴ They can be rapidly prepared on a lab scale by simple established procedures like dried film hydration or reverse phase evaporation. Homogeneous small or large unilamellar particles are usually obtained by sonication or extrusion through membranes with defined pore sizes.²⁵ A number of physicochemical methods for their characterization are available allowing the

determination of shape and size distributions (DLS, AFM, TEM), phase transitions (DSC) and lipid diffusion or domain formation for instance via spectroscopic methods especially based on fluorescence. Compared to solid surfaces, however visualization and high resolution imaging of artificial membrane structures can be challenging due to their soft (and dynamic) nature and small size with a typical diameter of around 100 nm and a bilayer thickness below 5 nm. Nevertheless synthetic vesicles are increasingly used for analytical and medicinal chemistry and in material science in recent years.



Scheme 1. Schematic self-assembly of small unilamellar vesicles with functionalized membranes. The structures and main phase transition temperatures (T_M) of common phospholipids as well as some examples of functional head groups and hydrophobic anchors for membrane-embedding are given: Polar heads include transition metal complexes based on Zn²⁺-cyclen or Cu²⁺-NTA, crown ether based hosts and fluorescent dyes like xanthene derivatives. Hydrophobic parts can be derived from (un-)saturated C₁₀-C₂₄ alkyl chains, cholesterol or hydrophobic dyes like pyrene.



Scheme 2. Structures of amphiphilic receptors and reporter dyes, peptide ligands and metal ion binding sites.

Probably the easiest way to modify and functionalize common phospholipid vesicles is to simply mix the lipid component with small amounts of artificial functional amphiphiles, which contain similar hydrophobic tails and a sufficiently polar head group, in order to embed these compounds in the lipid bilayers (cf. Scheme 1). Compared to completely synthetic assemblies of block copolymers known functional molecules like receptors, catalysts or chromophores are easily modified with hydrophobic anchors and incorporated into liposomes. The overall synthetic effort is reduced compared to covalent synthesis, (non-)covalently coated nanoparticles or polymersomes, as the functional compounds and the lipid vesicles are readily available. Thus vesicle and membrane properties can be easily combined with functional dopants to obtain particles in large variety with easily tunable and adjustable functions and properties. Compared to smaller micellar aggregates of functional amphiphiles they provide a greater diversity and stability, which for numerous applications can compete with that of solid nanoparticles. The distribution of the embedded functional amphiphiles is determined by dispersion interactions and other weak intermolecular forces and significantly affected by the experimental conditions, such as individual concentration, temperature, ionic strength and others. Controlling the distribution and the rational design of defined structural patterns is therefore like in every multi parameter system a challenge and the careful optimization of the conditions is often necessary to obtain the desired properties.

From bulk solution to two-dimensional surface arrays

(Transition-)metal complexes present a group of functional molecules which can be of particular interest for the embedding in vesicle membranes.²⁶ Not only is it known for long that natural cell membranes can complex calcium ions via acidic lipids to initiate the formation of rafts or aggregation and fusion processes.²⁷ Transition metals and their complexes are widely used in synthetic chemistry and catalysis and provide a perfect headgroup to be placed at the vesicle membrane-water interface. Compounds with established properties can be selected and modified with a sufficiently hydrophobic tail, which allows incorporation into the membrane bilayer. Similar to the immobilization on polymer or nanoparticle supports the embedding of transition metal catalysts in vesicle membranes can change their reactivity compared to bulk solution.²⁶

We have recently shown this for the hydrolysis of phosphodiester in neutral aqueous solution mediated by Zn²⁺-cyclen complexes (Scheme 2, compounds **1a** and **1b**). Such complexes have already been intensively studied and are well-known models for hydrolytic enzymes, which typically contain metal ions like zinc in their active center.^{28, 29} They promote the hydrolysis of active phosphodiester, like BNPP (Figure 1) in aqueous solution and the dinuclear bis-cyclen complex **1a**, developed in our group, belongs to the most active

catalysts for this reaction at neutral pH.³⁰ Instead of combining several zinc ion metal centers covalently to di- or oligonuclear complexes, a non-covalent self-assembly was achieved by embedding amphiphilic complexes with a C₁₈-alkyl chain (**1b**) in DSPC vesicle membranes.³¹ It was found that the vesicular catalysts containing tightly packed Zn²⁺-domains within their bilayer membranes outperformed the identical system in homogenous aqueous solution by several orders of magnitude regarding second order kinetics reaction rates and represented the most active artificial metal catalyst-system reported so far. Furthermore our self-assembled soft particles provided a more convenient preparation and higher activities compared to solid functional nanoparticles³² but still a sufficient long-term stability to readily cleave otherwise stable substrates like native plasmid DNA and even non-activated oligonucleotide strands. The observed performance increase can be explained by the high local concentration of catalytic centers in the membrane patches (see Figure 1a) and thus enhanced substrate attraction and conversion as well as the decreased polarity at the vesicle-water interface facilitating a nucleophilic attack of the phosphodiester substrates compared to bulk solution. Although the reactivity of our synthetic supramolecular catalysts is still far below those of natural nucleases they provide an interesting model as they offer the possibility to easily combine highly reactive catalytic centers (as already shown) with recognition sites to improve the selectivity.

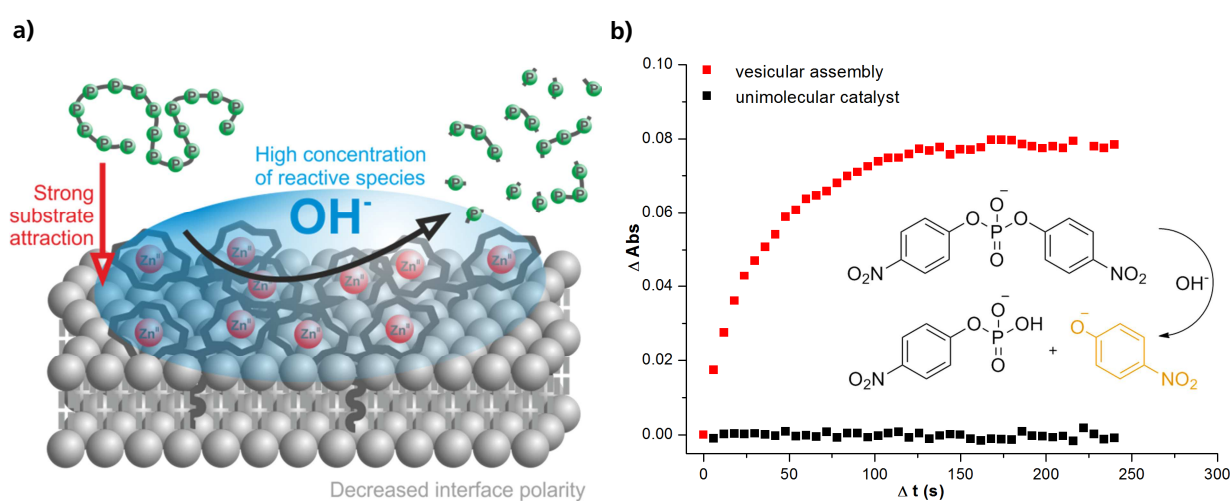


Figure 1. (a) Schematic domain of membrane-embedded Zn²⁺-catalysts and hydrolytic cleavage of phosphodiester substrates; (b) Kinetic traces of Zn²⁺-cyclen catalysts in homogenous aqueous (**1a**, black trace) solution and in vesicular assemblies (**1b**, red trace) showing a dramatic performance increase for the model substrate bis(paranitrophenyl)phosphate (BNPP).

The concept of a self-assembled vesicular multi-site catalyst has recently been expanded to different catalytic centers and particles by Uozumi et al.¹⁶

Metal ion functionalized vesicles also play an important role for molecular recognition at the membrane-water interfaces.³³ Transition metal complexes like the previously mentioned Zn²⁺-cyclens have found application as synthetic receptors,³⁴ which selectively bind

phosphate anions with milli- to micromolar affinities.³⁵ Several examples have been reported and combined with fluorescent labels via covalent connection³⁶ or indicator displacement assays³⁷ in order to develop luminescent chemosensors for all kinds of phosphate containing biomolecules. The assembly at a vesicle membrane interface can offer enhanced analyte selectivities and affinities here. The recognition takes place by multi-point interactions, which are difficult to achieve in solution as the covalent connection and synthesis of large receptor entities is tedious and time-consuming. Vesicle surface functionalization gives distinct interaction sites by incorporation of suitable amphiphiles into the lipid bilayer. For a proof of principle we have prepared vesicular multi-receptor surfaces from luminescent Zn²⁺-cyclen derivative **2** for sensing and differentiation of phosphorylated proteins.³⁸ While low-molecular phosphates can be selectively recognized using metal complexes in homogenous solution such systems are not useful for the sensing of more complex analytes like proteins with different degrees of phosphorylation. With **2** embedded in partially PEGylated DSPC membranes (cf. Figure 2) we could observe the selective binding of multiple phosphorylated α -S1-Casein, while a dephosphorylated sample or non-phosphorylated proteins, like BSA, did not trigger any response of the luminescent vesicle (Figure 3a). The affinities in the nanomolar range indicate a multi-dentate binding of the target protein, which is not possible by unimolecular receptors in bulk solution.

Labeled membranes as optical reporters and transducers

The coumarin-based fluorescence label attached to the Zn²⁺-cyclen binding sites of **2** furthermore allows a direct optical sensing via emission quenching if the chromophores are assembled at the less polar bilayer-water interface, which could again not be observed with non-amphiphilic derivatives in bulk solution (Figure 3b). This difference in emission response can be explained by the preorganization and the more rigid environment of the embedded labels compared to the much higher degree of freedom in bulk solution, which hampers the communication between the analyte binding site and the reporter dye.

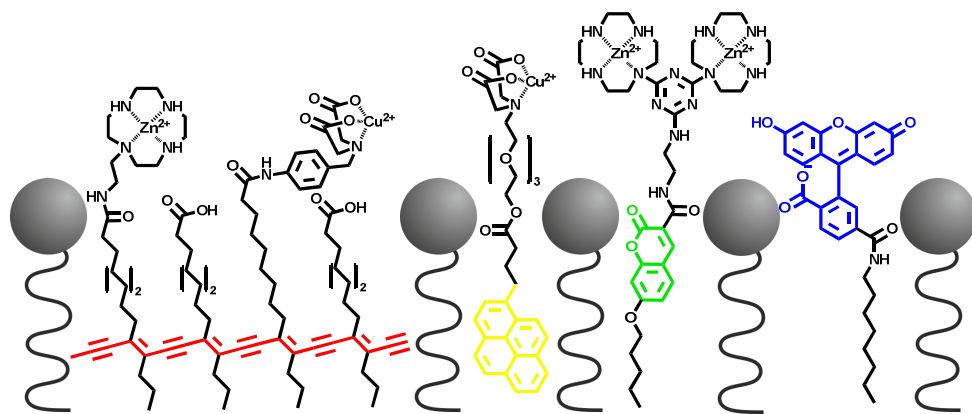


Figure 2. Labeling of vesicle membranes by polymerized lipids (red) or dyes embedded either in the hydrophobic core (yellow), the polar head group region (blue) or in between (green).

Organic dyes that are commonly used to signal the presence of an analyte however generally have short-lived fluorescence lifetimes and their emission interferes with the background from biological samples. The embedding of amphiphilic lanthanide complexes, e.g. Tb^{3+} compounds can solve this problem. The long lived phosphorescence emission at long wavelengths allows time-gated measurements and therefore eliminates background interference. For instance, luminescent thermosensitive vesicles based on Tb complexes were recently reported.³⁹ Furthermore binding events at artificial receptor-membranes can of course also be monitored by "label-free" techniques like ITC⁴⁰ or SPR⁴¹ which however are generally less sensitive than fluorescence based methods.

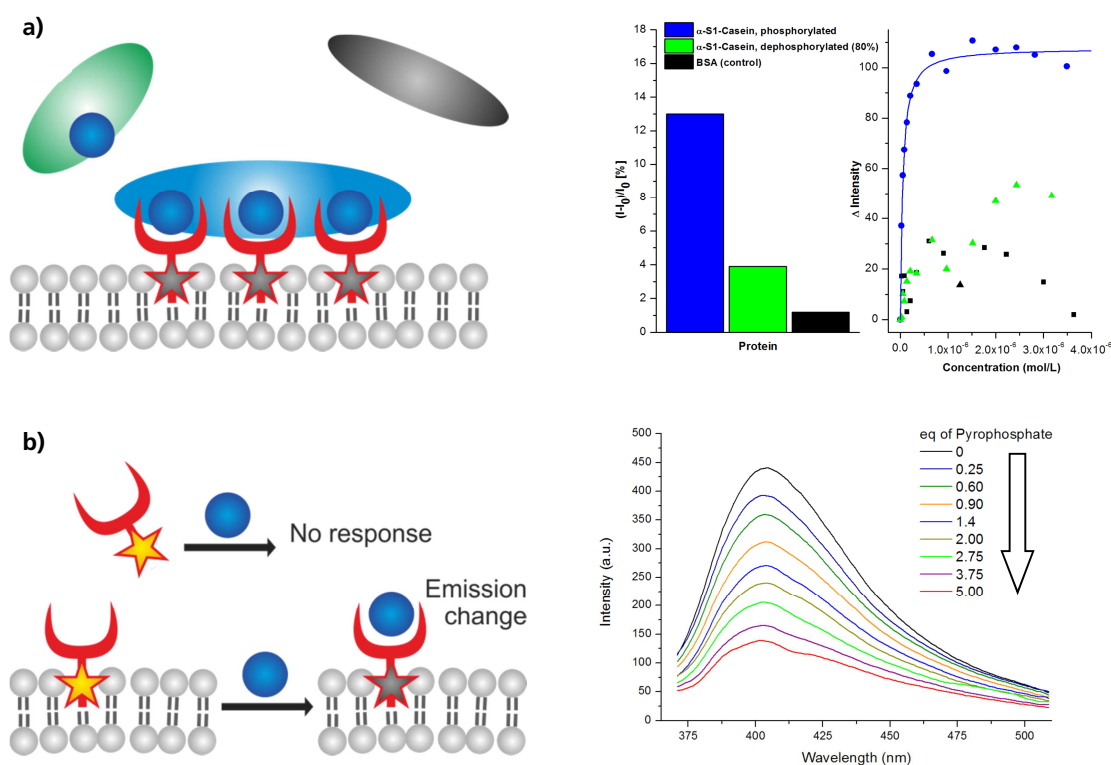


Figure 3. (a) By combining multiple binding sites (**2**) within a vesicle membrane multiply phosphorylated α -S1-Casein could be differentiated from other proteins; (b) Membrane-embedded dyes with attached binding sites can be used for direct detection of analyte binding: Fluorescence emission of vesicular **2** is quenched in the presence of pyrophosphate (PP) whereas the unimolecular derivative in homogeneous aqueous solution does not change its emission properties.

The embedding of dyes inside the hydrophobic core of lipid membranes has been used extensively for examining lipid arrangement and diffusion inside the bilayer sheets and thus for the elucidation of membrane structures. A very common approach here is the use of pyrene-labeled lipids (cf. Figure 2) as these can optically transduce spatial information of lipid distribution via their monomer/excimer emission(-ratio).⁴² Coloured or fluorescent vesicles can be obtained by the embedding of dyes, but also by using polydiacetylene (PDA)-modified lipids which are crosslinked by photopolymerization (cf. Figure 2). These particles respond to external stimuli like analyte binding, pH or temperature changes by blue-to-red colour transitions.⁴³ Here the particle membrane itself is used as optical reporter and

transducer and together with the embedding of selective receptors this approach allows the simple and rapid preparation of diverse colorimetric sensor materials,⁴⁴ which are applicable as test strips or thin films. The co-embedding of monomer ligands with metal ion binding ability like terpy, DPA, DP and DEA (cf. Scheme 2) enables optical discrimination of Zn-, Cd-, Mn-, Ag- and Hg-salts amongst various other alkali, alkaline earth and transition metals (Figure 4). The same sensing system with embedded receptors **3** and **5**⁴⁵ or quaternary ammonium groups⁴⁶ was furthermore used for the recognition of biological phosphate anions and allowed the discrimination of ATP and PP_i via colour and fluorescence emission changes of the vesicles, which presents a challenging task using luminescent metal complexes in homogeneous aqueous solution. While the intrinsic response of colorimetric vesicles can provide a convenient “naked-eye” detection the corresponding analyte affinities are usually only in the millimolar range. For most bioanalytic applications fluorescence spectroscopy is more suitable due to superior sensitivity.

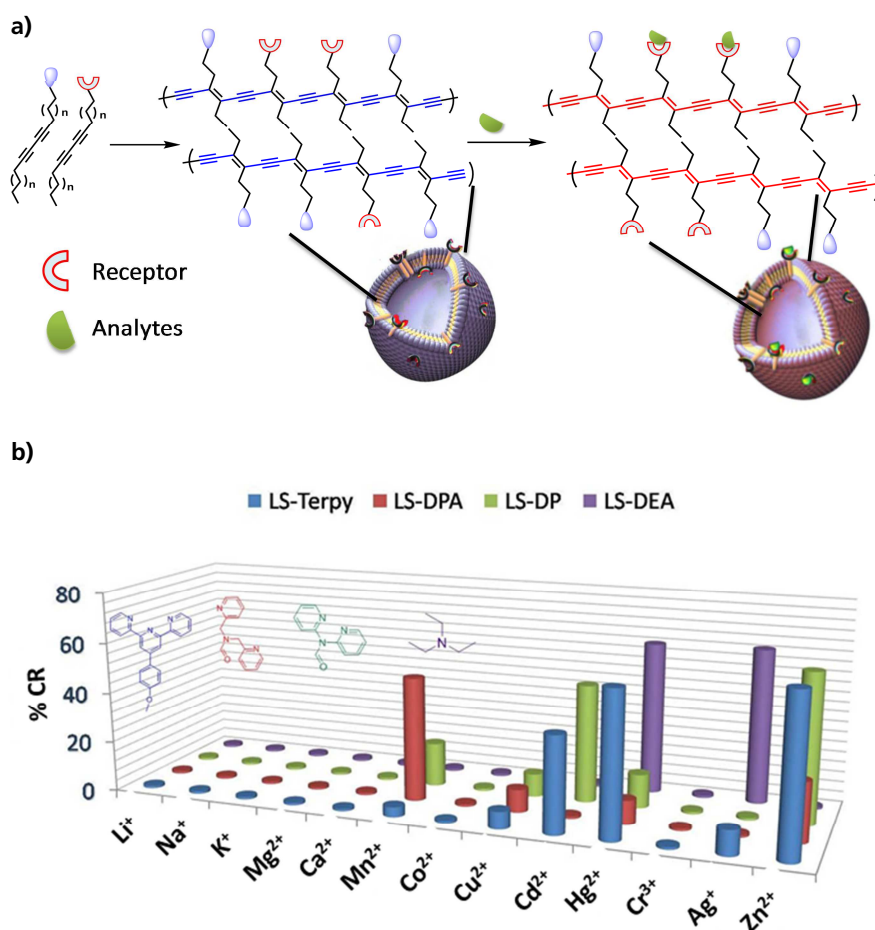


Figure 4. Intrinsic colorimetric sensing: Polymerized PDA-vesicle membranes with embedded metal ion binding sites like terpy, DPA, DP and DEA respond to the presence of different metals by a colour change.

Amphiphilic dyes with polar chromophores as headgroups also allow an easy labelling of vesicles and enable further interesting applications. We recently demonstrated this by developing modular chemosensors on the basis of self-assembled vesicle membranes with

embedded amphiphilic binding sites and reporter dyes.⁴⁷ Instead of covalently connecting a metal complex-binding site and a fluorescent reporter dye as parts of an optical chemosensor for small molecules in aqueous solution both components were co-embedded in DSPC vesicle membranes. We propose the formation of mixed receptor and dye patches in the lipid bilayers, which rearrange in the presence of the corresponding analytes. This results in an emission response of the environment-sensitive reporter dyes. By simple mixing of multiple receptors (“anionic” complex **6**, “cationic” complex **1** or “neutral” host **9**) and a reporter dye analytes, like histidine, phosphoserine and glycine could be selectively detected at sub-micromolar concentrations. Upon analyte binding a rearrangement of the mixed patches and a re-distribution of the dyes in separate phases is assumed and thus the optical output properties like wavelength and “turn-on” or “turn-off”-sensing could be easily adjusted by changing the properties of the embedded reporter dye. Compound **10** for instance leads to emission quenching, whereas carboxyfluorescein **11** responds with an increase in fluorescence intensity (Figure 5).

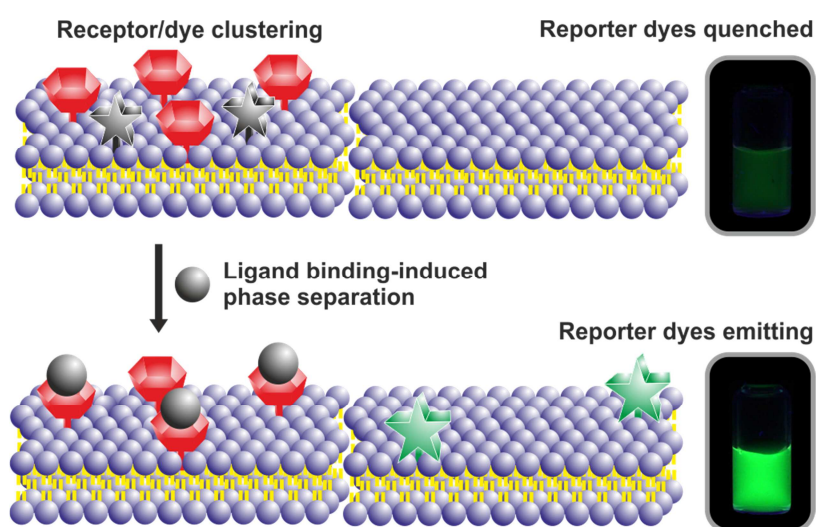


Figure 5. Co-embedding of binding sites and reporter dyes: Initial clusters of receptors and dyes undergo phase separation upon receptor-ligand binding which results in an emission response of the environment-sensitive fluorophores.

Vesicular assemblies therefore provide a handy scaffold for the non-covalent connection and local aggregation of functional organic molecules at lipid bilayer-water interfaces and the development of versatile sensing materials via embedded optical reporter groups (cf. Figure 2). The structure, packing and diffusion of embedded compounds is affected by intrinsic membrane properties, like lipid phase states and transitions, which furthermore allows the exploitation of dynamic rearrangement processes inside the bilayer sheets.

Dynamic functionalized interfaces responding to external stimuli

In reference to natural receptor-ligand interactions at biological membranes multiple receptor sites can also be combined in artificial bilayers for the recognition of multivalent ligands via receptor recruiting. As a simple model system we have recently studied⁴⁸ the binding of the divalent peptide **P1** towards gel-phase (DSPC) and fluid-phase (DOPC) membranes doped with two different binding sites: Complex **12** for the phosphorylated serine (pSer) moiety of **P1** and complex **6** for the His residue. To avoid additional fluorescent labels in the vesicle membranes here a fluorescent peptide **P1** was used, which changes its emission intensity upon binding to the vesicle surface. It was found that compared to aqueous solution the non-covalently assembled receptors in the lipid bilayer membranes can be dynamically arranged and form a 2:1 complex with increased affinities in the nanomolar range (cf. Figure 6a) if the membrane's phase state allows sufficient mobility at room temperature. For gel-phase vesicles made of DSPC instead just monodentate 1:1 binding of either the pSer or His residue was assumed due to considerably decreased affinities within the micromolar range. The concentrations of embedded binding sites were intentionally set to low levels (1 mol%) in order to keep the distinct functionalities dispersed in the initial particle states. If higher amounts of receptors were embedded the affinity to **P1** increases for DSPC vesicles, which indicates initial receptor clustering and as a result (partial) formation of 2:1 complexes. Additionally a non-labelled peptide **P2** was selectively recognized using membrane-embedded receptors that carry FRET-labels (**7** and **13**). At low concentrations (< 1 mol%) the labelled receptors are assumed to be dispersed within the lipid bilayers as only a limited energy transfer can be observed between FRET donor and acceptor label in the initial particle state. Upon binding of peptide **P2** however both **7** and **13** are recruited into close proximity, which induces a FRET emission (Figure 6b, c). The peptide to receptor binding occurs on the surface of a single vesicle and no aggregation or energy transfer between different vesicles was observed. With these results we could successfully demonstrate a ligand-induced formation of high-affinity epitopes for small peptides by dynamic receptor assembly within lipid bilayer membranes.

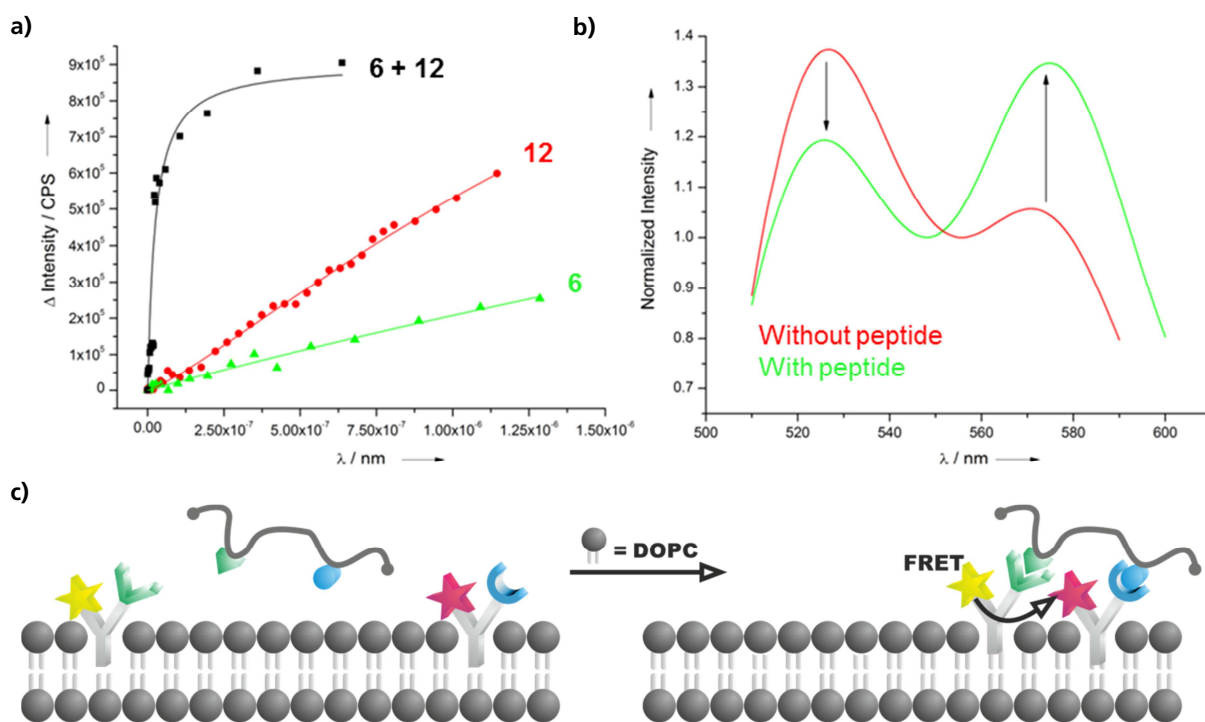


Figure 6. (a) Binding isotherms of **P1** showing increased affinities for combined receptors **12** and **6** in DOPC membranes; (b) FRET-response of heterodimeric receptor clustering in DOPC membranes in the presence of **P2**; (c) Schematic binding of multivalent ligands (**P2**) to FRET-labeled receptors **7** and **13**.

The dynamic formation of such binary “1:1” and ternary “1:2” ligand-to-receptor complexes via clustering of membrane-embedded metal complexes has also been reported by other groups. Using a minimalistic model Smith et al.⁴⁹ studied the association of the water-soluble anionic dye **CS** with POPC-vesicle bound Zn^{2+} -DPA complexes (cf. Scheme 2). The binding model changes with the receptor concentration in the membrane: For embedding of 10 mol% a 1:1 complex is dominant, whereas for higher loading levels of up to 30 mol% the predominant species is a 1:2 complex due to localizing of additional metal complexes. Additionally a cooperative binding of Cu^{2+} ions to membrane-bound dansyl-receptors has been previously described by Hunter, Williams et al. who reported complex formation of 4:1, 2:1 or 1:1 depending on the present receptor concentration in the lipid bilayers.⁵⁰ They observed increased (and interestingly also decreased) affinities compared to receptor-ligand binding in bulk solution which provides an indication how cells could control the formation of particular receptor-ligand clusters enabling a versatile response to external stimuli.

In the previously mentioned studies the aggregation of vesicle by crosslinking was suppressed using PEGylated lipids or not observed at all. Other reports however have also described the competing intra- and inter-membrane binding modes of multivalent ligands towards vesicular receptor surfaces (Figure 7a). In an approach to develop a simple model for cell adhesion Webb et al.^{51, 52} prepared DSPC vesicle membranes with pyrene-anchored Cu^{2+} -IDA complexes (**4**) and studied the effect of ligand valency via poly-histidine ligands. Receptor distributions were monitored by pyrene excimer-to-monomer emission and surface

affinities determined by isothermal titration calorimetry (ITC). They developed a binding model, which takes into account both intra- and intermembrane binding and observed an increasing crosslinking with increasing ligand valency (from mono-His to a 226-mer His), but no significantly increased affinities per binding unit. This was explained by the vesicles' difficulty of forming multiple bonds to the poly-His ligands due to adopted ligand conformations and the gel-phase membrane which especially at low loading levels may prevent receptor clustering resulting in predominate crosslinking over intramembrane chelation. The mechanism and functional determinants for molecular recognition and inter-vesicular docking, which finally lead to vesicle fusion have also been elucidated via other model systems.⁵³ Bong et al. for instance reported a synthetic fusion system based on vesicle-functionalization with vancomycin glycopeptide and a D -Ala- D -Ala dipeptide.⁵⁴

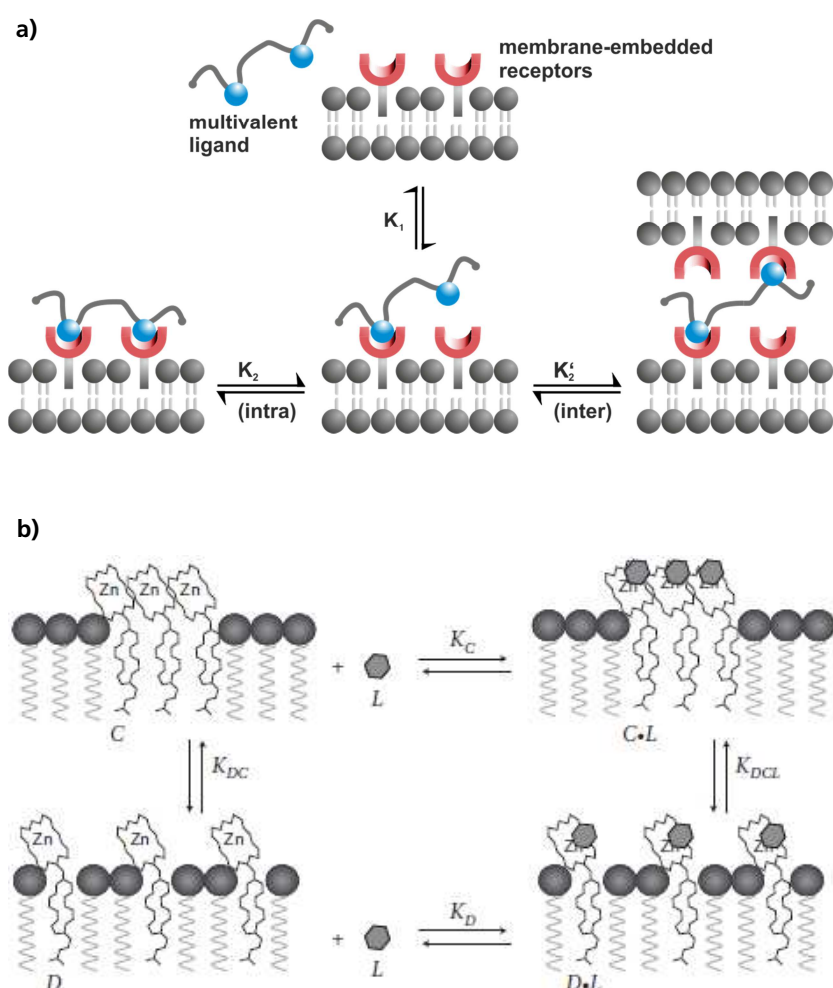


Figure 7. (a) Schematic inter- and intramembrane binding modes of multivalent ligands towards embedded receptors; (b) General thermodynamic cycle for receptor clustering induced by monovalent receptors and ligands (reprinted with permission from Ref. 59).

A reversible clustering of synthetic receptors in DSPC membranes in response to ligand binding was shown by Sasaki et al.⁵⁵⁻⁵⁷ In an approach towards developing metal ion sensors they embedded pyrene-labeled metal ion binding sites like IDA, BiPy or crown ethers (cf.

Scheme 2) in SUVs. The probe molecules initially formed small fluid-phase domains inside the gel-phase lipid bilayer, which can be observed by increased pyrene excimer emission. Upon coordination of metal ions with at least two positive charges (like Cu^{2+} , Pb^{2+} , Cr^{3+} and $\text{Fe}^{2/3+}$) the functionalized headgroups were driven away from each other by electrostatic repulsion and become dispersed in the surrounding DSPC domains. This fast and reversible membrane reorganization was also followed by the decreased E/M emission ratio. Using time-resolved fluorescence in a recent study the group also reported a favoured formation of nanodomains by phase separation of pyrene-labeled lipids (PLLs) in DSPC membranes whereas PLLs in fluid POPC membranes were found to be rather homogeneously distributed.⁵⁸

The relation of monovalent ligands to receptor clustering processes was demonstrated by Tomas et al.⁵⁹ who propose a combined binding-clustering thermodynamic cycle for the analysis of ligand interactions with membrane-embedded receptors (Figure 7b). Even without an apparent multivalent effect cluster formation between distinct amphiphilic metal complexes can be facilitated or hindered depending on electrostatic interactions. Variable amounts of negatively charged receptors based on Zn(II)-porphyrin (8) were incorporated into DMPC/cholesterol vesicles and examined in the absence/presence of various N-heterocyclic ligands. Positively charged ligands neutralized the receptor sites and favoured clustering due to less electrostatic repulsion. Negatively charged ligands however even increased the initial repulsive forces and resulted in greater spatial distances between the embedded metal complexes which were determined by UV-vis absorbance spectroscopy. This system provided another general model of addressable complexity, which can contribute to a better understanding of complex biological systems.

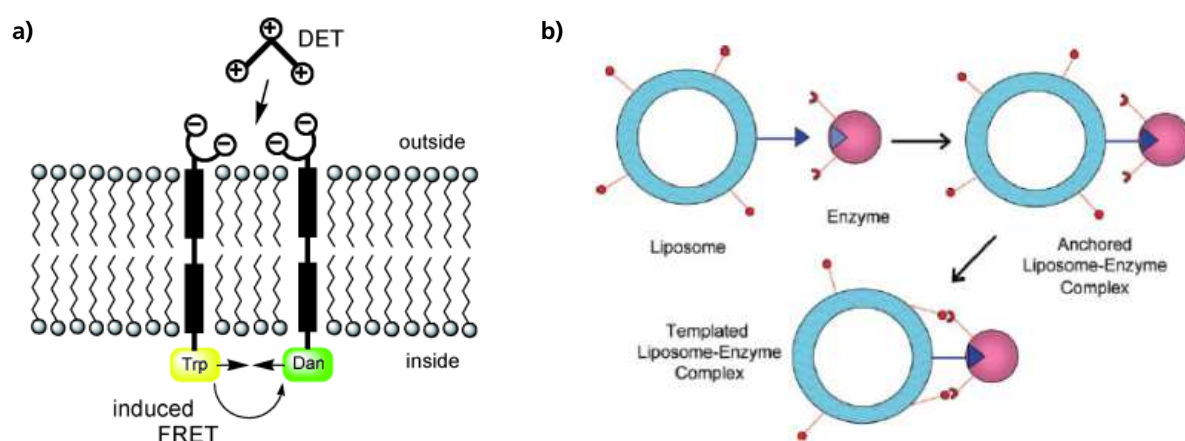


Figure 8. Applications of ligand-induced receptor clustering: (a) Artificial signal transduction across membranes (reprinted with permission from Ref. 61); (b) A multi-dentate vesicular enzyme inhibitor (reprinted with permission from Ref. 62).

In 2007 Hunter, Williams et al. reported the first transmission of binding information across lipid bilayers via a dansyl-transmembrane receptor and Cu^{2+} -ions as messenger.⁶⁰ In a later

study, Schrader et al. mimicked signal transduction across biological membranes by using cholesterol-based transmembrane building blocks functionalized with bisphosphonate dianions on one side and fluorescent dyes for FRET output on the other side.⁶¹ The anionic receptor sites located on the outside of 200 nm DPPC vesicles are assumed to be recruited by the presence of (poly)cations like diethylenetriammonium (DET). This way the complimentary Trp and dansyl labels on the other side of the membrane are brought into spatial proximity with the result of increased energy transfer (Figure 8a). As the membrane is impermeable for the messenger the transduction pathway is unidirectional from the recognition at the outer surface of the vesicle to the induced FRET output at the inner compartment, although the orientation of the transmembrane spanning compounds within the bilayer cannot be controlled and half of the recognition sites are not productive. Furthermore only a statistical third of all formed complexes are heterodimeric and useful for FRET. Although these models can of course not reflect the complexity of signal transduction processes at natural cell membranes or reproduce the corresponding affinities and selectivities with the latter approach it was nevertheless possible to create an entirely artificial signal transduction membrane system with selectivity for DET over other biological (poly)cationic species.

As a potential application of multivalent receptor recruiting at liposomal surfaces⁶² Mallik et al. finally suggested the design of “multi-prong” enzyme inhibitors. For this two rather simple compounds with a specific active site-anchor for the target enzyme and additional non-specific metal complex binding sites for surface exposed residues were combined in fluid vesicle membranes. For human carbonic anhydrase II (hCA II) it was shown that POPC vesicles containing both an amphiphilic benzenesulfonamide inhibitor and membrane-attached Cu^{2+} -IDA complexes exhibit a stronger inhibitory effect towards the enzyme than particles containing none or only one of these components. This effect was explained with the increased affinity of the multidentate vesicles which selectively anchor the active site hCA II and additionally complex surface exposed histidine residues via the dynamically organized Cu^{2+} -IDA sites (Figure 8b). This approach as a result could be transferred to different enzymes or other biological targets and may lead to the design of artificial antibodies for diagnostic applications.

As indicated by the reports presented herein the formation of functional lipid rafts and the (reversible) clustering of artificial membrane-embedded receptor units in response to external stimuli is usually detected by indirect spectroscopic methods, like UV/Vis- or fluorescence changes, or changes in ligand affinities/selectivities detected by other physicochemical methods. Thus imaging of such dynamic molecular rearrangements at the membrane-water interface provides a remaining challenge to support the current hypotheses and understanding for these systems by a “seeing is believing” approach.

Compared to solid particles and surfaces imaging of functionalized artificial bilayer membranes at molecular resolutions is still not accessible via standard techniques. The structural properties of such interfaces like the molecular ordering of surface layers are in discussion.⁶³

Despite the extremely easy and rapid preparation and variability of self-assembled functionalized vesicle membranes the control of spatial orientation of embedded functional molecules is a major challenge as some of the presented systems show. The random distribution of functional amphiphiles between the inner and outer leaflet of the bilayer sheets can be disadvantageous as it results in a loss of available interactions sites towards the exterior environment of the particles. This may be resolved by a post-functionalization approach: For this the vesicles are first assembled with randomly embedded “anchors” only and in a second step selectively functionalized on the outer surface in a covalent or non-covalent way. With conditions excluding “flip-flop”-transitions this could provide additional spatial control of functional entities in artificial bilayer membranes. On the other hand the different functionalization of membrane faces, as demonstrated e.g. with membrane spanning compounds provide opportunities for directed transport or signalling and overall more complex functions.

Summary and Outlook

The embedding of functional amphiphiles derived from well-known and accessible compounds into biomimetic vesicle membranes allows the preparation of versatile nanomaterials for catalytic transformations or sensing applications. Catalyst activities can be readily improved by local surface aggregation effects, binding units easily combined with transducing optical labels and much more complex analyte structures differentiated via multi-point interactions compared to aqueous solution systems. The reported examples of biomimetic functional membranes can contribute to a better understanding of biological membranes although their level of complexity is still much simpler compared to their natural models. Nevertheless, it is possible to mimic some basic functions with artificial functionalized membranes. To extend the presented concepts of dynamic receptor recruiting by multivalent ligands we are currently trying to store such kind of spatial information in initially fluid membranes via successive crosslinking of functional groups and thus providing a new kind of imprinted materials. Artificial membranes are furthermore suitable for processing and may be used for the preparation of functionalized surfaces and microarrays.⁶⁴

References

1. S. Singer, *Science*, 1992, **255**, 1671-1677.
2. A. Grakoui, S. K. Bromley, C. Sumen, M. M. Davis, A. S. Shaw, P. M. Allen and M. L. Dustin, *Science*, 1999, **285**, 221-227.
3. P. Scrimin and P. Tecilla, *Curr. Opin. Chem. Biol.*, 1999, **3**, 730-735.
4. K. Ariga, J. P. Hill and H. Endo, *Int J Mol Sci*, 2007, **8**, 864-883.
5. D. D. Lasic, *Biochem. J*, 1988, **256**, 1-11.
6. O. Onaca, R. Enea, D. W. Hughes and W. Meier, *Macromol. Biosci.*, 2009, **9**, 129-139.
7. D. D. Lasic, *Current Opinion in Solid State & Materials Science*, 1996, **1**, 392-400.
8. P. Walde, K. Cosentino, H. Engel and P. Stano, *ChemBioChem*, 2010, **11**, 848-865.
9. C. B. Minkenberg, F. Li, P. van Rijn, L. Florusse, J. Boekhoven, M. C. A. Stuart, G. J. M. Koper, R. Eelkema and J. H. van Esch, *Angew. Chem. Int. Ed.*, 2011, **50**, 3421-3424.
10. T. Fenske, H.-G. Korth, A. Mohr and C. Schmuck, *Chem. Eur. J.*, 2012, **18**, 738-755.
11. X. Zhang, S. Rehm, M. M. Safont-Sempere and F. Würthner, *Nat. Chem.*, 2009, **1**, 623-629.
12. T. Takeuchi and S. Matile, *J. Am. Chem. Soc.*, 2009, **131**, 18048-18049.
13. Q. Yan, R. Zhou, C. K. Fu, H. J. Zhang, Y. W. Yin and J. Y. Yuan, *Angew Chem Int Edit*, 2011, **50**, 4923-4927.
14. D. L. Giokas and A. G. Vlessidis, *Anal. Chim. Acta*, 2011, **683**, 156-169.
15. E. Mahon, T. Aastrup and M. Barboiu, *Chem. Commun.*, 2010, **46**, 2441-2443.
16. G. Hamasaka, T. Muto and Y. Uozumi, *Angew. Chem. Int. Ed.*, 2011, **50**, 4876-4878.
17. K. Letchford and H. Burt, *Eur. J. Pharm. Biopharm.*, 2007, **65**, 259-269.
18. V. Malinova, S. Belegriou, D. D. Ouboter and W. P. Meier, *Adv Polym Sci*, 2010, **224**, 113-165.
19. M. M. Tedesco, B. Ghebremariam, N. Sakai and S. Matile, *Angew. Chem. Int. Ed.*, 1999, **38**, 540-543.
20. C. P. Wilson and S. J. Webb, *Chem. Commun.*, 2008, 4007-4009.
21. S. Matile, H. Tanaka and S. Litvinchuk, in *Top. Curr. Chem.*, Springer Berlin / Heidelberg, 2007, pp. 219-250.
22. J. M. Moszynski and T. M. Fyles, *Org. Biomol. Chem.*, 2011, **9**, 7468-7475.
23. T. M. Fyles and B. Zeng, *Chem. Commun.*, 1996, 2295-2296.
24. T. Kunitake, *Angew. Chem. Int. Ed.*, 1992, **31**, 709-726.
25. D. D. Lasic, *Am. Sci.*, 1992, **80**, 20-31.

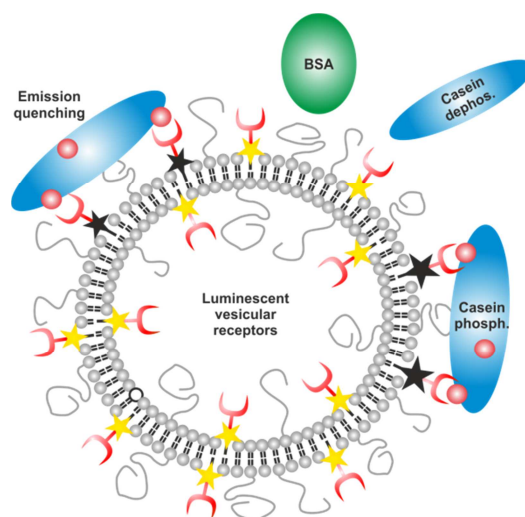
26. P. Tecilla, F. Mancin, P. Scrimin and U. Tonellato, *Coord. Chem. Rev.*, 2009, **253**, 2150-2165.
27. D. Papahadjopoulos, S. Nir and N. Duzgunes, *J. Bioenerg. Biomembr.*, 1990, **22**, 157-179.
28. F. Mancin and P. Tecilla, *New J. Chem.*, 2007, **31**, 800-817.
29. F. Mancin, P. Scrimin and P. Tecilla, *Chem. Commun.*, 2012, **48**, 5545-5559.
30. M. Subat, K. Woinaroschy, C. Gerstl, B. Sarkar, W. Kaim and B. König, *Inorg. Chem.*, 2008, **47**, 4661-4668.
31. B. Gruber, E. Kataev, J. Aschenbrenner, S. Stadlbauer and B. König, *J. Am. Chem. Soc.*, 2011, **133**, 20704-20707.
32. R. Bonomi, F. Selvestrel, V. Lombardo, C. Sissi, S. Polizzi, F. Mancin, U. Tonellato and P. Scrimin, *J. Am. Chem. Soc.*, 2008, **130**, 15744-15745.
33. J. Voskuhl and B. J. Ravoo, *Chem. Soc. Rev.*, 2009, **38**.
34. A. E. Hargrove, S. Nieto, T. Zhang, J. L. Sessler and E. V. Anslyn, *Chem. Rev.*, 2011, **111**, 6603-6782.
35. S.-i. Tamaru and I. Hamachi, ed. R. Vilar, Springer Berlin / Heidelberg, 2008, pp. 95-125.
36. E. Kimura and S. Aoki, *BioMetals*, 2001, **14**, 191-204.
37. B. T. Nguyen and E. V. Anslyn, *Coord. Chem. Rev.*, 2006, **250**, 3118-3127.
38. B. Gruber, S. Stadlbauer, K. Woinaroschy and B. König, *Org. Biomol. Chem.*, 2010, **8**, 3704-3714.
39. M. Bhuyan and B. König, *Chem. Commun.*, 2012, DOI:10.1039/C1032CC33279E.
40. O. Mertins and R. Dimova, *Langmuir*, 2011, **27**, 5506-5515.
41. L. S. Jung, J. S. Shumaker-Parry, C. T. Campbell, S. S. Yee and M. H. Gelb, *J. Am. Chem. Soc.*, 2000, **122**, 4177-4184.
42. H. J. Galla and W. Hartmann, *Chem. Phys. Lipids*, 1980, **27**, 199-219.
43. R. Jelinek and S. Kolusheva, ed. T. Schrader, Springer Berlin / Heidelberg, 2007, pp. 155-180.
44. X. Chen, G. Zhou, X. Peng and J. Yoon, *Chem. Soc. Rev.*, 2012, **41**, 4610-4630.
45. D. A. Jose, S. Stadlbauer and B. König, *Chem. Eur. J.*, 2009, **15**, 7404-7412.
46. H. Jeon, S. Lee, Y. Li, S. Park and J. Yoon, *J. Mater. Chem.*, 2012, **22**, 3795-3799.
47. B. Gruber, S. Stadlbauer, A. Späth, S. Weiss, M. Kalinina and B. König, *Angew. Chem. Int. Ed.*, 2010, **49**, 7125-7128.
48. B. Gruber, S. Balk, S. Stadlbauer and B. König, *Angew. Chem. Int. Ed.*, 2012, DOI: 10.1002/anie.201205701.
49. H. Jiang and B. D. Smith, *Chem. Commun.*, 2006, 1407-1409.

50. E. L. Doyle, C. A. Hunter, H. C. Phillips, S. J. Webb and N. H. Williams, *J. Am. Chem. Soc.*, 2003, **125**, 4593-4599.
51. R. J. Mart, K. P. Liem, X. Wang and S. J. Webb, *J. Am. Chem. Soc.*, 2006, **128**, 14462-14463.
52. X. Wang, R. J. Mart and S. J. Webb, *Org. Biomol. Chem.*, 2007, **5**, 2498-2505.
53. K. Meyenberg, A. S. Lygina, G. van den Bogaart, R. Jahn and U. Diederichsen, *Chem. Commun.*, 2011, **47**, 9405-9407.
54. Y. Gong, M. Ma, Y. Luo and D. Bong, *J. Am. Chem. Soc.*, 2008, **130**, 6196-6205.
55. D. Y. Sasaki, T. A. Waggoner, J. A. Last and T. M. Alam, *Langmuir*, 2002, **18**.
56. J. L. Pincus, C. Jin, W. Huang, H. K. Jacobs, A. S. Gopalan, Y. Song, J. A. Shelnett and D. Y. Sasaki, *J. Mater. Chem.*, 2005, **15**, 2938-2945.
57. D. Y. Sasaki, *Cell Biochem. Biophys.*, 2003, **39**, 145-161.
58. H. Siu, J. Duhamel, D. Y. Sasaki and J. L. Pincus, *Langmuir*, 2010, **26**, 10985-10994.
59. S. Tomas and L. Milanesi, *Nat. Chem.*, 2010, **2**, 1077-1083.
60. H. P. Dijkstra, J. J. Hutchinson, C. A. Hunter, H. Qin, S. Tomas, S. J. Webb and N. H. Williams, *Chem-Eur J*, 2007, **13**, 7215-7222.
61. K. Bernitzki and T. Schrader, *Angew. Chem. Int. Ed.*, 2009, **48**, 8001-8005.
62. A. I. Elegbede, M. K. Haldar, S. Manokaran, J. Kooren, B. C. Roy, S. Mallik and D. K. Srivastava, *Chem. Commun.*, 2007, 3377-3379.
63. I. V. Stiopkin, C. Weeraman, P. A. Pieniazek, F. Y. Shalhout, J. L. Skinner and A. V. Benderskii, *Nature*, 2011, **474**, 192-195.
64. K. M. Kim, D. J. Oh and K. H. Ahn, *Chem. Asian J.*, 2011, **6**, 122-127.

CHAPTER 2

LUMINESCENT VESICULAR RECEPTORS FOR THE RECOGNITION OF BIOLOGICALLY IMPORTANT PHOSPHATE SPECIES

The anion binding ability of bis-zinc cyclen complexes in buffered aqueous solution was investigated using indicator displacement assays (IDA) as well as luminescent labeled complexes. A high affinity to phosphate anions, such as UTP or pyrophosphate was observed in IDA while there was no observable binding of other anions. The binding affinity and as a result the selectivity between different phosphate anions correlates with their overall negative charge and steric demand. Complexes bearing luminescent labels did not respond to the presence of phosphate anions in homogeneous solution, but if embedded as amphiphiles in small unilamellar vesicle (SUV) membranes. The scope of possible anionic analytes was extended to phosphorylated protein surfaces by using such metal complex functionalized vesicles bearing oligoethylene glycol residues in an optimized amount on their surface to suppress non-specific interactions. Under physiological conditions these surface-modified vesicles show a selective response and nanomolar affinity for α -S1-Casein, which is multiple phosphorylated, while not responding to the corresponding dephosphorylated Casein or BSA. The vesicular luminescent metal complexes do currently not reach the sensitivity and selectivity of reported enzymatic assays or some chemosensors for phosphate anions, but they present a novel type of artificial receptors for molecular recognition. Membrane-embedding of multiple, different receptors and their possible structuring on the vesicular surface is expected to improve affinities and selectivities and may allow the design of artificial antibodies.



This chapter has been published:

B. Gruber, S. Stadlbauer, K. Woinaroschy and B. König, *Org. Biomol. Chem.* **2010**, *8*, 3704-3714.

Author contributions:

BG synthesized vesicles, performed CMS-, NMR- and MS-assays and wrote the manuscript; SS synthesized compounds **5** and **6**; KW synthesized compound **3** and performed PV-displacement assay; BK supervised the project and is corresponding author.

Introduction

Molecular recognition of phosphate anions under physiological conditions is of interest as they are ubiquitously present in nature:¹ in RNA and DNA, in phosphorylated saccharides and phosphorylated proteins.²⁻⁷ The nucleotide adenosine triphosphate (ATP) is the molecular currency of intracellular energy transfer,⁸ and pyrophosphate ($P_2O_7^{4-}$, PP_i), the product of ATP hydrolysis, plays an important role in intracellular signalling.⁹ Therefore the development of artificial phosphate anion receptors for use under physiological conditions is of continuous interest. Such sensors are useful tools for the detection of biologically important phosphates interest,¹⁰⁻¹² with applications in molecular biology, life and environmental sciences.

Recent reports reveal that transition metal complexes with vacant coordination sites are well suited to serve as phosphate ion binding sites.^{13, 14} A widely used binding unit in phosphate chemosensors is the zinc(II)-dipicolylamine (Dpa) complex as demonstrated by Hamachi,¹⁵⁻²¹ Hong²²⁻²⁴ and Smith.²⁵⁻²⁷ Macrocyclic 1,4,7,10-tetraazacyclododecane (cyclen) transition metal complexes were reported as phosphate binding sites by Kikuchi²⁸ and Kimura.²⁹⁻³² We have recently reported the use of zinc(II)-cyclen as promoters in ester hydrolysis,^{33, 34} detection of phosphorylated peptides³⁵ and proteins³⁶ and for a sterically guided molecular recognition of nucleotides, nucleobases and phosphates in supramolecular self-assembled systems.³⁷⁻³⁹

There are two typical ways to signal the binding of an analyte to a synthetic receptor: A luminescent group is located closely to the binding site and responds to the binding event by a change in its emission properties.^{40, 41} Alternatively, an indicator-displacement assay (IDA) based on the competitive binding of a pH indicator and the analyte to the non-labeled binding site is used to signal the interaction of the analyte and the receptor.⁴²⁻⁴⁵

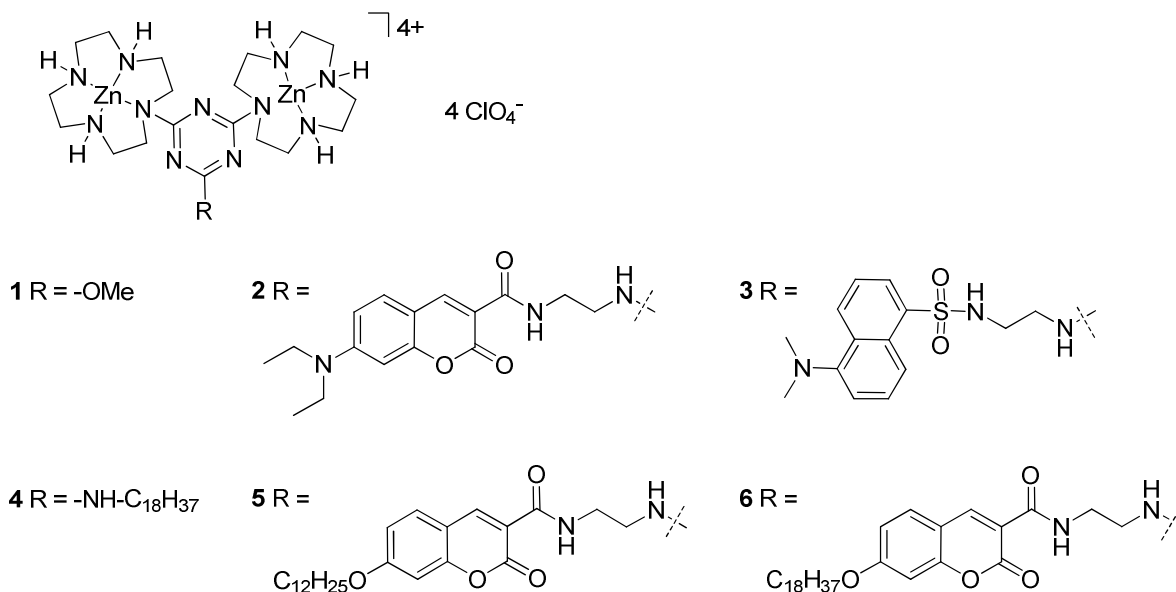
We describe here the preparation and binding properties of several 1,4,7,10-tetraazacyclododecane (cyclen) Zn(II) complexes and small unilamellar vesicles, which contain amphiphilic luminescent cyclen Zn(II) complexes as phosphate anion binding sites embedded in the vesicle membrane.

Results and Discussion

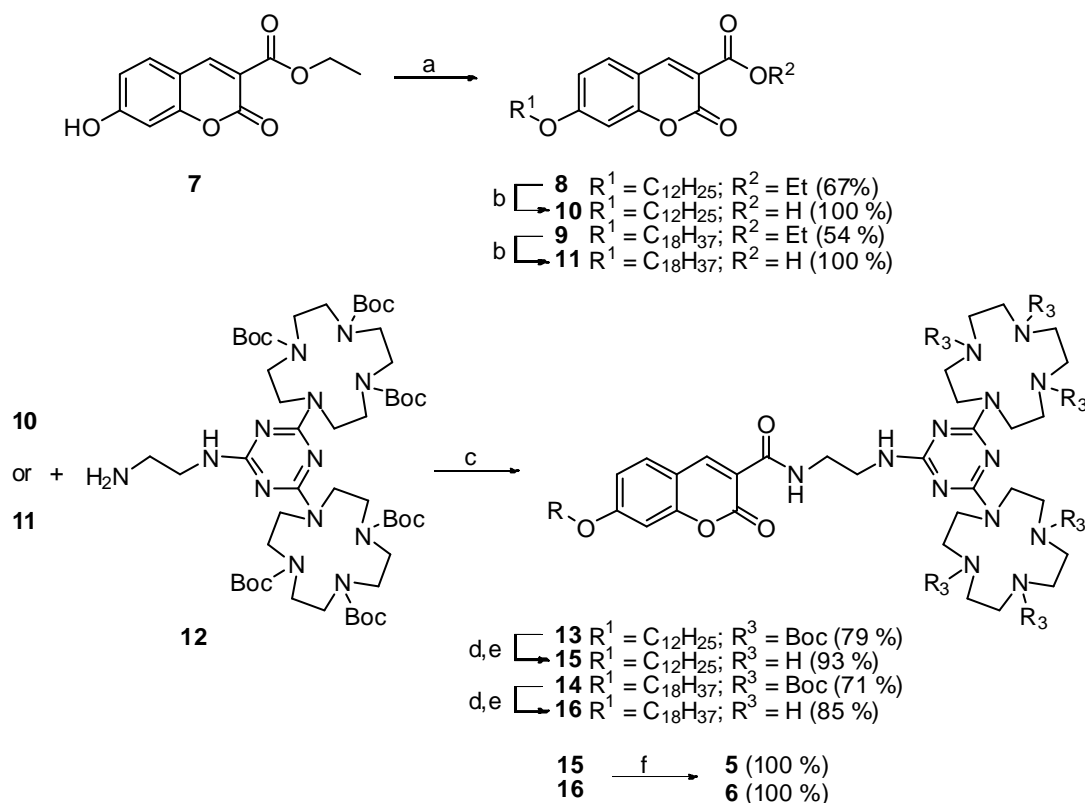
Syntheses of Zn(II)-cyclen complexes

The previously reported triazine-bis-zinc cyclen complex **1** was modified by the introduction of fluorescent groups (**2**, **3**), substitution with an alkyl chain (**4**) or both (**5**, **6**). Scheme 1 summarizes all prepared compounds. Complexes **1**,³⁴ **2**³⁶ and **4**^{37, 38} were synthesized as

previously reported and the preparation of compound **3** is described in the Supporting Information.



Scheme 1. Fluorescent and amphiphilic binuclear Zn(II)-cyclen complexes **1** - **6** for phosphate anion binding in aqueous media.



Scheme 2. Synthesis of fluorescent amphiphilic binuclear Zn(II)-cyclen complexes **5** and **6**. (a) Br-(CH₂)_n-CH₃ (n = 11 or 17), K₂CO₃, DMF, 80 °C, 20 h; (b) NaOH, THF, reflux, 5 h; (c) TBTU, HOBT, DIPEA, DMF,

40 °C, 2.5 h; (d) HCl/ether, RT, o/n; (e) basic ion exchanger resin H₂O, MeOH; (f) Zn(ClO₄)₂, MeOH, 65 °C, 20 - 24 h.

The synthesis of complexes **5** and **6** is shown in Scheme 2. Amphiphilic, fluorescent compounds **10** and **11** were obtained by Williamson ether synthesis with alkyl bromide on 8-hydroxycoumarin-3-carboxylic acid ethyl ester **7**⁴⁶ and subsequent saponification. Binuclear Zn(II)-cyclen complexes **5** and **6** were then prepared by amide formation using standard peptide coupling conditions in solution.

Removing of the Boc protecting groups and subsequent basic ion exchanger resin gave the free amine ligands which finally were treated with two equivalents of a methanolic solution of Zn(ClO₄)₄. Detailed experimental procedures and analytical data of the prepared compounds are provided in the Experimental Part and in the Supporting Information.

Preparation of Zn(II)-cyclen modified vesicles

Membrane-functionalized vesicles (vesicular receptors) were prepared from a mixture of commercially available synthetic phospholipid 1,2-distearoyl-sn-glycero-3-phosphocholine (DSPC) and amphiphilic Zn(II)-cyclen complexes **4**, **5**, **6** (10 mol% in respect to used DSPC) by the well-established film-hydration-method.⁴⁷ The resulting multilamellar vesicles (MLVs) were homogenized by extrusion to yield small unilamellar vesicles (SUVs) of a defined size of 80 - 100 nm.

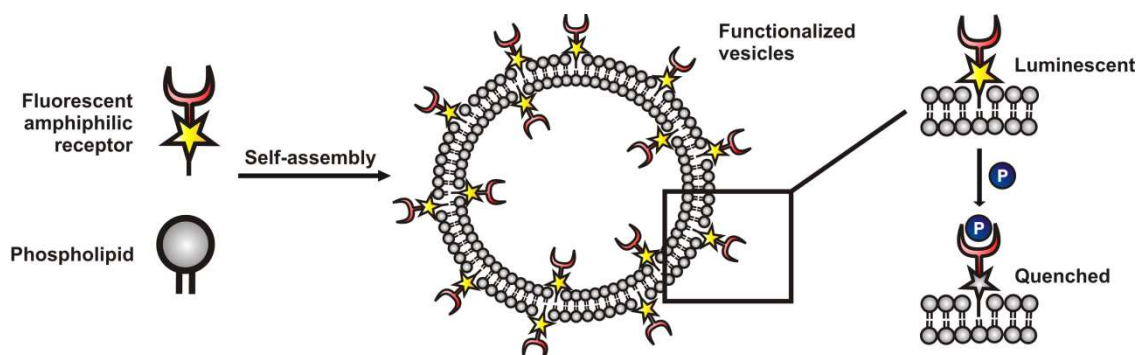


Figure 1. Scheme of functionalized vesicles with surface exposed receptors that respond to phosphate anions by decreasing fluorescence emission.

The individual receptor units of the obtained vesicles are assumed to be equally distributed in both layers of the liposomal membrane as reported for similar surface modified vesicles.⁴⁸ Thus, we established a correction factor f describing the outer surface exposed receptors as a fraction of its entire quantity of matter. This factor enables the determination of the effective concentration of available binding sites on the outer layer of the vesicle (for details see Experimental Part). As the main phase transition temperature (T_m) of DSPC vesicles is reported to be 54 °C,⁴⁹ no transverse (flip-flop) diffusion is assumed to occur at room temperature.

Characterization of vesicle dispersions

The particle size, particle number and sample dispersity of the prepared vesicle dispersions were determined by dynamic light scattering (DLS)^{50, 51} and the average hydrodynamic diameter of the functionalized vesicles was found to be 80 (\pm 5) nm. Generally, homogenized SUV dispersions are assumed to be free of impurities and thus no further purification is required. Nevertheless vesicles can be passed through size exclusion chromatography (SEC) columns to ensure complete exclusion of unimolecular amphiphiles or aggregates of lower molecular weight.⁵² All prepared vesicle dispersions were stored as buffered aqueous solutions at 6 °C and used within 2 weeks.

Phosphate anion binding studies

Zn(II) complexes of cyclen possess very high stability constants ($\log K_{\text{Zn-cyclen}} = 16.2$)^{53, 54} and as a result no decomplexation of the artificial receptors is assumed to occur under the conditions of the following binding studies. Initially, the binding properties of Zn(II)-cyclen **1** to various phosphate species were investigated in homogeneous aqueous solution by an indicator displacement assay utilizing pyrocatechol violet (PV) in HEPES buffered solution (10 mM, pH 7.4) by UV-VIS spectroscopy. Upon coordination to zinc cyclen complexes PV shows a colour change resulting from a decreasing absorption at $\lambda_{\text{max}} = 443$ nm and an increasing absorption at $\lambda_{\text{max}} = 636$ nm (Figure 2 Left).⁵⁵⁻⁵⁸ By addition of aliquots of aqueous solutions (HEPES buffer 10 mM, pH 7.4) of the sodium or potassium salts of ATP, ADP, cAMP, GTP, PPi, hydrogen phosphate and phenyl phosphate to a 1:1 mixture of **1** and PV (35 μ M each) the indicator is partially or fully displaced (Figure 2 Right).

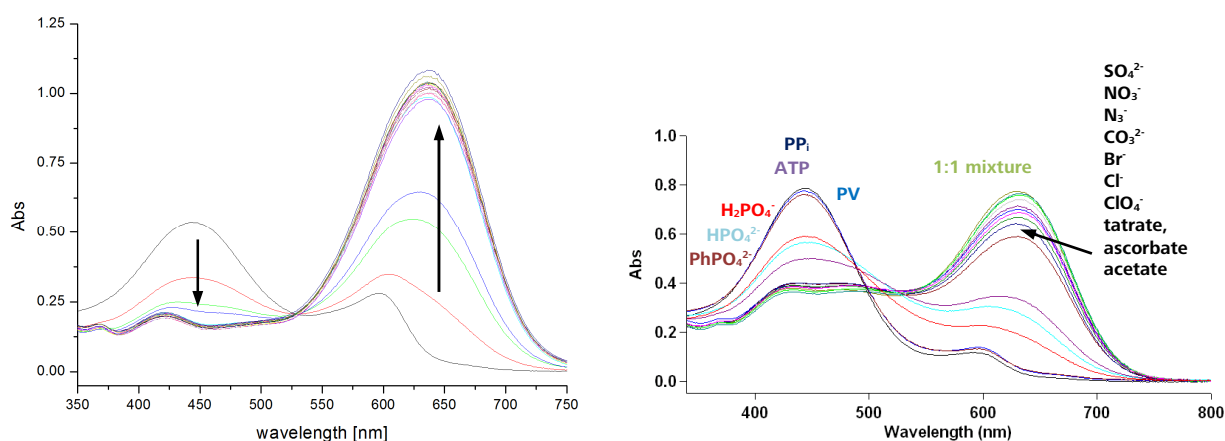


Figure 2. (Left) Addition of **1** (0-105 μ M) to a constant concentration of PV (35 μ M). Titrations were performed at 25 °C in 10 mM HEPES buffer, pH 7.4. (Right) UV/Vis spectra of a 1:1 mixture **1** and PV (50 μ M, $\lambda_{\text{max}} = 636$ nm) in the presence of various anions (250 μ M). Only phosphate anions are able to displace the indicator with $\lambda_{\text{max}} = 443$ nm. The displacement, and therefore the binding ability of **1**, is proportional to the number of negative charges on the phosphate.

The binding constants ($\log K$) of **1** to the different phosphate anions (Table 1) were derived from the concentrations of PV and the respective phosphate anion at 50% release of the

indicator. The addition of other anions, such as SO_4^{2-} , NO_3^- , N_3^- , CO_3^{2-} , Br^- , Cl^- , ClO_4^- , tartrate, ascorbate or acetate, did not displace the PV indicator from the metal complex: the absorption at $\lambda_{\text{max}} = 443 \text{ nm}$ remains unchanged and only a slight decrease at $\lambda_{\text{max}} = 636 \text{ nm}$ is observed.⁵⁹ Under the experimental conditions no hydrolysis of pyrophosphate or ATP was induced by the bis-zinc cyclen complexes over several hours as confirmed by HPLC-MS and NMR (see Supporting Information).

The binding affinity is clearly influenced by the number of negative charges on the phosphate and their steric demand, as was previously reported for other phosphate anion receptors.⁶⁰⁻⁶³ Nucleotides like ATP have four negative charges at the given pH and show the highest binding constants ($\log K \sim 6$) together with PPi , which has only three negative charges, but is sterically much less demanding and as a result also exhibits a very high charge density. Nucleoside diphosphates show affinities, which are up to one order of magnitude lower (~ 5) and similar to inorganic phosphate. Phenyl phosphate shows an again decreased affinity with a $\log K$ of 4.2. For cAMP ($\log K = 3.8$) partial displacement of the indicator was observed only upon addition of an excess of more than six equivalents of the analyte. As the IDA method represents an indirect method for the determination of the binding event, we used the Zn(II)-cyclen complexes **2** and **3**, which bear a fluorescence label and investigated their response in homogeneous aqueous buffered solution to phosphate anions (e.g. PPi , ATP, GTP, ADP, Na_2HPO_4 , GDP and other nucleotides). However, none of the added anions induced a significant change in the absorption or emission properties of **2** or **3** (See Supporting Information). The coordination of a phosphate anion obviously does not influence the photophysical properties of the covalently attached fluorophores.

Having acquired this information on phosphate anion binding of complexes **1**, **2** and **3** in homogeneous solution we turned our attention to self-assembled surface modified vesicles for anion sensing³⁹ and molecular recognition.^{48, 64} Thus a set of vesicular receptors modified by the amphiphilic phosphate binding moieties **4** – **6** were prepared.

A vesicular receptor (**VR-4**) with the hydrophobic binuclear Zn(II)-cyclen complex **4** was prepared and its binding affinity to various phosphate anions was investigated by IDA methods employing coumarin methyl sulfonate (CMS) as an indicator dye (rightright 3 Left). The highest binding constant was found for UTP (7.2), which exceeded the affinities of the other tested nucleotides ATP and GTP (both 6.5). This may be explained by the binding of both, phosphate and imide moieties of UTP to the Zn(II)-macrocycles (see SI).^{37, 38} However, no difference in binding affinities of the nucleoside diphosphates UDP and GDP was observed. GDP and UDP both show a binding constant of 5.2 as due to the weaker coordination capabilities of diphosphates the affinity is one to two orders of magnitude lower compared to the respective triphosphates. Pyrophosphate, due to its small size and

high charge density, exhibited a remarkable binding affinity with a log K value of 7.1. Fructose-1,6-bisphosphate also binds tightly (log K = 6.4), which might be explained by the favourable interaction with two bis-Zn(II)-cyclen moieties revealing additive or even cooperative action: following the binding of the first phosphate group, the binding of the second phosphate group is facilitated by the preformed substrate-receptor complex. Inorganic phosphate showed the same binding constant as the diphosphates GDP and UDP. At the given pH value inorganic phosphate exists predominantly as a dianion, having one negative charge less than GDP and UDP. The similar binding affinities might be explained by the lack of steric hindrance of inorganic phosphate as well as by an increase of its acidity upon complexation by the bis-Zn(II)-cyclen moieties resulting in an additional negative charge. The phosphate monoesters phenylphosphate and phosphoserine, in contrast, bind with an affinity one order of magnitude lower than inorganic phosphate, obviously due to their larger steric demands and only two acidic protons present at the phosphate moiety. For all tested and compared compounds the respective binding constants to the vesicular receptor were found to be higher than those to complex **1**. Only a minor increase was found for the monophosphates phenylphosphate and inorganic phosphate, whereas the difference in the binding constants for pyrophosphate amounted to an entire order of magnitude.

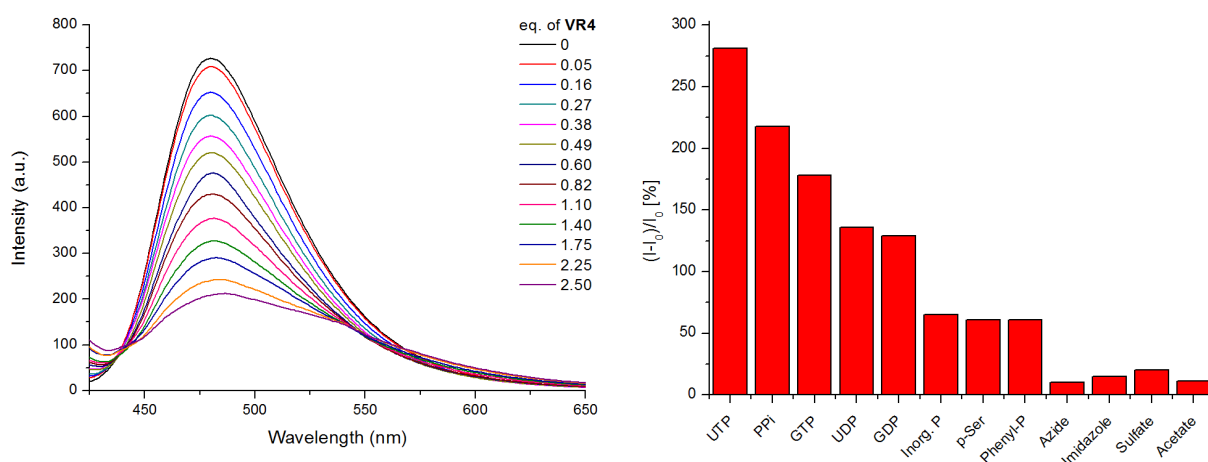


Figure 3. (Left) Fluorescence quenching of CMS in the presence of VR-4. (Right) Relative changes in emission intensity obtained by displacement with various analytes.

The ion selectivity of vesicular receptor **VR-4** was investigated by the addition of other anionic compounds like sulphate, azide and acetate (see Supporting Information and Figure 2 Right). Furthermore, imidazole was tested as a potential ligand as the bis-Zn(II)-cyclen moieties are known to have a weak affinity for histidine residues.⁶⁵ None of these compounds showed a considerable affinity towards the vesicular receptor **VR-4**. Thus, binding constants for these compounds could not be determined, but were estimated to be smaller than log K = 2.

Using the amphiphilic fluorescent binuclear Zn(II)-cyclen **6** and its corresponding vesicular receptor **VR-6** a direct signalling of the phosphate ion binding event was possible: upon addition of phosphate anions, such as PP_i , ATP, fructose-1,6-bisphosphate and inorganic phosphate, the emission intensity at 405 nm of the coumarin label decreased (Figure 3 Left). To the best of our knowledge this technique of anion sensing with membrane-embedded fluorescence-labeled metal complexes has not been reported so far. The determined binding affinities exceed the micro molar range and are consistent with the corresponding values obtained by the indicator displacement assay for the vesicular receptor **VR-4** and compound **1**. Modifying the tethered hydrophobic alkyl chain of the binuclear Zn(II)-cyclen complex from C_{18} to C_{12} (compound **5**) did not affect the binding affinity of the vesicular receptor **VR-5** to PP_i and ATP (Table 1).

Entry	Phosphate species	log K			
		1	VR-4	VR-5	VR-6
1	Pyrophosphate	5.9 ^[a]	7.1 ^[c]	6.6	6.6
2	UTP	5.4 ^[c]	7.2 ^[c]	–	–
3	ATP	5.9 ^[a]	6.5 ^[c]	6.6	6.6
4	GTP	5.8 ^[a]	6.5 ^[c]	–	–
5	GDP	– ^[b]	5.2 ^[c]	–	–
6	UDP	4.9 ^[c]	5.2 ^[c]	–	–
7	Fructose-1,6-bisphosphate	– ^[b]	6.4 ^[c]	–	6.1
8	Inorganic phosphate	4.9 ^[a]	5.2 ^[c]	–	5.5
9	p-Ser	– ^[b]	4.3 ^[c]	–	–
10	Ph-O- PO_3	4.0 ^[a]	4.2 ^[c]	–	–

Table 1. Summary of binding constants to various phosphate species obtained by indicator displacement assays in solution for the binuclear Zn(II)-cyclen motif. Error limits for the determined binding constants are ± 0.2 .

^[a] Binding affinities were obtained by IDA methods (indicator dye: PV) with UV-VIS absorption titration. ^[b] No binding experiments were performed. ^[c] Binding affinities were obtained by IDA methods (indicator dye: CMS) by emission titration ($\lambda_{\text{ex}} = 396 \text{ nm}$, $\lambda_{\text{em}} = 480 \text{ nm}$).

Monitoring of phosphate binding to compounds **2** and **3** by changes of their luminescence was not possible in aqueous solution, most likely due to the flexible linkage of binding and signalling sites. Compounds **5** and **6** are expected to be embedded with their alkyl chain and the coumarin dye into the vesicle bilayer, as reported for similar coumarin derivatives.^{66, 67} This should significantly restrict their movement in the highly ordered vesicle bilayer, which might be beneficial for the sensing properties.^{68, 69} In addition, the local polarity change at the fluorophore, which is a crucial factor for the response to phosphate binding, is expected to be larger at the vesicle membrane-water interface compared to bulk water.^{66, 67} Coumarin dye derivatives are known for their solvatochromism in various solvents of different polarity.⁷⁰⁻⁷³

Subsequently to the binding studies with low-molecular weight phosphate species, binding towards larger analytes bearing several phosphate anions was investigated to potentially take advantage of the numerous binding sites on the surface of the nanometer-sized vesicles. To demonstrate this, the affinities towards proteins with and without multiple phosphorylated sites were determined: α -S1-Casein from bovine milk bearing eight phosphorylated serine residues was expected to specifically interact with the zinc cyclen receptors on the vesicle surface. A (for the most part) dephosphorylated sample of the same protein and BSA were used as control to exclude non-specific vesicle-protein interactions.

The vesicular receptors (**VR-6**) exhibited, as expected, a significant non-specific interaction to all tested proteins regardless of the presence of phosphorylated sites (data not shown). Such non-specific interactions between proteins and liposome surfaces, for example due to electrostatic attraction, are well documented.⁷⁴

To suppress the non-specific interactions between the surfaces of liposome and protein and to gain selectivity for the phosphate anion zinc-cyclen receptor interaction the vesicular surface was shielded by polyethylene glycol (PEG) residues. Therefore vesicles were prepared from mixtures of DSPC and DSPC-PEG350 having an oligoethylene glycol residue attached to its polar head groups (See Supporting Information).

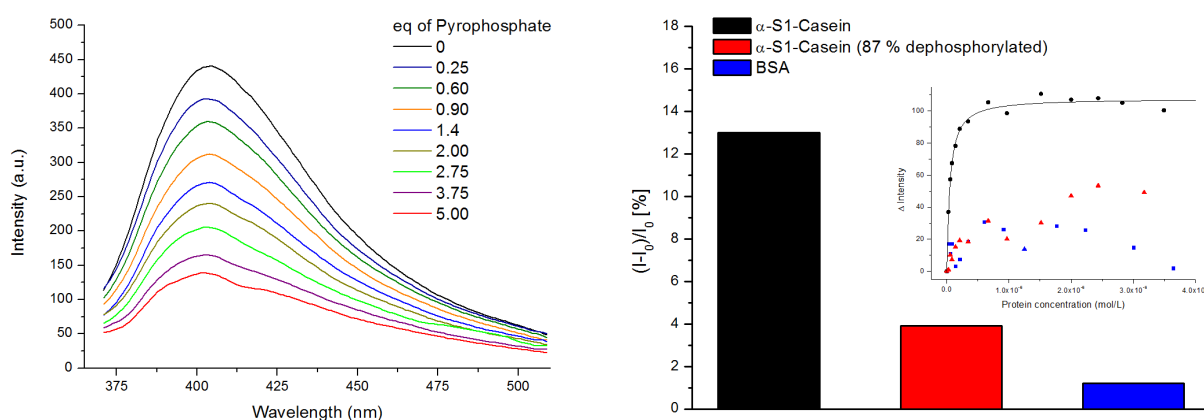


Figure 4. (Left) Fluorescence quenching of VR-6 in the presence of pyrophosphate anions. (Right) Relative emission response of VR-6P in the presence of different proteins (0.05 equivalents). Inset plot shows corresponding binding isotherms of α -S1-Casein, dephosphorylated α -S1-Casein and BSA to **VR-6P** [5×10^{-6} M Zn(II)].

At an optimum composition of about 6:4 DSPC to DSPC-PEG350 (**VR-6P**) the non-specific binding is suppressed sufficiently to allow a selective recognition of α -S1-Casein (Figure 4 Right). Due to its multiple phosphorylations the protein's affinity is in the nanomolar range and about two orders of magnitude higher than the affinity determined for a single phosphate group (Table 1). BSA shows only a very small relative change in fluorescence intensity as does the dephosphorylated α -S1-Casein sample, which still contains residual phosphate moieties. Furthermore the two control proteins do not give meaningful binding

isotherms. Vesicles with a lower PEG-content showed reduced or no selectivity, whereas a higher PEG-concentration on the vesicular surface decreases the binding affinity to the phosphate groups significantly (data not shown).

Conclusion

Indicator displacement assays revealed the binding of bis-zinc(II)-cyclen complex **1** or the vesicle embedded amphiphilic complex **4** to phosphate anions in buffered aqueous solution. Contrary, bis-zinc(II)-cyclen derivatives **2** and **3**, which are covalently modified with coumarin or dansyl labels, respectively, show no response to the presence of phosphate anions in homogeneous aqueous solution. Only if the amphiphilic coumarin labeled derivatives **5** and **6** are embedded into vesicular membranes, they show a luminescent response to the presence of phosphate anions. We explain this by the more confined environment of the fluorophore in the membrane if compared to homogeneous solution and the change of this environment and the localization of the fluorophore upon phosphate anion binding. Such membrane embedded luminescent metal complexes responding to the presence of anions have not been reported before and may find applications in sensory surfaces or particles. The binding affinity of all bis-zinc(II)-cyclen complexes towards phosphate anions correlates with the overall charge the steric demand of the anions. The discrimination of low molecular phosphate species by the vesicular receptors is not sufficient for practical analytical applications, but they provide an ideal scaffold for the molecular recognition of biologically important multivalent targets. This is illustrated by their specific interaction with a phosphorylated protein. To suppress non-specific interactions an optimized amount of PEG-modified amphiphiles was used to prepare the functionalized vesicles, which showed a selective response and nanomolar affinity to the phosphorylated protein α -S1-Casein. The simple method of their preparation may allow the development of more complex vesicles responding with even higher affinity and selectivity by the combination of different synthetic receptors into the membrane surface. Our ongoing investigations focus on the preparation of new receptor building blocks and chromophores and the recognition of multivalent ligands by multi-receptor vesicles.

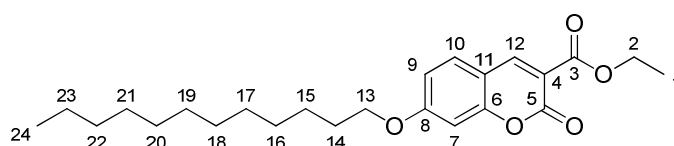
Experimental Part

General methods and material

Fluorescence spectra were recorded on a 'Cary Eclipse' fluorescence spectrophotometer and absorption spectra on a "Cary BIO 50" UV/VIS/NIR spectrometer from Varian. All measurements were performed in 1 cm quartz cuvettes (Hellma) and UV-grade solvents (Baker or Merck) at 25 °C. DLS measurements were carried out on a Malvern Zetasizer 3000 at 25 °C using 1 cm disposable cuvettes (Sarstedt) using automatically optimized settings.

NMR Spectra: Bruker Avance 600 (1H: 600.1 MHz, 13C: 150.1 MHz, T = 300 K), Bruker Avance 400 (1H: 400.1 MHz, 13C: 100.6 MHz, T = 300 K), Bruker Avance 300 (1H: 300.1 MHz, 13C: 75.5 MHz, T = 300 K). The chemical shifts are reported in [ppm] relative to external standards (solvent residual peak). The spectra were analyzed by first order, the coupling constants are given in Hertz [Hz]. Characterization of the signals: s = singlet, d = doublet, t = triplet, q = quartet, m = multiplet, bs = broad singlet, psq = pseudo quintet, dd = double doublet, dt = double triplet, ddd = double double doublet. Integration is determined as the relative number of atoms. Assignment of signals in 13C-spectra was determined with DEPT-technique (pulse angle: 135 °) and given as (+) for CH₃ or CH, (-) for CH₂ and (C_q) for quaternary C_q. Error of reported values: chemical shift: 0.01 ppm for 1H-NMR, 0.1 ppm for 13C-NMR and 0.1 Hz for coupling constants. The solvent used is reported for each spectrum. Mass Spectra: Varian CH-5 (EI), Finnigan MAT 95 (CI; FAB and FD), Finnigan MAT TSQ 7000 (ESI). Xenon serves as the ionization gas for FAB. IR Spectra were recorded with a Bio-Rad FTS 2000 MX FT-IR and Bio-Rad FT-IR FTS 155. Melting Points were determined on Büchi SMP or a Lambda Photometrics OptiMelt MPA 100. Thin layer chromatography (TLC) analyses were performed on silica gel 60 F-254 with 0.2 mm layer thickness and detection via UV light at 254 nm / 366 nm or through staining with ninhydrin in EtOH. Column chromatography was performed on silica gel (70–230 mesh) from Merck. Commercially available starting materials and solvents were used without any further purification except stated otherwise. Optional drying and purification was performed according to accepted general procedures.^{75, 76} Elemental analyses were carried out by the centre for chemical analysis of the Faculty of Chemistry and Pharmacy at the University of Regensburg.

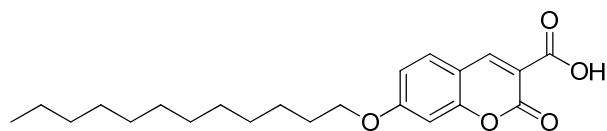
Synthesis



7-Dodecyloxy-2-oxo-2H-chromene-3-carboxylic acid ethyl ester (**8**)

Under nitrogen atmosphere hydroxy-coumarin ethylester **7** (779 mg, 3.3 mmol) was dissolved in dry DMF (12 mL) and K₂CO₃ (2.68 g, 11.6 mmol) was added. Subsequently 1-bromododecane (1.2 mL, 5.0 mmol) was given dropwise to the stirred to suspension. The reaction mixture was stirred over night (20 h) at 80 °C. The reaction progress was monitored by TLC (chloroform). K₂CO₃ was filtered off and the filtrate was concentrated. The crude product was purified by flash column chromatography on flash silica gel (chloroform; R_f = 0.48) yielding compound **8** (537 mg, 1.33 mmol, 40%) as yellow solid. **MP**: 71 °C. – **1H-NMR** (400 MHz; CDCl₃): δ (ppm) = 0.87 (t, ³J = 7.1 Hz, 3 H, COSY: C²⁴H₃), 1.17-1.36 (m, 16 H, COSY: C¹⁶H₂ – C²³H₂), 1.38 (t, ³J = 7.1 Hz, 3 H, COSY: C¹H₃), 1.43-1.51 (m, 2 H, COSY: C¹⁵H₂),

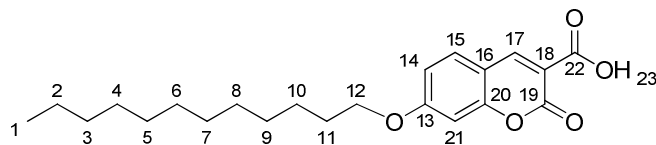
1.81 (quin, 2 H, COSY: C¹⁴H₂), 4.03 (t, ³J = 6.1 Hz, 2 H, COSY: C¹³H₂), 4.39 (q, ³J = 7.1 Hz, 2 H, COSY: C²H₂), 6.78 (d, ³J = 1.9 Hz, 1 H, HMBC: C⁷H), 6.87 (dd, ³J = 1.9 Hz, 8.5 Hz, 1 H, COSY: C¹⁰H), 7.48 (d, ³J = 8.5 Hz, 1 H, COSY: C⁹H), 8.49 (s, 1 H, HMBC: C¹²H). – ¹³C-NMR (100 MHz; CDCl₃): δ (ppm) = 14.1 (+, 1 C, HSQC, COSY: C²⁴H₃), 14.3 (+, 1 C, HSQC, COSY: C¹H₃), 22.6, 29.26, 29.29, 29.47, 29.52, 29.59, 31.9 (–, 8 C, HSQC, COSY: C¹⁶H₂ – C²³H₂), 25.9 (–, 1 C, HSQC, COSY: C¹⁵H₂), 28.8 (–, 1 C, HSQC, COSY: C¹⁴H₂), 61.3 (–, 1 C, HSQC, COSY: C²H₂), 70.0 (–, 1 C, HSQC, COSY: C¹³H₂), 100.8 (+, 1 C, HSQC, HMBC: C⁷H), 114.0 (+, 1 C, HSQC, COSY: C¹⁰H), 130.6 (+, 1 C, HSQC, COSY: C⁹H), 149.0 (+, 1 C, HSQC, HMBC: C¹⁰H), 111.4 (C_q, 1 C, HMBC: C¹¹), 113.9 (C_q, 1 C, HMBC: C⁶), 157.2 (C_q, 1 C, HMBC: C⁵), 157.6 (C_q, 1 C, HMBC: C⁴), 163.5 (C_q, 1 C, HMBC: C³), 164.7 (C_q, 1 C, HMBC: C⁸). – IR (KBr) [cm⁻¹]: $\tilde{\nu}$ = 2918, 2847, 1748, 1693, 1598, 1553, 1469, 1434, 1378, 1301, 1213, 1110, 1027, 793, 722. – UV (CHCl₃): λ_{max} (lg ε) = 352 nm (4.423). – MS (CI (NH₃): m/z (%) = 403.2 (100) [MH⁺], 420.2 (38) [M + NH₄⁺]. – HRMS Calcd for C₂₄H₃₄O₅: 402.2406; Found: 402.2398. – MF: C₂₄H₃₄O₅ – FW: 402.54 g/mol



7-Dodecyloxy-2-oxo-2H-chromene-3-carboxylic acid (**9**)

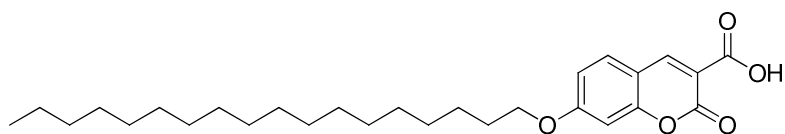
Under nitrogen atmosphere hydroxy-coumarin ethylester **7** (1.3 g, 5.6 mmol) was dissolved in dry DMF and K₂CO₃ (2.7 g, 19.5 mmol) was added. Subsequently 1-ocatedecylamine (2.8 g, 8.4 mmol) was given dropwise to the stirred to suspension. The reaction mixture was stirred over night (20 h) at 60 °C. The reaction progress was monitored by TLC (chloroform). K₂CO₃ was filtered off and the filtrate was concentrated. The crude product was purified by flash column chromatography on flash silica gel (chloroform; R_f = 0.34) yielding compound **9** (1.4 g, 2.8 mmol, 50%) as yellow solid. **MP**: 84 °C. – ¹H-NMR (300 MHz; CDCl₃): δ (ppm) = 0.87 (t, ³J = 6.7 Hz, 3 H, CH₃), 1.12-1.35 (m, 28 H, CH₂), 1.39 (t, ³J = 7.1 Hz, 3 H, CH₃), 1.43-1.54 (m, 2 H, CH₂), 1.81 (quin, 2 H, CH₂), 3.63 (t, ³J = 6.6 Hz, 1.7 H, CH₂), 4.02 (t, ³J = 6.6 Hz, 0.3 H, CH₂), 4.39 (t, ³J = 7.1 Hz, 2 H, CH₂), 6.79 (d, ³J = 2.2 Hz, 1 H, CH), 6.87 (dd, ³J = 2.3 Hz, 8.6 Hz, 1 H, CH), 7.48 (d, ³J = 8.8 Hz, 1 H, CH), 8.49 (s, 1 H, CH). – ¹³C-NMR (75 MHz; CDCl₃): δ (ppm) = 14.1 (+, 1 C, CH₃), 14.3 (+, 1 C, CH₃), 22.7 (–, 1 C, CH₂), 25.8 (–, 0.2 C, CH₂), 25.9 (–, 0.8 C, CH₂), 28.9 (–, 1 C, CH₂), 29.32 (–, 1 C, CH₂), 29.38 (–, 1 C, CH₂), 29.46 (–, 0.2 C, CH₂), 29.54 (–, 0.8 C, CH₂), 29.59 (–, 1 C, CH₂), 29.67, 29.71 (–, 8 C, CH₂), 31.9 (–, 0.9 C, CH₂), 32.8 (–, 0.1 C, CH₂), 61.7 (–, 0.8 C, CH₂), 63.1 (–, 0.2 C, CH₂), 69.0 (–, 1 C, CH₂), 100.8 (+, 1 C, CH), 111.5 (C_q, 1 C), 113.8 (C_q, 1 C), 114.0 (+, 1 C, CH), 130.7 (+, 1 C, CH), 149.1 (+, 1 C, CH), 157.3 (C_q, 1 C), 157.7 (C_q, 1 C), 163.5 (C_q, 1 C), 164.8 (C_q, 1 C). – IR (ATR) [cm⁻¹]: $\tilde{\nu}$ = 2916, 2849, 1746, 1702, 1624, 1510, 1472, 1376, 1228, 1180, 1040, 847, 793, 718. – UV (CHCl₃): λ_{max} (lg ε) = 352 nm (4.246). – MS

(EI): m/z (%) = 486.3 (20) [M^+], 440.4 (12) [$M^+ - EtOH$], 247.0 (50) [$M^+ - C_{17}H_{35}$], 234.0 (100) [$M^+ - C_{18}H_{36}$], 189.0 (90) [$M^+ - C_{18}H_{36} - EtO$]. – **HRMS** Calcd for $C_{30}H_{46}O_5$ 486.3345; Found: 486.3347. – **MF**: $C_{30}H_{46}O_5$ – **FW**: 486.70 g/mol



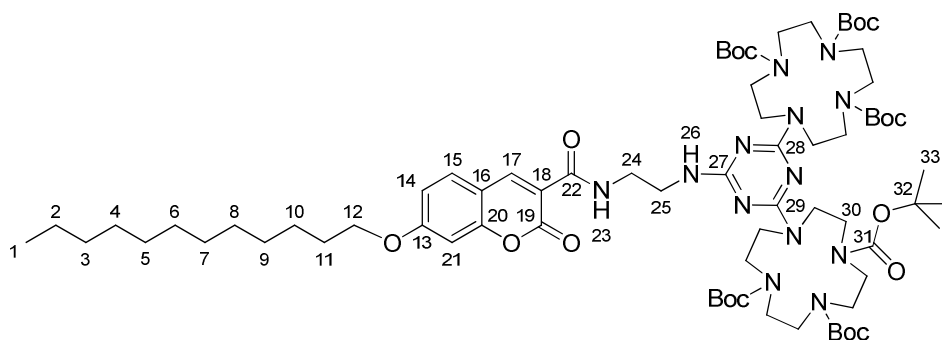
7-Dodecyloxy-2-oxo-2H-chromene-3-carboxylic acid (**10**)

Ethyl ester of compound **8** (386 mg, 0.96 mmol) was dissolved in THF (6.0 mL) and heated to reflux. Subsequently 2 M NaOH (15.4 mL) were added and the solution was refluxed for 5 h. Reaction control was performed by TLC (chloroform). The reaction mixture was cooled to room temperature and further to 0 °C by an ice bath. The yellow solution was acidified with 1 M HCl until a white precipitate was formed which was isolated by filtration and washed with cold water. Compound **10** was obtained as a white solid (360 mg, 0.96 mmol, 100%). **MP**: 126 °C. – **¹H-NMR** (600 MHz; $CDCl_3$): δ (ppm) = 0.87 (t, $^3J = 7.0$ Hz, 3 H, HSQC, COSY: C^1H_3), 1.16-1.33 (m, 14 H, HSQC, COSY: $C^2H_2 - C^8H_2$), 1.33-1.42 (m, 2 H, HSQC, COSY: C^9H_2), 1.47 (quin, $^3J = 7.4$ Hz, 2 H, HSQC, COSY: $C^{10}H_2$), 1.84 (quin, $^3J = 7.6$ Hz, 2 H, HSQC, COSY: $C^{11}H_2$), 4.08 (t, $^3J = 6.5$ Hz, 2 H, HSQC, COSY: $C^{12}H_2$), 6.89 (d, $^4J = 2.0$ Hz, 1 H, HSQC, COSY: $C^{14}H_2$), 6.99 (dd, $^3J = 8.8$ Hz, $^4J = 2.2$ Hz, 1 H, HSQC, COSY: $C^{15}H_2$), 7.62 (d, $^3J = 8.7$ Hz, 1 H, HMBC, HSQC: $C^{21}H_2$), 8.84 (s, 1 H, HMBC, HSQC: $C^{17}H_2$), 12.16 (bs, 1 H, HSQC: COOH²³). – **¹³C-NMR** (150 MHz; $CDCl_3$): δ (ppm) = 14.1 (+, 1 C, HSQC, COSY: C^1H_3), 22.6, 29.29, 29.46, 29.51, 29.58, 29.59, 31.9 (–, 7 C, HMBC, HSQC: $C^2H_2 - C^8H_2$), 25.8 (–, 1 C, HSQC, COSY: $C^{10}H_2$), 28.8 (–, 1 C, HSQC, COSY: $C^{11}H_2$), 29.23 (–, 1 C, HSQC, COSY: C^9H_2), 69.4 (–, 1 C, HSQC, COSY: $C^{12}H_2$), 101.2 (+, 1 C, HSQC, COSY: $C^{14}H$), 110.6 (C_{qr} , 1 C, HMBC, HSQC: C^{18}), 112.1 (C_{qr} , 1 C, HMBC, HSQC: C^{16}), 115.4 (+, 1 C, HSQC, COSY: $C^{15}H$), 131.6 (+, 1 C, HMBC, HSQC: $C^{21}H$), 151.2 (+, 1 C, HMBC, HSQC: $C^{17}H$), 157.1 (C_{qr} , 1 C, HMBC, HSQC: C^{20}), 163.1 (C_{qr} , 1 C, HMBC, HSQC: C^{19}), 164.6 (C_{qr} , 1 C, HMBC, HSQC: C^{22}), 165.9 (C_{qr} , 1 C, HMBC, HSQC: C^{13}). – **IR** (ATR) [cm^{-1}]: $\tilde{\nu} = 2914, 2846, 1734, 1686, 1619, 1560, 1504, 1466, 1429, 1384, 1258, 1217, 1121, 922, 807, 720$. – **UV** ($CHCl_3$): λ_{max} ($\lg \epsilon$) = 277 (4.305), 358 nm (4.418). – **MS** (ESI(–), EE/MeOH + 10 mmol/L NH_4Ac): m/z (%) = 373.1 (100) [$M - H^+$], 329.1 (13) [$M - CO_2$], 747.4 (8) [$2 M - H^+$]. – **HRMS** Calcd for $C_{22}H_{30}O_5$: 374.2093; Found: 374.2088. – **MF**: $C_{22}H_{30}O_5$ – **FW**: 374.48 g/mol



7-Octadecyloxy-2-oxo-2H-chromene-3-carboxylic acid (**11**)

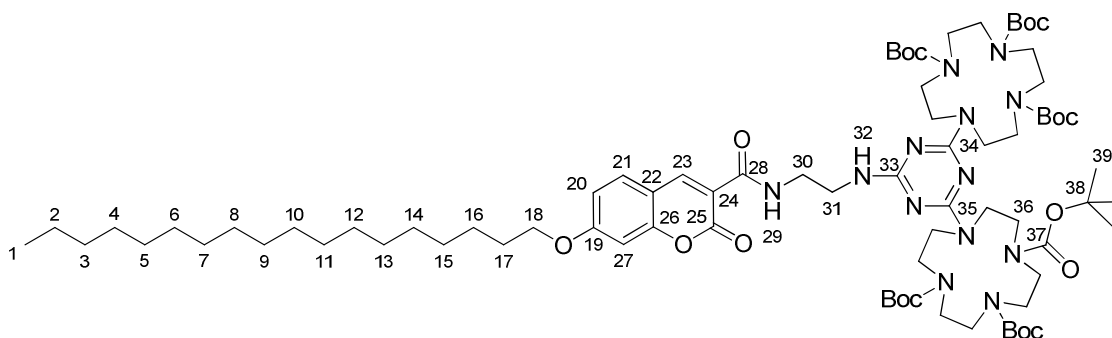
Ethyl ester of compound **9** (297 mg, 0.61 mmol) was dissolved in THF (5.0 mL) and heated to reflux. Subsequently 2 M NaOH (10.3 mL) were added and the solution was refluxed for 4 h. Reaction control was performed by TLC (chloroform). The reaction mixture was cooled to room temperature and further to 0 °C by an ice bath. The yellow solution was acidified with 1 M HCl until a white precipitate was formed which was isolated by filtration and washed with cold water. After drying in vacuum 278 mg (0.61 mmol, 100%) of compound **11** were obtained as a white solid. **MP**: 125 °C. – **¹H-NMR** (300 MHz; CDCl₃): δ (ppm) = 0.86 (t, ³J = 6.7 Hz, 3 H, CH₃), 1.03-1.38 (m, 28 H, CH₂), 1.41-1.58 (m, 2 H, CH₂), 1.68-1.97 (m, 2 H, CH₂), 3.64 (t, ³J = 6.7 Hz, 0.2 H, CH₂), 4.08 (t, ³J = 6.4 Hz, 1.8 H, CH₂), 6.89 (d, ⁴J = 2.5 Hz, 1 H, CH), 6.99 (dd, ³J = 8.8 Hz, ⁴J = 2.5 Hz, 1H, CH), 7.62 (d, ³J = 8.8 Hz, 1 H CH), 8.84 (s, 1 H, CH). – **¹³C-NMR** (75 MHz; CDCl₃): δ (ppm) = 14.1 (+, 1 C, CH₃), 22.7 (–, 1 C, CH₂), 25.9 (–, 1 C, CH₂), 28.8 (–, 1 C, CH₂), 29.3 (–, 1 C, CH₂), 29.4, (–, 1 C, CH₂), 29.53 (–, 1 C, CH₂), 29.58 (–, 1 C, CH₂), 29.67 (–, 2 C, CH₂), 29.71 (–, 6 C, CH₂), 31.9 (–, 1 C, CH₂), 69.4 (–, 1 C, CH₂), 101.2 (+, 1 C, CH), 110.6 (C_q, 1 C), 112.2 (C_q, 1 C), 115.5 (+, 1 C, CH), 131.7 (+, 1 C, CH), 151.3 (+, 1 C, CH), 157.1 (C_q, 1 C), 163.2 (C_q, 1 C), 164.6 (C_q, 1 C), 166.0 (C_q, 1 C). – **IR** (ATR) [cm⁻¹]: $\tilde{\nu}$ = 2915, 2850, 1733, 1686, 1622, 1560, 1505, 1471, 1383, 1256, 1221, 1122, 1005, 820, 798. – **UV** (CHCl₃): λ_{max} (lg ε) = 358 nm (4.009). – **MS** (ESI(+), DCM/MeOH + 10 mmol/L NH₄Ac): m/z (%) = 459.3 (100) [MH⁺], 476.3 (25) [M + NH₄⁺]. – **HRMS** Calcd for C₂₈H₄₂O₅ 458.3032; Found: 458.3026. – **MF**: C₂₈H₄₂O₅ – **FW**: 458.64 g/mol



7-Dodecyloxy-2-oxo-2H-chromene-3-carboxylic acid {2-[4,6-bis-(1,4,7,10 tetraaza-cyclododec-1-yl)-[1,3,5]triazin-2-yl]-ethyl}-1,4,7-tricarboxylic acid tri-tert-butyl ester (**13**)

7-Dodecyloxy-2-oxo-2H-chromene-3-carboxylic acid **10** (200 mg, 0.53 mmol), DIPEA (368 μ L, 2.14 mmol), TBTU (189 mg, 0.59 mmol), and HOBt (90 mg, 0.59 mmol) were dissolved under nitrogen atmosphere in dry DMF/THF (2 mL/4 mL) under ice cooling and stirred for 1 h. Subsequently **12** (635 mg, 0.59 mmol) dissolved in DMF (2 mL) was added dropwise. The reaction was allowed to warm to room temperature and was stirred 30 min at rt and 2.5 h at 40 °C. The reaction progress was monitored by TLC (ethyl acetate/petrol ether). After completion of the reaction the solvent was removed and the crude product was purified by flash column chromatography on flash silica gel (ethyl acetate/petrol ether 1:1; R_f = 0.25) yielding compound **13** (608 mg, 79%) as a lightly yellow solid. **MP**: 113 °C. – **¹H-NMR** (400 MHz; CDCl₃): δ = 0.85 (t, 3J = 6.9 Hz, 3 H, HSQC, COSY: C¹H₃), 1.20-1.33 (m, 18 H, HSQC, COSY: C²H₂ – C¹⁰H₂), 1.41 (s, 18 H, HSQC, COSY: C³³H₃), 1.42 (s, 36 H, HSQC, COSY: C³³H₃), 1.80 (quin, 3J = 7.3 Hz, 2 H, HSQC, COSY: C¹¹H₂), 3.02-3.89 (m, 36 H, HSQC, COSY: C²⁴H₂, C²⁵H₂, C³⁰H₂), 4.02 (t, 3J = 6.5 Hz, 2 H, HSQC, COSY: C¹²H₂), 4.99 (bs, 1 H, HMBC, HSQC: NH²³), 6.81 (d, 4J = 2.2 Hz, 1 H, HMBC, HSQC, COSY: C²¹H₂), 6.90 (dd, 4J = 2.3 Hz, 3J = 8.8 Hz, 1 H, HMBC, HSQC, COSY: C¹⁴H), 7.54 (d, 3J = 8.8 Hz, 1 H, HMBC, HSQC, COSY: C¹⁵H), 8.79 (s, 1 H, HMBC, HSQC: C¹⁷H), 8.87 (m, 1 H, HMBC, HSQC: NH²⁶). – **¹³C-NMR** (100 MHz; CDCl₃): δ = 14.0 (+, 1 C, HSQC, COSY: C¹H₃), 22.6, 25.9, 29.23, 29.26, 29.46, 29.49, 29.55, 29.57, 31.8 (–, 9 C, HSQC, COSY: C²H₂ – C¹⁰H₂), 28.43, 28.47 (+, 18 C, HSQC, COSY: C³³H₃), 28.8 (–, 1 C, HSQC, COSY: C¹¹H₂), 39.8, 40.6 (–, 2 C, HSQC, COSY: C²⁴H₂, C²⁵H₂), 50.2 (–, 16 C, HSQC, COSY: C³⁰H₂), 69.0 (–, 1 C, HMBC, HSQC: C¹²H₂), 79.7 (C_q, 6 C, HMBC, HSQC: C³²), 100.7 (+, 1 C, HMBC, HSQC, COSY: C²¹H), 112.1 (C_q, 1 C, HMBC, HSQC: C¹⁶), 114.35 (+, 1 C, HMBC, HSQC, COSY: C¹⁴H), 114.41 (C_q, 1 C, HMBC, HSQC: C¹⁹), 130.8 (+, 1 C, HMBC, HSQC, COSY: C¹⁵H), 148.3 (+, 1 C, HMBC, HSQC, COSY: C¹⁷H), 156.3 (C_q, 6 C, HMBC, HSQC: C³¹), 156.7 (C_q, 1 C, HMBC, HSQC: C²⁰), 161.7 (C_q, 1 C, HMBC, HSQC: C¹⁸), 162.7 (C_q, 1 C, HMBC, HSQC: C²²), 164.5 (C_q, 1 C, HMBC, HSQC: C¹³), 165.9 (C_q, 3 C, HMBC, HSQC: C²⁷, C²⁸, C²⁹). – **IR** (KBr) [cm⁻¹]: $\tilde{\nu}$ = 2973, 2929, 2878, 1686, 1603, 1535, 1501, 1466, 1408, 1247, 1160, 1026, 971, 858, 776. – **UV** (CHCl₃): λ_{\max} (lg ϵ) = 351 nm (4.336). – **MS**

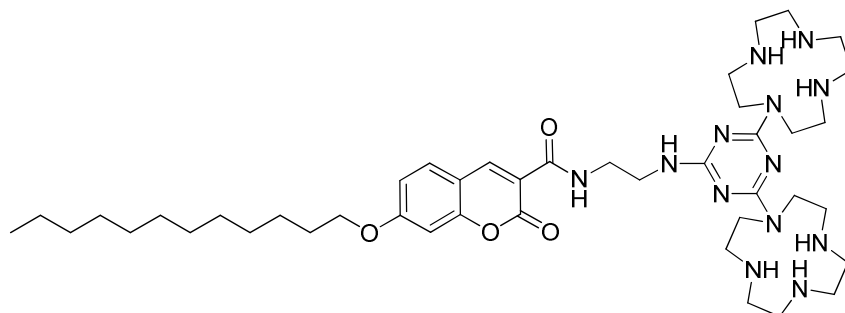
(ESI(+), EE/MeOH + 10 mmol/L NH₄Ac): m/z (%) = 1437.3 (100) [MH⁺], 569.0 (12) [M + 2 H⁺ - 3 Boc]²⁺, 518.9 (20) [M + 2 H⁺ - 4 Boc]²⁺, 468.8 (17) [M + 2 H⁺ - 5 Boc]²⁺, 418.8 (13) [M + 2 H⁺ - 6 Boc]²⁺.



7-Octadecyloxy-2-oxo-2H-chromene-3-carboxylic acid {2-[4,6-bis-(1,4,7,10 tetraaza-cyclododec-1-yl)-[1,3,5]triazin-2-ylamino]-ethyl}-1,4,7-tricarboxylic acid tri-tert-butyl ester (**14**)

7-Octadecyloxy-2-oxo-2H-chromene-3-carboxylic acid **11** (160 mg, 0.35 mmol), DIPEA (360 μ L, 2.09 mmol), TBTU (123 mg, 0.38 mmol), and HOBt (59 mg, 0.38 mmol) were dissolved under nitrogen atmosphere in dry DMF/THF (2 mL / 4 mL) under ice cooling and stirred for 1 h. Subsequently **12** (415 mg, 0.38 mmol) dissolved in DMF (2 mL) was added dropwise. The reaction was allowed to warm to room temperature and was stirred 30 min at rt and 4.5 h at 40 °C. The reaction progress was monitored by TLC (ethyl acetate/petrol ether). After completion of the reaction the solvent was removed and the crude product was purified by flash column chromatography on flash silica gel (ethyl acetate/petrol ether 1:1; R_f = 0.25) yielding compound **14** (375 mg, 71%) as a colourless solid. **MP**: 108 °C. – ¹H-NMR (600 MHz; CDCl₃): δ = 0.86 (t, ³J = 7.2 Hz, 3 H, HSQC, HMBC: C¹H₃), 1.24 (m, 28 H, HSQC, HMBC: C²H₂ – C¹⁵H₂), 1.31-1.64 (m, 56 H, HSQC, HMBC: boc-CH₃, C¹⁶H₂), 1.78-1.83 (m, 2 H, HSQC, HMBC: C¹⁷H₂), 3.00-3.92 (m, 36 H, HSQC, HMBC: cyclen-C³⁶H₂, C³⁰H₂, C³¹H₂), 4.02 (t, ³J = 6.5 Hz, 2 H, HSQC, HMBC: C¹⁸H₂), 5.04 (bs, 1 H, HSQC, HMBC: N³²H), 6.82 (d, ⁴J = 2.3 Hz, 1 H, HSQC, HMBC: C²⁷H), 6.90 (dd, ³J = 8.7 Hz, ⁴J = 2.3 Hz, 1 H, HSQC, HMBC: C²⁰H), 7.55 (d, ³J = 8.7 Hz, 1 H, HSQC, HMBC: C²¹H), 8.79 (s, 1 H, HSQC, HMBC: C²³), 8.88 (m, 1 H, HSQC, HMBC: N²⁹H). – ¹³C-NMR (150 MHz; CDCl₃): δ = 14.1 (+, 1 C, HSQC, HMBC: C¹H₃), 22.6 (–, 1 C), 25.9 (–, 1 C), 29.26 (–, 1 C), 29.30 (–, 1 C), 29.52 (–, 1 C), 29.59 (–, 2 C), 29.61 (–, 1 C), 29.63 (–, 5 C), 31.9 (–, 1 C) HSQC, HMBC: C²H₂ – C¹⁶H₂), 28.4, 28.5 (+, 18 C, HSQC, HMBC: C³⁹H₃), 28.8 (–, 1 C, HSQC, HMBC: C¹⁷H₂), 39.7 (–, 1 C, HSQC, HMBC: C³⁰H₂), 40.6 (–, 1 C, HSQC, HMBC: C³¹H₂), 50.3 (–, 16 C, HSQC, HMBC: C³⁶H₂), 69.0 (–, 1 C, HSQC, HMBC: C¹⁸H₂), 79.7 (C_q, 6 C, HSQC: C³⁷), 100.7 (+, 1 C, HSQC, HMBC: C²⁷H), 112.4 (C_q, 1 C, HSQC, HMBC: C²²), 114.37 (+, 1 C, HSQC, HMBC: C²⁰H), 114.39 (C_q, 1 C, HSQC, HMBC: C²⁴), 130.9 (+, 1 C, HSQC, HMBC: C²¹H), 148.3 (+, 1 C, HSQC,

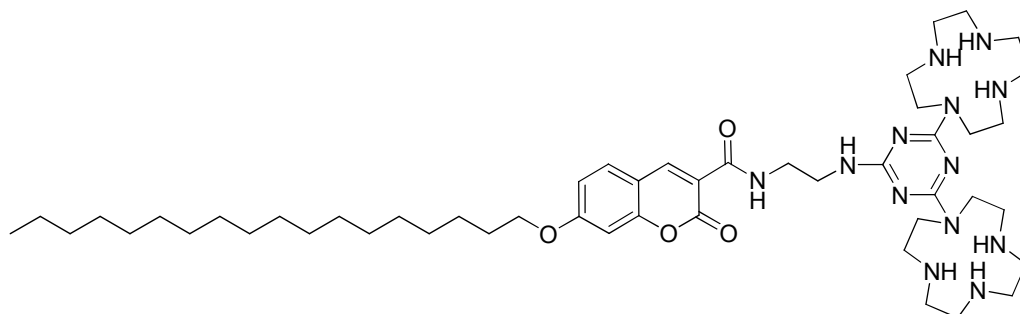
HMBC: C²³H), 156.7 (C_q, 7 C, HSQC, HMBC: C²⁶, C³⁸), 161.7 (C_q, 1 C, HSQC, HMBC: C²⁵), 162.7 (C_q, 1 C, HSQC, HMBC: C²⁸), 164.5 (C_q, 1 C, HSQC, HMBC: C¹⁹), 165.9 (C_q, 3 C, HSQC, HMBC: C³³, C³⁴, C³⁵). – UV (CHCl₃): λ_{max} (lg ε) = 350 nm (4.333). – MS (ESI(+), DCM/MeOH + 10 mmol/L NH₄Ac): m/z (%) = 1521.4 (100) [MH⁺], 769.7 (46) [MH⁺ + NH₄⁺]²⁺, 761.2 [M + 2 H⁺]²⁺.



7-Dodecyloxy-2-oxo-2H-chromene-3-carboxylic acid {2-[4,6-bis-(1,4,7,10 tetraaza-cyclododec-1-yl)-[1,3,5]triazin-2-ylamino]-ethyl}-amide (**15**)

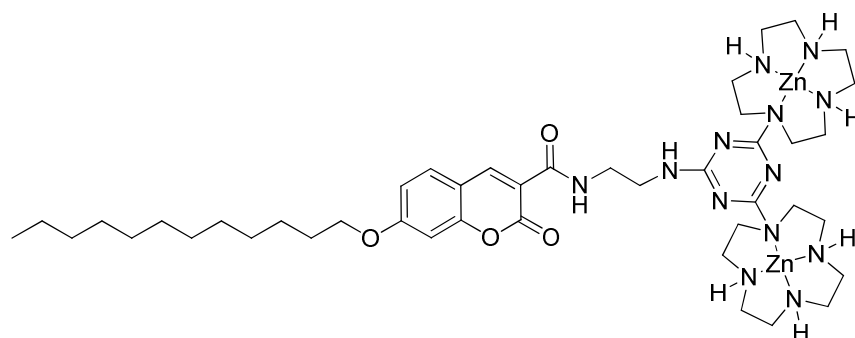
Compound **13** (200 mg, 0.14 mmol) was dissolved in DCM (4 mL) and cooled to 0 °C. Subsequently TFA (901 μL, 11.7 mmol) was added. The solution was stirred 15 min at 0 °C and additionally 20 h at room temperature. The solvent was removed in vacuo, yielding quantitatively the protonated TFA salt of compound **15** as a pale yellow solid. To obtain the free base of compound **15** a weak basic ion exchanger resin was swollen for 15 min in water and washed neutral with water. A column was charged with resin (1.1 g, 40 mmol hydroxy equivalents at a given capacity of 5 mmol/g). The hydrochloride salt was dissolved in water / MeOH (8:2), applied to the column and eluted with water / MeOH (8:2). The elution of the product was controlled by pH indicator paper (pH > 10) and was completed when pH became neutral. The eluate was concentrated and lyophilised to yield 110 mg (93%) of free base **15**, as pale yellow solid. **MP**: 174°C. – ¹H-NMR (400 MHz; CDCl₃): δ = 0.85 (t, ³J = 6.9 Hz, 3 H, CH₃), 1.19-1.37 (m, 16 H, CH₂), 1.39-1.49 (m, 2 H, CH₂), 1.80 (quin, ³J = 7.2 Hz, 2 H, CH₂), 2.82-3.84 (m, 36 H, CH₂), 4.02 (t, ³J = 6.2 Hz, 2 H, CH₂), 6.80 (d, ⁴J = 1.8 Hz, 1 H, CH), 6.93 (dd, ³J = 8.7 Hz, ⁴J = 1.7 Hz, 1 H, CH), 7.02 (bs, 1H, NH), 7.66 (d, ³J = 8.8 Hz, 1 H, CH), 8.73 (s, 1 H, CH), 9.18 (bs, 1 H, NH). – ¹³C-NMR (100 MHz; CDCl₃): δ = 14.0 (+, 1 C, CH₃), 22.6 (–, 1 C, CH₂), 25.9 (–, 1 C, CH₂), 28.8 (–, 1 C, CH₂), 29.27 (–, 2 C, CH₂), 29.46 (–, 1 C, CH₂), 29.51 (–, 1 C, CH₂), 29.56 (–, 2 C, CH₂), 31.8 (–, 1 C, CH₂), 39.2 (–, 1 C, CH₂), 39.3 (–, 1 C, CH₂), 42.5 (–, 1 C, CH₂), 43.3 (–, 2 C, CH₂), 43.7 (–, 1 C, CH₂), 44.8 (–, 4 C, CH₂), 45.8 (–, 4 C, CH₂), 46.9 (–, 4 C, CH₂), 69.1 (–, 1 C, CH₂), 100.8 (+, 1 C, CH), 111.9 (C_q, 1 C), 113.4 (C_q, 1 C), 114.5 (+, 1 C, CH), 131.3 (+, 1 C, CH), 148.5 (+, 1 C, CH), 156.8 (C_q, 1 C), 161.6 (C_q, 1 C), 163.7 (C_q, 1 C), 164.9 (C_q, 1 C), 165.9 (C_q, 1 C), 167.2 (C_q, 1 C), 168.0 (C_q, 1 C). – IR (ATR) [cm⁻¹]: ν̃ = 2926, 2855, 1676, 1597, 1536, 1496, 1418, 1366, 1297, 1198, 1174, 1120, 1017, 795, 719. – UV (CHCl₃): λ_{max} (lg ε) = 352 nm (4.197).

– **LC-MS** (+ c ESI Q1MS): m/z (%) = 418.7.0 (100) $[M + 2 H^+]^{2+}$, 836.6 (10) $[MH^+]$. – **HRMS** Calcd for $C_{43}H_{74}N_{13}O_4$ 836.5987; Found: 836.5960.



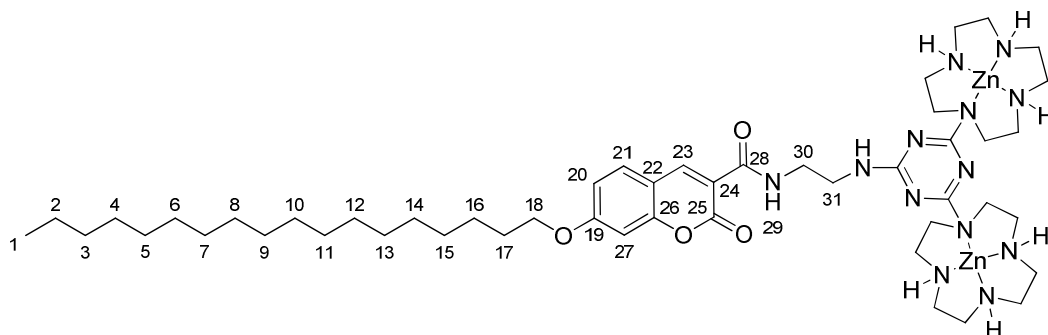
7-Octadecyloxy-2-oxo-2H-chromene-3-carboxylic acid {2-[4,6-bis-(1,4,7,10 tetraaza-cyclododec-1-yl)-[1,3,5]triazin-2-ylamino]-ethyl}-amide (**16**)

Compound **14** (375 mg, 0.26 mmol) was dissolved in DCM (4 mL) and cooled to 0 °C. Subsequently HCl/ether (14 mL) was added. The solution was stirred 15 min at 0 °C and additionally 24 h at room temperature. The solvent was removed in vacuo, yielding quantitatively the protonated HCl salt of compound **16** as a pale yellow solid. To obtain the free base of compound **16** a weak basic ion exchanger resin was swollen for 15 min in water and washed neutral with water. A column was charged with resin (1.9 g, 40 mmol hydroxy equivalents at a given capacity of 5 mmol/g). The hydrochloride salt was dissolved in water / MeCN (5:1), loaded onto the column and eluated with water / MeCN (5:1). The elution of the product was controlled by pH indicator paper (pH > 10) and was completed when pH again was neutral. The eluate was concentrated and lyophilised to yield 200 mg (85%) of free base **16**, as colourless solid. **MP**: 179 °C. – **IR** (ATR) $[cm^{-1}]$: $\tilde{\nu}$ = 3347, 2921, 2850, 1708, 1594, 1538, 1496, 1418, 1362, 1274, 1222, 1142, 1017, 809, 739. – **UV** ($CHCl_3$): λ_{max} (lg ϵ) = 354 nm (4.360). – **LC-MS** (+ c ESI Q1MS): m/z (%) = 460.8 (100) $[M + 2 H^+]^{2+}$, 920.7 (5) $[MH^+]$. – **HRMS** Calcd. for $C_{49}H_{86}N_{13}O_4$ 920.6926; Found: 920.6901. No meaningful NMR data were obtained most likely due to slow molecular motion of parts of the molecule on the NMR timescale.



Binuclear Zn(II)-cyclen-coumarin- C_{12} (**6**)

A solution of compound **15** (50 mg, 60 μ mol) in MeOH (1 mL) was heated to 65 °C and subsequently a methanolic solution of $Zn(ClO_4)_2$ (0.1 M, 1.2 mL, 120 μ mol) was added dropwise. After stirring the reaction mixture for 20 h at 65 °C, the methanol was removed in vacuo. The residue was dissolved in water and was lyophilized yielding complex **5** as a colourless solid in quantitative yield (82 mg). **MP**: 232 °C. – **IR** (ATR) [cm^{-1}]: $\tilde{\nu}$ = 3537, 3303, 2929, 2854, 1702, 1599, 1546, 1424, 1347, 1283, 1224, 1058, 964, 848. – **UV** ($CHCl_3$): λ_{max} (lg ϵ) = 353 nm (3.740). – **MS** (ESI(+), DCM/MeOH + 10 mmol/L NH_4Ac): m/z (%) = 540.9 (100) [$M^{4+} + 2 CH_3COO^-$] $^{2+}$, 561.9 (26) [$M^{4+} + ClO_4^- + CH_3COO^-$] $^{2+}$, 510.9 (20) [$M^{4+} - H^+ + CH_3COO^-$] $^{2+}$.



Binuclear Zn(II)-cyclen-coumarin- C_{18} (**5**)

Compound **16** (100 mg, 0.11 mmol) was dissolved in 5 mL of water and heated to 65 °C yielding a clear yellow solution. Subsequently zinc(II)-perchlorate (81 mg, 0.22 mmol) dissolved in 5 ml of water was added slowly to the stirred reaction mixture, which was stirred for additional 24 h at 65 °C. The solvent was removed in vacuo and the residue was redissolved in water and lyophilized to yield 158 mg (quantitative) of **6** as a lightly yellow solid. **MP**: 209 °C. – **1H -NMR** (600 MHz; $CDCl_3$ / CD_3CN 1:1): δ = 0.86 (t, 3J = 7.1 Hz, 3 H, HSQC, HMBC: C^1H_3), 1.20-1.31 (m, 26 H, HSQC, HMBC: $C^2H_2 - C^{14}H_2$), 1.31-1.37 (m, 2 H, HSQC, HMBC, ROESY: $C^{15}H_2$), 1.41-1.46 (2 H, HSQC, HMBC, ROESY: $C^{16}H_2$), 1.73-1.80 (m, 2 H, HSQC, HMBC, ROESY: $C^{17}H_2$), 2.51-3.57 (m, 36 H, HSQC, HMBC: cyclen- CH_2 , $C^{30}H_2$, $C^{31}H_2$), 4.06 (t, 3J = 6.5 Hz, 2 H, HSQC, HMBC: $C^{18}H_2$), 6.11 (s, 1 H, HSQC, ROESY: cyclen-NH), 6.20 (s, 1 H, HSQC, ROESY:

cyclen-NH), 6.29 (s, 1 H, HSQC, ROESY: cyclen-NH), 6.44 (s, 1 H, HSQC, ROESY: cyclen-NH), 6.87 (d, $^4J = 2.2$ Hz, 1 H, HSQC, HMBC, ROESY: C²⁷H), 6.95 (dd, $^3J = 8.7$ Hz, $^4J = 2.3$ Hz, 1 H, HSQC, HMBC, ROESY: C²⁰H), 7.74 (d, $^3J = 8.7$ Hz, 1 H, HSQC, HMBC, ROESY: C²¹H), 8.85 (s, 1 H, HSQC, HMBC, ROESY: C²³H), 9.22 (m, 1 H, HSQC, ROESY: NH²⁹). – ¹³C-NMR (150 MHz; CDCl₃ / CD₃CN 1:1): $\delta = 14.3$ (+, 1 C, HSQC, HMBC: C¹H₃), 26.3 (–, 1 C, HSQC, HMBC, ROESY: C¹⁶H₂), 23.1, 29.7, 29.94, 29.97, 30.1, 32.3 (–, 13 C, HSQC, HMBC: C²H₂ – C¹⁴H₂), 29.3 (–, 1 C, HSQC, HMBC, ROESY: C¹⁷H₂), 29.75 (–, 1 C, HSQC, HMBC: C¹⁵H₂), 39.9, 42.6, 44.3, 45.8, 45.9, 46.3, 46.9 3 (–, 18 C, HSQC, HMBC, ROESY: cyclen-CH₂, C³⁰H₂, C³¹H₂), 69.8 (–, 1 C, HSQC, HMBC, ROESY: C¹⁸H₂), 101.4 (+, 1 C, HSQC, HMBC, ROESY: C²⁷H), 112.8 (C_q, 1 C, HSQC, HMBC: C²²), 113.8 (C_q, 1 C, HSQC, HMBC: C²⁴), 115.1 (+, 1 C, HSQC, HMBC, ROESY: C²⁰H), 132.3 (+, 1 C, HSQC, HMBC, ROESY: C²¹H), 149.8 (+, 1 C, HSQC, HMBC, ROESY: C²³H), 157.5 (C_q, 1 C, HSQC, HMBC: C²⁶), 162.1 (C_q, 1 C, HSQC, HMBC: C²⁵), 164.8 (C_q, 1 C, HSQC, HMBC: C²⁸), 165.6 (C_q, 1 C, HSQC, HMBC: C¹⁹). – IR (ATR) [cm⁻¹]: $\tilde{\nu} = 3355, 2919, 2851, 1705, 1655, 1612, 1534, 1426, 1276, 1225, 1051, 926$. – UV (CHCl₃): λ_{\max} (lg ϵ) = 355 nm (3.523). – MS (ESI(+), EE/MeOH + 10 mmol/L NH₄Ac): m/z (%) = 583.0 (100) [M⁴⁺ + 2 CH₃COO]²⁺.

Vesicle preparation and characterization

In a small round-bottom flask 2 - 12 mg (2.5 - 15 μ mol) of DSPC were dissolved in 5 - 10 mL of chloroform and 10 mol% of the respective amphiphilic receptors were added. After warming to 75 °C under vigorous shaking, the solvent was slowly removed under reduced pressure to yield a thin lipid film. Traces of solvent were removed by high vacuum. An appropriate amount of buffer (HEPES 25 mM, pH 7.4) was added to obtain lipid concentrations of 1.5 – 2.5 mM and heating to 75 °C for 15-30 min yielded a turbid MLV-suspension. SUV-dispersions were obtained by extrusion through 100 nm-pore size polycarbonate membranes with a LiposoFast liposome extruder from Avestin.^{47, 77}

Vesicle dispersions were separated from low molecular weight solutes on minicolumns of Sephadex LH-20 gel filtration media as described in literature.⁵²

Vesicle	Molar composition	Size	λ_{ex}	λ_{em}
VR-4	DSPC/4 10:1	80 \pm 5 nm	-	-
VR-5	DSPC/5 10:1	95 \pm 5 nm	349 nm	406 nm
VR-6	DSPC/6 10:1	95 \pm 5 nm	349 nm	406 nm
VR-6P	DSPC/DSPC-PEG350/ 6 5.6:4.4:1	100 \pm 5 nm	349 nm	406 nm

Table 2. Vesicle compositions, size distribution and emission properties.

Binding studies

All titrations were carried out at 25 °C in HEPES buffer (25 mM, pH 7.4) and corrected for dilution. Data analysis was performed with Origin 8 software.

Receptor concentration on vesicle surface

For all binding studies the concentration of vesicular receptors refers to the outer surface exposed binding units according to Equation 1.

$$f = \frac{\sigma_o}{\sigma_o + \sigma_i}$$

Equation 1. Correction factor f for surface exposed receptor molecules as a fraction of its entire quantity of matter.

The ratio of outer surface (σ_o) and inner (σ_i) surface of the respective vesicles was calculated using the hydrodynamic diameters obtained from dynamic light scattering and the assumption that the bilayer thickness for the prepared vesicles generally amounts to 5 nm.^{78, 79}

Indicator displacement assays (IDA)

Evaluation of the indicator binding towards receptors **1** and **VR-4** was performed by utilizing Hill plots, whereas for the subsequent displacement titrations a competitive binding model was used.⁸⁰ For all titrations the initial indicator concentration was 3.5×10^{-5} M for PV and 5.0×10^{-7} M for CMS. After each addition, the cuvette was shaken for 1 minute before the absorption (PV: $\lambda_{\max} = 636$ nm) or fluorescence spectrum (CMS: $\lambda_{\text{ex}} = 396$ nm, $\lambda_{\text{em}} = 480$ nm) was recorded.

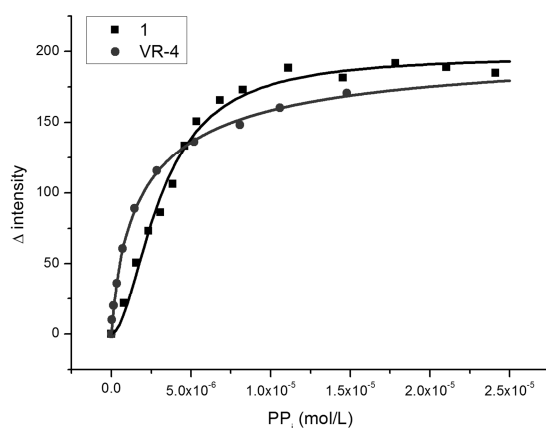


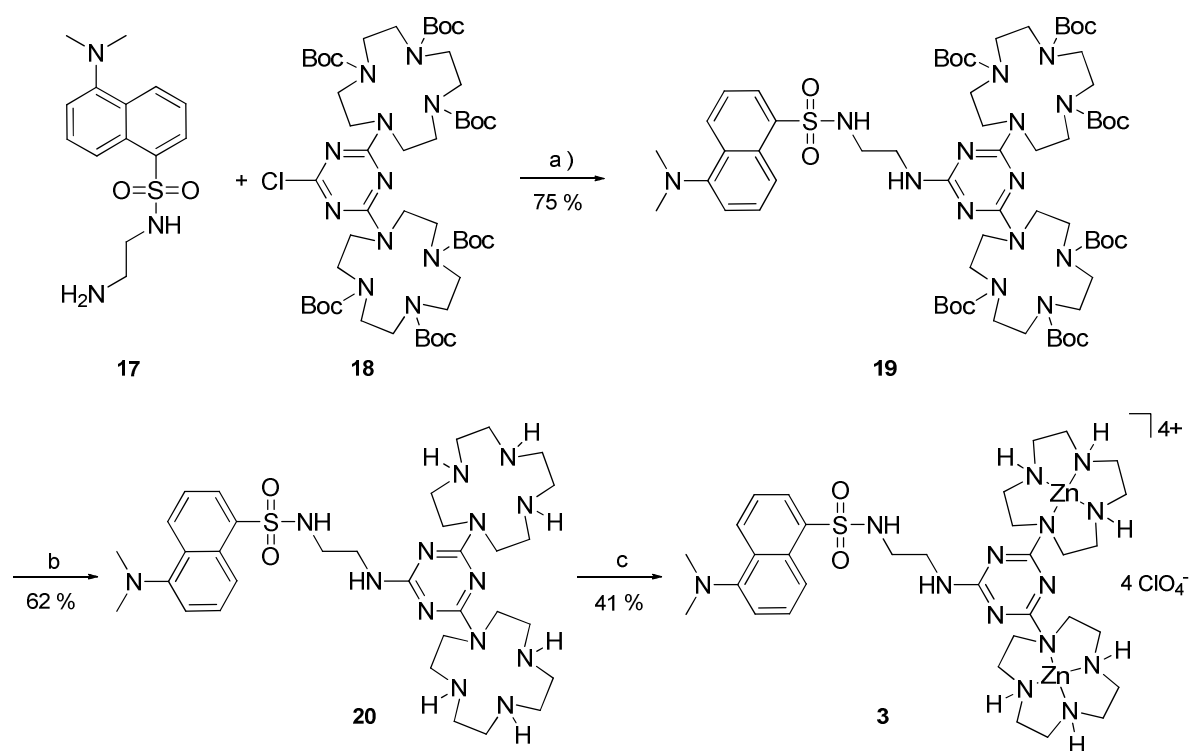
Figure 5. Comparison of binding isotherms obtained by indirect IDA methods of **1** and **VR-4** to PP_i .

Vesicular receptor binding monitored by direct emission

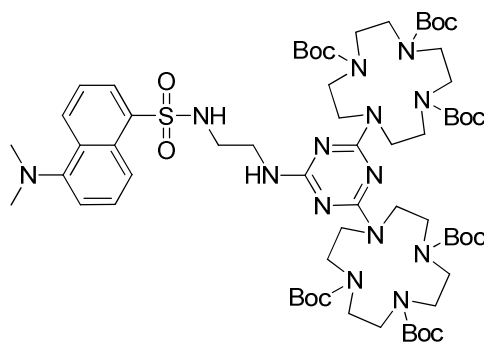
Evaluation of phosphate binding towards the vesicular receptors **VR-5** and **VR-6** was performed by plotting Δ emission values against the analyte concentration and employing non-linear curve fitting using the Hill equation. The initial concentration of vesicular receptors for all titrations was 5.0×10^{-7} M, after each analyte addition, the cuvette was shaken for 1 minute before the fluorescence spectrum ($\lambda_{\text{ex}} = 348$ nm, $\lambda_{\text{em}} = 406$ nm) was recorded.

Supporting Information

Synthesis and characterization of compound 3

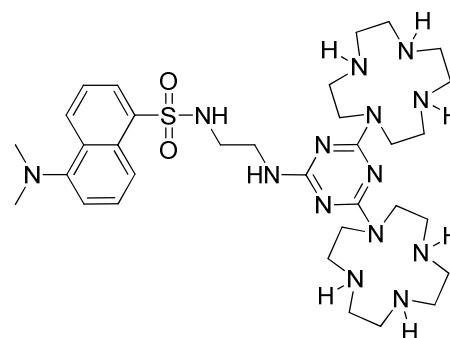


Scheme S1. Synthesis of fluorescent bis-Zn(II) cyclen complex **3**. (a) 5-Dimethylamino-naphthalene-1-sulfonic acid (2-amino-ethyl)-amide **17**, K_2CO_3 , dioxane, reflux, 72 h; (b) TFA, DCM RT 12 h, basic ion exchanger resin; (c) $\text{Zn}(\text{ClO}_4)_2$, H_2O , 65 °C.



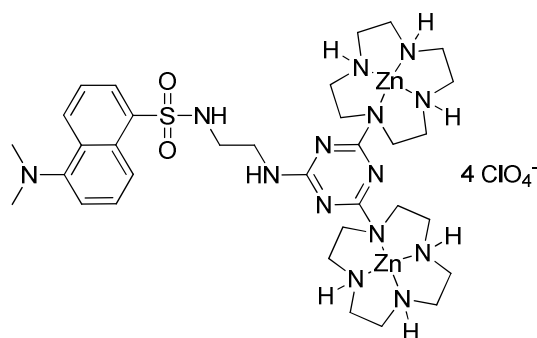
5-Dimethylamino-naphthalene-1-sulfonic acid {2-[4,6-bis-(1,4,7,10-tetraaza-cyclododec-1-yl)-[1,3,5]triazin-2-ylamino]-ethyl}-1,4,7-tricarboxylic acid tri-tert-butyl ester (**19**)

A solution of **18** (0.89 g, 0.84 mmol) in 25 mL of dioxane was stirred under nitrogen for 5 min, then a solution of 5-dimethylamino-naphthalene-1-sulfonic acid (2-amino-ethyl)-amide **17** (0.62 g, 2.1 mmol) in dioxane (75 mL) was added dropwise and K_2CO_3 (0.58 g, 4.2 mmol, 5 eq.) was added. The mixture was refluxed for 72 h at 140 °C under nitrogen atmosphere. After completion, all inorganic salts were filtered off, the solvent was removed under reduced pressure and the crude product was purified by column chromatography on neutral alumina (EE/PE 3:7 to 2:3). Compound **19** was obtained as a yellow solid (0.82 g, 75%). **MP**: 113 °C (sublimation). – **¹H-NMR** (400 MHz; $CDCl_3$): δ = 1.41 (bs, 54 H, CH_3 -Boc), 2.86 (s, 6 H, CH_3N), 3.10-3.68 (m, 36 H, CH_2 chain and CH_2 cyclen), 4.77 (bs, 1 H, $NHSO_2$), 6.95 (bs, 1 H, NH-triazine), 7.13 (d, 1 H, 3J = 7.6 Hz, CH), 7.47 (dd, 1 H, 3J = 7.6, 8.7 Hz, CH), 7.48 (dd, 1 H, 3J = 7.3, 8.5 Hz, CH), 8.21 (d, 1 H, 3J = 7.3 Hz, CH), 8.36 (d, 1 H, 2J = 8.7 Hz, CH), 8.5 (d, 1 H, 2J = 8.5 Hz, CH). – **¹³C-NMR** (400 MHz; $CDCl_3$): δ = 28.5 (+, CH_3 -Boc), 41.8 (–, CH_2NHSO_2), 43.6 (–, CH_2NH -triazine), 45.4 (+, $(CH_3)_2N$), 50.09, 50.16, 50.25, 50.29 (–, CH_2 cyclen), 79.78, 80.1, 80.3 (C_q , Boc), 115.0, 123.1, 127.78, 127.82, 129.8, 129.8, 129.9, 129.9 (+, CH); 135.08 (C_q , Cq- SO_2), 151.7 (C_q , Cq-N- $(CH_3)_2$), 156.2 (C_q , Boc), 165.8 (C_q , triazine). – **IR** (KBr) [cm^{-1}]: $\tilde{\nu}$ = 3267, 2975, 2933, 2361, 2200, 1686, 1541, 1499, 1474, 1410, 1366, 1321, 1249, 1163, 1106, 1050, 970, 946, 858, 777. – **UV** (CH_2Cl_2): λ_{max} ($\lg \epsilon$) = 340 nm (3.655). – **MS** (ESI, DCM/MeOH + 10 mmol/l NH_4Ac): m/z (%) = 1313.9 (100) [MH]⁺. – $C_{63}H_{104}N_{14}O_{14}S$ (1313.66 g/mol): calcd.: C 57.59, H 7.98, N 14.93; found: C 57.22, H 8.11, N 14.66.

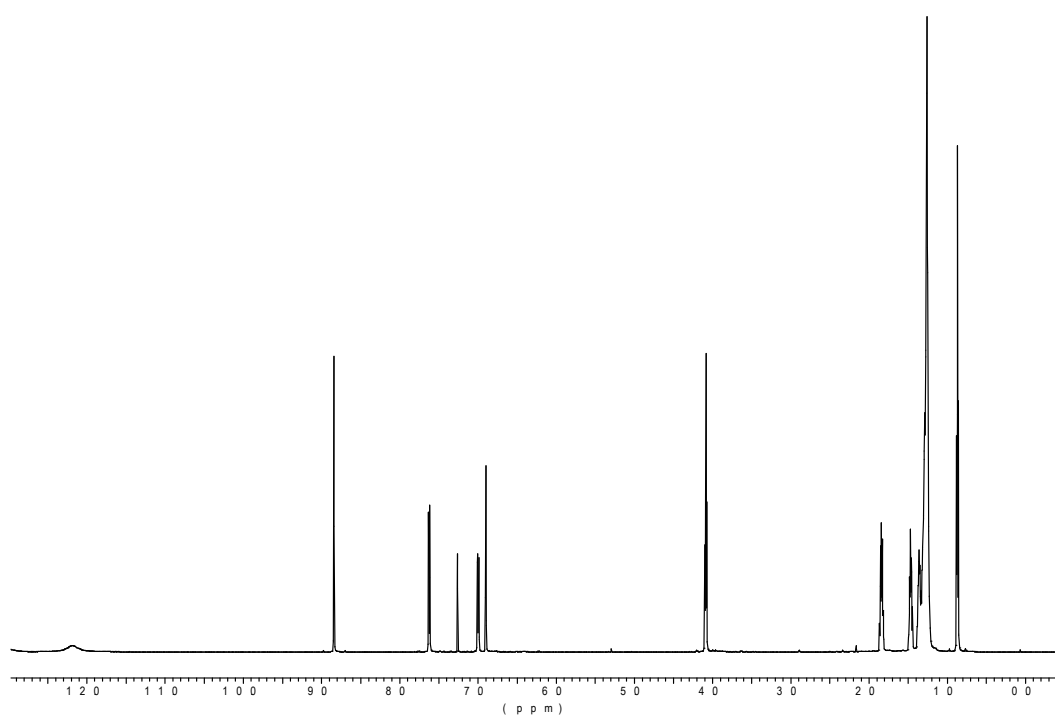
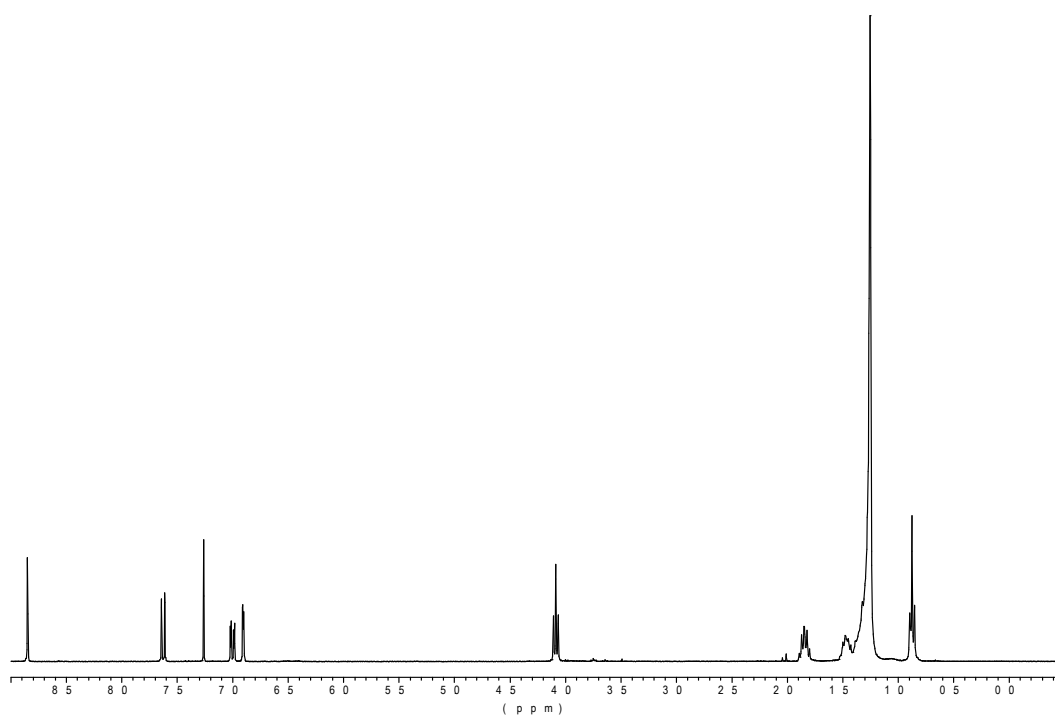


5-Dimethylamino-naphthalene-1-sulfonic acid {2-[4,6-bis-(1,4,7,10-tetraaza-cyclododec-1-yl)-[1,3,5]triazin-2-ylamino]-ethyl}-amide (**20**)

A solution of **19** (0.77 g, 0.59 mmol) in CH_2Cl_2 was treated with TFA (3.6 mL, 47 mmol) and the reaction mixture was stirred for 24 h. After completion of the reaction the solvent was removed under reduced pressure, the obtained pale yellow solid (quantitative yield) was dissolved in water and passed through a column of pre-swelled (pH = 7) basic ion exchanger resin. The fractions having a basic pH were collected and the resulting aqueous solution was lyophilised. The product was obtained as a yellow solid (0.26 g, 62%). **MP**: 92 °C. – **$^1\text{H NMR}$** (300 MHz; MeOD): δ = 2.62 (bs, 8 H, CH_2 cyclen), 2.70 (bs, 8 H, CH_2 cyclen), 2.87 (s, 14 H, $(\text{CH}_3)_2\text{N}$ and CH_2 cyclen), 3.00 (t, 2 H, $^3J = 6.0$ Hz, CH_2NH -triazine), 3.32 (t, 2 H, $^3J = 6.0$ Hz, CH_2NHSO_2), 3.7 (bs, 8 H, CH_2 cyclen), 7.23 (d, 1 H, $^3J = 7.6$ Hz, CH), 7.50 (dd, 1 H, $^3J = 7.6, 8.6$ Hz, CH), 7.55 (dd, 1 H, $^3J = 7.3, 8.5$ Hz, CH), 8.17 (d, 1 H, $^3J = 7.3$ Hz, CH), 8.26 (d, 1 H, $^3J = 8.6$ Hz, CH), 8.53 (d, 1 H, $^3J = 8.5$ Hz, CH). – **$^{13}\text{C NMR}$** (300 MHz; MeOD): δ = 41.2 (–, CH_2NHSO_2), 44.5 (–, CH_2NH -triazine), 45.8 (–, $(\text{CH}_3)_2\text{N}$), 46.9, 48.6, 48.7, 48.9 (–, CH_2 cyclen), 116.28 (+, CH), 120.4 (+, CH), 124.2 (+, CH), 129.0 (+, CH), 130.1 (+, CH), 131.0 (C_q), 131.1 (+, CH), 131.2 (C_q), 136.9 (C_q , $\text{C}_q\text{-SO}_2$), 153.2 (C_q , $\text{C}_q\text{-N}(\text{CH}_3)_2$), 167.2 (C_q , C_q -triazine cyclen), 168.0 (C_q , C_q -triazine NH). – **IR** (KBr) [cm^{-1}]: $\tilde{\nu}$ = 3397, 2938, 2840, 2361, 2200, 1542, 1497, 1416, 1362, 1294, 1142, 1063, 940, 792, 625, 572. – **UV** (CH_2Cl_2): λ_{max} ($\lg \epsilon$) = 336 nm (3.766). – **MS** (ESI, TFA/ $\text{AcN}/\text{H}_2\text{O}$): m/z (%): 357.4 (100) [$\text{M} + 2 \text{H}^+$] $^{2+}$, 713.6 (20) [MH] $^+$. – **HRMS** Calcd for $\text{C}_{33}\text{H}_{56}\text{N}_{14}\text{O}_2\text{S}$: 712.4331; found: 712.4421.

Bis-Zn(II)-cyclen dansyl (**3**)

Compound **20** (120 mg, 0.17 mmol) was dissolved in 1 mL of water and heated to 65 °C to give a clear yellow solution. Subsequently zinc(II)-perchlorate (64 mg, 172 μmol) dissolved in 1 ml of water was added slowly. The pH was adjusted by addition of 1 M NaOH (approx. 2 mL) to pH 7. The reaction mixture was stirred for additional 23 h at 70 °C. The solvent was removed in vacuo and the residue was redissolved in water and lyophilized. The crude product (200 mg) was recrystallized from an EtOH / H₂O (4:1) mixture as a yellow solid (89 mg, 41%). **MP**: 180-182°C. – **¹H NMR** (300 MHz; CD₃CN): δ = 2.65-2.90 (m, 18 H, CH₂ cyclen, (CH₃)₂N), 2.94-3.15 (m, 14 H, CH₂ cyclen, CH₂NHSO₂), 3.23-3.46 (m, 6 H, CH₂ cyclen, CH₂NH-triazine), 4.24-4.44 (m, 4 H, CH₂ cyclen), 6.11 (m, 1 H, NH-triazine), 7.23 (d, 1 H, ³J = 7.4 Hz, CH), 7.53 (dd, 1 H, ³J = 7.4, 8.8 Hz, CH), 7.57 (dd, 1 H, ³J = 7.4, 8.2 Hz, CH), 8.15 (d, 1 H, ³J = 7.4 Hz, CH), 8.18 (d, 1 H, ³J = 8.8 Hz, CH), 8.51 (d, 1 H, ³J = 8.2 Hz, CH). – **¹³C NMR** (300 MHz; CD₃CN): δ = 41.9 (–, CH₂NH-triazine), 43.0 (–, CH₂NHSO₂), 44.4 (+, (CH₃)₂N), 45.3, 45.8, 46.1, 46.4 (–, CH₂ cyclen), 114.8, 118.3, 123.1, 127.9, 128.6, 128.9, 129.3, 129.9 (+, CH), 135.0 (C_q, C_q-SO₂), 151.7 (C_q, C_q-N-(CH₃)₂), 165.5 (C_q, C_q-triazine). – **IR** (KBr) [cm⁻¹]: $\tilde{\nu}$ = 3427, 3283, 2931, 2361, 2200, 1636, 1560, 1419, 1346, 1312, 1143, 1110, 1090, 979, 795, 627, 575. – **UV** (HEPES pH 7.4, 25 mM): λ_{ex} (lg ε) = 330 nm (3.575), 227 (4.637). – **MS** (ESI(+), H₂O/MeOH + 10 mmol/L NH₄Ac): m/z (%) = 479.1 (100) [M⁴⁺ + 2 CH₃COO]²⁺, 449.1 (82) [M⁴⁺ – H⁺ + CH₃COO]²⁺, 420.1 (20) [M⁴⁺ – 2 H⁺]²⁺. – C₃₃H₅₆N₁₄O₁₈SCl₄Zn₂ · EtOH (1241.52 g/mol): Calcd.: C 32.65, H 4.85, N 15.23; found: C 32.52, H 4.87, N 15.04.

^1H -NMR spectra of selected compounds**Figure S1.** Compound **10** (600 MHz; CDCl_3).**Figure S2.** Compound **11** (300 MHz; CDCl_3).

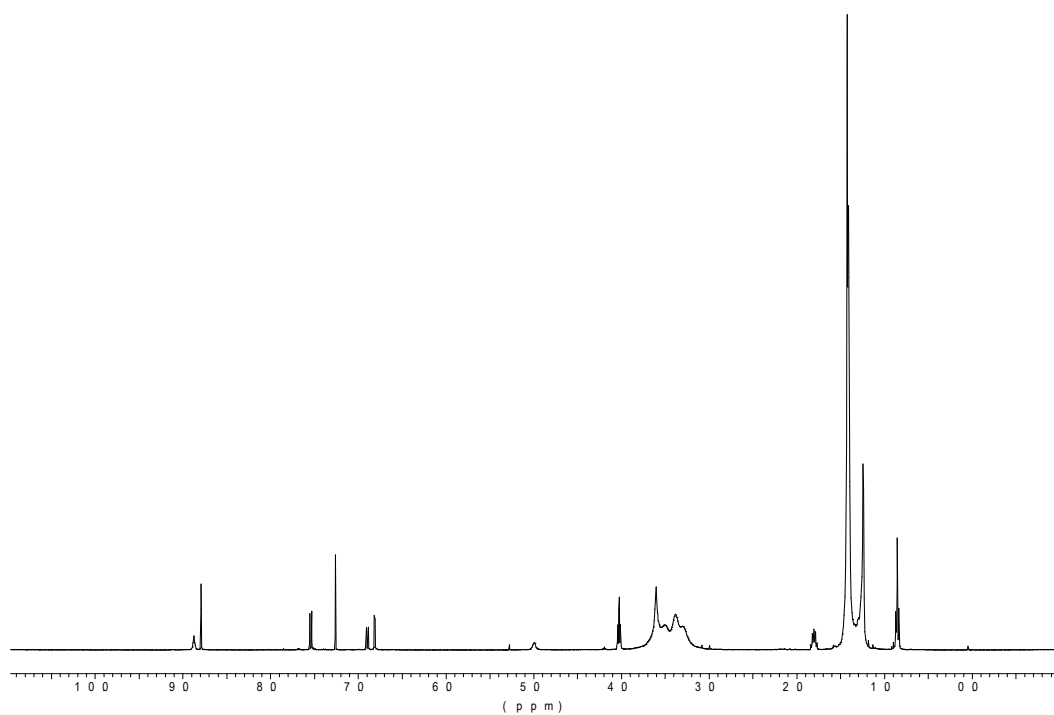


Figure S3. Compound **13** (400 MHz; CDCl_3).

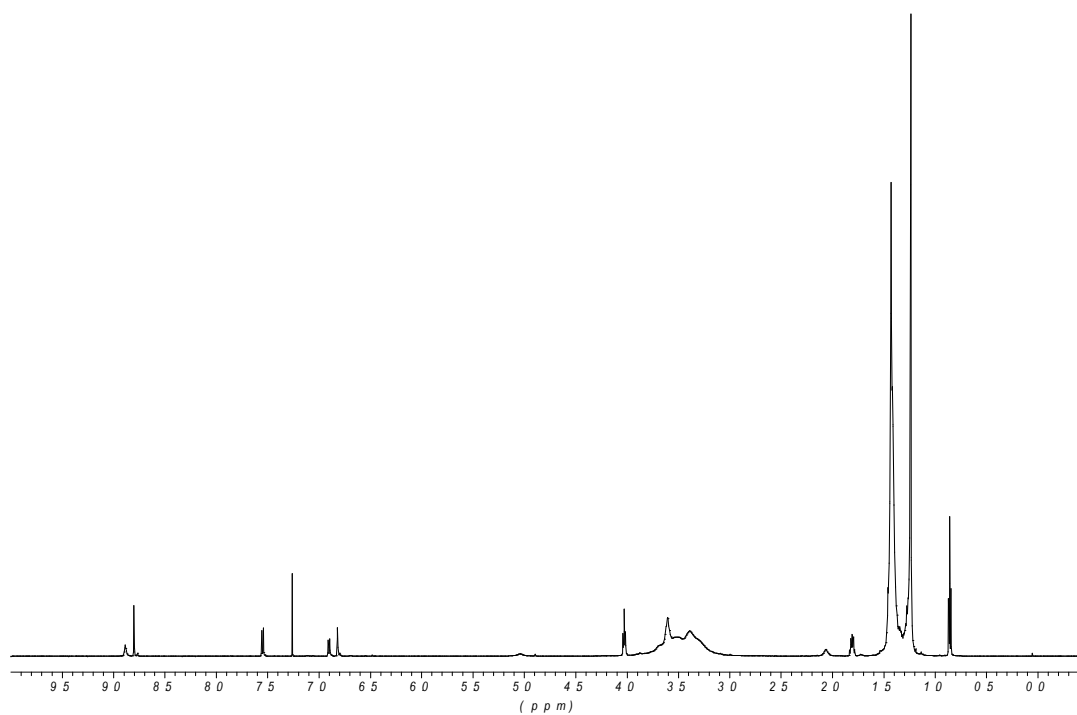


Figure S4. Compound **14** (600 MHz; CDCl_3).

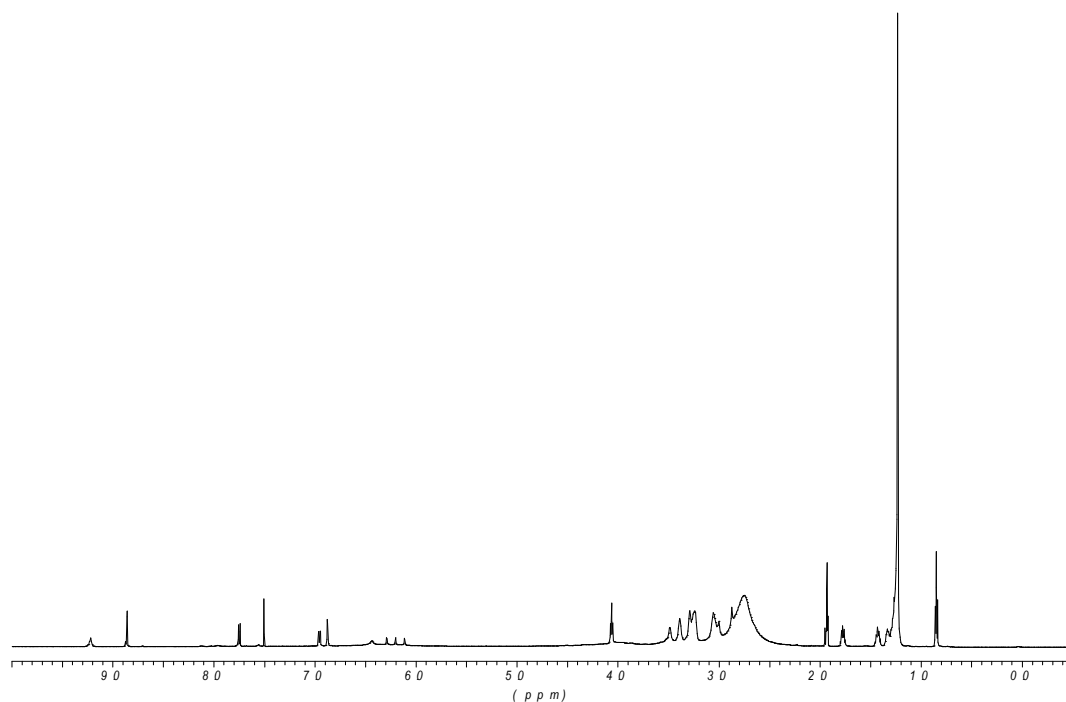


Figure S5. Compound **5** (600 MHz; CDCl_3 / MeOH 1:1).

Hydrolytic stability of ATP under assay conditions

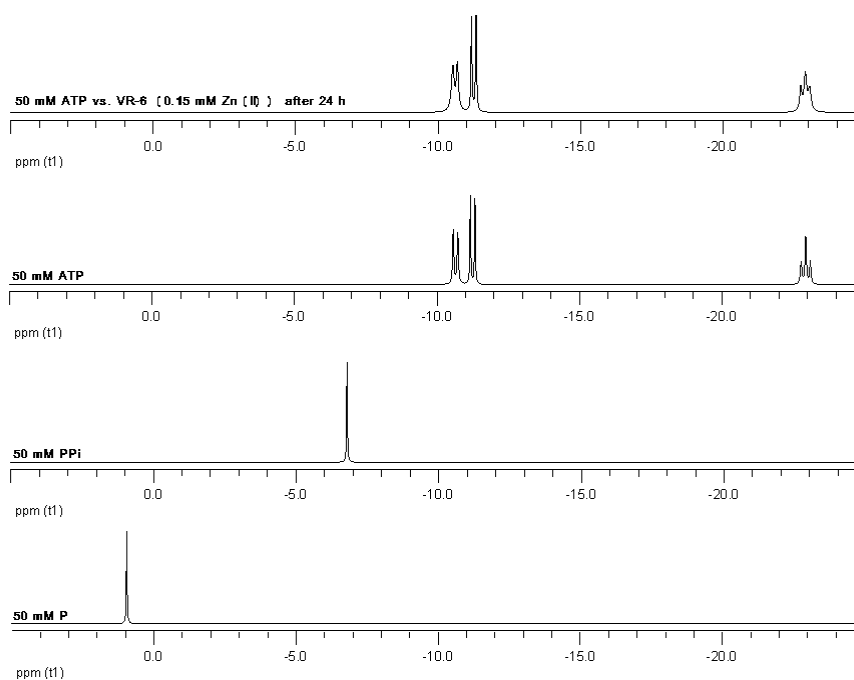


Figure S6. ^{31}P -NMR spectrum of ATP (50 mM) in the presence of **VR-6** (0.15 mM $[\text{Zn}^{2+}]$) after 24 hours. ^{31}P -NMR spectra of ATP, pyrophosphate and inorganic phosphate are included for comparison. All samples were measured in HEPES buffer (pH 7.4) with 10% D_2O .

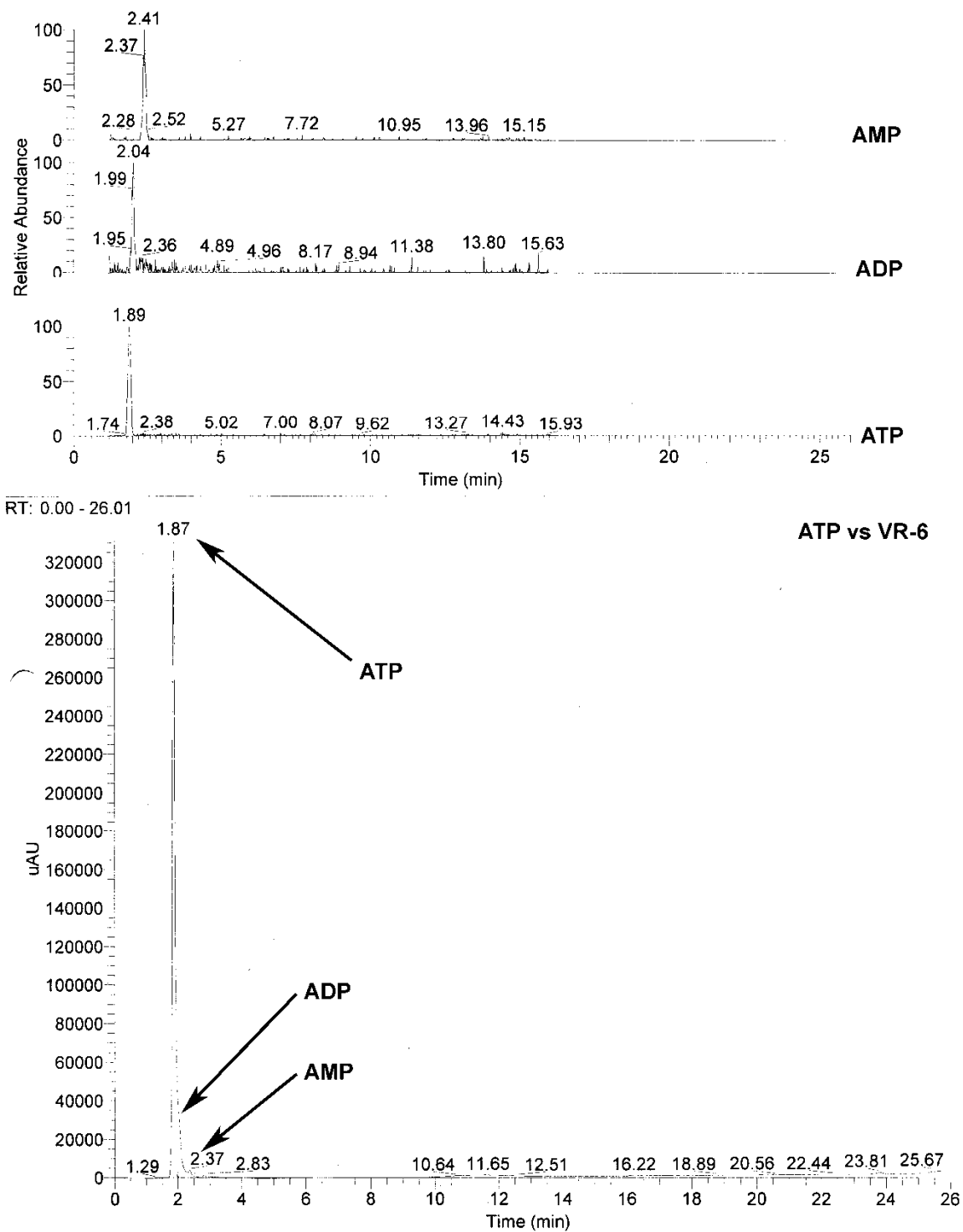


Figure S7. LC-MS chromatograms for AMP, ADP, ATP and ATP sample incubated with **VR-6**.

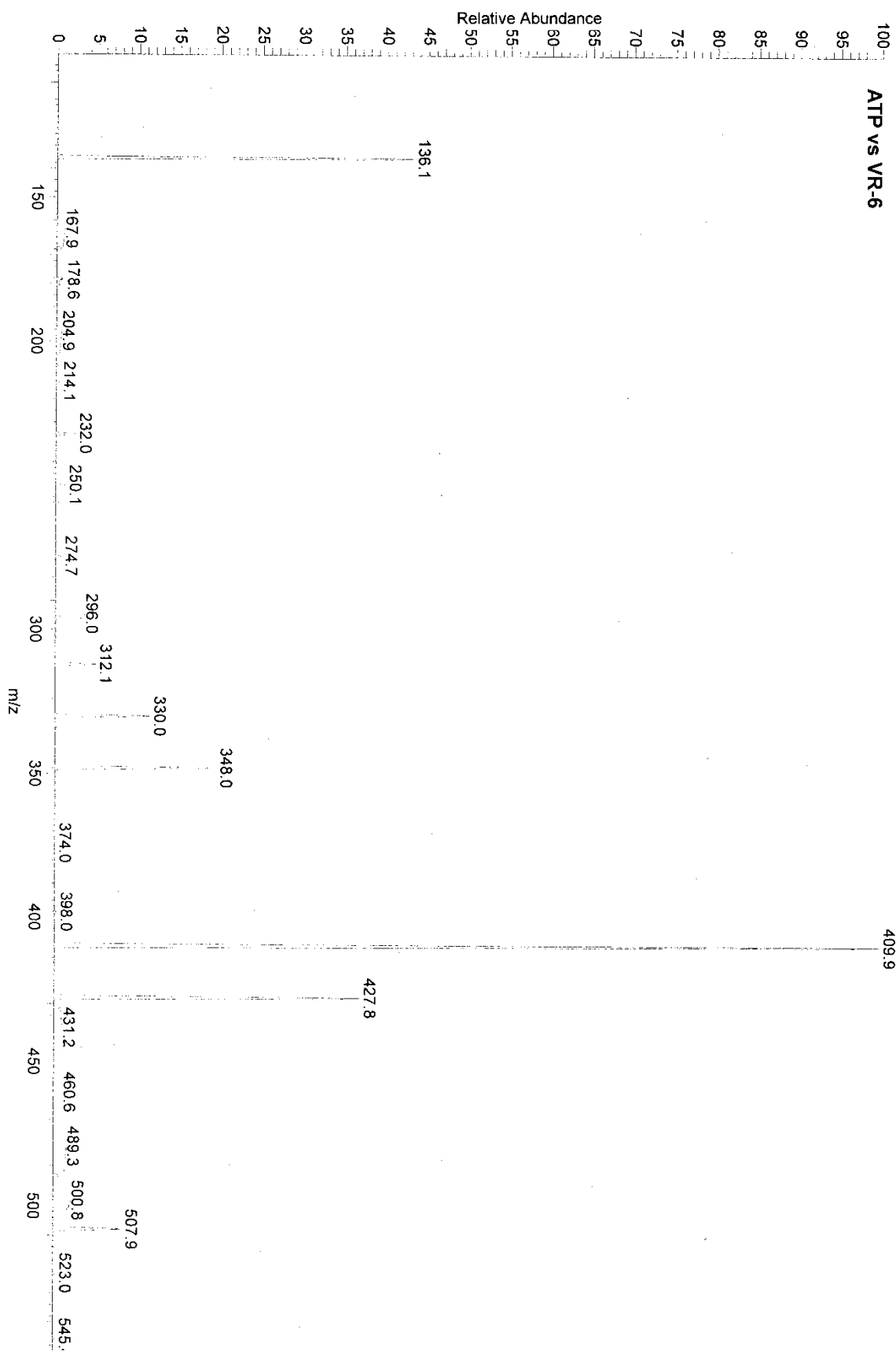


Figure S9. MS for ATP sample incubated with **VR-6** (RT = 1.87 min).

Indicator Displacement Assays

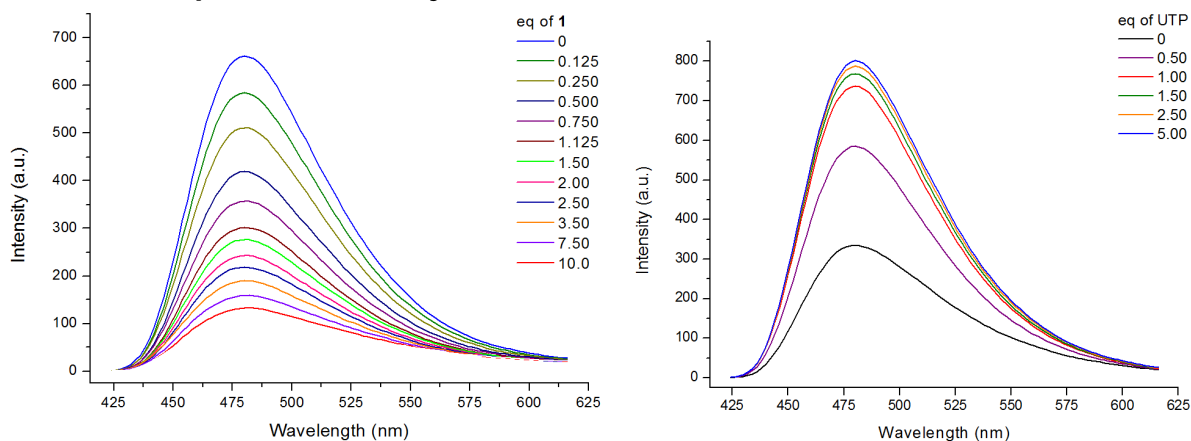


Figure S10. Quenching of CMS emission (5×10^{-6} M) in the presence of **1** in 25 mM HEPES buffer ($\lambda_{\text{ex}} = 396$ nm) and displacement by re-titration with UTP.

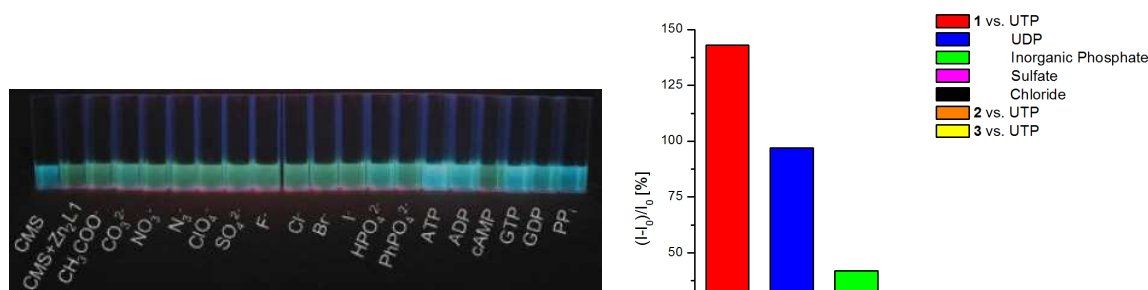


Figure S11. (Left) Color of a mixture of 80 μM CMS and 40 μM **1** upon irradiation in the presence and absence of various anions (800 μM) and phosphate anions (80 μM). Titrations were performed at 25 $^{\circ}\text{C}$ in 10 mM Hepes buffer, pH 7.4. (Right) Relative intensity changes of **1**/CMS in the presence of selected analytes and comparison to the emission response of **2** and **3**.

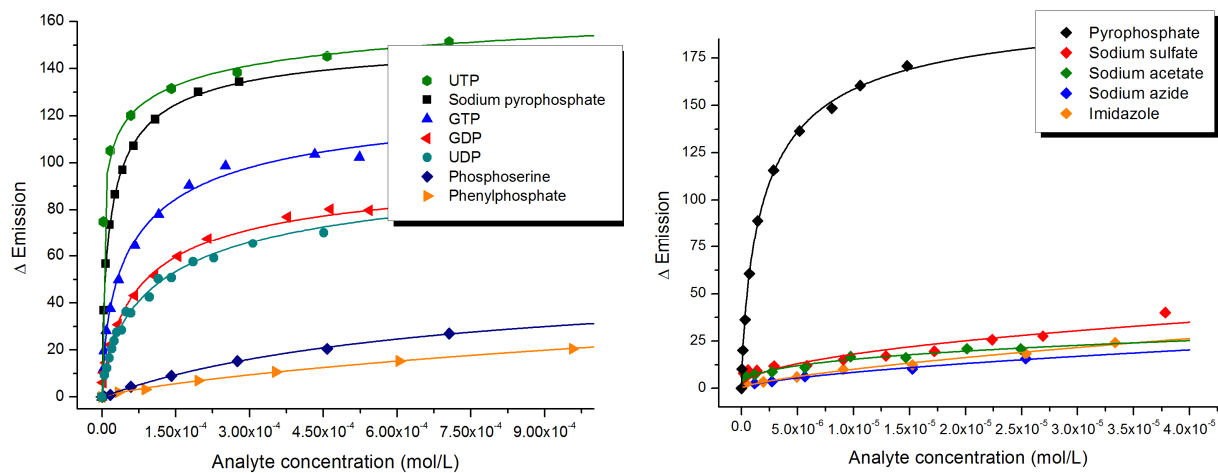


Figure S12. Binding isotherms obtained by indicator displacement assay (IDA) for vesicular receptor VR-4 and various phosphate anions and anion selectivity of vesicular receptor VR-4.

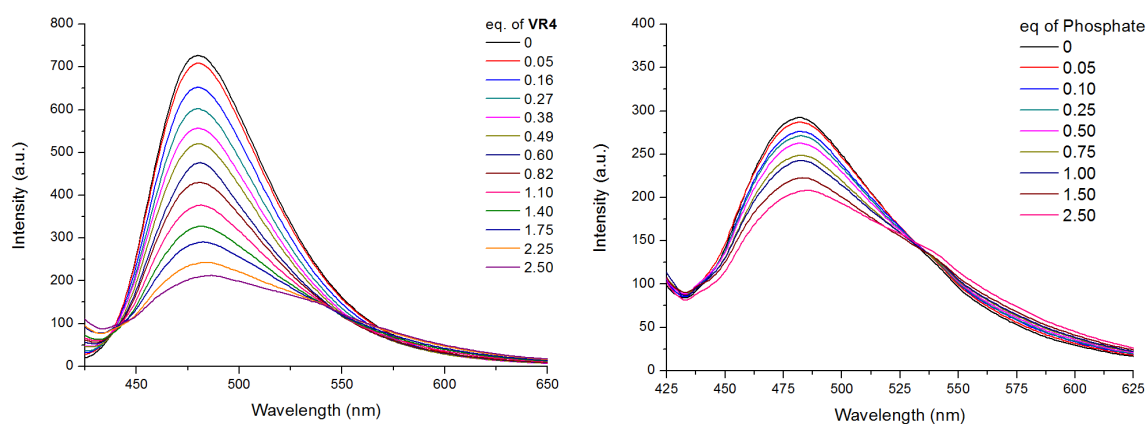


Figure S13. Quenching of CMS emission (5×10^{-6} M) in the presence of **VR-4** in 25 mM HEPES buffer ($\lambda_{\text{ex}} = 396$ nm) and displacement by re-titration with inorganic phosphate.

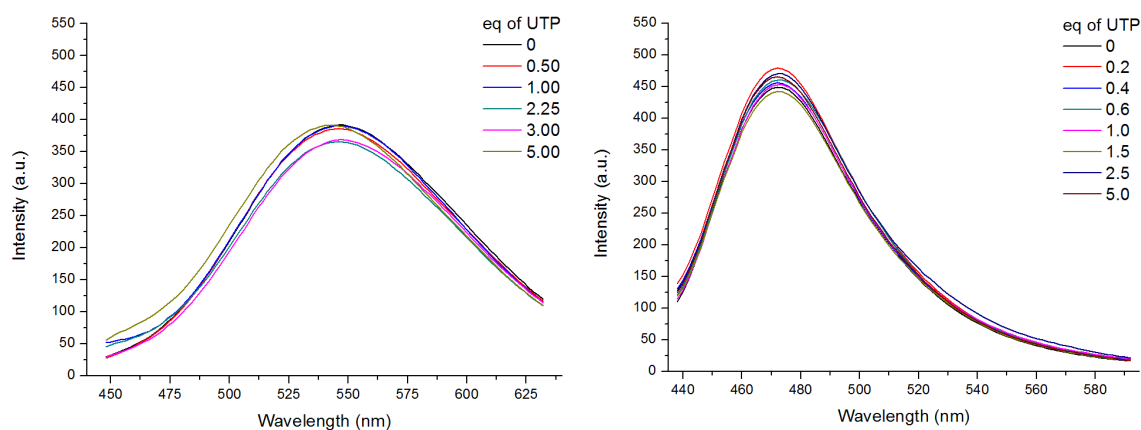


Figure S14. Lack of emission response of **2** and **3** (5×10^{-6} M) in 25 mM HEPES buffer (pH 7.4) in the presence of UTP (λ_{ex} (**2**) = 330 nm, λ_{ex} (**3**) = 335 nm).

NMR titration of **1** vs. UDP

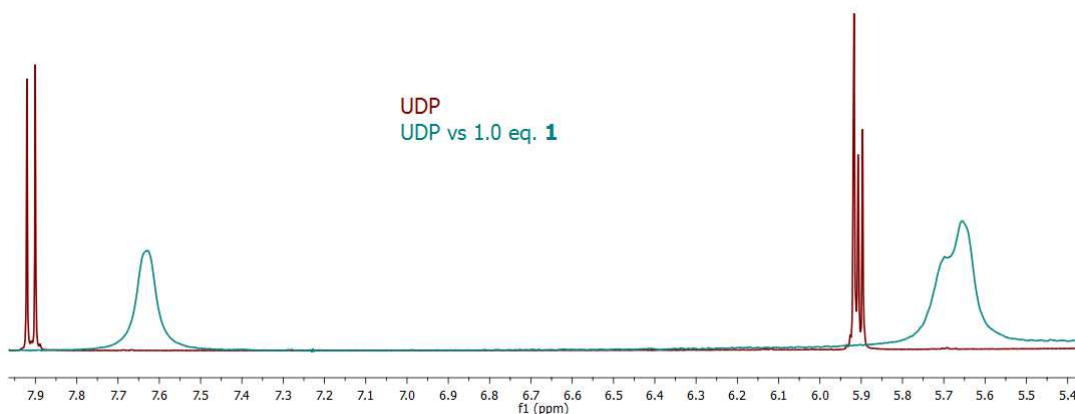


Figure S15. ¹H-NMR spectrum of UDP (25 mM) and UDP in the presence of **1** (1.0 eq). The selected region of the spectrum shows the shift and signal broadening of the imide moiety of UDP and therefore indicates a binding to the Zn(II) complex **1**. All samples were measured in H₂O/D₂O (9:1) at 400 MHz with water suppression.

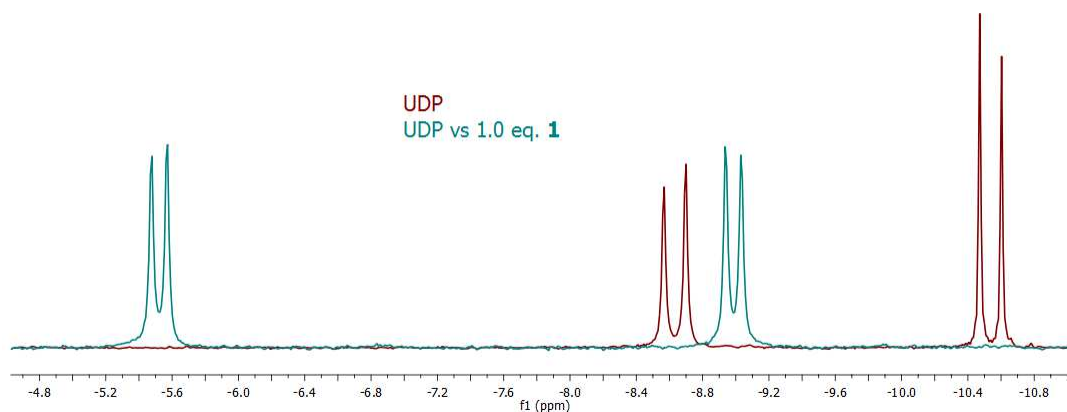


Figure S16. ^{31}P -NMR spectrum of UDP (25 mM) and UDP in the presence of **1** (1.0 eq). The selected region of the spectrum shows the shift of the phosphate moieties of UDP and therefore indicates a binding to the Zn(II) complex **1**. All samples were measured in $\text{H}_2\text{O}/\text{D}_2\text{O}$ (9:1) at 400 MHz.

Structures of DSPC and DSPC-PEG350

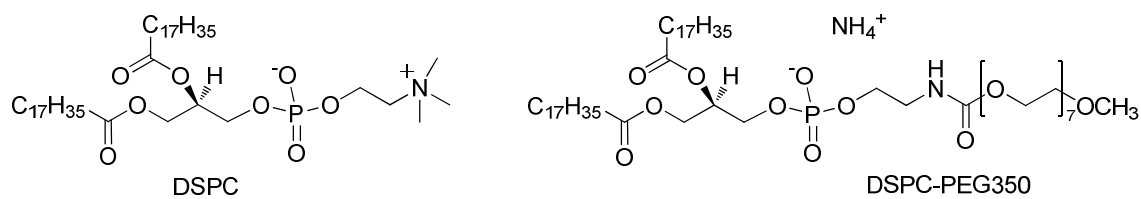


Figure S17. 1,2-distearoyl-*sn*-glycero-3-phosphocholine (**DSPC**) and 1,2-distearoyl-*sn*-glycero-3-phosphoethanolamine-*N*-[methoxy(polyethylene glycol)-350] (**DSPC-PEG350**).

References

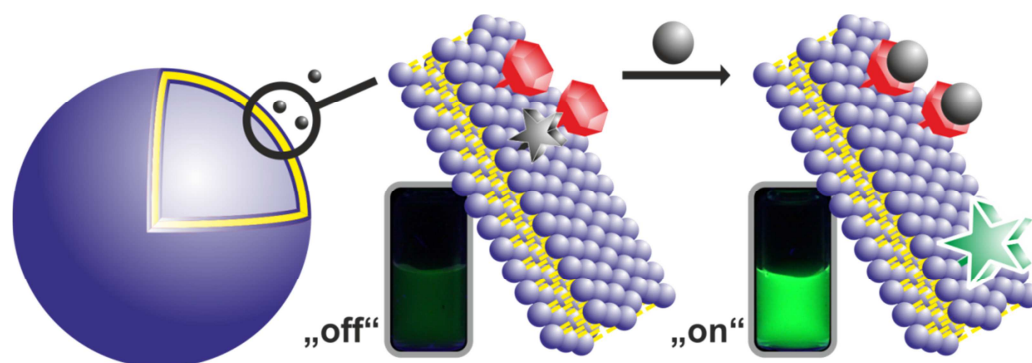
1. J. J. R. Fraústo da Silva and R. J. P. Williams, *The Biological Chemistry of the Elements*, Clarendon Press, Oxford, 1991.
2. S. Aoki and E. Kimura, *Rev. Mol. Biotechnol.*, 2002, **90**, 129-155.
3. R. L. P. Adams, J. T. Knowler and D. P. Leader, *The Biochemistry of Nucleic Acids Tenth Edition*, 1986.
4. W. Saenger, *Principles of Nucleic Acid Structure*, Springer, New York, 1998.
5. L. N. Johnson and R. J. Lewis, *Chem. Rev.*, 2001, **101**, 2209-2242.
6. T. Hunter, *Cell*, 2000, **100**, 113-127.
7. M. B. Yaffe, *Nat. Rev. Mol. Cell Biol.*, 2002, **3**, 177-186.
8. W. N. Lipscomb and N. Sträter, *Chem. Rev.*, 1996, **96**, 2375-2433.
9. H. R. Horton, L. A. Moran, K. G. Scrimgeour, M. D. Perry and J. D. Rawn, *Principles of Biochemistry 4th ed.*, Pearson Prentice Hall, NY, 2006.

10. X. Lin, X. Wu, Z. Xie and K.-Y. Wong, *Talanta*, 2006, **70**, 32-36.
11. J. J. Wang and P. L. Bishop, *Environ. Technol.*, 2005, **26**, 381-388.
12. J. D. R. Thomas, *Pure Appl. Chem.*, 2001, **73**, 31-38.
13. S.-i. Tamaru and I. Hamachi, ed. R. Vilar, Springer Berlin / Heidelberg, 2008, pp. 95-125.
14. M. Kruppa and B. König, *Chem. Rev.*, 2006, **106**, 3520-3560.
15. T. Anai, E. Nakata, Y. Koshi, A. Ojida and I. Hamachi, *J. Am. Chem. Soc.*, 2007, **129**, 6232-6239.
16. A. Ojida, Y. Mito-oka, M. Inoue and I. Hamachi, *J. Am. Chem. Soc.*, 2002, **124**, 6256-6258.
17. A. Ojida, H. Nonaka, Y. Miyahara, S.-i. Tamaru, K. Sada and I. Hamachi, *Angew. Chem. Int. Ed.*, 2006, **45**, 5518-5521.
18. A. Ojida, S.-k. Park, Y. Mito-oka and I. Hamachi, *Tetrahedron Lett.*, 2002, **43**, 6193-6195.
19. A. Ojida, I. Takashima, T. Kohira, H. Nonaka and I. Hamachi, *J. Am. Chem. Soc.*, 2008, **130**, 12095-12101.
20. T. Sakamoto, A. Ojida and I. Hamachi, *Chem. Commun.*, 2009, 141-152.
21. J. Wongkongkatep, Y. Miyahara, A. Ojida and I. Hamachi, *Angew. Chem. Int. Ed.*, 2006, **45**, 665-668.
22. D. H. Lee, S. Y. Kim and J.-I. Hong, *Angew. Chem. Int. Ed.*, 2004, **43**, 4777-4780.
23. H. K. Cho, D. H. Lee and J.-I. Hong, *Chem. Commun.*, 2005.
24. D. H. Lee, J. H. Im, S. U. Son, Y. K. Chung and J.-I. Hong, *J. Am. Chem. Soc.*, 2003, **125**, 7752-7753.
25. W. M. Leevy, J. R. Johnson, C. Lakshmi, J. Morris, M. Marquez and B. D. Smith, *Chem. Commun.*, 2006.
26. W. M. Leevy, S. T. Gammon, H. Jiang, J. R. Johnson, D. J. Maxwell, E. N. Jackson, M. Marquez, D. Piwnica-Worms and B. D. Smith, *J. Am. Chem. Soc.*, 2006, **128**, 16476-16477.
27. C. Lakshmi, R. G. Hanshaw and B. D. Smith, *Tetrahedron*, 2004, **60**, 11307-11315.
28. S. Mizukami, T. Nagano, Y. Urano, A. Odani and K. Kikuchi, *J. Am. Chem. Soc.*, 2002, **124**, 3920-3925.
29. T. Koike, S. Kajitani, I. Nakamura, E. Kimura and M. Shiro, *J. Am. Chem. Soc.*, 1995, **117**, 1210-1219.
30. E. Kimura, T. Shiota, T. Koike, M. Shiro and M. Kodama, *J. Am. Chem. Soc.*, 1990, **112**, 5805-5811.
31. E. Kimura, S. Aoki, T. Koike and M. Shiro, *J. Am. Chem. Soc.*, 1997, **119**, 3068-3076.
32. S. Aoki, M. Zulkefeli, M. Shiro, M. Kohsako, K. Takeda and E. Kimura, *J. Am. Chem. Soc.*, 2005, **127**, 9129-9139.
33. M. Subat, K. Woinaroschy, C. Gerstl, B. Sarkar, W. Kaim and B. König, *Inorg. Chem.*, 2008, **47**, 4661-4668.

34. M. Subat, K. Woinaroschy, S. Anthofer, B. Malterer and B. König, *Inorg. Chem.*, 2007, **46**, 4366-4356.
35. A. Grauer, A. Riechers, S. Ritter and B. König, *Chem. Eur. J.*, 2008, **14**, 8922-8927.
36. A. Riechers, F. Schmidt, S. Stadlbauer and B. König, *Bioconjugate Chem.*, 2009, **20**, 804-807.
37. D. S. Turygin, M. Subat, O. A. Raitman, V. V. Arslanov, B. König and M. A. Kalinina, *Angew. Chem. Int. Ed.*, 2006, **45**, 5340-5344.
38. D. S. Turygin, M. Subat, O. A. Raitman, S. L. Selector, V. V. Arslanov, B. König and M. A. Kalinina, *Langmuir*, 2007, **23**, 2517-2524.
39. D. A. Jose, S. Stadlbauer and B. König, *Chem. Eur. J.*, 2009, **15**, 7404-7412.
40. R. Martinez-Manez and F. Sancenon, *Chem. Rev.*, 2003, **103**, 4419-4476.
41. S. K. Kim, D. H. Lee, J. I. Hong and J. Yoon, *Acc. Chem. Res.*, 2009, **42**, 23-31.
42. L. Zhu, Z. Zhong and E. V. Anslyn, *J. Am. Chem. Soc.*, 2005, **127**, 4260-4269.
43. M. K. Coggins, A. M. Parker, A. Mangalum, G. A. Galdamez and R. C. Smith, *Eur. J. Org. Chem.*, 2009, **2009**, 343-348.
44. B. T. Nguyen and E. V. Anslyn, *Coord. Chem. Rev.*, 2006, **250**, 3118-3127.
45. S. L. Wiskur, H. Ait-Haddou, J. J. Lavigne and E. V. Anslyn, *Acc. Chem. Res.*, 2001, **34**, 963-972.
46. B. S. Creaven, D. A. Egan, K. Kavanagh, M. McCann, A. Noble, B. Thati and M. Walsh, *Inorg. Chim. Acta*, 2006, **359**, 3976-3984.
47. J. Lasch, *Liposomes*, Oxford University Press, 2003.
48. A. I. Elegbede, M. K. Haldar, S. Manokaran, J. Kooren, B. C. Roy, S. Mallik and D. K. Srivastava, *Chem. Commun.*, 2007, 3377-3379.
49. M. Ueno, S. Katoh, S. Kobayashi, E. Tomoyama, S. Ohsawa, N. Koyama and Y. Morita, *J. Colloid Interface Sci.*, 1990, **134**, 589-592.
50. B. J. Berne, *Dynamic Light Scattering*, John Wiley, 1976.
51. B. Ruozi, G. Tosi, F. Forni, M. Fresta and M. A. Vandelli, *Eur. J. Pharm. Sci.*, 2005, **25**, 81-89.
52. D. W. Fry, J. C. White and I. D. Goldman, *Anal. Biochem.*, 1978, **90**, 809-815.
53. M. Kodama and E. Kimura, *J. Chem. Soc., Dalton Trans.*, 1977.
54. T. Chen, X. Wang, Y. He, C. Zhang, Z. Wu, K. Liao, J. Wang and Z. Guo, *Inorg. Chem.*, 2009, **48**, 5801-5809.
55. H. Ait-Haddou, S. L. Wiskur, V. M. Lynch and E. V. Anslyn, *J. Am. Chem. Soc.*, 2001, **123**, 11296-11297.
56. M. S. Han and D. H. Kim, *Angew. Chem. Int. Ed.*, 2002, **41**, 3809-3811.
57. M. S. Han and D. H. Kim, *Bioorg. Med. Chem. Lett.*, 2003, **13**, 1079-1082.
58. B. P. Morgan, S. He and R. C. Smith, *Inorg. Chem.*, 2007, **46**, 9262-9266.

59. We explain the observed slight decrease in absorption by the polarity change of the solution due to an increase of the ionic strength.
60. R. G. Hanshaw, S. M. Hilkert, H. Jiang and B. D. Smith, *Tetrahedron Lett.*, 2004, **45**, 8721-8724.
61. T. Zhang and E. V. Anslyn, *Tetrahedron*, 2004, **60**, 11117–11124.
62. C. Li, M. Numata, M. Takeuchi and S. Shinkai, *Angew. Chem. Int. Ed.*, 2005, **44**, 6371-6374.
63. D. A. Jose, S. Mishra, A. Ghosh, A. Shrivastav, S. K. Mishra and A. Das, *Org. Lett.*, 2007, **9**, 1979-1982.
64. J. Voskuhl and B. J. Ravoo, *Chem. Soc. Rev.*, 2009, **38**.
65. M. Kruppa, D. Frank, H. Leffler-Schuster and B. König, *Inorg. Chim. Acta*, 2006, **359**, 1159-1168.
66. R. Kraayenhof, G. J. Sterk and H. W. Wong Fong Sang, *Biochemistry (Mosc)*. 1993, **32**, 10057-10066.
67. R. M. Epand and R. Kraayenhof, *Chem. Phys. Lipids*, 1999, **101**, 57-64.
68. A. Chattopadhyay and S. Mukherjee, *Biochemistry (Mosc)*. 1993, **32**, 3804-3811.
69. A. Chattopadhyay and S. Mukherjee, *Langmuir*, 1999, **15**, 2142-2148.
70. R. S. Moog, W. W. Davis, S. G. Ostrowski and G. L. Wilson, *Chem. Phys. Lett.*, 1999, **299**, 265-271.
71. N. M. Correa and N. E. Levinger, *The Journal of Physical Chemistry B*, 2006, **110**, 13050-13061.
72. B. R. Gayathri, J. R. Mannektla and S. R. Inamdar, *J. Mol. Struct.*, 2008, **889**, 383-393.
73. J. R. Mannektla, B. G. Mulimani and S. R. Inamdar, *Spectrochim. Acta, Pt. A: Mol. Biomol. Spectrosc.*, 2008, **69**, 419-426.
74. V. Orlin D, *Adv. Biophys.*, 1997, **34**, 139-157.
75. Author collective, *Organikum, 17th Edition*, VEB Deutscher Verlag der Wissenschaften, Berlin, 1988.
76. S. Hünig, G. Märkl and J. Sauer, *Einführung in die apparativen Methoden in der Organischen Chemie, 2nd Edition*, Würzburg / Regensburg, 1994.
77. R. C. MacDonald, R. I. MacDonald, B. P. M. Menco, K. Takeshita, N. K. Subbarao and L.-r. Hu, *Biochim. Biophys. Acta*, 1991, **1061**, 297-303.
78. P. Balgavy, M. Dubnickova, N. Kucerka, M. A. Kiselev, S. P. Yaradaikin and D. Uhrikova, *Biochim. Biophys. Acta*, 2001, **1512**, 40-52.
79. J. F. Nagle and S. Tristram-Nagle, *Biochim. Biophys. Acta*, 2000, **1469**, 159-195.
80. K. A. Connors, *Binding Constants - The Measurement of Molecular Complex Stability*, John Wiley & Sons, 1987.

CHAPTER 3

MODULAR CHEMOSENSORS FROM SELF-ASSEMBLED VESICLE MEMBRANES WITH AMPHIPHILIC BINDING SITES AND REPORTER DYES

Tiny analysts: Co-embedding of amphiphilic binding sites and environment-sensitive dyes in vesicular membranes allows rapid and easy preparation of self-assembled modular chemosensors. The fluorescent particles thus obtained respond to the presence of analytes by changes in their emission intensity.

This chapter has been published:

B. Gruber, S. Stadlbauer, A. Späth, S. Weiss, M. Kalinina and B. König, *Angew. Chem.* **2010**, *122*, 7280-7284; *Angew. Chem. Int. Ed.* **2010**, *49*, 7125-7128.

Author contributions:

BG synthesized vesicles, performed binding studies and wrote the manuscript; SS synthesized compound **2**; AS synthesized compound **3**; SW synthesized compound **4**; MK contributed to data interpretation and manuscript writing; BK supervised the project and is corresponding author.

Introduction

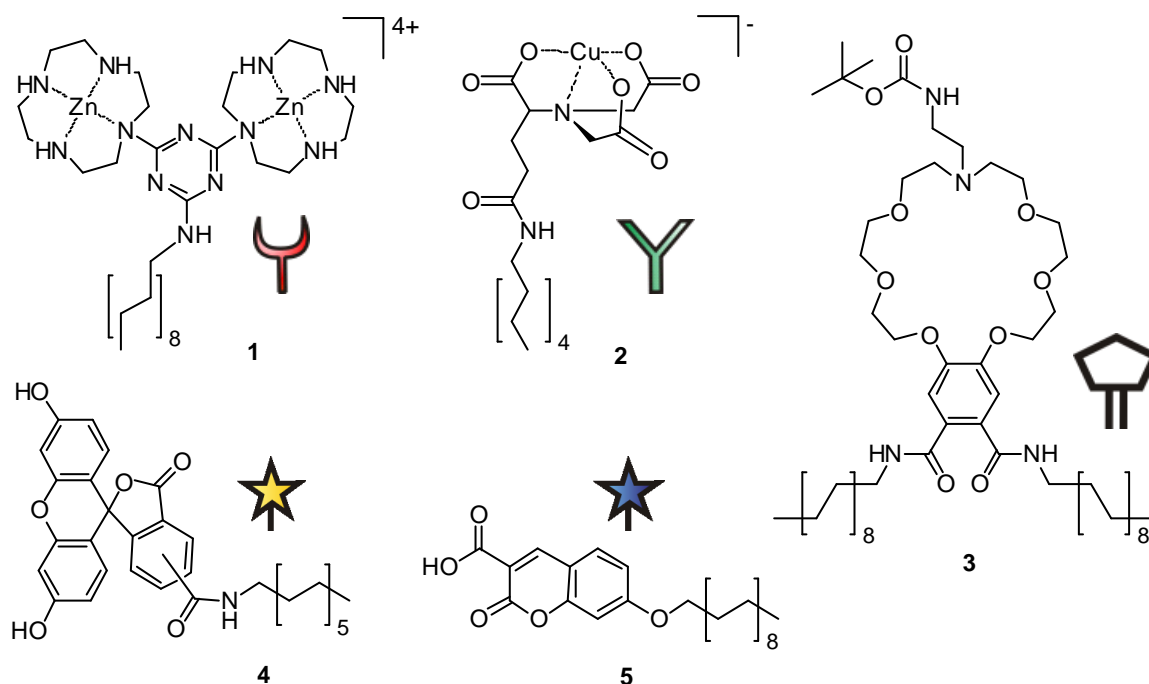
Transition metal complexes with vacant coordination sites have found wide use as binding sites in the development of molecular probes and chemosensors.^{1, 2} Such probes typically consist of the guest binding site and a luminescent reporter group that enables convenient monitoring of ligand binding events. The luminescent moiety can either be a part of the actual molecular chemosensor, usually in close proximity to the analyte binding site,^{3, 4} or a separate dye that is first non-covalently attached to the binding site and later displaced by the analyte (indicator displacement assay).⁵ Both strategies have drawbacks, as the rational design of luminescent chemosensors is still difficult and their synthesis laborious, while the response of indicator displacement assays is typically not reversible. We present here a novel approach to signal analyte binding by non-covalent co-embedding of amphiphilic non-fluorescent binding sites⁶⁻⁸ and reporter dyes into the membrane of small unilamellar vesicles. The receptor binding is communicated through the membrane to the co-embedded dyes,⁹ which change their emission properties. We demonstrate a simple and versatile approach to combine several different recognition sites with fluorescent reporter groups in a lipid bilayer.¹⁰⁻¹²

Results and Discussion

Three amphiphilic artificial binding sites, 1,4,7,10-tetraazacyclododecane (cyclen) Zn(II) complex **1** for phosphate anion binding,¹³⁻¹⁷ a nitrilotriacetic acid (NTA) Cu(II) complex **2** for the recognition of imidazole-derivatives¹ and a benzo-azacrown ether (BACE) **3** as host for ammonium ions,^{18, 19} and two amphiphilic fluorophores (Scheme 1) were incorporated into vesicle membranes. Compounds **1** and **5** were reported previously by us,^{8, 20} syntheses of compounds **2**, **3** and **4** are described in the Supporting Information to this paper. The widely used carboxyfluorescein (CF) dye was selected due to its sensitivity to local electrostatic potential^{21, 22} and easy derivatization with alkyl amines. The sensitivity of coumarin derivative **5** to changes in the local environment was already observed in an earlier study.²³

Luminescent vesicular receptors (LVR; Figure 1) with phospholipid bilayer embedded receptors and fluorescent dyes were prepared following our previously reported protocol.⁸ Vesicles **LVR-1,5**, containing co-embedded cyclen Zn(II) complex **1** and coumarin derivative **5**, exhibit a strong fluorescence emission with a maximum intensity at 408 nm. In the presence of increasing amounts of phosphate anions, like pyrophosphate (PP_i) or phospho-serine (pSer) this emission intensity is significantly reduced (Figure 2, left). The embedded Zn(II) cyclen complexes retain their known selectivity for phosphate anions and the addition of other anions gave no emission response (see Supporting Information for data). We explain this change in emission intensity by a rearrangement of the membrane structure induced by the phosphate anion coordination towards the embedded receptor molecules: Dye **5** and

artificial receptor **1** if embedded together in the lipid bilayer are not supposed to be homogeneously distributed but to form relatively closely arranged mixed patches in the membrane as its structure is disturbed by the rather bulky embedded molecules. Such non-uniform distribution translates into a different environment for dye molecules within the membrane. While a certain portion of dye molecules remains free enough to provide initial emission, those molecules, which are in a close proximity to the ligand, are “switched-off” due to the interactions of receptor and dye. These interactions are imposed by the tightly packed membrane structure of surrounding lipid phase and do not occur in homogeneous aqueous solution.²⁴ Binding of bulky phosphate anions to the receptors changes solvation and charge of the binding sites and thereby changes the miscibility of the receptor and dyes. These phase state alterations, in turn, cause a segregation of the patches and the surrounding zone and thus the lateral expelling of dye molecules from the mixed phase. Similar phenomena, though more complex in nature, underlie the response of cell membranes, which are essentially composed of lipids with various embedded active sites, to external stimuli and substrates.²⁵⁻²⁷ Environment sensitive dyes like coumarin derivatives are known to respond to such altered conditions resulting from the binding event^{28, 29} - in this case by a decrease of their emission intensity.



Scheme 1. Amphiphilic artificial binding sites based on Zn(II) cyclen (**1**), Cu(II) NTA (**2**) and BACE (**3**) and amphiphilic fluorescent reporter dyes derived from carboxy-fluorescein (**4**) and coumarin (**5**).

Apparent binding constants were determined from emission titration binding isotherms and are summarized in Table 1. The obtained affinities for PP_i and pSer are in the micromolar range and in good agreement with previously determined affinities by different methods.⁸ To confirm that the specific anion - metal complex interaction is responsible for the emission

response and exclude effects of unspecific adsorption the measurements were repeated with vesicles that do not contain Zn(II) cyclen binding sites. These vesicles also exhibit blue fluorescence, but indeed give no emission response on excess addition (50 - 100 eq) of PP_i or pSer (data not shown).

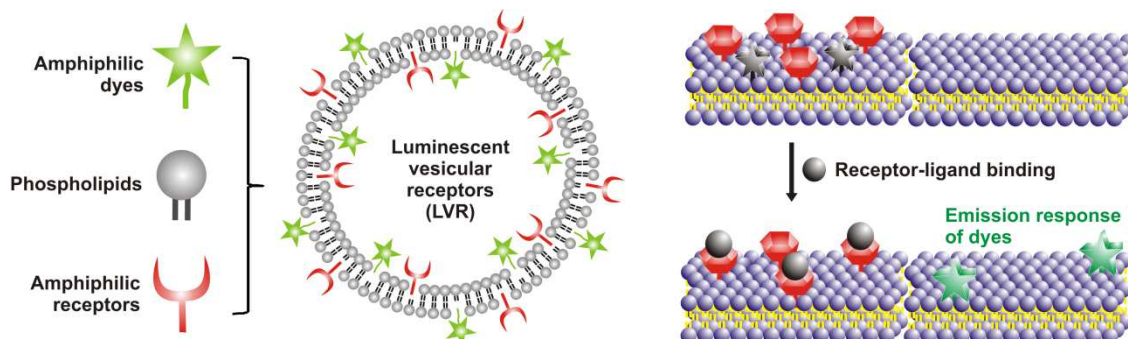


Figure 1. Preparation of luminescent vesicular receptors (LVR) and their analyte response: Self-assembly of lipids, amphiphilic artificial receptors and amphiphilic fluorescent dyes in buffered aqueous solution yields surface-modified vesicles that respond to receptor-ligand binding by a change in their emission intensity.

Different reporter dyes can be used to adjust the optical properties of the vesicular receptors: **LVR-1,4** obtained from co-embedding of Zn(II) cyclen complexes **1** and amphiphilic carboxyfluorescein **4** showed green fluorescence emission with a maximum intensity at 520 nm if excited at 495 nm. As the optical response of environment-sensitive dyes depends on their structure and properties as well as on their miscibilities with the substrate-free and occupied receptor it can be quite varying and upon addition of increasing amounts of phosphate anions the emission at 520 nm now shows a strong increase (Figure 2, right). The apparent binding constants derived from the binding isotherms of **LVR-1,4** and of **LVR-1,5** however are identical for pSer and for PP_i (Table 1) within the error of the experiment. This fits to our above hypothesis and gives rise to the assumption that a variety of dyes can be employed as long as they change their emission properties upon an alteration of their environment. As vesicles functionalized with **4** show emission increase upon guest binding ("switch-on" fluorescence), which is more desirable for most analytic applications than an emission decrease ("switch-off"), compound **4** was used as reporter dye for all subsequent binding studies.³⁰

To provide more experimental support for our mechanistic hypothesis we also prepared **LVR-1,4** with different concentrations of receptors and dyes. As a result the relative emission response to a certain amount of analyte increases, respectively decreases, with an increasing, respectively decreasing, amount of embedded receptors and dyes (see Supporting Information for data), which perfectly fits to our suggested model of receptor/dye patches.

Next, the amphiphilic Cu(II) nitrilotriacetic acid (NTA) complex **2** was investigated as binding site. Cu(II) NTA complexes coordinate imidazole ligands and are widely used in immobilized metal affinity chromatography (IMAC),³¹ e.g. for the separation of His-tagged biomolecules.^{32, 33} Vesicles **LVR-2,4** containing the Cu(II) NTA complexes **2** and the CF dye **4** were prepared; the particles showed emission at 520 nm analogous to **LVR-1,4**. Binding studies revealed that now in presence of imidazole derivatives the emission intensity considerably increased, while other additives - cationic or anionic - induced no response (see Supporting Information for data). The analyte selectivity of the functionalized vesicle is therefore determined by the selectivity of the embedded Cu(II) NTA complexes.

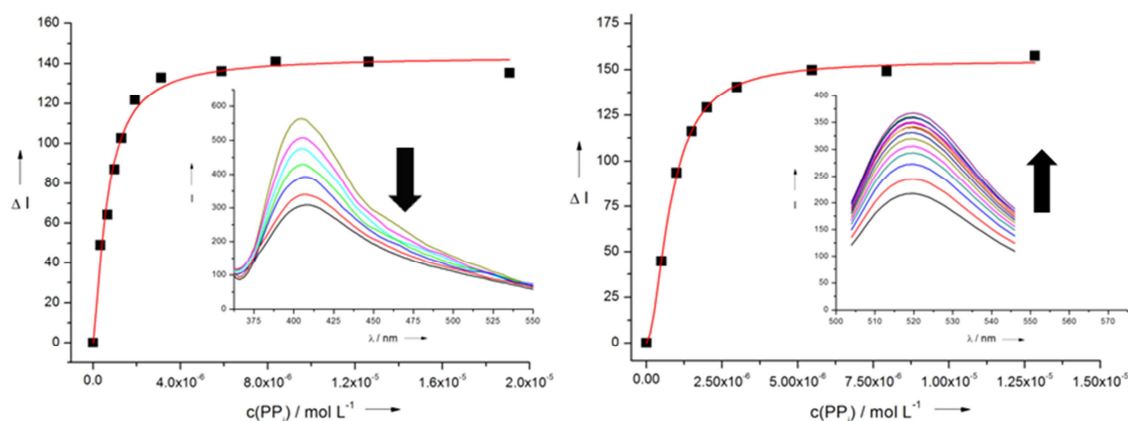


Figure 2. (Left) Binding isotherm obtained from emission titration of **LVR-1,5** vs. PP_i ($\lambda_{\text{ex}} = 349$ nm, $\lambda_{\text{em}} = 405$ nm); (Right) Binding isotherm obtained from emission titration of **LVR-1,4** vs. PP_i ($\lambda_{\text{ex}} = 495$ nm, $\lambda_{\text{em}} = 520$ nm).

To increase the complexity, two different binding sites were incorporated simultaneously in one vesicle: **LVR-1,2,4** contains cationic³⁴ Zn(II) cyclen complexes **1** and anionic^[14] Cu(II) NTA complexes **2** as binding sites, and CF **4** reporter groups. The particles exhibit green fluorescence at 520 nm, which increases in the presence of either phosphate anions or imidazoles (Figure S5). Binding affinities for PP_i and pSer were similar as determined for **LVR-1,4**, whereas the derived log *K* values for 4-Me-Im and His were found to be up to one order of magnitude lower than for **LVR-2,4**, but still in the micromolar range and thus higher than for Cu(II) NTA complexes in homogeneous aqueous solution.³⁵ The selectivities of the individual binding sites for their corresponding ligands were retained. The vesicles containing both metal complexes did not respond by change of their emission to other analytes, such as ammonium or sulfate ions (Figure S5). We therefore assume that our suggested model for a binary system (with one receptor and one dye) also works with ternary (two receptors and one dye) or even more complex systems.³⁶ Furthermore, the addition of phosphate and imidazole derivatives to **LVR-1,2,4** can be sequential, with each guest producing an incremental increase in fluorescence intensity. This again supports our suggested model of (multi-)receptor and dye patches in the membrane which are rearranged to some extent by an additional binding of analytes to the receptor moieties.

	Receptor(s)	Reporter	Ligand	log K (± 0.1)
LVR1-4	1	4	PP _i	6.2
LVR1-4	1	4	pSer	5.9
LVR1-5	1	5	PP _i	6.0
LVR1-5	1	5	pSer	5.9
LVR2-4	2	4	4-Me-Im	7.1
LVR2-4	2	4	His-OMe	7.1
LVR1-2-4	1 + 2	4	PP _i	6.0
LVR1-2-4	1 + 2	4	pSer	5.8
LVR1-2-4	1 + 2	4	4-Me-Im	6.2
LVR1-2-4	1 + 2	4	His-OMe	6.1
LVR1-2-3-4	1 + 2 + 3	4	PP _i	6.1
LVR1-2-3-4	1 + 2 + 3	4	4-Me-Im	6.0
LVR1-2-3-4	1 + 2 + 3	4	Gly-OMe	5.8

Table 1. Binding affinities of luminescent vesicular receptors (LVR) to several analytes derived from emission titrations.

To increase the complexity of the vesicular receptors even further, a third binding site was added to the cationic and anionic transition metal complex receptors **1** and **2**. Therefore we prepared the amphiphilic benzo-aza-crown ether derivative **3**^{18, 19} and incorporated it together with **1**, **2** and **4** into the luminescent vesicles **LVR-1,2,3,4** bearing now three fundamentally different molecular recognition sites on the bilayer surface. The benzo-aza-crown ether moiety is a well established low affinity binding site for the molecular recognition of ammonium ions. Incorporated in the luminescent vesicles the crown ether's binding selectivity is combined with the optical properties of the bilayer-embedded fluorescent dye. The emission properties of **LVR-1,2,3,4** and binding affinities towards phosphate and imidazole are again in good agreement with **LVR-1,2,4** (Table 1). However, **LVR-1,2,3,4** in contrast to **LVR-1,2,4** responds also to the presence of ammonium ions like the C-terminal protected amino acid glycine (Gly-OMe) by increase in emission intensity. The binding affinity for Gly-OMe was determined as $\log K = 5.8$, which exceeds ammonium ion affinities for the benzo-aza-crown ether moiety in aqueous solution by three to four orders of magnitude. We explain the significant binding affinity increase by the improved signaling mechanism using the embedded dye and the special properties affecting intermolecular interactions at the interface of hydrophobic membrane and water. Such effects are reported for related examples.^{20, 37-41}

To finally demonstrate the reversibility of the receptor-ligand binding on the vesicular surface the vesicles were separated from bound analytes via size exclusion chromatography and reused for emission titrations with nearly identical results (see Figure S6).

Conclusion

In summary, a novel kind of luminescent vesicular chemosensors for the recognition of biologically important ions and molecules was obtained by self-assembly of lipids, amphiphilic binding sites and environment-sensitive reporter dyes. As a proof of principle three different amphiphilic binding sites **1 - 3**, based on Zn(II) cyclen or Cu(II) NTA complexes and benzo-aza-crown ether, and two fluorescent dyes, based on coumarin and carboxyfluorescein, were co-embedded into membranes of unilamellar vesicles. Although not covalently linked or directly coordinated to a single receptor site like in classical indicator displacement systems, the reporter dyes signal analyte binding to the receptor sites by changes of their emission properties. We explain this response by an analyte binding induced rearrangement of the doped bilayer membrane. Embedding of bulky binding sites and dyes leads to phase separation and the initial formation of patches with gathered receptors and dyes. Subsequent receptor binding events change conditions like solvation and charge in the local receptor environment and release dye molecules for signalling action. This redistribution of dye molecules finally explains the emission response of the environment-sensitive dyes. This "substrate catch - dye release" signalling mechanism based on the delicate interplay between binding events and phase properties of local environment of the receptor site also provides an opportunity for fine tuning of the system response by simple altering the ligand-to-dye ratio and vesicle composition. Vesicles prepared from mixtures of binding sites show an additive response corresponding to the selectivity of all incorporated receptors. Analytes, such as pSer, His-OMe and Gly-OMe bind reversibly and are detected at (sub-)micromolar concentrations. The key advantage of the self-assembled functionalized nanoparticles is the non-covalent pooling of multiple binding sites and fluorescent reporter groups reducing the synthetic effort in chemosensor preparation. It is likely that many other binding sites and luminescent probes can be combined in the demonstrated way, which paves an easy way to analytical nanoparticles adjustable at will in their binding and response properties.

Experimental Part and Supporting Information

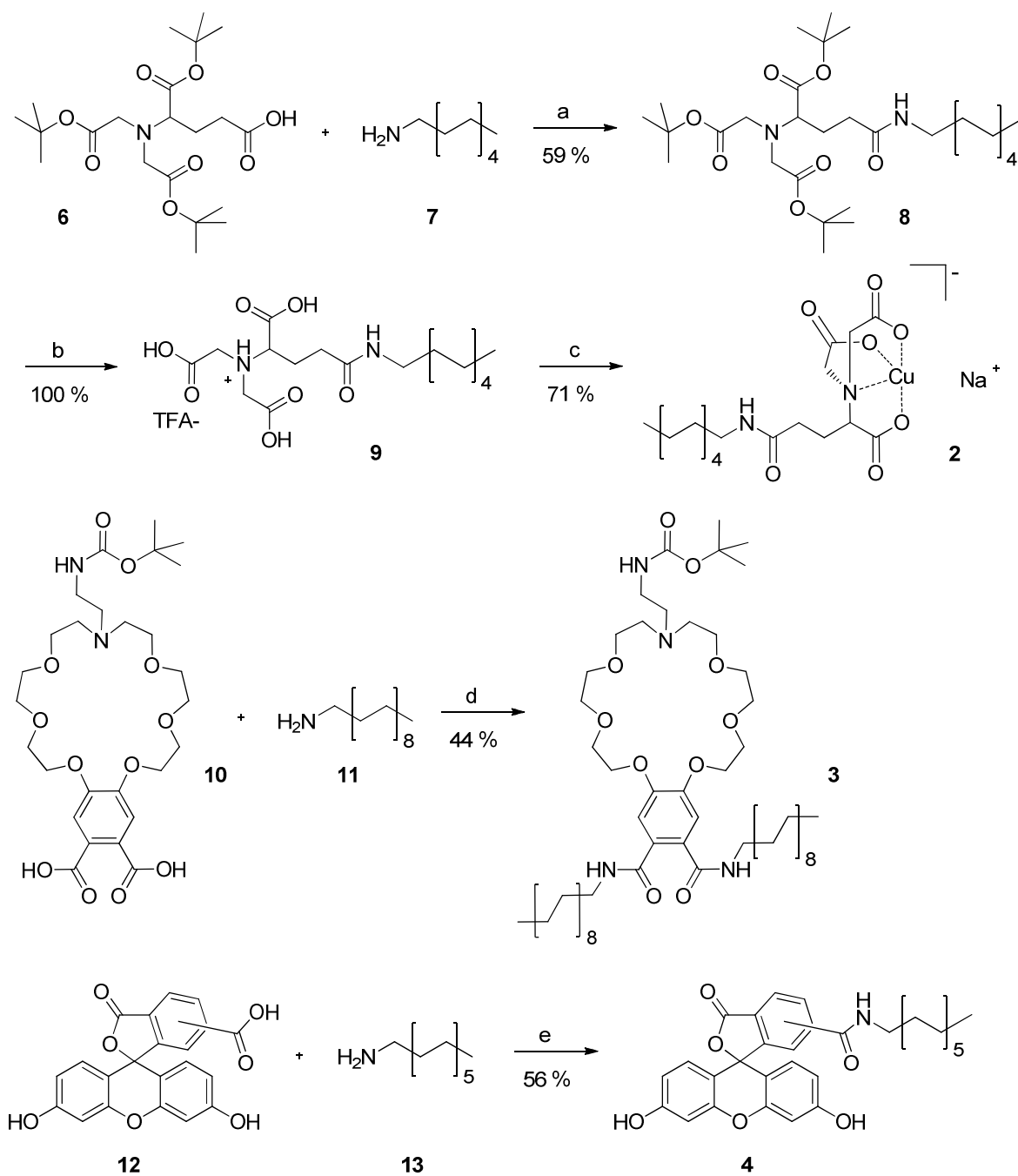
General methods and material

Fluorescence spectra were recorded on a 'Cary Eclipse' fluorescence spectrophotometer and absorption spectra on a "Cary BIO 50" UV/VIS/NIR spectrometer from Varian. All measurements were performed in 1 cm quartz cuvettes (Hellma) and UV-grade solvents (Baker or Merck) at 25 °C. DLS measurements were carried out on a Malvern Zetasizer NanoZS at 25 °C using 1 cm disposable cuvettes (Sarstedt) using automatically optimized

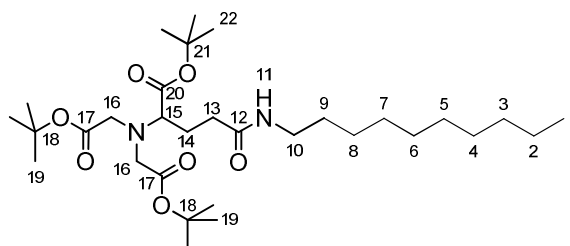
settings. NMR Spectra: Bruker Avance 600 (1H: 600.1 MHz, 13C: 150.1 MHz, T = 300 K), Bruker Avance 400 (1H: 400.1 MHz, 13C: 100.6 MHz, T = 300 K), Bruker Avance 300 (1H: 300.1 MHz, 13C: 75.5 MHz, T = 300 K). The chemical shifts are reported in [ppm] relative to external standards (solvent residual peak). The spectra were analyzed by first order, the coupling constants are given in Hertz [Hz]. Characterization of the signals: s = singlet, d = doublet, t = triplet, q = quartet, m = multiplet, bs = broad singlet, psq = pseudo quintet, dd = double doublet, dt = double triplet, ddd = double double doublet. Integration is determined as the relative number of atoms. Assignment of signals in 13C-spectra was determined with DEPT-technique (pulse angle: 135 °) and given as (+) for CH₃ or CH, (-) for CH₂ and (C_q) for quaternary C_q. Error of reported values: chemical shift: 0.01 ppm for 1H-NMR, 0.1 ppm for 13C-NMR and 0.1 Hz for coupling constants. The solvent used is reported for each spectrum. Mass Spectra: Varian CH-5 (EI), Finnigan MAT 95 (CI; FAB and FD), Finnigan MAT TSQ 7000 (ESI). Xenon serves as the ionization gas for FAB. IR Spectra were recorded with a Bio-Rad FTS 2000 MX FT-IR and Bio-Rad FT-IR FTS 155. Melting Points were determined on Büchi SMP or a Lambda Photometrics OptiMelt MPA 100. Thin layer chromatography (TLC) analyses were performed on silica gel 60 F-254 with 0.2 mm layer thickness and detection via UV light at 254 nm / 366 nm or through staining with ninhydrin in EtOH. Column chromatography was performed on silica gel (70–230 mesh) from Merck. Commercially available starting materials and solvents were used without any further purification except stated otherwise. Optional drying and purification was performed according to accepted general procedures.^{42, 43} Elemental analyses were carried out by the centre for chemical analysis of the Faculty of Chemistry and Pharmacy at the University of Regensburg.

Synthesis

The amphiphilic Cu(II) NTA complex **2** was prepared in three steps starting from the N-alkylated⁴⁴ glutamic acid derivative **6**. Amide formation with **7** under standard peptide coupling conditions gave **8**, which was transformed into **2** by ester cleavage and copper complex formation (Scheme 1). The crown ether building block **10** was prepared as published^{18, 19} and alkyl chains were introduced by peptide coupling of **11** with EDC and HOBT to give **3**. Amphiphilic carboxyfluorescein **4** was prepared by amide formation of 5/6-carboxyfluorescein **12** with dodecylamine **11**.

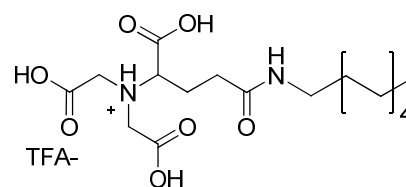


Scheme S1. Synthesis of amphiphiles **2**, **3** and **4**. (a) EDC, HOBT, DIPEA, DMF, 40 °C; (b) TFA, RT; (c) $\text{Cu}_2(\text{OH})_2\text{CO}_3$, MeOH; (d) EDC, HOBT, DIPEA, CHCl_3 , DMF; (e) DMF, DIPEA, HOBT, DCC.



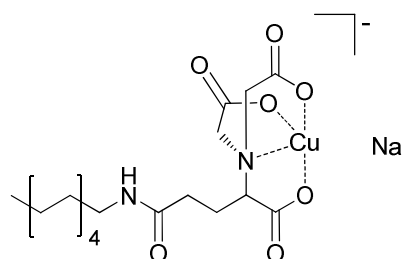
2-(Bis-tert-butoxycarbonylmethyl-amino)-4-decylcarbamoyl-butyl ester tert-butyl ester (**8**):

Under N_2 -atmosphere compound **6**⁴⁴ (472 mg, 1.09 mmol), DIPEA (0.94 mL, 5.47 mmol), EDC (0.23 mL, 1.31 mmol), and HOBt (177 mg, 1.31 mmol) were dissolved in DMF (10 mL) under ice cooling. Decylamine **7** (0.26 mL, 1.31 mmol) dissolved in DMF was added slowly. The reaction was allowed to warm to r.t. and was stirred over night (20 h) at 40 °C. The reaction progress was monitored by TLC (EE). After completion the solution was mixed with water (25 mL) and extracted with citric acid (3x) and sat. NaCl (3x). The organic layer was dried over $MgSO_4$. The solvent was evaporated and the crude was purified using column chromatography on silica gel (EE/PE 1:1, $R_f = 0.65$) yielding **8** (365 mg, 0.64 mmol, 59%) as a colourless solid after drying in vacuum. **¹H-NMR** (600 MHz; $CDCl_3$): δ (ppm) = 0.80-0.90 (t, $^3J = 7.1$ Hz, 3 H, HSQC: C^1H_3), 1.19-1.32 (m, 14 H, $C^2H_2 - C^8H_2$), 1.41-1.42 (s, 9 H, $C^{22}H_3$), 1.43-1.44 (s, 18 H, $C^{19}H_3$), 1.45-1.51 (m, 2 H, HMBC: C^9H_3), 1.73-1.83 (m, 1 H, HMBC: $C^{14}H_2$ diastereotop), 2.01-2.13 (m, 1 H, HMBC: $C^{14}H_2$ diastereotop), 2.32-2.40 (m, 1 H, HMBC: $C^{13}H_2$ diastereotop), 2.47-2.54 (m, 1 H, HMBC: $C^{13}H_2$ diastereotop), 3.09-3.17 (m, 1 H, HMBC: $C^{10}H_2$ diastereotop), 3.18-3.26 (m, 2 H, HMBC: $C^{10}H_2$ diastereotop, $C^{15}H$), 3.32-3.47 (dd, $^4J = 17.1$ Hz, $^4J = 41.9$ Hz, 4 H, HMBC: $C^{16}H_2$), 6.75-6.83 (t, 1 H, $^3J = 5.3$ Hz, HSQC: $N^{11}H$). – **¹³C-NMR** (150 MHz; $CDCl_3$): δ (ppm) = 14.1 (+, 1 C, HSQC: C^1), 22.6 (–, 1 C, HSQC: C^1), 26.6 (–, 1 C, HSQC: C^{14}), 27.0 (–, 1 C, HSQC: C^1), 28.07 (+, 6 C, HSQC: C^{19}), 28.15 (+, 3 C, HSQC: C^{22}), 29.2 (–, 1 C, HSQC: C^1), 29.3 (–, 1 C, HSQC: C^1), 29.52 (–, 1 C, HSQC: C^1), 29.55 (–, 1 C, HSQC: C^1), 29.6 (–, 1 C, HSQC: C^1), 31.8 (–, 1 C, HSQC: C^9), 32.7 (–, 1 C, HSQC: C^{13}), 39.5 (–, 1 C, HMBC: C^{10}), 54.5 (–, 2 C, HMBC: C^{16}), 64.8 (+, 1 C, HSQC: C^{15}), 80.9 (C_q , 2 C, HMBC: C^{18}), 81.4 (C_q , 1 C, HMBC: C^{21}), 170.8 (C_q , 2 C, HMBC: C^{17}), 171.8 (C_q , 1 C, HMBC: C^{20}), 173.0 (C_q , 2 C, HMBC: C^{17}). – **IR** (KBr) [cm^{-1}]: $\tilde{\nu} = 3000, 2927, 2854, 1730, 1649, 1541, 1456, 1368, 1149$. – **MS** (ESI(+), DCM/MeOH + 10 mmol NH_4Ac): m/z (%) = 571.6 (100) [MH^+], 515.5 (8) [$MH^+ - C_4H_8$], 593.6 (5) [MNa^+]. – **Elemental analysis** calcd. (%) for $C_{31}H_{58}N_2O_7$: C 65.23, H 10.24, N 4.91; found C 64.84, H 10.20, N 4.66. – **MF**: $C_{31}H_{58}N_2O_7$ – **FW**: 570.82 g/mol



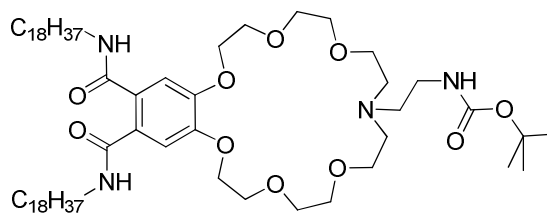
2-(Bis-carboxymethyl-amino)-4-decylcarbamoyl-butyric acid triflate (**9**)

Compound **8** (107 mg, 0.19 mmol) was suspended in TFA (4 mL). The reaction mixture was stirred at room temperature for 20 h. Reaction progress was monitored by TLC (EE). TFA was evaporated in vacuo and the triflate salt of compound **9** was redissolved in water and was lyophilized giving product **9** (98 mg, 0.19 mmol, 100%) as a white hygroscopic solid. **¹H-NMR** (300 MHz; CD₃OD): δ (ppm) = 0.81-0.96 (t, ³J = 6.7 Hz, 3 H, CH₃), 1.18-1.40 (m, 14 H, CH₂), 1.41-1.60 (m, 2 H, CH₂), 1.78-2.17 (m, 2 H, Glu-CH₂), 2.29-2.49 (t, ³J = 7.0 Hz, 2 H, Glu-CH₂), 3.05-3.22 (t, ³J = 7.0 Hz, 2 H, CH₂), 3.42-3.52 (m, 1 H, CH), 3.53-3.73 (m, 4 H, N-CH₂). – **¹³C-NMR** (75 MHz; CD₃OD): δ (ppm) = 14.5 (+, 1 C, CH₃), 23.8 (–, 1 C, CH₂), 27.2 (–, 1 C, CH₂), 28.1 (–, 1 C, CH₂), 30.4 (–, 1 C, CH₂), 30.5 (–, 2 C, CH₂), 30.8 (–, 2 C, CH₂), 33.1 (–, 1 C, CH₂), 33.7 (–, 1 C, CH₂), 40.5 (–, 1 C, CH₂), 54.9 (–, 2 C, N-CH₂), 66.0 (+, 1 C, CH), 175.3 (C_q, 1 C, CONH), 175.5 (C_q, 1 C, CHCOOH), 175.8 (C_q, 2 C, NCH₂COOH). – **IR** (KBr) [cm⁻¹]: $\tilde{\nu}$ = 3340, 3028, 2921, 2852, 2547, 1725, 1643, 1538, 1427, 788, 715. – **MS** (ESI(+), H₂O/MeCN): m/z (%) = 401.2 (100) [M - H⁺], 457.2 (15) [starting material - 2 C₄H₈ + H⁺], 803 (6) [2M-H⁺]. – **MF**: C₁₉H₃₄N₂O₇ · TFA – **FW**: 516.51 g/mol; without TFA: 402.49 g/mol



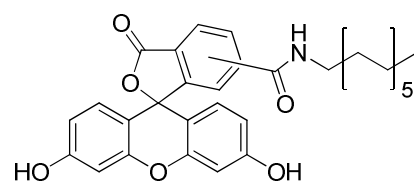
Glu-NTA-2-(Bis-carboxymethyl-amino)-4-decylcarbamoyl-butyric acid (**2**)

Compound **36** (40 mg, 0.08 mmol) and Cu₂(OH)₂CO₃ (8.6 mg, 0.04 mmol) were dissolved in methanol (6 mL). The mixture was stirred at room temperature over night, subsequently for 3 h at 60 h and was filtered immediately. The resulting blue solution was concentrated under reduced pressure, redissolved in water and lyophilized yielding **43** (35 g, 0.06 mmol, 71%) without further purification as a blue solid. **MP**: 173-175 °C. – **IR** (KBr) [cm⁻¹]: $\tilde{\nu}$ = 2925, 2854, 2362, 1724, 1448, 1378, 1240, 1112, 906. – **MS** (ESI(+), H₂O/MeCN): m/z (%) = 462.3 (100) [A⁻], 415.3 (35) [A⁻ - H₂O - CH₃], 374.2 (15) [A⁻ - CO₂]. – **MF**: C₁₉H₃₁N₂O₇CuH(H₂O)₂ · TFA – **FW**: 614.07 g/mol; A⁻ (without TFA, H₂O, H): 463.01 g/mol



14-[2-^{tert}Butyloxycarbonylamino-ethyl]-6,7,9,10,13,14,15,16,18,19,21,22-sodecahydro-12H-5,8,11,17,20,23-hexaoxa-14-aza-benzocycloheicosene-2,3-dicarboxylic acid dioctadecyl amide (**3**)

A solution of **10**^{18, 19} (150 mg, 0.25 mmol) in chloroform (3.5 mL) and DMF (0.5 mL) containing HOBt (70 mg, 0.50 mmol) and EDC (80 mg, 0.50 mmol) was stirred in a nitrogen atmosphere at 0 °C for 30 minutes. Octadecylamine **11** (132 mg, 0.50 mmol) in chloroform (2.0 mL) containing DIPEA (50 mg, 0.07 mL, 0.50 mmol) was added and the mixture was stirred 2 h under nitrogen slowly warming up to ambient temperature. Again HOBt (35 mg, 0.25 mmol) and EDC (40 mg, 0.25 mmol) were added, stirring was continued for 2 h at room temperature, then the solution was heated to 70 °C over night. After cooling to room temperature the solution was filtered over celite and the solvent was removed at reduced pressure. The residue was purified by column chromatography. ¹H-NMR (300 MHz, CDCl₃): δ [ppm] = 0.87 (t, 6 H, 6.3 Hz), 1.18 – 1.35 (m, 60 H), 1.32 – 1.37 (m, 4 H), 1.41 (s, 9 H), 1.55 (m, 4 H), 2.57 (m, 2 H), 2.70 (m, 4 H), 3.01 (m, 2 H), 3.31 (m, 4 H), 3.53 (m, 4 H), 3.66 (m, 4 H), 3.74 (m, 4 H), 3.89 (m, 4 H), 4.21 (m, 4 H), 5.56 (bs, 1 H), 7.15 (s, 2 H); - ¹³C-NMR (75 MHz, CDCl₃): δ [ppm] = 14.1 (+, 1 C), 22.7 (-, 2 C), 27.0 (-, 2 C), 28.5 (+, 3 C), 29.3 – 29.8 (-, 30 C), 31.9 (-, 1 C), 38.1 (-, 1 C), 40.4 (-, 1 C), 53.6 (-, 2 C), 54.4 (-, 1 C), 69.1 (-, 2 C), 69.6 (-, 2 C), 69.6 (-, 2 C), 70.6 (-, 2 C), 71.1 (-, 2 C), 78.7 (C_{quat}, 1 C), 113.8 (+, 2 C), 127.8 (C_{quat}, 2 C), 149.6 (C_{quat}, 2 C), 156.2 (C_{quat}, 1 C), 168.9 (C_{quat}, 2 C); - IR (neat): ν (cm⁻¹) = 3314 (m), 3264 (m), 2948 (s), 2849 (s), 1687 (m), 1648 (m), 1626 (m), 1538 (m), 1506 (m), 1461 (m), 1338 (m), 1280 (s), 1203 (m), 1124 (s), 1106 (m), 1059 (m), 974 (m), 874 (m), 725 (m), 654 (m); - MS (ESI-MS, CH₂Cl₂/MeOH + 10 mmol NH₄OAc): e/z (%) = 1090.0 (100, MH⁺); - MF: C₆₃H₁₁₆N₄O₁₀ - FW: 1089.65 g/mol



N-dodecyl-3',6'-dihydroxy-3-oxo-3H-spiro[isobenzofuran-1,9'-xanthene]-6-carboxamide (**4**, mixture of 5' and 6' isomer):

HOBt (119 mg, 0.88 mmol) and DIPEA (217 mg, 1.68 mmol) were added to a solution of Carboxyfluorescein **12** (300 mg, 0.80 mmol, mixture of 5' and 6' isomer) in 4 mL DMF.

Cooling the mixture in an ice bath was followed by addition of DCC (181 mg, 0.88 mmol) and after 15 minutes dodecan-1-amine **13** (148 mg, 0.80 mmol). The reaction mixture was stirred overnight and DMF removed completely. Addition of 20 mL NaHSO₄ solution (5% w/w) precipitated an orange solid (268 mg, 56%) which was filtered off and dried under high vacuum. **MP**: 234 °C (Decomp.). – **¹H NMR** (300 MHz, MeOD): 0.88 (t, J = 6.19 Hz, 3 H), 1.20 – 1.70 (m, 20 H), 3.25 – 3.50 (m, 2 H), 6.45 – 6.75 (m, 6 H), 7.20 – 8.45 (m, 3 H). – **LC-MS**: Column: Phenomenex Luna C18, 2.5μ; 50 x 2 mm HST; flow: 0.40 ml/min; solvent A (water + 0.1% TFA), solvent B (MeCN); gradient: 0 (min) [95% A + 5% B]; 8 (min) [2% A + 98% B]; 11 (min) [2% A + 98% B]; 12 (min) [95% A + 5% B]; 15 (min.) [95% A + 5% B]. **MS**: *m/z* (%) [*t*_{r1} = 9.09 min.; *t*_{r2} = 9.20]: 544 (100, MH⁺).

Vesicle preparation

In small glass reaction vessels 1 - 5 μmol of DSPC were dissolved in chloroform and optionally 5 mol% of dissolved compounds **1**, **2**, **3**, **4** and **5** were added and mixed. The solvent was completely removed under reduced pressure and an appropriate amount of buffer (HEPES 25 mM, pH 7.4) was added to obtain lipid concentrations of 1 - 2 mM. Heating to 75 °C and vigorous shaking for 5 - 10 minutes yielded a turbid multi-lamellar vesicle suspension. Small uni-lamellar dispersions were obtained by extrusion through 100 nm-pore size polycarbonate membranes with a LiposoFast liposome extruder from Avestin.⁴⁵

Vesicle dispersions were separated from low molecular weight solutes on minicolumns of Sephadex LH-20 gel filtration media by a previously described procedure.⁴⁶

Binding studies

For all binding studies the receptor concentration refers to the outer surface exposed binding sites, as only these should be accessible, with the assumption that embedded compounds distribute equally in both layers of the vesicle membrane.⁴⁷ The ratio of outer and inner surface of the respective vesicles was calculated using the hydrodynamic diameters obtained from dynamic light scattering⁴⁸ and the assumption that the bilayer thickness for the prepared vesicles amounts to 5 nm.^{49, 50}

All titrations were carried out at 25 °C in HEPES buffer (25 mM, pH 7.4) and corrected for dilution. Binding affinities were determined by non-linear fitting using Origin 8 software.

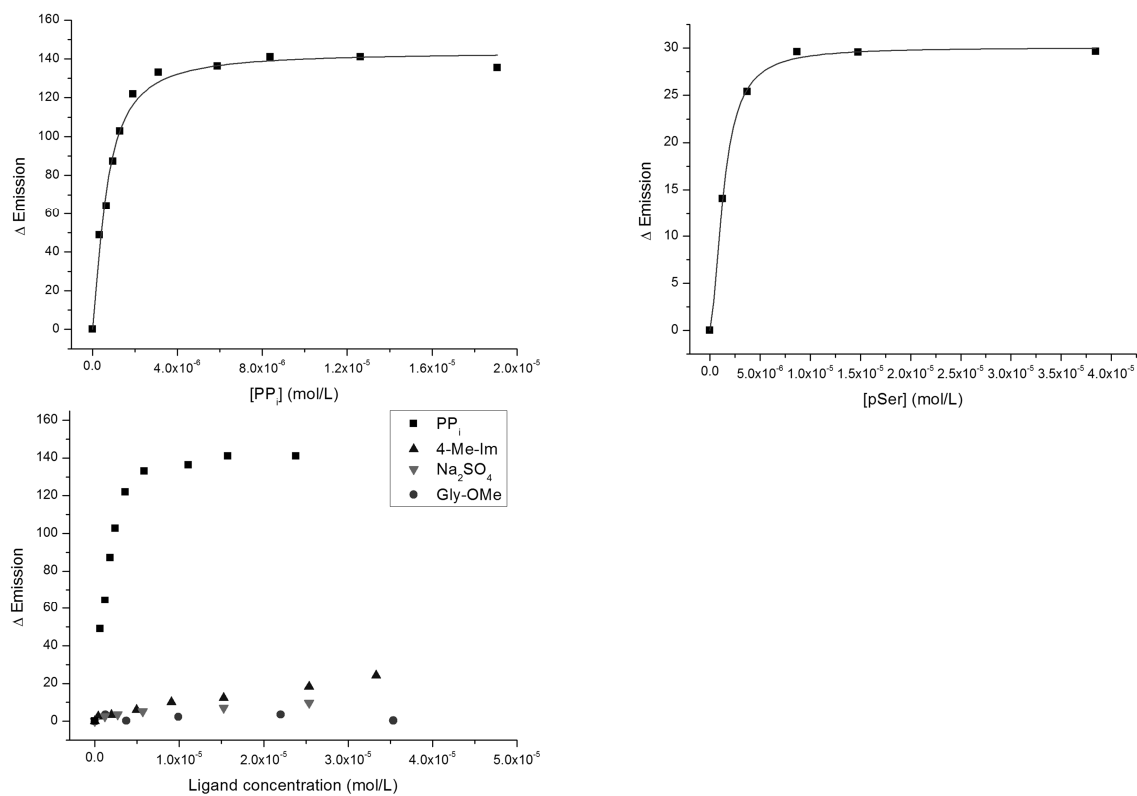


Figure S1. Fluorescence emission titrations of LVR1-5 with different ligands.

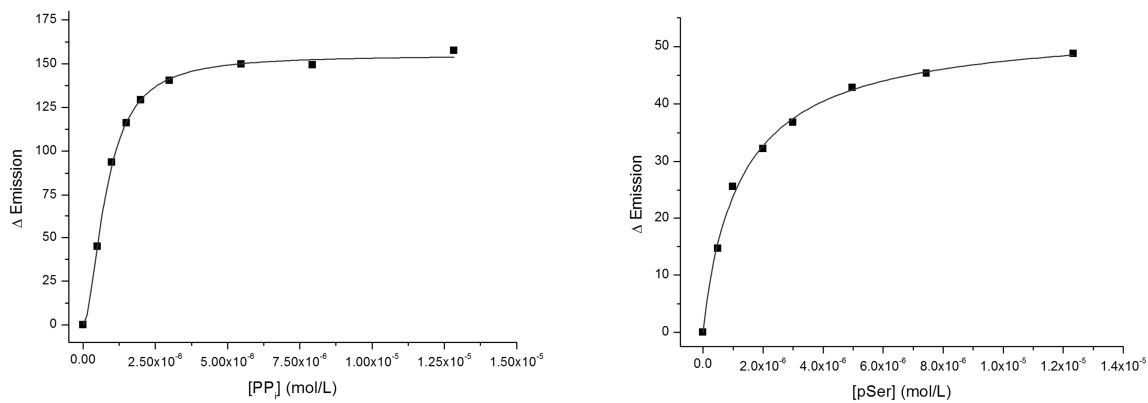


Figure S2. Fluorescence emission titrations of LVR1-4 with different ligands.

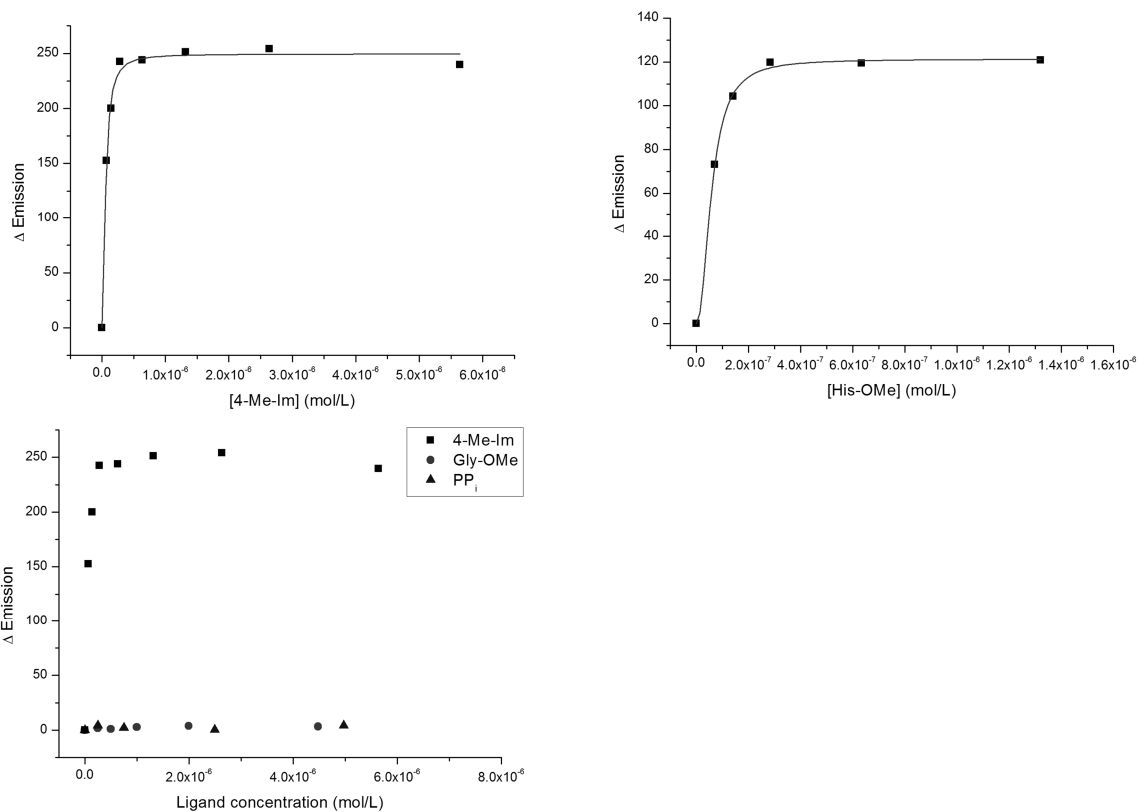


Figure S3. Fluorescence emission titrations of LVR2-4 with different ligands.

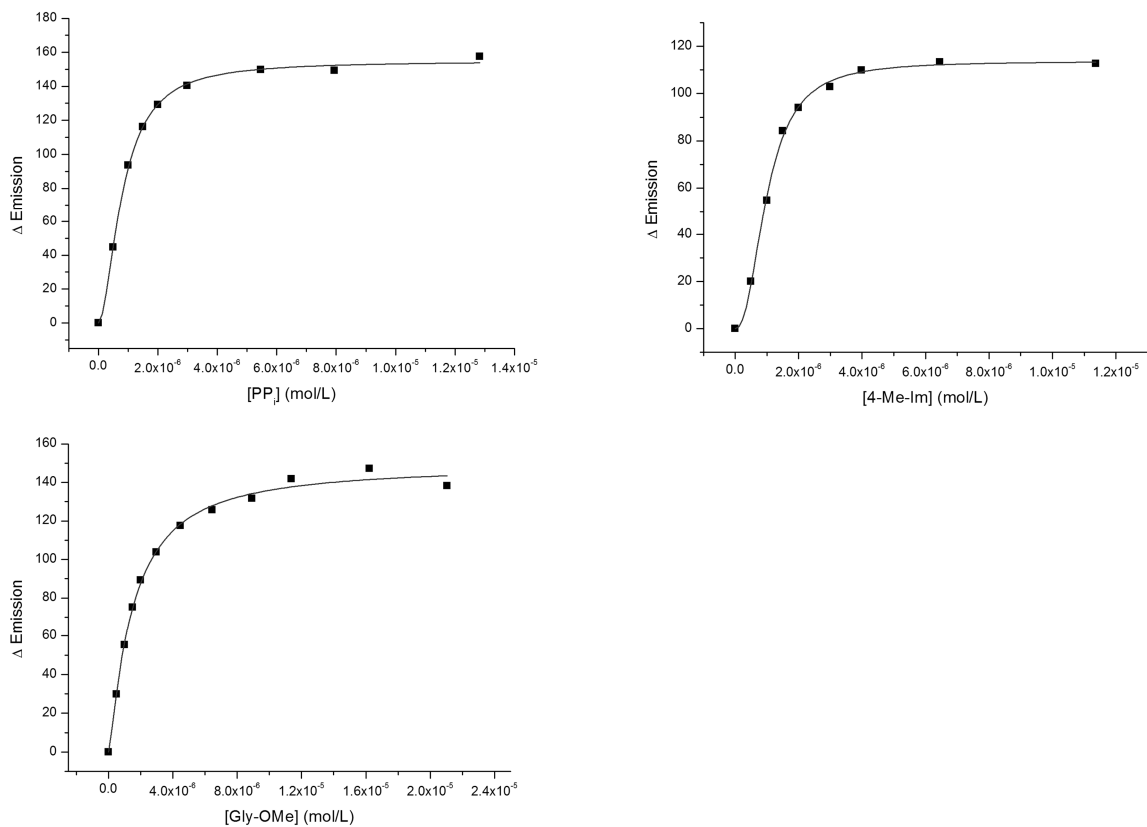


Figure S4. Fluorescence emission titrations of LVR1-2-3-4 with different ligands.

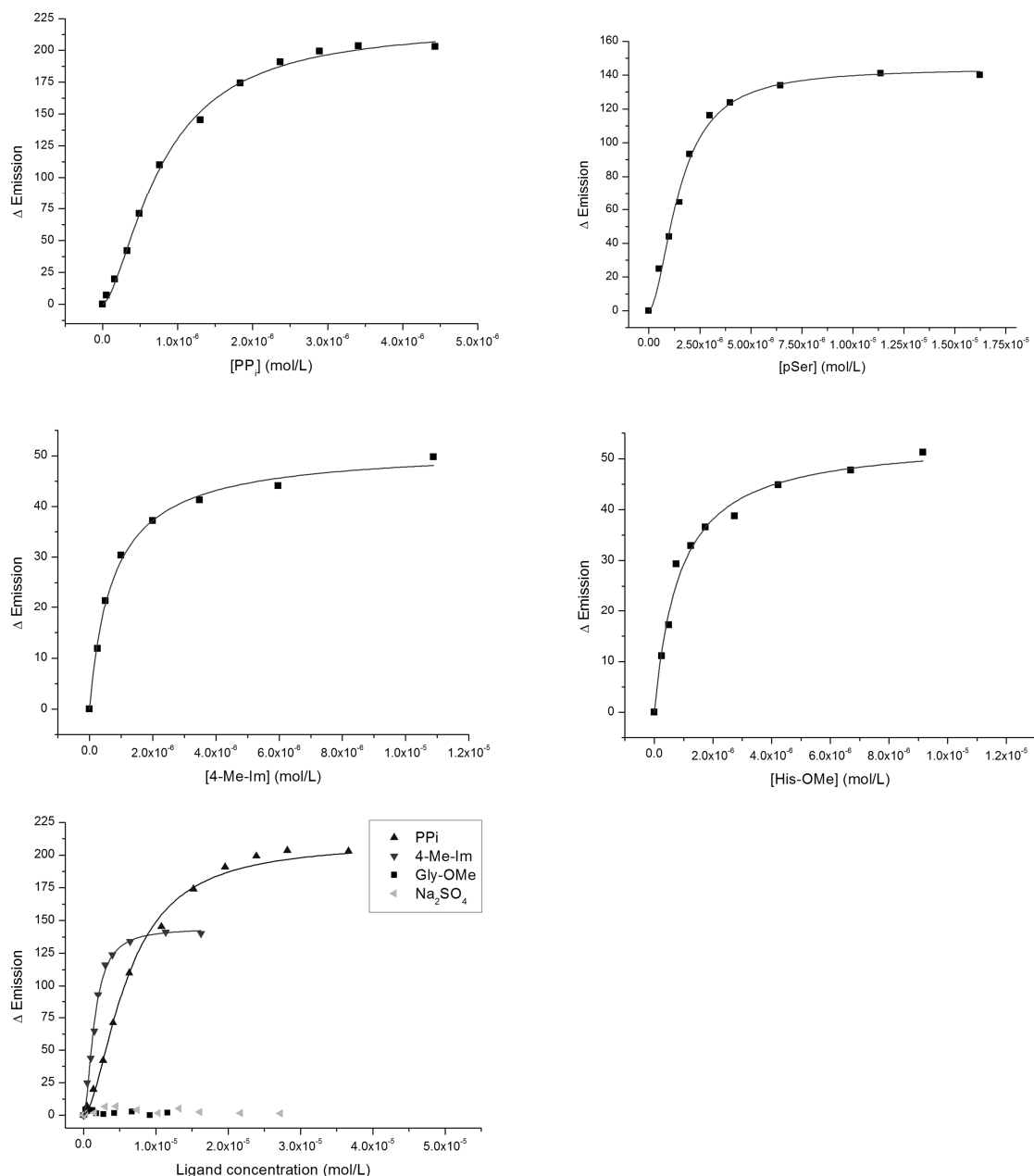


Figure S5. Fluorescence emission titrations of **LVR1-2-4** with different ligands.

Reversibility of binding events

To demonstrate the reversibility of the receptor-ligand binding on the vesicular surface and the vesicle reuse they were passed over small spin columns filled with size exclusion chromatography gel⁴⁶ after emission titration and saturation with analytes. The procedure separates the vesicles from the analyte ions or molecules. The emission titrations were then repeated with the restored vesicles under the same conditions as before. The results for **LVR1-2-4** are depicted in Figure 9 (left) and clearly show that obtained binding isotherms before (red) and after (blue) the size exclusion column are nearly identical with only a slight

decrease in fluorescence output. The derived binding constant for 4-Me-Im remains unchanged within the error of the experiment ($\log K = 6.2$ before, respectively 6.1 after the size exclusion chromatography). The results for PP_i were analogous (Figure 9 right).

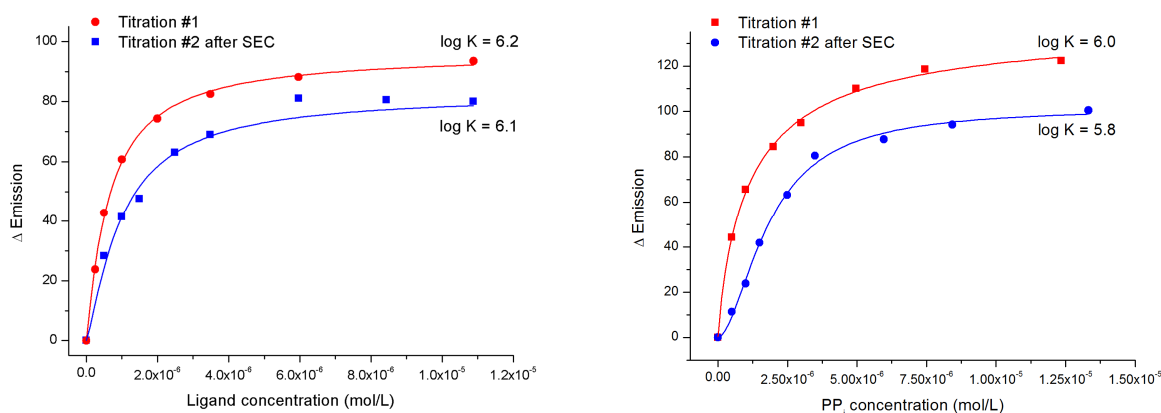


Figure S6. (Left) Emission titrations of **LVR1-2-4** with 4-Me-Im before (red) and after (blue) ligand saturation and subsequent removal by size exclusion chromatography; (Right) Analogous experiment using PP_i instead of 4-Me-Im.

Mechanistic studies

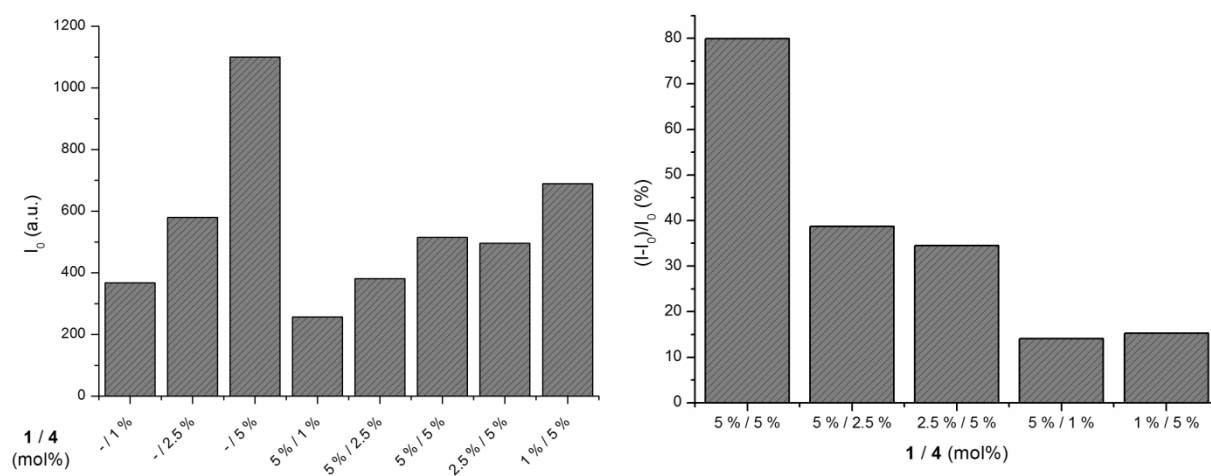


Figure S7. Absolute emission intensities (left) of **LVR-1,4** (5×10^{-6} M dye) at different receptor/dye ratios and corresponding relative changes (right) in the presence of 10 eq. PP_i .

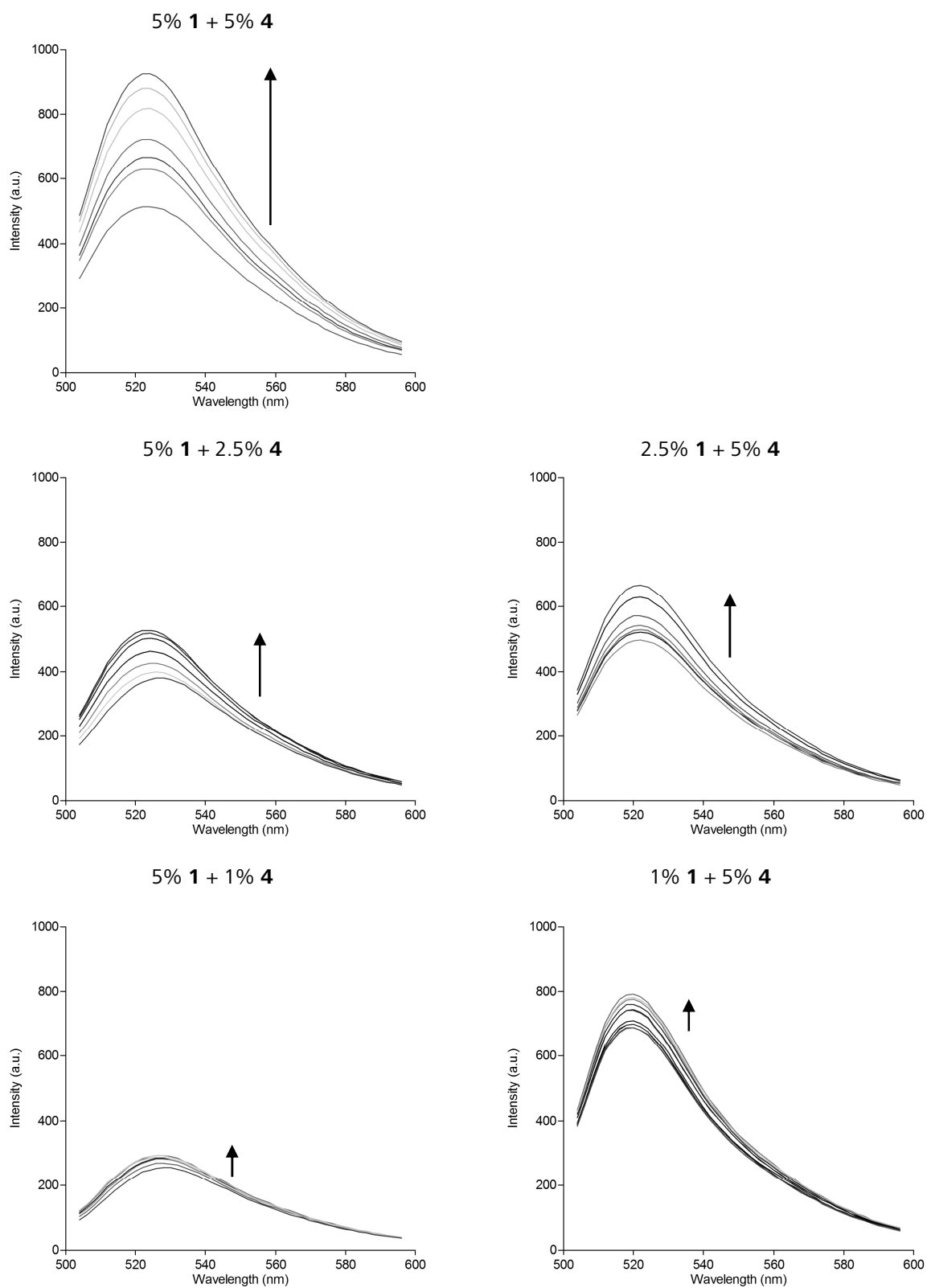


Figure S8. Dependence of emission response on receptor and dye concentration: Fluorescence spectra of **LVR-1,4** (5×10^{-6} M) at different receptor/dye ratios in the presence of increasing amounts of PPi (max 10 eq).

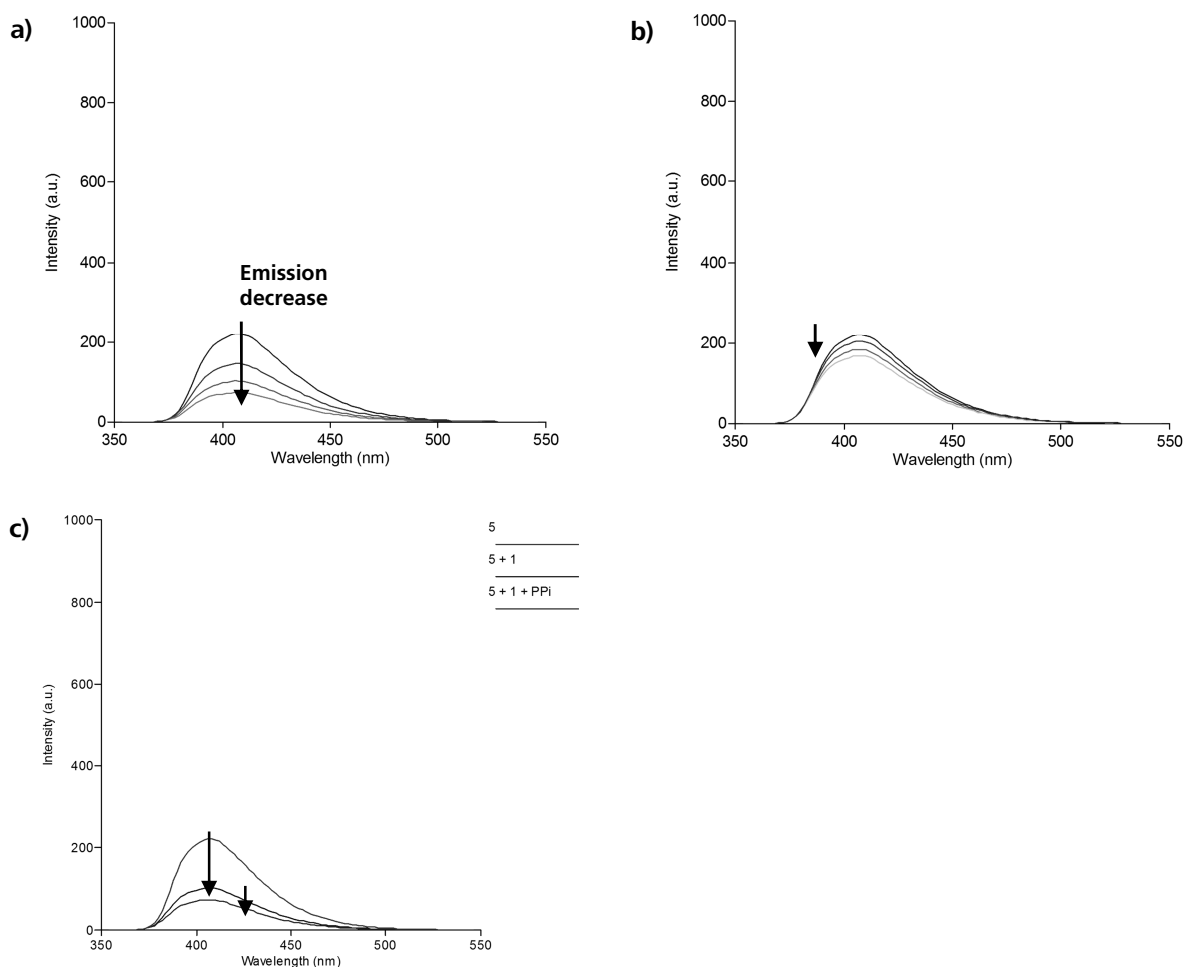


Figure S9. Receptor-dye interactions in non-polar organic solvents (CHCl₃:MeCN 10:1): (a) Dye **5** (5 × 10⁻⁵ M) vs. receptor **1** (0.5 - 1.5 eq); (b) Control (solvent addition only); (c) "Displacement" with PPi (> 100 eq. added as solid).

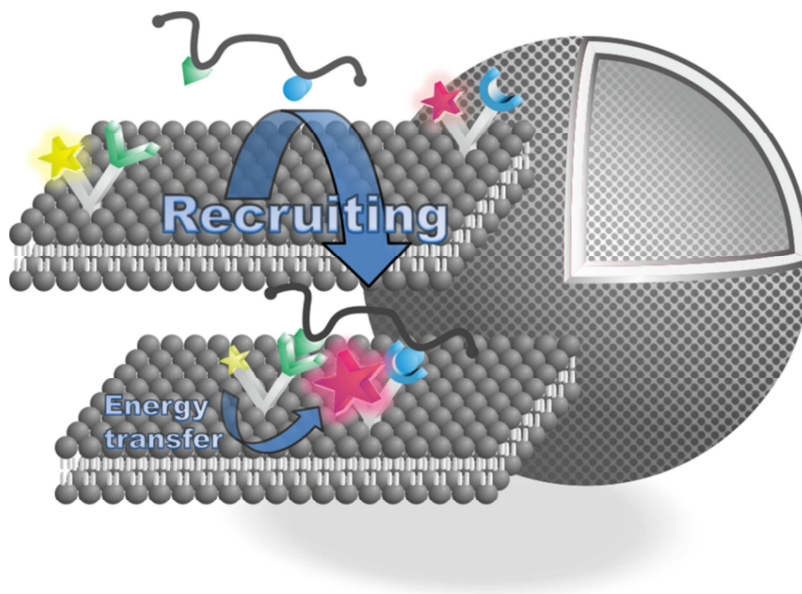
References

1. M. Kruppa and B. König, *Chem. Rev.*, 2006, **106**, 3520-3560.
2. A. Ojida, Y. Mito-oka, M. Inoue and I. Hamachi, *J. Am. Chem. Soc.*, 2002, **124**, 6256-6258.
3. S. K. Kim, D. H. Lee, J. I. Hong and J. Yoon, *Acc. Chem. Res.*, 2009, **42**, 23-31.
4. R. Martinez-Manez and F. Sancenon, *Chem. Rev.*, 2003, **103**, 4419-4476.
5. B. T. Nguyen and E. V. Anslyn, *Coord. Chem. Rev.*, 2006, **250**, 3118-3127.
6. D. A. Jose, S. Stadlbauer and B. König, *Chem. Eur. J.*, 2009, **15**, 7404-7412.
7. D. A. Jose and B. König, *Org. Biomol. Chem.*, 2010, **8**, 655-662.
8. B. Gruber, S. Stadlbauer, K. Woinaroschy and B. König, *Org. Biomol. Chem.*, 2010, **8**, 3704-3714.
9. T. Parasassi, E. K. Krasnowska, L. Bagatolli and E. Gratton, *J. Fluoresc.*, 1998, **8**, 365-373.

10. T. Takeuchi and S. Matile, *J. Am. Chem. Soc.*, 2009, **131**, 18048-18049.
11. S. Matile, H. Tanaka and S. Litvinchuk, in *Top. Curr. Chem.*, Springer Berlin / Heidelberg, 2007, pp. 219-250.
12. M. M. Tedesco, B. Ghebremariam, N. Sakai and S. Matile, *Angew. Chem. Int. Ed.*, 1999, **38**, 540-543.
13. S. Mizukami, T. Nagano, Y. Urano, A. Odani and K. Kikuchi, *J. Am. Chem. Soc.*, 2002, **124**, 3920-3925.
14. S. Aoki, M. Zulkefeli, M. Shiro, M. Kohsako, K. Takeda and E. Kimura, *J. Am. Chem. Soc.*, 2005, **127**, 9129-9139.
15. E. Kimura, T. Shiota, T. Koike, M. Shiro and M. Kodama, *J. Am. Chem. Soc.*, 1990, **112**, 5805-5811.
16. T. Koike, S. Kajitani, I. Nakamura, E. Kimura and M. Shiro, *J. Am. Chem. Soc.*, 1995, **117**, 1210-1219.
17. E. Kimura, S. Aoki, T. Koike and M. Shiro, *J. Am. Chem. Soc.*, 1997, **119**, 3068-3076.
18. C. P. Mandl and B. König, *J. Org. Chem.*, 2005, **70**, 670-674.
19. A. Späth and B. König, *Tetrahedron*, 2009, **65**, 690-695.
20. D. S. Turygin, M. Subat, O. A. Raitman, V. V. Arslanov, B. König and M. A. Kalinina, *Angew. Chem. Int. Ed.*, 2006, **45**, 5340-5344.
21. M. Przybylo, A. Olzynska, S. Han, A. Ozyhar and M. Langner, *Biophys. Chem.*, 2007, **129**, 120-125.
22. M. Langner, H. Pruchnik and K. Kubica, *Z. Naturforsch., C: Biosci.*, 2000, **55**, 418-424.
23. A. Riechers, F. Schmidt, S. Stadlbauer and B. König, *Bioconjugate Chem.*, 2009, **20**, 804-807.
24. To some extent an interaction between receptors and dye/analyte molecules could be modeled in a "bad" non-polar organic solvent mimicking the environment in the bilayer membrane (see SI).
25. I. D. Alves, Z. Salamon, V. J. Hruby and G. Tollin, *Biochemistry (Mosc)*. 2005, **44**, 9168-9178.
26. E. L. Elson, E. Fried, J. E. Dolbow and G. M. Genin, *Annu. Rev. Biophys.*, 2010, **39**, 207-226.
27. K. Simons and W. L. C. Vaz, *Annu. Rev. Biophys. Biomol. Struct.*, 2004, **33**, 269-295.
28. M. Langner, J. Gabrielska and S. A. Przystalski, *Appl. Organomet. Chem.*, 2000, **14**, 25-33.
29. M. Langner and H. Kleszczynska, *Cell. Mol. Biol. Lett.*, 1997, **2**, 15-24.
30. The different responses can be explained on the basis of our suggested hypothesis. The carboxyfluorescein derived dye presents rather bulky head groups providing a comparatively large free volume, which contradicts to a tight packing in homogeneous phase. When expelled from the receptor-ligand proximity during patch segregation, the dye's molecular structure suggests that it tends to distribute more or less separately within the lipid-enriched phase surrounding the patch. This results in the emission increase due to the enhanced sterical "freedom" of the dye. The coumarin derived dye presents relatively compact aromatic heads, which can stack and form tightly arranged assemblies around the phosphate-bound patch during segregation that causes self-quenching.

31. I. Paunovic, R. Schulin and B. Nowack, *J. Chromatogr. A*, 2005, **1100**, 176-184.
32. A. N. Kapanidis, Y. W. Ebricht and R. H. Ebricht, *J. Am. Chem. Soc.*, 2001, **123**, 12123-12125.
33. C. R. Goldsmith, J. Jaworski, M. Sheng and S. J. Lippard, *J. Am. Chem. Soc.*, 2006, **128**, 418-419.
34. This refers to the charge of the coordinated metal ion in the amphiphilic ligand neglecting the counter-ion.
35. D. Hopgood and R. J. Angelici, *J. Am. Chem. Soc.*, 1968, **90**, 2508-2513.
36. At this moment data for detailed phase diagram plotting are not fully obtained, we actively pursue this goal.
37. K. Ariga and T. Kunitake, *Acc. Chem. Res.*, 1998, **31**, 371-378.
38. R. Zadnand and T. Schrader, *J. Am. Chem. Soc.*, 2005, **127**, 904-915.
39. S. Kolusheva, O. Molt, M. Herm, T. Schrader and R. Jelinek, *J. Am. Chem. Soc.*, 2005, **127**, 10000-10001.
40. K. Ariga, A. Kamino, X. Cha and T. Kunitake, *Langmuir*, 1999, **15**, 3875-3885.
41. N. Sakai and S. Matile, *J. Am. Chem. Soc.*, 2003, **125**, 14348-14356.
42. Author collective, *Organikum, 17th Edition*, VEB Deutscher Verlag der Wissenschaften, Berlin, 1988.
43. S. Hünig, G. Märkl and J. Sauer, *Einführung in die apparativen Methoden in der Organischen Chemie, 2nd Edition*, Würzburg / Regensburg, 1994.
44. S. Lata, A. Reichel, R. Brock, R. Tampe and J. Piehler, *J. Am. Chem. Soc.*, 2005, **127**, 10205-10215.
45. R. C. MacDonald, R. I. MacDonald, B. P. M. Menco, K. Takeshita, N. K. Subbarao and L.-r. Hu, *Biochim. Biophys. Acta*, 1991, **1061**, 297-303.
46. D. W. Fry, J. C. White and I. D. Goldman, *Anal. Biochem.*, 1978, **90**, 809-815.
47. A. I. Elegbede, M. K. Haldar, S. Manokaran, J. Kooren, B. C. Roy, S. Mallik and D. K. Srivastava, *Chem. Commun.*, 2007, 3377-3379.
48. A. J. Jin, D. Huster, K. Gawrisch and R. Nossal, *Eur. Biophys. J.*, 1999, **28**, 187-199.
49. J. F. Nagle and S. Tristram-Nagle, *Biochim. Biophys. Acta*, 2000, **1469**, 159-195.
50. P. Balgavy, M. Dubnickova, N. Kucerka, M. A. Kiselev, S. P. Yaradaikin and D. Uhrikova, *Biochim. Biophys. Acta*, 2001, **1512**, 40-52.

CHAPTER 4

DYNAMIC INTERFACE IMPRINTING: HIGH AFFINITY PEPTIDE BINDING SITES ASSEMBLED BY ANALYTE-INDUCED RECRUITING OF MEMBRANE RECEPTORS

Dynamic molecular recognition events at biological membrane receptors play a key role in cell signalling. We have prepared artificial membranes with embedded synthetic receptors which dynamically arrange and selectively respond to external stimuli like small peptide ligands.

This chapter has been published:

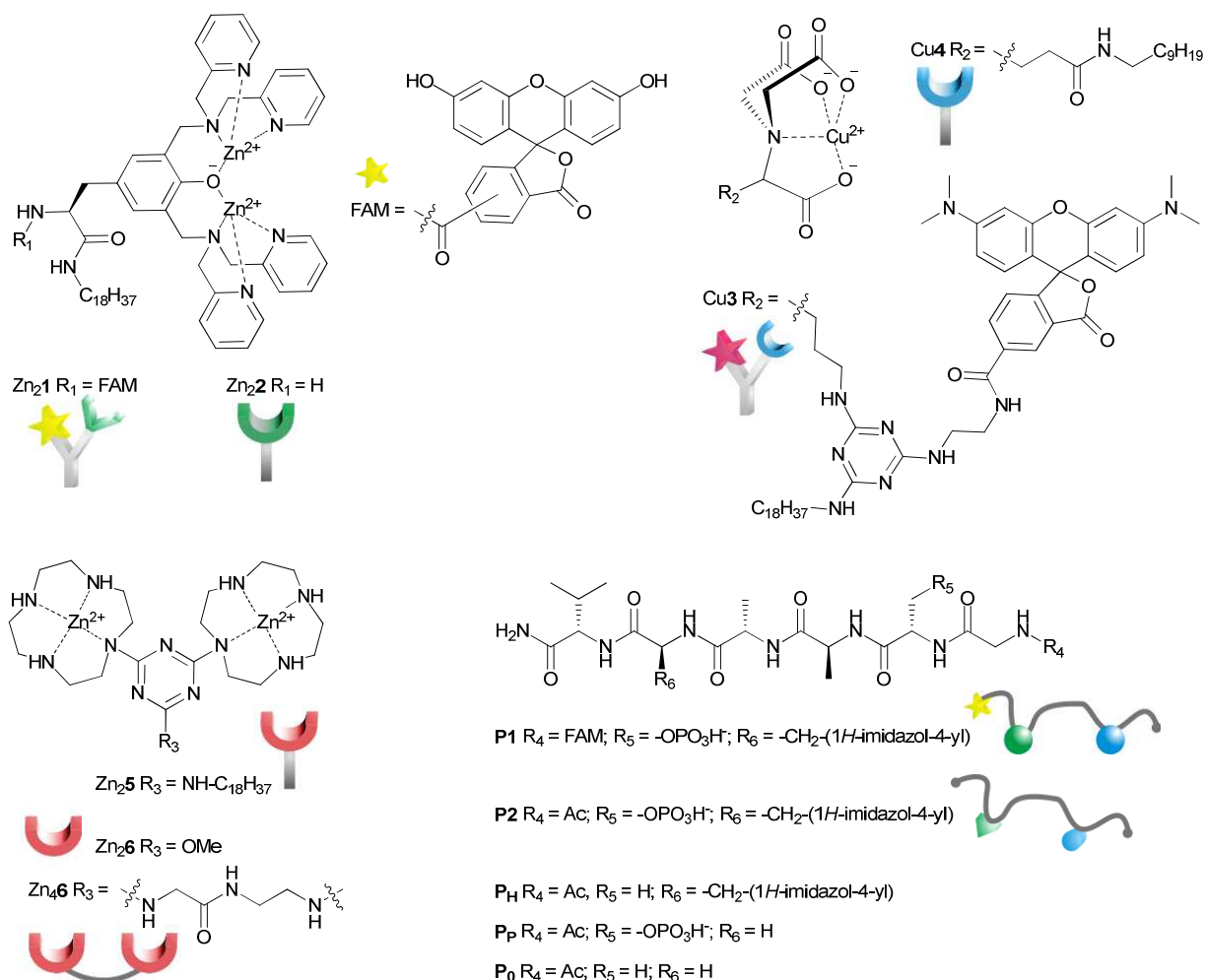
B. Gruber, S. Balk, S. Stadlbauer and B. König, *Angew. Chem.* **2012**, DOI: 10.1002/ange.201205701; *Angew. Chem. Int. Ed.*, **2012**, DOI: 10.1002/anie.201205701 (Hot Paper).

Author contributions:

BG designed experiments, synthesized vesicles, performed binding studies and wrote the manuscript; SB synthesized compound **Cu3** and performed FRET binding studies; SS synthesized compounds **Cu4**, **Zn21**, **Zn22**; BK supervised the project and is corresponding author.

Introduction

Molecular recognition between membrane-associated receptors and external ligands as stimuli is important for many biological processes.¹⁻³ The dynamic formation of domains and the clustering of receptors in fluid membranes play a key role e.g. in signal transduction leading to highly specific binding of competing multivalent ligands.⁴⁻⁶



Scheme 1. Structures of synthetic receptors and ligands (counterions omitted).

Various model systems for biological membranes have been developed to understand and mimic multivalent interactions at interfaces⁷⁻¹² as well as for applications in delivery, sensing and catalysis.¹³⁻¹⁸ The principle of template-guided assembly has also been extensively exploited in molecular imprinting,^{19, 20} but the non-covalent arrangement of binding sites in precisely defined distances still remains a challenge. We have investigated a concept that mimics immunological synapses, where receptors are recruited at a membrane interface, spatially organized by the binding partner and this orientation triggers a specific response.²¹⁻²³ Our vesicles with membrane-embedded luminescent receptors produce a characteristic optical response in the presence of small peptides as external ligands.

Depending on the functional groups present in the peptide, suitable receptors with complementary binding sites are recruited and arranged in the fluid membrane, which triggers a FRET signal.

Results and Discussion

We have previously reported on the recognition of small biomolecules and phosphorylated proteins by multi-site interactions^{24, 25} at the lipid-water interface using synthetic vesicle membranes with embedded artificial receptors based on transition metal complexes of 1,4,7,10-tetraazacyclododecane (cyclen) and nitrilotriacetic acid (NTA). We now expand this concept to the dynamic recruiting of synthetic receptors allowing the multivalent recognition of phosphorylated peptides. The selective recognition of phospho-serine (pSer) and histidine (His) moieties in model-peptide **P1** by metal-complex binding sites was investigated in a previous study in homogeneous solution.²⁶ It was found that in buffered aqueous solution Zn(II)-cyclen receptor $Zn_2\mathbf{6}$ binds peptide **P1** with $\lg K = 4.8$, while dimer $Zn_4\mathbf{6}$, allowing a simultaneous two-prong interaction to pSer and His, shows an affinity of $\lg K = 7.5$ (see Table 1, entries 1 and 2 and Supporting Information). Instead of covalently connecting two receptor sites, as in $Zn_4\mathbf{6}$, distinct binding sites are now simply embedded in synthetic lipid bilayers. Recruiting and self-organization by the peptide ligand allows the divalent binding of both pSer and His residues of **P1** at the membrane interface.

First we embedded $Zn_2\mathbf{5}$ (1 mol%) in vesicular lipid bilayers from 1,2-distearoyl-sn-glycero-3-phosphocholine (DSPC) using previously reported procedures (see Supporting Information). The emission intensity of peptide **P1** increases significantly upon binding to the surface receptors (see SI) and a binding constant of $\lg K = 5.9$ (Table 1, entry 3) at ambient temperature was derived. This value is in good agreement with the recognition of pSer by a single $Zn_2\mathbf{5}$ receptor²⁴ and reasonable, because DSPC's high phase transition temperature (54 °C)²⁷ restricts diffusion and thus participation of more than a single metal complex binding site in the peptide recognition (cf. Figure 1, Top). Binding affinities could only be enhanced by drastically increasing the vesicle receptor loading to 10 mol% (Table 1, entry 4) resulting in the formation of tightly packed metal complex patches.¹⁶ However, replacing the saturated DSPC lipid by unsaturated 1,2-dioleoyl-sn-glycero-3-phosphocholine (DOPC), which has a much lower transition temperature of -20 °C,²⁷ leads to an increase in peptide **P1** binding affinity by more than two orders of magnitude (Table 1, entry 5). The embedded receptor sites can now diffuse in the membrane at room temperature allowing complex formation of one **P1** with two $Zn_2\mathbf{5}$ units by a dynamic assembly process (Figure 1, Top). Unchanged particle sizes determined by dynamic light scattering (Supporting Information, Figure S11) confirm binding of the peptide to receptors of one vesicle (intra-

membrane binding mode) and excludes peptide crosslinking of different vesicles (inter-membrane binding).

Entry	Lipid	Receptor	Mol%	Lg K
1	-	Zn ₂ 6	-	4.8 ^a
2	-	Zn ₄ 6	-	7.5 ^a
3	DSPC	Zn ₂ 5	1	5.9
4	DSPC	Zn ₂ 5	10	8.1
5	DOPC	Zn ₂ 5	1	8.6
6	DSPC	Zn ₂ 2	1	6.2
7	DSPC	Cu4	1	5.0
8	DSPC	Zn ₂ 2 + Cu4	1 (each)	6.3
9	DOPC	Zn ₂ 2	1	5.5
10	DOPC	Cu4	1	5.8
11	DOPC	Zn ₂ 2 + Cu4	1 (each)	8.8

^a from Ref [26]

Table 1. Summary of apparent binding constants for peptide **P1** by synthetic receptors in homogeneous solution (entry 1 and 2) and embedded in vesicle membranes (HEPES buffer, pH 7.4, 25 °C).

The experiments show that analyte induced recruiting of binding sites in a fluid membrane leads to higher binding affinities due to multipoint interaction. Next, vesicle membranes with two different embedded receptors, which bind selectively either pSer or His of **P1**, were investigated. The synthesis of amphiphilic Cu(II)-NTA complex **Cu4** for the recognition of histidine was reported previously,²⁴ the synthesis of the amphiphilic Zn(II)-3,5-bis-[(bis-pyridin-2-ylmethyl-amino)-methyl]-4-hydroxy-phenyl (DPA) complex **Zn₂2** for the selective recognition of phosphate²⁸ is described in the Supporting Information. Stable metal complex-doped DOPC and DSPC vesicle membranes were prepared using **Zn₂2** or **Cu4** and a mixture of both (1 mol% each). For DSPC membranes with one type of receptor embedded the emission titrations with **P1** revealed monovalent binding either to Zn-DPA or to Cu-NTA coordination,²⁹ with lg *K* = 5.0 and 6.2, resp. (Table 1, entries 6 and 7). Job's plots with **P1** as limiting reagent confirm the 1:1 stoichiometry of the binding event (Figure S18). Combining both receptors in gel-phase DSPC-membranes (Figure 1, Bottom) does not increase the binding affinity for peptide **P1** (lg *K* = 6.3; Table 1, entries 6, 7, 8). The binding isotherm for the receptor vesicles bearing both complexes resembles the average of the binding properties of the individual receptor vesicles (see SI for data). This is explained by a random, but fixed position of lipid bilayer embedded metal complex receptors, which prevents the formation of a ternary **Zn₂2-P1-Cu4** complex (see SI for Job's plots). DOPC membranes, in contrast, show a completely different behaviour: Whereas vesicles with either **Zn₂2** or **Cu4** as embedded receptors give similar binding isotherms and affinity constants (lg *K* = 5.5 and

5.8, resp.; Table 1, entries 9, 10), the liquid-crystalline membrane containing both receptor binding sites shows a significantly higher affinity for peptide **P1** in the nanomolar range ($\lg K = 8.8$, Table 1, entry 11 and Figure 1, bottom). We explain this by the divalent binding of **P1** by a heterodimeric Zn_2 - and Cu-receptor assembly in the fluid lipid bilayer (cf. Figure 1, Bottom) resulting from peptide induced self-organization of the membrane receptors. The Job's plot analysis (Figure S19) supports this conclusion.

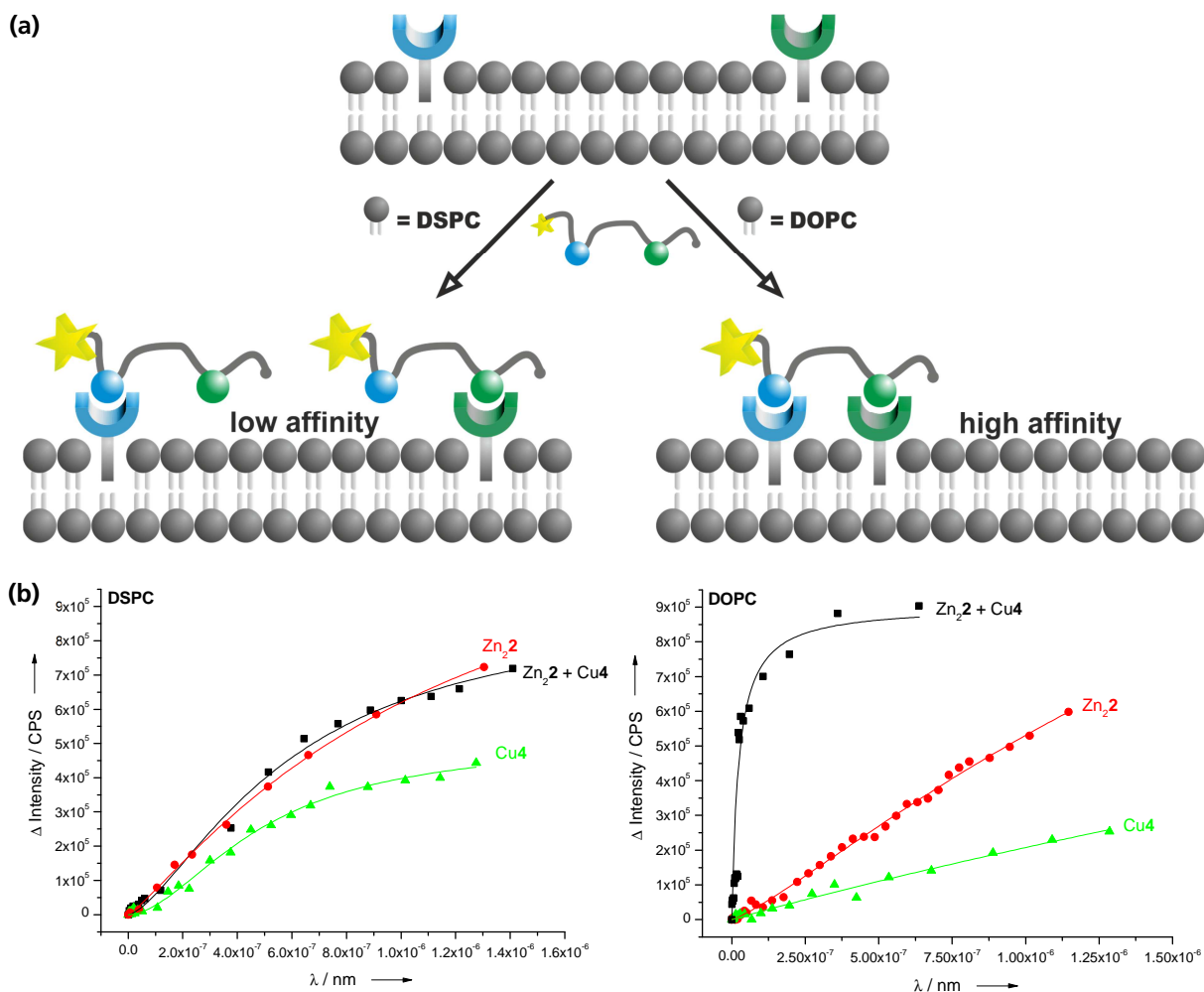


Figure 1. (a) (Top) Schematic receptor assembly in vesicle membranes: Fixed receptors in gel-phase DSPC-membranes vs. analyte-induced clustering in fluid DOPC-membranes; (b) Emission titrations of **P1** vs. DSPC and DOPC- membranes containing Zn_2 , Cu_3 or both receptors.

For bioanalytical applications, the labelling of the peptide analyte must be avoided. Therefore amphiphilic receptor binding sites that signal the presence of the target analyte by induced FRET were developed: $Zn(II)$ -DPA complex (Zn_2) is labelled with carboxyfluorescein (FAM) and $Cu(II)$ -NTA complex Cu_3 is rhodamine (TMR) labelled. FRET techniques are widely used in molecular biology to measure distances within bio-molecules or to explore membrane structures.³⁰ We use the FRET signal, which is induced by the close distance of the membrane-embedded luminescent binding sites to signal the presence of peptide **P2**, which in contrast to **P1**, does not carry a fluorescent label. Divalent binding of

P2 to the membrane embedded binding sites recruits **Zn₂1** and **Cu3** into close proximity and therefore within the Förster distance of 5.5 nm³¹ resulting in a FRET signal as optical output (Figure 2, Top).³²

The vesicles responded to the presence of the target peptide **P2** with a significant FRET-signature. Formation of a **Zn₂1-P2-Cu3** ternary complex leads to energy transfer of the donor label FAM at 490 nm to the acceptor label TMR at 580 nm (Figures 2, Bottom and S22). However, an excess of the target peptide is necessary to reach the maximum energy transfer. Control experiments with monovalent ligands (**P_P**, **P_H** and **P₀**) did not change the observed emission spectra significantly (Figure S23). We exclude inter-vesicular FRET via crosslinking of distinct vesicles as the solution particle size remains unchanged in the presence of **P2** (Figures S24, 25). Additionally, vesicles were purified by size exclusion chromatography before binding experiments to remove traces of amphiphilic receptors or micellar aggregates from the solution and the concentrations of the embedded receptors were verified by Zn- and Cu-element analysis using ICP-AES (see SI).³³

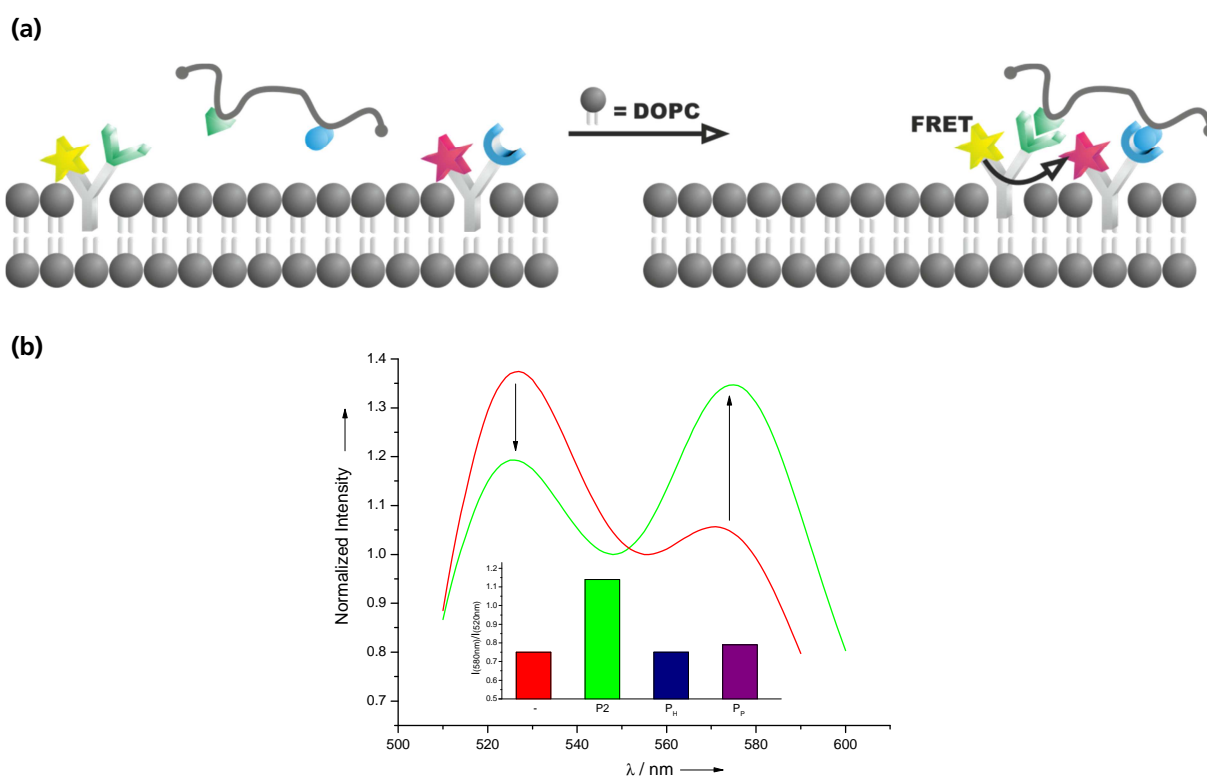


Figure 2. (a) Schematic recruiting of labelled membrane receptors by a peptide ligand resulting in a FRET signal; (b) Fluorescence spectra of DOPC vesicles containing labelled receptors **Zn₂1** + **Cu3** (1 mol% each) in the absence (red) and presence (green) of peptide **P2**. Relative FRET emission ratio ($I_{580\text{nm}}/I_{520\text{nm}}$) of **P2** and monovalent **P_H** and **P_P** as control (inset).

As additional control experiments, DOPC and DSPC vesicles with only one of the two binding sites were prepared and used for emission titrations with increasing amounts of corresponding ligands (pSer/**P_P** for **Zn₂1** and His/**P_H** for **Cu3**). As expected, no significant change in the optical properties of the fluorescent receptor-vesicles was observed (Figure

S21). DSPC vesicles with both co-embedded receptors Zn₂1 and Cu3 (0.1 mol% each) show a small energy transfer between the FAM- and TMR-labels in the absence of the peptide ligand (Figure S20), which might be explained by the partial formation of Zn₂1/Cu3 heterodimers. Upon addition of any mono- or divalent ligand no change in emission was detected, as the gel-phase state of the DSPC membranes at room temperature limits the diffusion of the embedded metal complexes (Figure S22).

Conclusion

In conclusion, we demonstrated the specific recognition of peptides by dynamic interface imprinting of synthetic binding sites embedded in vesicle membranes. The amphiphilic metal complex binding sites are recruited in the membrane by the target peptide resulting in multivalent interactions and nanomolar binding affinity. The use of amphiphilic binding sites with FRET pair chromophores, leads to self-organization of a specific analyte epitope at the lipid-water interface and a FRET signal indicating the presence of the target analyte.

The experimental data prove that dynamic binding site recruitment in fluid membranes by analytes (dynamic interface imprinting, DII) leads to the formation of high affinity epitopes. The process allows the specific detection of functional groups in peptides with nanomolar affinity. To further improve the sensitivity and selectivity of functionalized luminescent vesicles in chemical bioanalysis the number and nature of simultaneously embedded binding sites may be increased, including peptides or nucleotides as recognition moieties. The combined use of several chromophores in the membrane gives a specific spectroscopic output depending on their spatial arrangement. Such functionalized luminescent vesicles may in some applications replace antibody based assays.

Experimental Part and Supporting Information

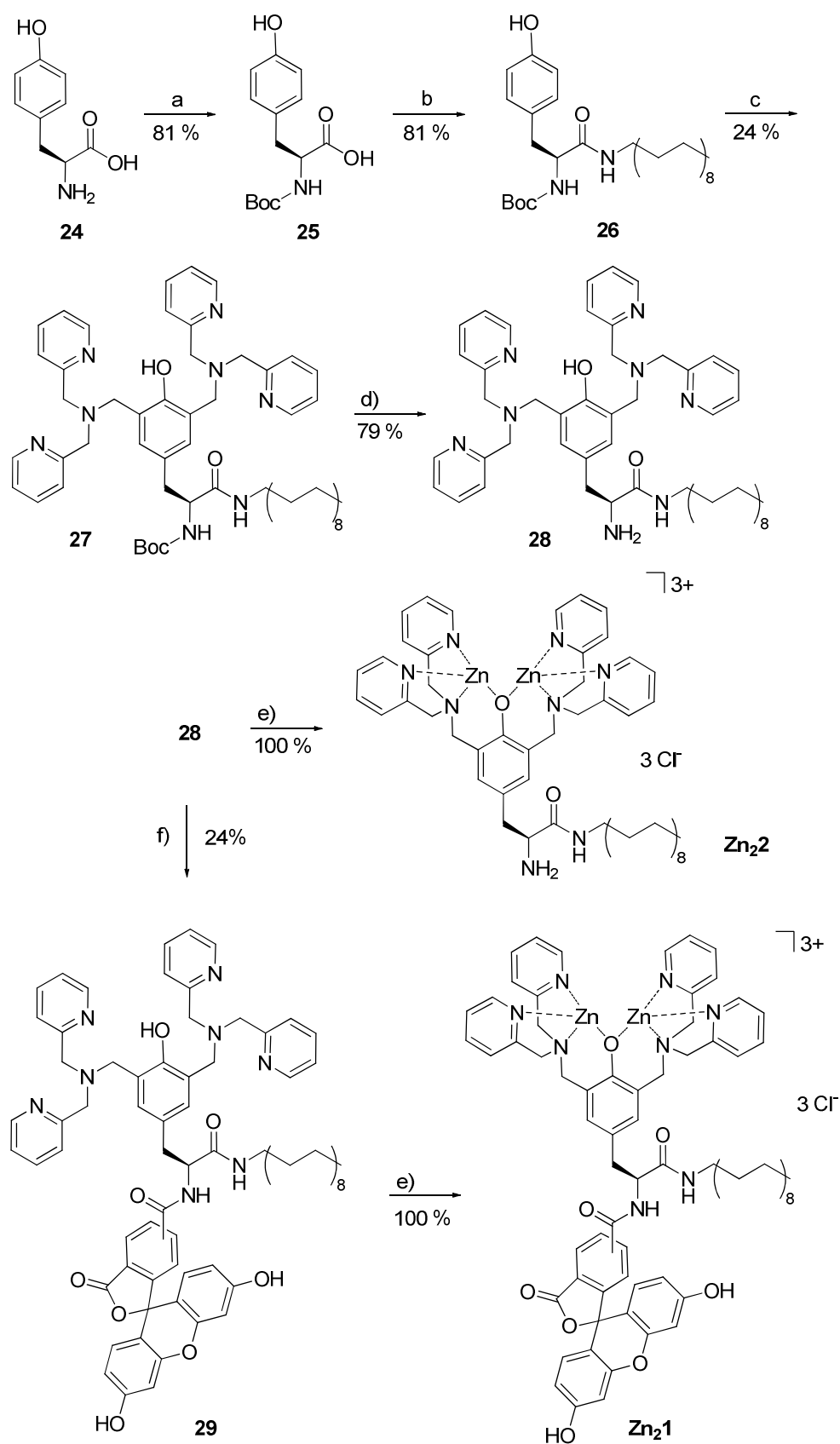
General methods and material

Fluorescence measurements were performed with UV-grade solvents (Baker or Merck) in 1 cm quartz cuvettes (Hellma) and recorded on a Varian 'Cary Eclipse' fluorescence spectrophotometer with temperature control. Absorption was recorded on a Varian Cary BIO 50 UV/VIS/NIR Spectrometer with temperature control by use of a 1 cm quartz cuvettes (Hellma) and Uvasol solvents (Merck or Baker). PCS measurements were performed on a Malvern Zetasizer Nano at 25 °C using 1 cm disposable polystyrene cuvettes (VWR). NMR spectra were recorded on Bruker Avance 600 (¹H: 600.1 MHz, ¹³C: 150.1 MHz, T = 300 K), Bruker Avance 400 (¹H: 400.1 MHz, ¹³C: 100.6 MHz, T = 300 K), Bruker Avance 300 (¹H: 300.1 MHz, ¹³C: 75.5 MHz, T = 300 K). The chemical shifts are reported in δ [ppm] relative to external standards (solvent residual peak). The spectra were analyzed by first order, the coupling constants are given in Hertz [Hz]. Characterization of the signals: s = singlet, d =

doublet, t = triplet, q = quartet, m = multiplet, bs = broad singlet, psq = pseudo quintet, dd = double doublet, dt = double triplet, ddd = double double doublet. Integration is determined as the relative number of atoms. Assignment of signals in ^{13}C -spectra was determined with DEPT-technique (pulse angle: 135°) and given as (+) for CH_3 or CH, (-) for CH_2 and (C_q) for quaternary C. Error of reported values: chemical shift: 0.01 ppm for ^1H -NMR, 0.1 ppm for ^{13}C -NMR and 0.1 Hz for coupling constants. The solvent used is reported for each spectrum. Mass spectra were measured on Varian CH-5 (EI), Finnigan MAT 95 (CI; FAB and FD), Finnigan MAT TSQ 7000 (ESI) with Xenon as ionisation gas for FAB. IR spectra were recorded on Bio-Rad FTS 2000 MX FT-IR and Bio-Rad FT-IR FTS 155. Melting Points were determined on Büchi SMP or a Lambda Photometrics OptiMelt MPA 100. Thin layer chromatography (TLC) analyses were performed on silica gel 60 F-254 with a 0.2 mm layer thickness. Detection via UV light at 254 nm / 326 nm or through staining with ninhydrin in EtOH. Column chromatography was performed on silica gel (70–230 mesh) from Merck. Commercially available solvents of standard quality were used. Starting materials were used without any further purification. Phospholipids were purchased from Avanti Polar Lipids Inc. Commercially available solvents of standard quality were used. If not otherwise stated, purification and drying was done according to accepted general procedures.³⁴ Elemental analyses were carried out by the centre for chemical analysis of the Faculty of chemistry and pharmacy of the University of Regensburg.

Synthesis of amphiphilic bis-Zn(II)-DPA complexes Zn₂1 and Zn₂2

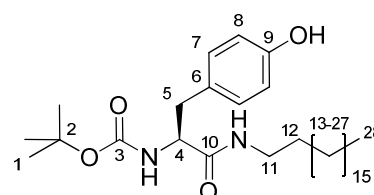
Receptor Zn₂1 and Zn₂2 were prepared from a tyrosine based bis-DPA metal chelating lipid which was synthesized according to a modified protocol of the procedure for the binuclear tyrosine based bis-DPA reported by Hamachi *et al.*³⁵ Derivatization of the tyrosine scaffold on large scale was possible by standard peptide solution chemistry.



Scheme S1. Synthesis of amphiphilic tyrosine based bis-dpa zinc complexes. (a) Boc₂O, DCM, RT, 20 h; (b) EDC, HOBT, DIPEA, DMF, toluene, 60 °C, 22h; (c) 2,2'-dipicoloylamine, paraformaldehyde, H₂O, ⁱPrOH, 80 °C, 30 min, reflux, 17 h; (d) HCl / ether, DCM, RT, 16 h; (e) ZnCl₂, MeOH, RT, 2 - 3 h; (f) 5/6-carboxyfluorescein, DIPEA, TBTU, HOBT, DMF, 40 °C, 22 h.

Amide formation of **25**³⁶ with octadecylamine gave amphiphilic tyrosine derivative **26** in good yields. *Mannich* type reaction using 2,2'-dipicolylamine and paraformaldehyde according to literature known procedure gave the protected metal chelating lipid **27**.³⁵ Removal of the Boc group in acidic conditions (HCl/ether) yielded compound **28** which was finally treated with two equivalents of ZnCl₂ to give **Zn₂2**.

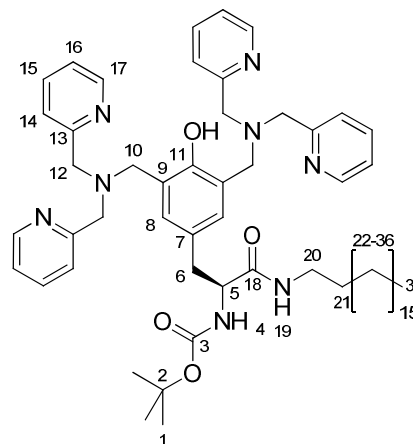
A fluorescein label was introduced by amide formation of **28** with an isomeric mixture of 5/6-carboxy fluorescein. Subsequent treatment with ZnCl₂ gave the fluorescent amphiphilic binuclear tyrosine based metal complex **Zn₂1**.



[2-(4-Hydroxy-phenyl)-1-octadecylcarbamoyl-ethyl]-carbamic acid tert-butyl ester
(**26**)

Boc-Tyr-OH **25** (2.50 g, 8.9 mmol), DIPEA (5.0 mL, 29.3 mmol), EDC (1.73 mL, 9.8 mmol), and HOBt (1.32 g, 9.8 mmol) were dissolved in DMF (4 mL) under ice cooling and stirred for 45 min. Subsequently a solution of octadecylamine (2.89 g, 9.8 mmol) in 25 mL DMF was added slowly. The reaction was allowed to warm to room temp. and was stirred over night (22 h) at 60 °C. The reaction progress was monitored by TLC (CHCl₃ / MeOH 9:1). After completion of the reaction the solvent was removed and the crude product was loaded on flash silica gel and purified by flash column chromatography (CHCl₃ / MeOH 95:5, *R_f* = 0.40) yielding **26** (3.82 g, 7.2 mmol, 81 %) as a colourless solid. **MP**: 115 °C. – **¹H-NMR** (600 MHz; CDCl₃): δ (ppm) = 0.87 (t, ³J = 7.0 Hz, 3 H, C²⁸H₃), 1.25 (s, 30 H, C¹³H₂ – C²⁷H₂), 1.36 (bs, 2 H, COSY: C¹²H₂), 1.42 (s, 9 H, COSY: C¹H₃), 2.83-3.02 (m, 2 H, COSY: C⁵H₂), 3.07-3.24 (m, 2 H, COSY: C¹¹H₂), 4.21 (m, 1 H, HMBC, COSY: C⁴H), 5.17 (bs, 1 H, COSY: NH^a), 5.91 (bs, 1 H, COSY: NH^b), 6.74 (d, ²J = 8.5 Hz, 2 H, HMBC: C⁸H), 7.02 (d, ²J = 7.7 Hz, 2 H, HMBC: C⁷H). – **¹³C-NMR** (150 MHz; CDCl₃): δ (ppm) = 14.1 (+, 1 C, C²⁸H₃), 22.7 (–, 1 C, alkyl-CH₂), 26.8 (–, 1 C, alkyl-CH₂), 28.3 (+, 3 C, C¹H₃), 29.2 (–, 1 C, alkyl-CH₂), 29.3 (–, 1 C, alkyl-CH₂), 29.5 (–, 1 C, C¹²H₂), 29.60, 29.65, 29.69 (–, 10 C, alkyl-CH₂), 31.9 (–, 1 C, alkyl-CH₂), 37.9 (–, 1 C, C⁵H₂), 39.6 (–, 1 C, C¹¹H₂), 56.2 (+, 1 C, HMBC: C⁴H₃), 80.3 (C_q, 1 C, C²), 115.6 (+, 2 C, HMBC: C⁷H), 130.4 (+, 2 C, HMBC: C⁸H), 128.1 (C_q, 1 C, HMBC: C⁶), 155.2 (C_q, 1 C, HMBC: C⁹), 155.6 (C_q, 1 C, HMBC: C³), 171.3 (C_q, 1 C, HMBC: C¹⁰). – **IR** (ATR) [cm⁻¹]: $\tilde{\nu}$ [cm] = 3335, 3306, 2959, 2917, 1682, 1655, 1523, 1468, 1367, 1295, 1236, 1168, 1046, 896, 799. – **MS** (ESI(+), DCM/MeOH + 10 mmol/L NH₄Ac): *m/z* (%) = 533.6 (100) [MH⁺], 477.4 (19) [MH⁺ - C₄H₈]⁺, 555.5 (36) [MNa⁺]. – **Elemental analysis** calcd. (%)

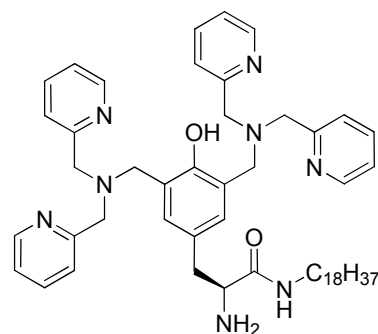
for $C_{32}H_{56}N_2O_4$: C 72.14, H 10.59, N 5.26; found C 72.13, H 10.63, N 5.00. – **MF**: $C_{32}H_{56}N_2O_4$ – **FW**: 532.81 g/mol



(2-{3,5-Bis-[(bis-pyridin-2-ylmethyl-amino)-methyl]-4-hydroxy-phenyl}-1-octadecyl carbamoyl-ethyl)- carbamic acid tert-butyl ester (**27**)

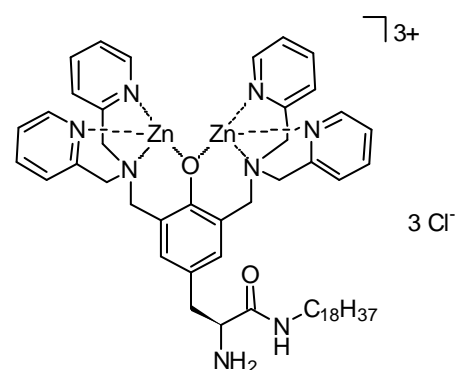
2,2'-Dipicolylamine (2.35 g, 11.8 mmol) and paraformaldehyde (0.56 g, 18.9 mmol) were dissolved in 30 mL water / isopropanol (5:3) and the pH was adjusted to 8 by adding 1 M NaOH. After stirring at 80 °C for 35 min, compound **26** (2.51 g, 4.7 mmol) was added, and the reaction mixture was refluxed for 17 h. After cooling to room temperature the solvent was evaporated and the residue was dissolved in ethyl acetate. The solution subsequently was washed with saturated $NaHCO_3$ (3x) and brine (3x) followed by drying over $MgSO_4$. After removal of the solvent in vacuo the crude product was purified by flash column chromatography on flash silica gel (ethyl acetate / MeOH 2:1, $R_f = 0.1$) obtaining **27** (1.1 g, 1.15 mmol, 24 %) as a colourless oil. 1H -NMR (400 MHz; acetone- d_6): δ (ppm) = 0.86 (t, $^3J = 6.9$ Hz, 3 H, $C^{37}H_3$), 1.14-1.28 (m, 30 H, $C^{22}H_2 - C^{36}H_2$), 1.29 (s, 11 H, HSQC: C^1H_3 , $C^{21}H_2$), 2.87 (dd, $^3J = 13.5$ Hz, $^2J = 6.5$ Hz, 1 H, HSQC, COSY: C^6H_2), 2.94 (dd, $^3J = 13.5$ Hz, $^2J = 7.4$ Hz, 1 H, HSQC, COSY: C^6H_2), 3.02 (dd, $^3J = 12.9$ Hz, $^2J = 6.6$ Hz, 2 H, HSQC: $C^{20}H_2$), 3.74 (d, $^2J = 13.7$ Hz, 2 H, HMBC, COSY: $C^{10}H_2$), 3.80 (d, $^2J = 13.7$ Hz, 2 H, HMBC, COSY: $C^{10}H_2$), 3.85 (s, 8 H, COSY: $C^{12}H_2$), 3.34 (dd, $^3J = 14.4$ Hz, $^2J = 7.1$ Hz, 1 H, COSY: $C^{20}H_2$), 5.98 (d, $^3J = 8.2$ Hz, 1 H, HSQC, COSY: N^4H), 7.10 (s, 2 H, HMBC, COSY: C^8H), 7.20 (ddd, $^3J = 7.4$ Hz, 4.9 Hz, 1.1 Hz, 4 H, HMBC: $C^{16}H$), 7.29 (bs, 1 H, HSQC, COSY: $N^{19}H$), 7.55 (d, $^3J = 7.8$ Hz, 4 H, HMBC: $C^{14}H$), 7.69 (dt, $^3J = 7.7$ Hz, $^2J = 1.9$ Hz, 4 H, HMBC: $C^{15}H$), 8.52 (m, 4 H, HMBC: $C^{17}H$), 10.96 (bs, 1 H, HSQC: OH). – ^{13}C -NMR (100 MHz; acetone- d_6): δ (ppm) = 14.3 (+, 1 C, $C^{37}H_3$), 23.3 (–, 1 C, alkyl- CH_2), 27.5 (–, 1 C, alkyl- CH_2), 28.5 (+, 3 C, C^1H_3), 29.9 (–, 1 C, alkyl- CH_2), 30.22 (–, 1 C, alkyl- CH_2), 30.27 (–, 1 C, alkyl- CH_2), 30.4 (–, 9 C, alkyl- CH_2 , solvent peak), 32.6 (–, 1 C, alkyl- CH_2), 38.8 (–, 1 C, COSY: C^6H_2), 39.7 (–, 1 C, HSQC: $C^{20}H_2$), 55.3 (–, 2 C, HMBC, COSY: $C^{10}H_2$), 60.1 (–, 4 C, HMBC, COSY: $C^{12}H_2$), 56.9 (+, 1 C, HMBC: C^5H_3), 79.0 (C_q , 1 C, HMBC, HSQC, C^2), 122.8 (+, 4 C, HMBC: $C^{16}H$), 123.8 (+, 4 C, HMBC: $C^{14}H$), 124.6 (C_q , 2 C, HMBC: C^9), 127.7 (C_q , 1 C, HMBC: C^7),

131.3 (+, 2 C, HMBC, COSY: C⁸H), 137.3 (+, 4 C, HMBC, COSY: C¹⁵H), 149.7 (+, 4 C, HMBC, COSY: C¹⁷H), 155.8 (C_q, 1 C, HMBC: C¹¹), 155.8 (C_q, 1 C, HMBC: C¹¹), 159.9 (C_q, 1 C, HMBC: C³), 160.2 (C_q, 4 C, HMBC: C¹³), 171.9 (C_q, 1 C, HMBC: C¹⁸). – IR (ATR) [cm⁻¹]: $\tilde{\nu}$ [cm] = 3383, 2922, 2852, 1706, 1656, 1590, 1569, 1433, 1364, 1288, 1245, 1167, 1048, 995, 791. – MS (ESI(+), DCM/MeOH + 10 mmol/L NH₄Ac): m/z (%) = 478.5 (100) [M + 2 H⁺]²⁺, 955.8 (85) [MH⁺]. – **Elemental analysis** calcd. (%) for C₅₈H₈₂N₈O₄: C 72.92, H 8.65, N 11.73; found C 72.38, H 8.34, N 11.63 – **MF**: C₅₈H₈₂N₈O₄ – **FW**: 955.35 g/mol



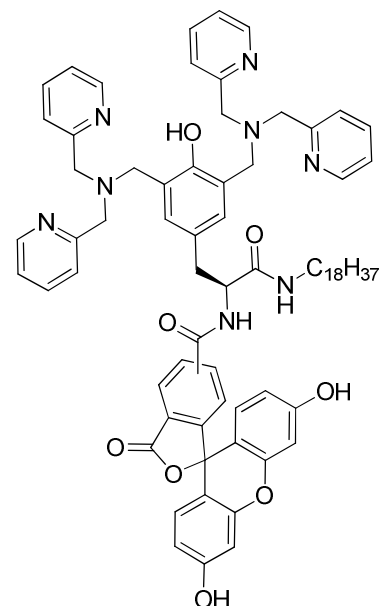
2-Amino-3-{3,5-bis-[(bis-pyridin-2-ylmethyl-amino)-methyl]-4-hydroxy-phenyl}-N-octadecyl-propionamide (**28**)

Boc protected **27** (700 mg, 0.73 mmol) was dissolved in DCM under ice cooling and mixed with HCl/ether (3.7 mL; 1 mL / 0.2 mmol Boc group). The reaction was allowed to warm to room temp. and was stirred for additional 16 hours. After completion the reaction mixture was evaporated to dryness, the residue was suspended in saturated NaHCO₃ and extracted with ethyl acetate (4x). Subsequently the organic phase was dried over MgSO₄ and the solvent was removed in vacuo yielding **28** (497 mg, 0.58 mmol, 79 %) as a pale yellow oil. **¹H-NMR** (300 MHz; DMSO-d₆): δ (ppm) = 0.82 (t, ³J = 6.9 Hz, 3 H, CH₃), 1.04 (bs, 4 H, alkyl-CH₂), 1.19 (s, 28 H, alkyl-CH₂), 2.57 (dd, ³J = 13.5 Hz, ²J = 7.1 Hz, 1 H, Tyr-CH₂), 2.73 (dd, ³J = 13.5 Hz, ²J = 7.1 Hz, 1 H, Tyr-CH₂), 2.91 (m, 2 H, CH₂), 3.29 (t, ³J = 6.4 Hz, 1 H, CH), 3.65 (s, 4 H, Ar-CH₂-pyr), 3.74 (s, 8 H, N-CH₂-pyr), 6.98 (s, 2 H, Ar-CH), 7.21 (m, 4 H, Pyr-CH), 7.46 (d, ³J = 8.0 Hz, 4 H, Pyr-CH), 7.70 (dt, ³J = 7.6 Hz, 1.7 Hz, 4 H, pyr-CH), 8.47 (dd, ³J = 4.4 Hz, 0.3 Hz, 4 H, pyr-CH). – **¹³C-NMR** (75 MHz; DMSO-d₆): δ (ppm) = 13.8 (+, 1 C, CH₃), 22.0 (–, 1 C, alkyl-CH₂), 26.1 (–, 1 C, alkyl-CH₂), 28.52 (–, 1 C, alkyl-CH₂), 28.57 (–, 1 C, alkyl-CH₂), 28.78, 28.81, 28.89 (–, 11 C, alkyl-CH₂), 31.4 (–, 1 C, alkyl-CH₂), 38.0 (–, 1 C, CH₂), 40.2 (–, 1 C, CH₂), 53.9 (–, 2 C, CH₂), 55.9 (+, 1 C, CH), 58.8 (–, 4 C, CH₂), 122.1 (+, 4 C, CH), 122.5 (+, 4 C, CH), 123.1 (C_q, 1 C), 127.4 (C_q, 1 C), 129.8 (+, 2 C, CH), 136.5 (+, 4 C, CH), 148.5 (+, 4 C, CH), 153.7 (C_q, 1 C), 158.5 (C_q, 4 C), 173.5 (C_q, 1 C). – IR (ATR) [cm⁻¹]: $\tilde{\nu}$ [cm] = 2921, 2852, 1658, 1590, 1522, 1474, 1433, 1372, 1233, 1149, 1048, 996, 754. – MS (ESI(+), DCM/MeCN/TFA): m/z (%) = 428.4 (100) [M + 2 H⁺]²⁺, 299.6 (16) [M + 3 H⁺ + MeCN]³⁺, 855.8 (14) [MH⁺], 286 (12) [M + 3 H⁺]. – **HRMS** Calcd for C₅₃H₇₅N₈O₂ 855.6013; Found: 855.6000. – **MF**: C₅₃H₇₄N₈O₂ – **FW**: 855.23 g/mol



Amphiphilic binuclear Zn(II)-Dpa complex (**Zn₂2**)

To a solution of compound **28** (36.5 mg, 43 μ mol) in MeOH (2 mL) was added dropwise a methanolic solution of ZnCl₂ (100 mM, 858 μ L, 86 μ mol). After stirring the reaction mixture for 2 h at room temperature, the methanol was removed in vacuo. The residue was dissolved in water and was lyophilized yielding complex **12** as a colourless solid in quantitative yield. **MP**: 147 °C. – **IR** (ATR) [cm^{-1}]: $\tilde{\nu}$ = 2924, 2852, 1676, 1608, 1573, 1477, 1440, 1303, 1270, 1156, 1100, 1053, 1023, 763. – **UV** (MeOH): λ_{max} (log ϵ) = 261 nm (4.076), 296 (3.436). – **MS** (ESI(+), H₂O/MeOH + 10 mmol/L NH₄Ac): m/z (%) = 1099.7 (100) [$\text{M}^{3+} + 2 \text{CH}_3\text{COO}^-$]⁺, 520.4 (69) [$\text{M}^{3+} + \text{CH}_3\text{COO}^-$]²⁺. – **MF**: C₅₃H₇₄N₈O₂Zn₂Cl₄ – **FW**: 1127.79 g/mol



Isomeric mixture of amphiphilic, fluorescein labeled Dpa ligand (**29**)

A isomeric mixture of 5/6-carboxyfluorescein (246 mg, 0.65 mmol), DIPEA (323 μ L, 1.87 mmol), TBTU (315 mg, 0.98 mmol), and HOBt (133 mg, 0.98 mmol) were dissolved under nitrogen atmosphere in dry DMF (4 mL) under ice cooling and stirred for 1 h. Subsequently **28** (400 mg, 0.47 mmol) in 4 mL DMF was added slowly. The reaction was allowed to warm

to room temperature and was stirred 22 h at 40 °C. The reaction progress was monitored by TLC (CHCl₃ / MeOH 9:1). After completion of the reaction the solvent was removed and the crude product was purified by preparative HPLC yielding the isomers **29** as an orange-yellow solid. **MP**: 97 – 99 °C. – **UV** (MeOH): λ_{\max} (log ϵ) = 224 (4.629), 260 (4.158), 454 (3.500), 481 (3.481). – **IR** (ATR) [cm⁻¹]: $\tilde{\nu}$ [cm] = 2924, 2853, 1757, 1670, 1609, 1438, 1377, 1246, 1178, 1126, 955, 837, 798, 755, 719. – **MS** (ESI(+), DCM/MeCN/TFA): m/z (%) = 607.6 (100) [M + 2 H⁺]²⁺, 405.3 (65) [M + 3 H⁺]²⁺, 1213.9 (11) [MH⁺]. – **LC-MS** (+ p ESI Q1MS ; RT 40 min): m/z (%) = 607.6 (100) [M + 2 H⁺]²⁺, 1213.9 (65) [MH⁺]⁺, 405.3 (38) [M + 3 H⁺]²⁺. – **MF**: C₇₄H₈₄N₈O₈ – **FW**: 1213.53 g/mol

Purification by preparative HPLC:

Column: LabID75 Phenomenex Luna 250 x 21.2 mm 10 μ m / Ser.Nr. 453159-3

Flow: 21 mL / min

Concentration 10 mg / mL

Injection volume: 500 μ L

Detection wavelength: 220 nm

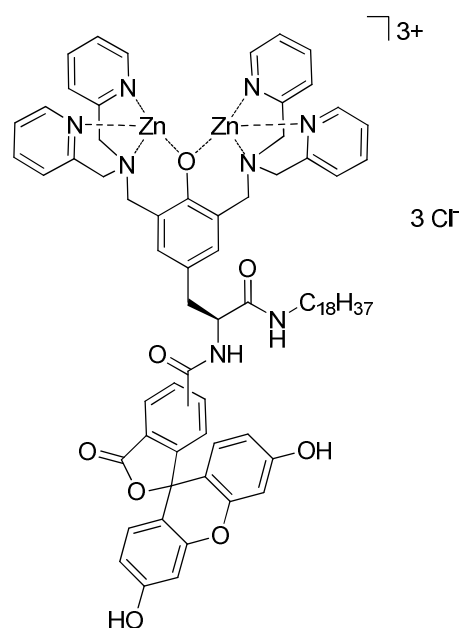
Gradient: 0 min – 5 % MeCN / H₂O (+ 0.0059 % TFA)

43 min – 72 % MeCN / H₂O (+ 0.0059 % TFA)

45 min – 98 % MeCN / H₂O (+ 0.0059 % TFA)

55 min – 98 % MeCN / H₂O (+ 0.0059 % TFA)

Retention time: ca. 42 min



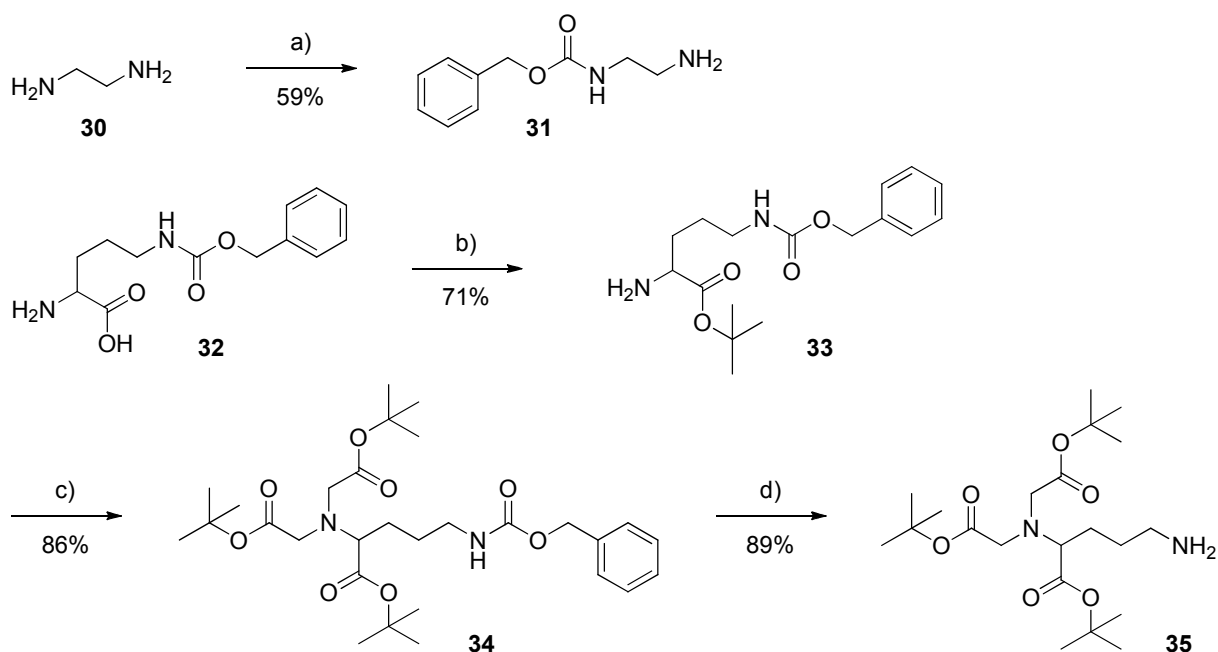
Fluorescent binuclear Zn(II)-Dpa complex (**Zn₂1**)

To a solution of compound **29** (10.5 mg, 8.7 μ mol) in MeOH (2 mL) was added dropwise a methanolic solution of MnCl₂ (100 mM, 174 μ L, 17.4 μ mol). After stirring the reaction

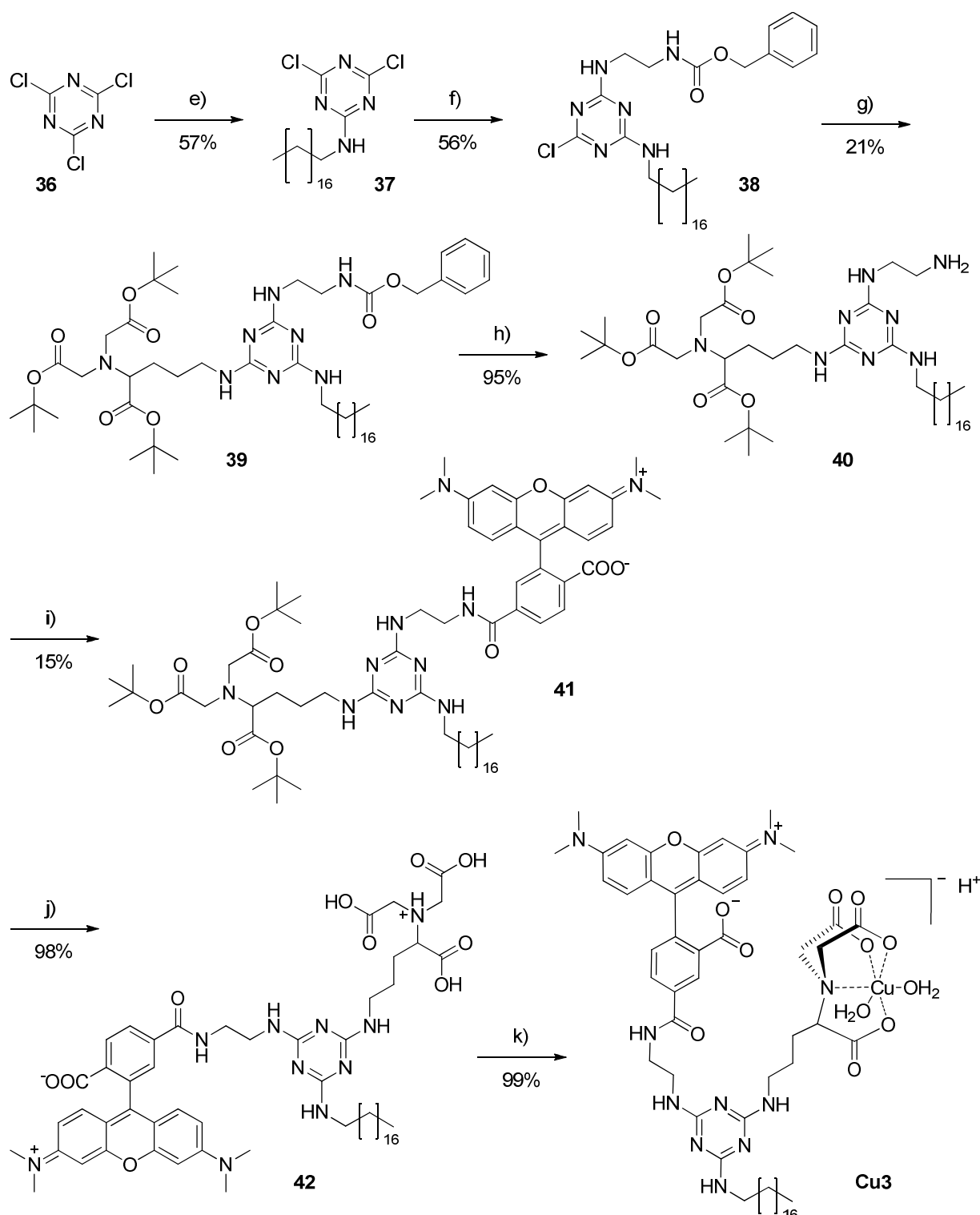
mixture for 2.5 h at room temperature, the methanol was removed in vacuo. The residue was dissolved in water and was lyophilized yielding complex **14** as an orange solid in quantitative yield (13 mg, 8.7 μmol). **MS** (ESI(+), $\text{H}_2\text{O}/\text{MeOH} + 10 \text{ mmol/L NH}_4\text{Ac}$): m/z (%) = 701.7 (100) $[\text{M}^{3+} + \text{CH}_3\text{COO}^-]^+$, 1398.0 (8) $[\text{M}^{3+} - \text{H}^+ + \text{CH}_3\text{COO}^-]^+$, 1458.0 (7) $[\text{M}^{3+} + 2 \text{CH}_3\text{COO}^-]^+$. – **MF**: $\text{C}_{74}\text{H}_{84}\text{N}_8\text{O}_8\text{Zn}_2\text{Cl}_4$ – **FW**: 1486.10g/mol

Synthesis of amphiphilic Cu(II)-NTA complex Cu3

Receptor **Cu3** was prepared by connecting a carboxytetramethylrhodamine label, an ornithine based NTA binding site and a hydrophobic anchor via a central cyanuric chloride linker and complexation of the amphiphilic ligand with Cu(II).



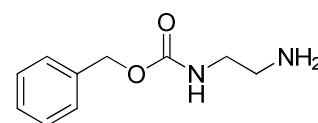
Scheme S2. Synthesis of an amphiphilic, fluorescent copper complex: (a) Cbz chloride, DCM, 0°C, 3 h; (b) tert butyl acetate, HClO_4 , RT, 72 h; (c) bromo tert butyl acetate, DMF, 55°C, 20 h; (d) Pd/C, H_2 , EtOH, RT, 72 h.



Scheme S3. Synthesis of an amphiphilic, fluorescent copper complex: (e) octadecylamine, K_2CO_3 , acetone, RT, 20 h; (f) Cbz-diamine **31**, K_2CO_3 , acetone, 50°C, 48 h; (g) NTA-precursor **35**, collidine, dioxane, 140°C (MW), 1.5 h; (h) Pd/C, H_2 , EtOH, RT, 48 h; (i) carboxytetramethylrhodamine, TBTU, HOBT, DIPEA, DMF, 0°C, 1 h / 40°C, 24 h; (j) TFA, RT, 24 h; (k) $Cu_2(OH)_2CO_3$, MeOH, 60°C, 4 h.

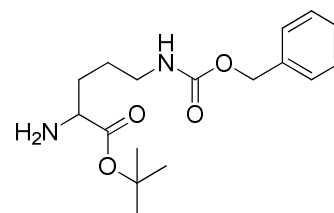
Ethylenediamine **30** is Cbz-protected to give mono-amine **31**. Cbz-protected L-ornithine **32** is converted into the butyl acetate ester **33**. The amine group of **33** reacts in a nucleophilic substitution with bromo-tert-butyl-acetate to give **34** and yields after deprotection the free

amine **35**. To introduce the hydrophobic anchor octadodecanylamine **13** is tethered by nucleophilic substitution to cyanuric chloride **36** yielding compound **37**. Subsequently Cbz-protected ethylenediamine **31** is attached to **37** yielding **38** to connect carboxytetramethylrhodamine as fluorescent label. Next, the NTA-precursor **35** is coupled to the unprotected functional group of the linker **38** via nucleophilic substitution yielding **39**. Hydrogenolytic Cbz-deprotection gives compound **40**, which is tethered to an *in situ* formed active ester of carboxytetramethylrhodamine. Treatment of **41** with TFA leads to the free acid **42**. In a last step copper is chelated by the acid groups of the NTA-complex **42** yielding the target receptor **Cu3**.



Synthesis of benzyl (2-aminoethyl)carbamate (**31**)

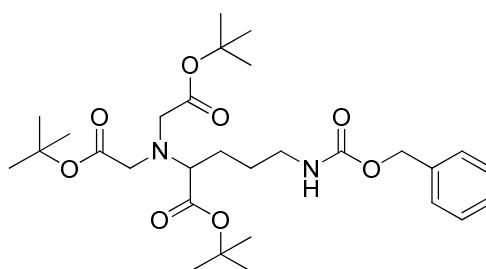
Ethylenediamine **30** (12.1 mL, 180 mmol) was dissolved in DCM (240 mL) and a solution of benzyl chloroformate (2.5 mL, 18 mmol) in DCM (60 mL) was added dropwise over 1.5 h at 0 °C. The reaction mixture was stirred at this temperature for further 1.5 h and at room temperature overnight. The formed precipitate was filtered off, the filtrate was washed three times with brine (150 mL) and the organic phase was dried over MgSO₄. Evaporation of the solvent leads to a pale-yellow, crystalline raw product which was purified via column chromatography (silica gel, CHCl₃/MeOH/Et₃N 70:29:1; R_f = 0.09). The product **31** (2.07 g, 10.7 mmol, 59 %) was obtained as pale-yellow oil which crystallizes at 0 °C. ¹H-NMR (400 MHz, CDCl₃), δ [ppm]: 1.70 (2 H, bs, NH₂-CH₂), 2.73 (2 H, pt, H₂N-CH₂-CH₂), 3.17 (2 H, dd, CH₂-CH₂-NH), 5.05 (2 H, s, O-CH₂-C), 5.65 (1 H, bs, CH₂-NH-C), 7.29 (5 H, m, CH_{arom}). – ¹³C-NMR (100 MHz, CDCl₃), δ [ppm]: 156.84 (NH-CO₂), 136.64 (CH₂-C-C₅H₅), 128.51, 128.48, 128.02 (C-C₅H₅), 66.60 (O-CH₂-C), 43.71 (CH₂-CH₂-NH), 41.62 (H₂N-CH₂-CH₂). – MS (ESI(+), H₂O + 0.1% FA/MeCN + 0.1% FA): m/z (%) = 195.1 (100) [MH⁺].



Synthesis of tertbutyl protected 2-amino-5-(((benzyloxy)carbonyl)amino)pentanoic acid (**33**)

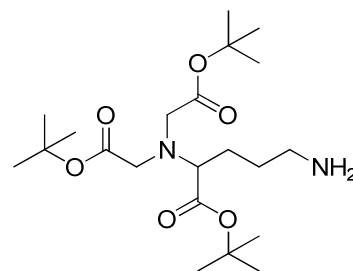
Benzyloxycarbonyl ornithine **32** (10.00 g, 37.55 mmol) was dissolved in tert butyl acetate (471 mL, 3.47 mol), perchloric acid (70 %, 5.64 mL, 67.59 mmol) was added and the solution was stirred at rt for 72 h. The reaction mixture was cooled to 0°C and four times extracted

with 0.5 M hydrochloric acid (300 mL). 2 M sodium hydroxide solution was added to the aqueous phase and the target molecule was extracted from the basic solution with diethyl ether (three times, 200 mL), dried over Na₂SO₄ and the solvent was removed in vacuo. **33** was obtained as yellow oil (8.61 g, 26.71 mmol, 71 %). – ¹H-NMR (400 MHz, CDCl₃): δ [ppm] = 1.43 (s, 9H, CH₃), 1.55 – 1.70 (m, 4H, 2x CH₂), 3.18 (m, 2H, CH₂-NH), 3.30 (m, 1H, CH), 5.05 (s, 2H, CH₂-Cbz), 5.25 (s, 1H, NH), 7.25 – 7.36 (m, 5H, CH_{aromat.}). – ¹³C-NMR (100 MHz, CDCl₃): δ [ppm] = 26.0 (CH₃), 28.2 (CH₂), 40.9 (CH₂), 54.4 (CH), 66.6 (CH₂), 81.3 (CH_{quart.}), 128.6 (CH_{arom.}), 137.0 (C_{quart,arom.}), 156.5 (C_{carbonyl}), 175.0 (C_{carbonyl}). – MS (ESI(+), H₂O + 0.1% FA/MeCN + 0.1% FA): m/z (%) = 323.0 (100) [MH⁺], 645.4 (36) [2MH⁺].



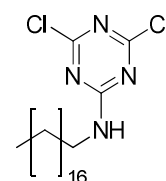
Synthesis of di-tert-butyl 2,2'-((5-(((benzyloxy)carbonyl)amino)-1-(tert-butoxy)-1-oxopentan-2-yl)azanediyl)diacetate (**34**)

Two-fold protected ornithine **33** (8.61 g, 26.71 mmol), tert butyl bromoacetate (15.50 mL, 106.82 mmol) and DIPEA (22.71 mL, 133.53 mmol) were dissolved in dry DMF (100 mL) under nitrogen atmosphere and the mixture was stirred at 55 °C for 20 h. Subsequently the solvent was removed under vacuo yielding a dark brown solid which was suspended in ethyl acetate (60 mL) and filtered off. The residue was washed three times with hexane/ethyl acetate (3:1, 120 mL). After evaporation a brown oil (17.54 g) was obtained. The crude product was purified via column chromatography (flash silical gel, hexanes/EA 3:1; R_f = 0.27) to give **34** as pale yellow solid (12.74 g, 23.mmol, 86 %). – ¹H-NMR (400 MHz, CDCl₃): δ [ppm] = 1.38 (s, 27H, CH₃), 1.55 – 1.70 (m, 4H, 2x CH₂), 3.16 – 3.25 (m, 3H, CH and CH₂-NH), 3.30 – 3.44 (m, 4H, 2x CH₂-Ntert.), 5.00 (s, 2H, CH₂-Cbz), 5.22 (s, 1H, NH), 7.21 – 7.27 (m, 5H, CH_{aromat.}). – ¹³C-NMR (100 MHz, CDCl₃): δ [ppm] = 26.0 (CH₃), 28.2 (CH₂), 40.6 (CH₂), 54.0 (CH), 65.1 (CH₂), 66.4 (CH₂), 81.2 (CH_{quart.}), 128.0 (CH_{arom.}), 136.8 (C_{quart,arom.}), 156.5 (CH_{carbonyl}), 175.1 (CH_{carbonyl}). – MS (ESI(+), H₂O + 0.1% FA/MeCN + 0.1% FA): m/z (%) = 551.2 (100) [MH⁺].



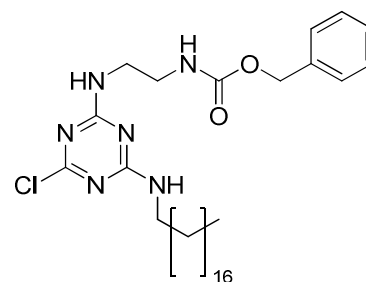
Synthesis of di-tert-butyl 2,2'-((5-amino-1-(tert-butoxy)-1-oxopentan-2-yl)azanediyl)diacetate (**35**)

Cbz-protected NTA-precursor **34** (484 mg, 0.51 mmol) was dissolved in ethanol (15 mL) and Pd/C (500 mg) was added. The reaction mixture was stirred at rt and under hydrogen atmosphere (30 bar) for 72 h. Subsequently Pd/C was filtered off via celite and the solvent was evaporated yielding the yellow oil **35** (372 mg, 0.45 mmol, 89%). ¹H-NMR (300 MHz, CDCl₃) δ [ppm] = 5.00 (bs, 1 H, NH), 3.41 (s, 2 H, CH₂-N), 3.38 (s, 2 H, CH₂-N), 3.31 (m, 1 H, CH-N), 2.85 (m, 2H, CH₂-NH₂), 1.52- 1.87 (m, 4 H, 2x CH_{2alkyl}), 1.41 - 1.38 (m, 27 H, CH₃). – ¹³C-NMR (100 MHz, CDCl₃) δ [ppm] = 171.82 (COO), 170.68 (COO), 81.40 (CO_{quart.}), 81.03 (CO_{quart.}), 65.21 (CH-N), 57.79 (CH₂-N), 40.36 (CH₂-NH₂), 28.13 (CH_{2alkyl}), 28.04 (CH₃), 27.04 (CH₂-CH), 18.30 (CH₃). – MS (ESI(+), H₂O + 0.1% FA/MeCN + 0.1% FA): m/z (%) = 417.3 (100) [MH⁺].



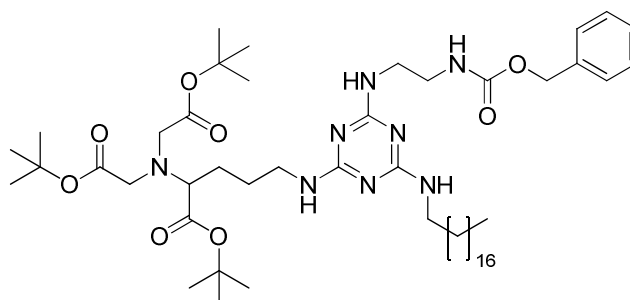
Synthesis of 4,6-dichloro-N-propyl-1,3,5 triazin-2-amine (**37**)

Octadecylamine (1.02 g, 5.50 mmol) was dissolved in acetone (40 mL) and a solution of 2,4,6-trichloro-1,3,5-triazine **36** (1.47 g, 5.44 mmol) in acetone (25 mL) and water (5 mL) was added at 0 °C, followed by the addition of K₂CO₃ (2.25 g, 16.28 mmol) in water (10 mL). The reaction mixture was stirred at 0 °C for further 30 min and at rt for 20 h. After the solvent was removed in vacuo the residue was washed with brine (5 mL) and extracted three times with CHCl₃ (25 mL). The organic phases were dried over MgSO₄ and the solvent was evaporated to give a white powder (2.20 g). The crude product was purified via silica column chromatography (hexanes/EA 10:1; R_f = 0.37) yielding the white solid **37** (1.30 g, 3.11 mmol, 57 %). – ¹H-NMR (300 MHz, CDCl₃) δ [ppm] = 3.47 (q, 2H, CH₂-NH), 1.59 (m, 2H, CH_{2alkyl}), 1.25 -1.32 (m, 30H, 15 x CH_{2alkyl}), 0.88 (t, 3H, CH₃). – ¹³C NMR (100 MHz, CDCl₃) δ [ppm] = 171.01 (C_{arom.}-NH), 165.83 (C_{arom.}-Cl), 41.58 (CH_{2alkyl}), 31.94 (CH_{2alkyl}), 29.48 (CH_{2alkyl}), 26.64 (CH_{2alkyl}), 22.71 (CH_{2alkyl}), 14.14 (CH₃). – MS (ESI(+), H₂O + 0.1% FA/MeCN + 0.1% FA): m/z (%) = 417.2 (100) [MH⁺].



Synthesis of benzyl (2-((4-chloro-6-(propylamino)-1,3,5-triazin-2-yl)amino)ethyl)carbamate (**38**)

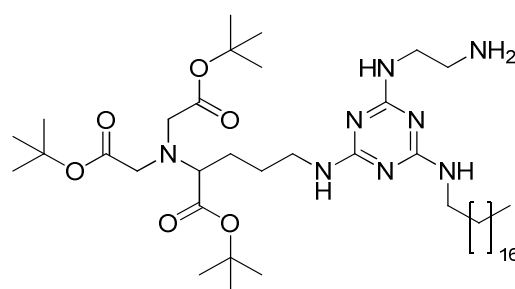
Amphiphilic triazine **37** (4.50 g, 10.80 mmol) was dissolved in acetone (50 mL) followed by the addition of Cbz-protected ethylenediamine **31** (2.10 g, 10.80 mmol) and K_2CO_3 (7.46 g, 54.00 mmol). The mixture was stirred at 50 °C for 40 h before the solvent was removed in vacuo. The residue was redissolved in $CHCl_3$ (100 mL) and washed three times with a water/brine solution (2:1, 100 mL). The organic phases was dried over $MgSO_4$ and the solvent was evaporated. The obtained crude product was recrystallized from EA yielding **38** as a light brown solid (3.46 g, 6.01 mmol, 56 %). 1H -NMR (300 MHz, $CDCl_3$) δ [ppm] = 7.29 (m, 5 H, CH_{arom}), 5.08 (s, 2 H, CH_2 -Cbz.), 3.56 (m, 2 H, CH_{2alkyl}), 3.27- 3.45 (m, 4 H, CH_2 - CH_2), 1.53 (t, 2 H, CH_{2alkyl}), 1.25 (bs, 30 H, 15 x CH_{2alkyl}), 0.88 (t, 3 H, CH_3). – ^{13}C -NMR (100 MHz, $CDCl_3$) δ [ppm] = 136.53 (C_{arom}), 128.07- 128.54 (CH_{arom}), 66.72 (CH_2 - CH_2), 41.05 (CH_{2alkyl}), 31.94 (CH_{2alkyl}), 29.38 - 29.72 (CH_{2alkyl}), 22.71 (CH_{2alkyl}), 14.14 (CH_3). – MS (ESI(+), H_2O + 0.1% FA/MeCN + 0.1% FA): m/z (%) = 574.4 (100) [MH^+].



Synthesis of di-tert-butyl 2,2'-((5-((4-((2-(((benzyloxy)carbonyl)amino)ethyl)amino)-6-(octadecylamino)-1,3,5-triazin-2-yl)amino)-1-(tert-butoxy)-1-oxopentan-2-yl)azanediyl)diacetate (**39**)

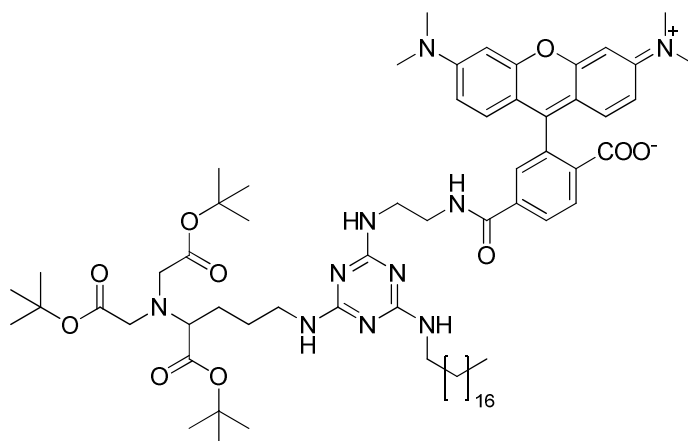
Amine **35** (1.00 g, 2.47 mmol) was suspended in dioxane (10 mL) followed by the addition of the two-fold substituted triazine **38** (1.42 g, 2.47 mmol) and collidine (1.63 μ l, 12.37 mmol). The reaction was carried out in a microwave (150 W, 1.7 bar) at 140 °C for 1.5 h. After evaporation a brown oil was obtained. The crude product was purified via column

chromatography (flash silica gel, EA/hexanes/ Et_3N 75:20:5; $R_f = 0.43$) to give product **39** as a dark yellow oil (0.48 g, 0.51 mmol, 21 %). $^1\text{H-NMR}$ (300 MHz, CDCl_3) δ [ppm] = 7.29 - 7.33 (m, 5 H, CH_{arom}), 5.07 (s, 2 H, $\text{CH}_2\text{-Cbz}$), 3.26 - 3.50 (m, 13 H, CH and 6 x $\text{CH}_{2\text{alkyl}}$), 1.70 (m, 2 H, $\text{CH}_{2\text{alkyl}}$), 1.64 (m, 2 H, $\text{CH}_{2\text{alkyl}}$), 1.50 (t, 2 H, $\text{CH}_{2\text{alkyl}}$), 1.43 (bs, 30 H, $\text{CH}_{2\text{alkyl}}$), 1.24 (bs, 27 H, CH_3), 0.88 (t, 3 H, CH_3). – $^{13}\text{C-NMR}$ (100 MHz, CDCl_3) δ [ppm] = 172.22 (COO), 170.66 (COO), 136.73 (CH_{arom}), 128.45 (CH_{arom}), 127.96 (CH_{arom}), 81.11 (CO_{quart}), 80.67 (CO_{quart}), 66.49 (CHCOO), 65.1. (CH_2O), 53.82 ($\text{CH}_2\text{-N}$), 40.68 ($\text{CH}_2\text{-NH}$), 40.39 ($\text{CH}_2\text{-NH}$), 31.92 - 26.22 ($\text{CH}_{2\text{alkyl}}$), 26.97 (CH_3), 22.69 ($\text{CH}_2\text{-CH}_3$), 14.12 (CH_3). – **MS** (ESI(+), H_2O + 0.1% FA/MeCN + 0.1% FA): m/z (%) = 478.4 (100) [$\text{M} + 2 \text{H}^+$] $^{2+}$, 955.8 (64) [MH^+].



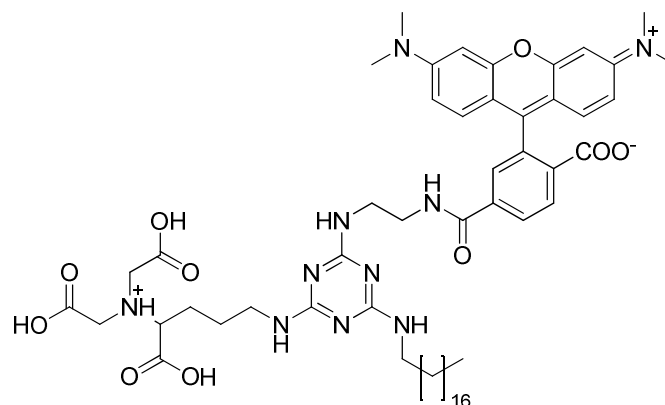
Synthesis of di-tert-butyl 2,2'-(5-((4-((2-aminoethyl)amino)-6-(octodecylamino)-1,3,5-triazin-2-yl)amino)1-(tert-butoxy)-1-oxopentan-2-yl)azanediyl)diacetate (**40**)

Cbz-protected spacer moiety **39** (190 mg, 0.20 mmol) was dissolved in ethanol (15 mL) and Pd/C (500 mg) was added. The reaction mixture was stirred at rt and under hydrogen atmosphere (30 bar) for 48 h. Subsequently Pd/C was filtered off via celite and the solvent was evaporated yielding **40** as light-yellow oil (156 mg, 0.19 mmol, 95%). $^1\text{H-NMR}$ (300 MHz, CDCl_3) δ [ppm] = 3.26 – 3.58 (m, 13 H, CH and 6 x $\text{CH}_{2\text{alkyl}}$), 1.71 (m, 2 H, $\text{CH}_{2\text{alkyl}}$), 1.64 (m, 2 H, $\text{CH}_{2\text{alkyl}}$), 1.55 (t, 2 H, $\text{CH}_{2\text{alkyl}}$), 1.42 (bs, 30 H, $\text{CH}_{2\text{alkyl}}$), 1.24 (bs, 27 H, CH_3), 0.88 (t, 3 H, CH_3). – $^{13}\text{C-NMR}$ (100 MHz, CDCl_3) δ [ppm] = 172.22 (COO), 170.66 (COO), 136.73 (CH_{arom}), 128.45 (CH_{arom}), 127.96 (CH_{arom}), 81.11 (CO_{quart}), 80.67 (CO_{quart}), 66.49 (CHCOO), 65.1. (CH_2O), 53.82 ($\text{CH}_2\text{-N}$), 40.68 ($\text{CH}_2\text{-NH}$), 40.39 ($\text{CH}_2\text{-NH}$), 31.93 - 26.22 ($\text{CH}_{2\text{alkyl}}$), 26.97 (CH_3), 22.69 ($\text{CH}_2\text{-CH}_3$), 14.13 (CH_3). – **MS** (ESI(+), H_2O + 0.1% FA/MeCN + 0.1% FA): m/z (%) = 411.2 (70) [$\text{M} + 2 \text{H}^+$] $^{2+}$, 431.8 (100) [$\text{M} + 2 \text{H}^+ + \text{MeCN}$] $^{2+}$, 821.7 (30) [MH^+].



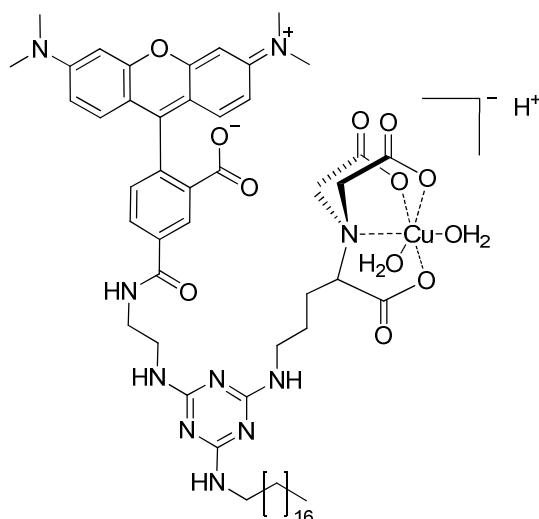
Synthesis of 4-((2-((4-((4-(bis(2-(tert-butoxy)-2-oxoethyl)amino)-5-(tert-butoxy)-5-oxopentyl)amino)-6-(octadecylamino)-1,3,5-triazin-2-yl)amino) ethyl)carbonyl)-2-(6-(dimethylamino)-3-(dimethyliminio)-3H-xanthen-9-yl)benzoate (**41**)

Carboxytetramethylrhodamine (180 mg, 0.42 mmol), TBTU (148 mg, 0.46 mmol), HOBt (62 mg, 0.46 mmol) and DIPEA (284 μ L, 1.67 mmol) were dissolved in dry DMF (4.5 mL) under nitrogen atmosphere at 0°C and the reaction mixture was stirred at rt. After 1 h a solution of the receptor-precursor **40** (343 mg, 0.42 mmol) in dry DMF (3 mL) was added dropwise over 35 min. The reaction mixture was warmed to 45 °C and stirred for another 40 h. Subsequently the solvent was removed and the pink residue was purified via column chromatography (flash silica gel, EA/MeOH/Et₃N 75:20:5) to give **41** as magenta oil. (76 mg, 0.06 mmol, 15 %). ¹H-NMR (300 MHz, CDCl₃) δ [ppm] = 0.80 (t, 3 H, CH₃), 1.11 (m, 2 H, CH₂ alkyl), 1.17 (m, 28 H, CH₂ alkyl), 1.27 (m, 2 H, CH₂ alkyl), 1.35 (s, 27 H, CH₃ Boc), 1.45 – 1.73 (m, 4 H, CH₂ alkyl), 3.00 (m, 12 H, CH₃-N), 3.16-3.55 (m, 13 H, CH₂ and CH), 7.22 (s, 1H, arom.), 7.34 – 7.49 (m, 4 H, arom), 7.64 – 7.67 (m, 4H, arom.). – ¹³C-NMR (100 MHz, CDCl₃) δ [ppm] = 8.7, 14.1, 22.7, 28.0, 28.3, 29.7, 31.9, 45.7, 53.4, 110.7, 110.9, 118.5, 124.0, 125.1, 127.8. – MS (ESI(+), H₂O + 0.1% FA/MeCN + 0.1% FA): m/z (%) = 1234.0 (100) [MH⁺].



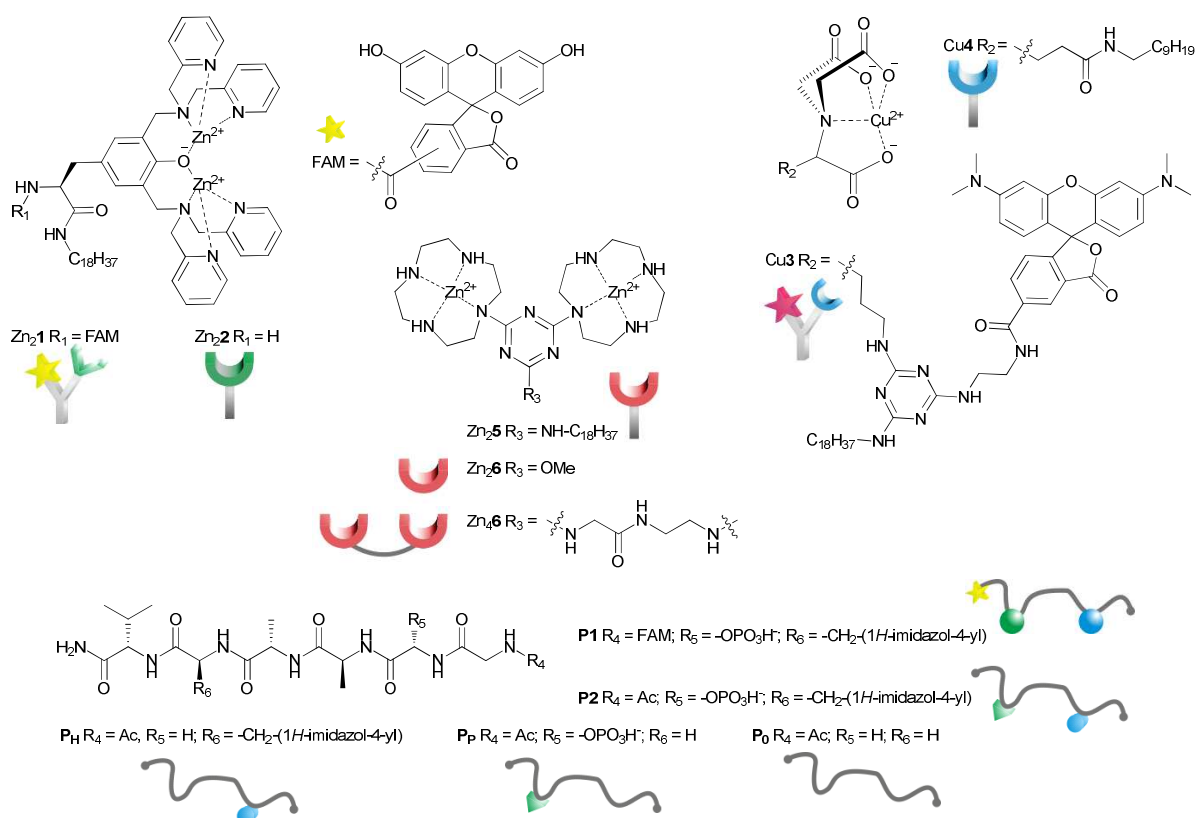
Synthesis of 4-((2-((4-((4-(bis(carboxymethyl)ammonio)-4-carboxybutyl) amino)-6-(octadecylamino)-1,3,5-triazin-2-yl)amino)ethyl)carbamoyl)-2-(6-(dimethylamino)-3-(dimethyliminio)-3H-xanthen-9-yl)benzoate (**42**)

41 (92 mg, 0.08 mmol) was dissolved in TFA (1.6 mL, 20.77 mmol) and stirred at rt for 30 h. TFA was evaporated in vacuo, the residue was suspended in water (3 mL) and lyophilized giving product **42** (83 mg, 0.08 mmol, 98 %) as a magenta solid. $^1\text{H-NMR}$ (600 MHz, CDCl_3) δ [ppm] = 0.86 (t, 3 H, CH_3), 1.15 – 1.28 (m, 28 H, CH_2 alkyl), 1.36-1.38 (m, 4 H, CH_2 alkyl), 1.39 – 1.42 (m, 12 H, CH_3), 3.09 – 3.15 (m, 5 H, $\text{CH}-(\text{CH}_2)_2$), 3.16 – 3.20 (m, 8 H, CH_2 -NH), 3.69 – 3.71 (m, 4 H, CH_2 -COOH), 6.61 (bs, 1 H, NH), 6.74 (bs, 1 H, NH), 6.98 (bs, 1 H, NH), 7.39 (t, 1H, $\text{CH}_{\text{arom.}}$), 7.41 – 7.53 (m, 4 H, $\text{CH}_{\text{arom.}}$), 7.56 (d, 1H, $\text{CH}_{\text{arom.}}$), 7.75 – 7.83 (m, 2H, $\text{CH}_{\text{arom.}}$), 8.02 (d, 1H, $\text{CH}_{\text{arom.}}$), 8.61 (bs, 1 H, NH), 9.12 (bs, 1 H, NH). – $^{13}\text{C-NMR}$ (150 MHz, CDCl_3) δ [ppm] = 14.1 (+, 1 C, CH_3), 17.3 (+, 2 C, CH_3), 18.5 (+, 2 C, CH_3), 22.6 (-, 1 C, CH_2 alkyl), 28.8 – 29.7 (-, 16 C, CH_2 alkyl), 31.9 (-, 1 C, CH_2 alkyl), 40.6 (+, 1 C, CH), 41.0 (-, 1 C, $\text{CH}-(\text{CH}_2)_2$), 42.5 (-, 1 C, $\text{CH}-(\text{CH}_2)_2$), 46.3 (-, 4C, CH_2 -NH), 54.4 (-, 2 C, CH_2 -COOH), 109.8 (+, 1 C, $\text{CH}_{\text{arom.}}$), 112.6 (+, 1 C, $\text{CH}_{\text{arom.}}$), 114.1 (+, 1 C, $\text{CH}_{\text{arom.}}$), 114.7 (-, 1 C, C_q), 114.8 (-, 1 C, C_q), 116.7 (-, 1 C, C_q), 118.6 (-, 1 C, C_q), 119.7 (+, 1 C, $\text{CH}_{\text{arom.}}$), 124.8 (+, 1 C, $\text{CH}_{\text{arom.}}$), 127.0 (+, 1 C, $\text{CH}_{\text{arom.}}$), 128.1 (+, 1 C, $\text{CH}_{\text{arom.}}$), 128.6 (+, 1 C, $\text{CH}_{\text{arom.}}$), 128.9 (+, 1 C, $\text{CH}_{\text{arom.}}$), 130.4 (-, 1 C, C_q), 130.9 (-, 1 C, C_q), 136.6 (-, 1 C, C_q), 142.5 (-, 1 C, C_q), 157.0 (-, 1 C, C_q), 157.3 (-, 1 C, C_q), 160.6 (-, 1 C, C_q), 160.9 (-, 1 C, C_q), 161.1 (-, 1 C, C_q), 161.4 (-, 1 C, C_q). – **MS** (ESI(+), DCM/MeOH + 0.1% FA): m/z (%) = 533.5 (100) $[\text{M} + 2 \text{H}]^{2+}$, 1065.7 (26) $[\text{MH}]^+$.



Synthesis of the amphiphilic, labeled Cu(II)-NTA-complex (**Cu3**)

Deprotected **42** (83.0 mg, 0.08 mmol) was dissolved in MeOH (1.5 mL) and a suspension of $\text{Cu}(\text{OH})_2\text{CO}_3$ and a very small amount of MeOH was added. The reaction was completed by stirring the mixture at rt for 20 h and at 60°C for 3 h. Subsequently the warm solution was filtered immediately and the solvent was evaporated. The residue was suspended in water (2 mL) and lyophilized yielding **Cu3** (89.0 mg, 0.08 mmol, 99 %) as a dark magenta solid. **MS** (ESI(-), $\text{H}_2\text{O}/\text{MeOH} + 10 \text{ mmol/L NH}_4\text{Ac}$): m/z (%) = 1124.4 (100) [$\text{M} - \text{H} - 2 \text{H}_2\text{O}$]⁻.



Scheme S4. Structures and symbols of (non-)amphiphilic receptors and ligands (counterions omitted).

Receptor-ligand binding in homogeneous (Zn_26 , Zn_46) and vesicular (Zn_25) solution

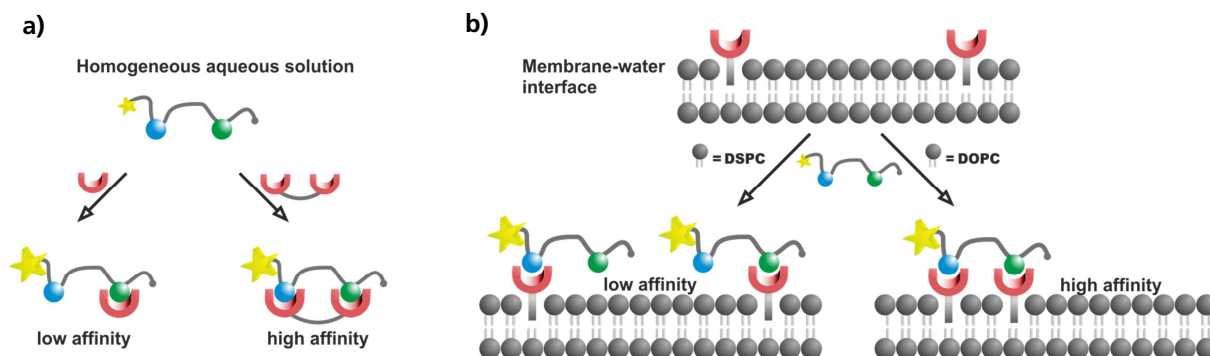


Figure S1. (a) Schematic recognition of **P1** in homogeneous aqueous solution by previously developed receptors²⁶ Zn_26 and Zn_46 ; (b) Schematic recognition of **P1** by membrane-embedded receptor Zn_25 in DSPC and DOPC vesicles.

Vesicles

Preparation

In small glass reaction vessels 1 - 5 μ mol of DOPC or DSPC were dissolved in chloroform and optionally 0.1-10 mol% of dissolved metal complexes were added and mixed. The solvent was completely removed under reduced pressure at 25 °C (DOPC) or 75 °C (DSPC) and an appropriate amount of buffer (HEPES 10 mM, pH 7.4) was added to obtain lipid concentrations of 1 - 2 mM. Vigorous shaking at 25 °C (DOPC) or 75 °C (DSPC) for 5 - 10 minutes yielded a turbid multi-lamellar vesicle suspension. Small uni-lamellar dispersions were obtained by extrusion through 100 nm-pore size polycarbonate membranes with a LiposoFast liposome extruder from Avestin.³⁷

Metal complex concentration

For all vesicles the receptor concentration refers to the outer surface exposed binding sites, as only these should be reactive, with the assumption that embedded compounds distribute equally in both layers of the vesicle membrane and the bilayer thickness for the prepared vesicles amounts to 5 nm.^{11, 38-40}

Dynamic light scattering (DLS)

Vesicle size distributions were determined using Dynamic light scattering (DLS). The standard size distribution of species obtained after extrusion is the following:

	Diam. (nm)	% Intensity	Width (nm)
Z-Average (d.nm): 92,99	Peak 1: 98,42	100,0	24,62
Pdl: 0,039	Peak 2: 0,000	0,0	0,000
Intercept: 0,922	Peak 3: 0,000	0,0	0,000
Result quality Good			

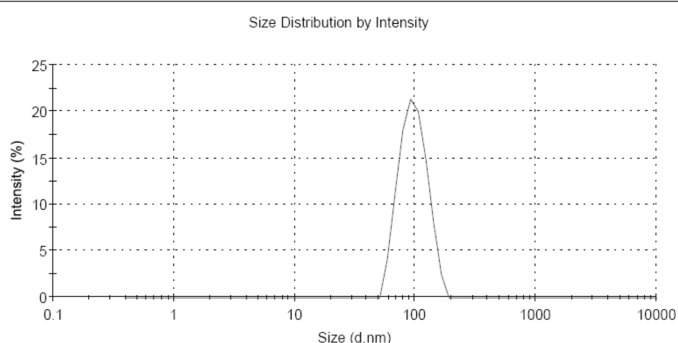


Figure S2. Typical size distribution of 100nm-sized vesicles.

Size exclusion chromatography (SEC)

In order to remove low molecular weight solutes vesicles can be purified by size exclusion chromatography via small spin columns.⁴¹ For this Sephadex LH-20 SEC medium was swollen in buffer solution prior to use. 5 mL bed volume per mL vesicle suspension was transferred into a small plastic syringe with filter support and removed plunger and the solvent removed by centrifugation (Eppendorf bench top centrifuge, 15 sec @ 4400 rpm). Vesicle solutions were added onto the column and recovered by subsequent centrifugation.

Cu- and Zn-quantification via atomic emission spectroscopy (ICP-AES)

In order to verify the receptor concentration of prepared vesicles their total metal content was measured via ICP-AES on a Spectro Flame-EOP spectrometer. Standard curves were recorded in Millipore water to quantify Cu and Zn in stock solutions of **Cu3** and **Zn₂1**. Metal contents were again determined after receptor-embedding in vesicle membranes and purification of vesicular solutions via SEC.

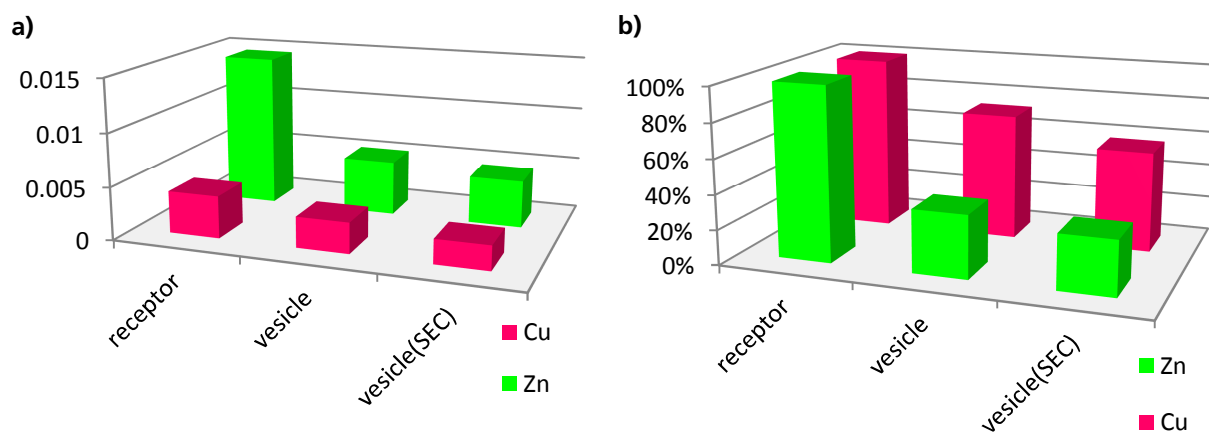


Figure S3. (a) Absolute (in mM) and (b) relative concentrations of Cu- and Zn in stock solutions of **Cu3** and **Zn21** and corresponding vesicle preparations before and after purification via SEC.

Supporting experimental data for Zn₂5-vesicles vs. P1

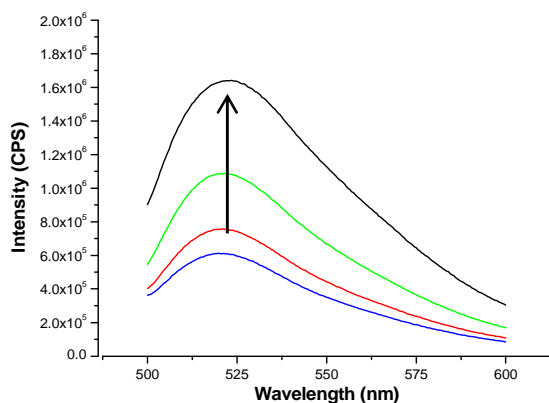


Figure S4. Raw emission spectra of **P1** in the presence of increasing amounts of receptor-vesicles.

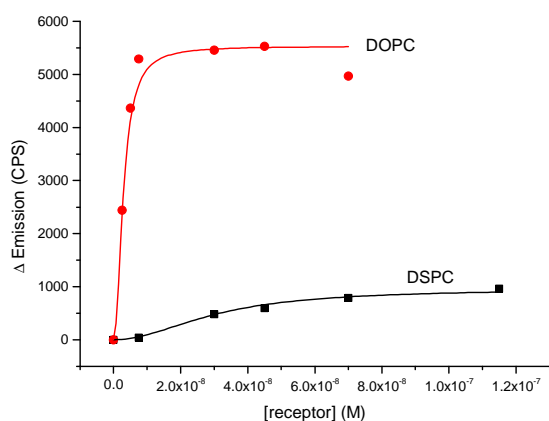


Figure S5. Emission response of **Zn₂5** doped (1 mol% each) DOPC and DSPC vesicle membranes.

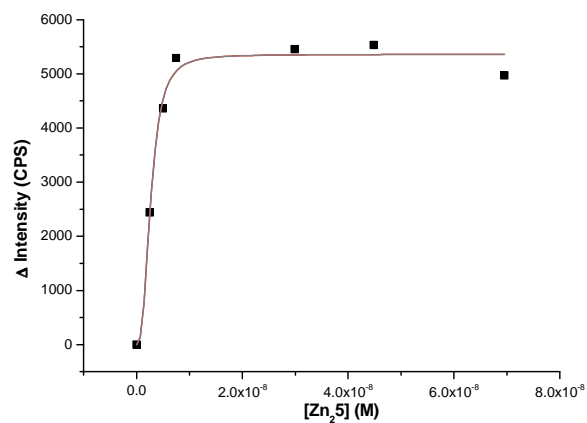


Figure S6. Non-linear curve fitting of DOPC-vesicles doped with 1 mol% Zn_25 .

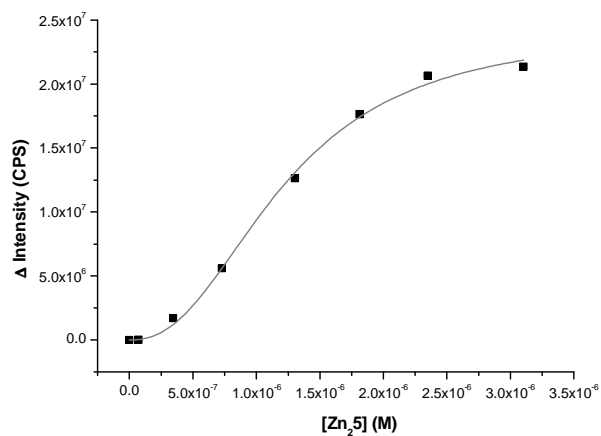


Figure S7. Non-linear curve fitting of DSPC-vesicles doped with 1 mol% Zn_25 .

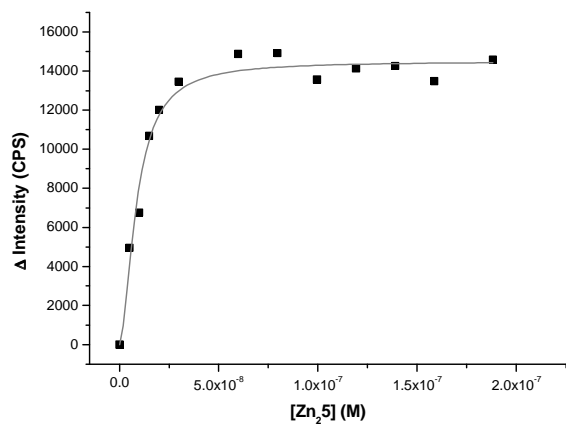


Figure S8. Non-linear curve fitting of DSPC-vesicles doped with 10 mol% Zn_25 .

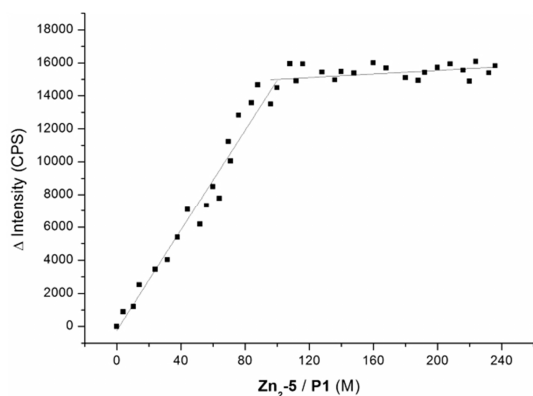


Figure S9. Job's Plot (limiting reagent method) of **P1** vs. DSPC-vesicles doped with 1 mol% **Zn₂5**.

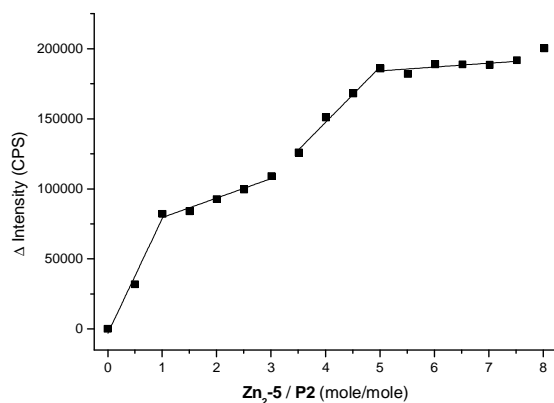


Figure S10. Job's Plot (limiting reagent method) of **P1** vs. DSPC-vesicles doped with 1 mol% **Zn₂5**.

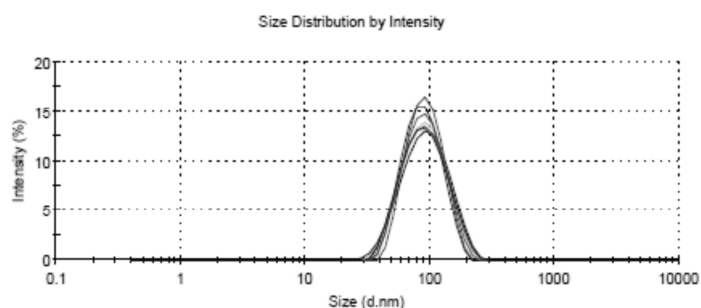


Figure S11. Size distributions of vesicles doped with 1 mol% **Zn₂5** in the presence of increasing amounts of **P1** (0.5 – 200 eq.) showing no apparent crosslinking of membranes.

Supporting experimental for Zn₂/Cu₄-vesicles vs. P1

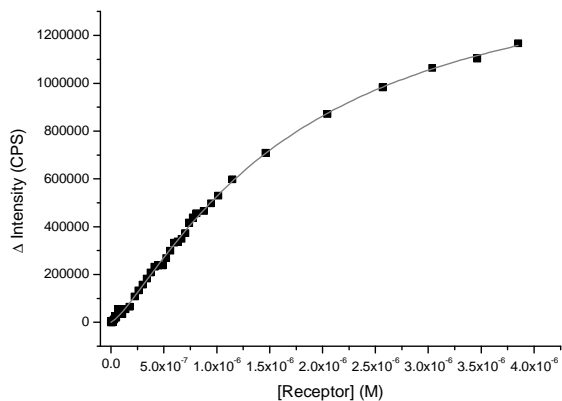


Figure S12. Non-linear curve fit for **Zn₂2** (1 mol%) in DOPC-vesicles.

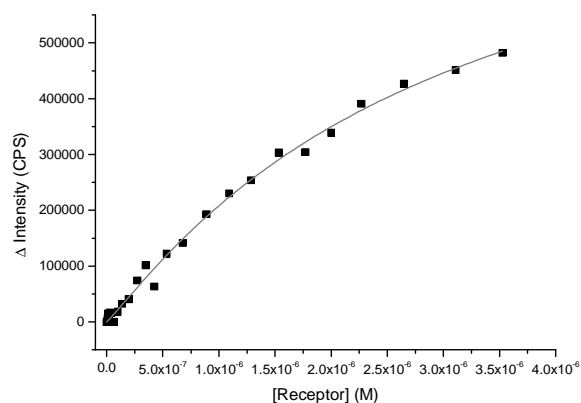


Figure S13. Non-linear curve fit for **Cu₄** (1 mol%) in DOPC-vesicles.

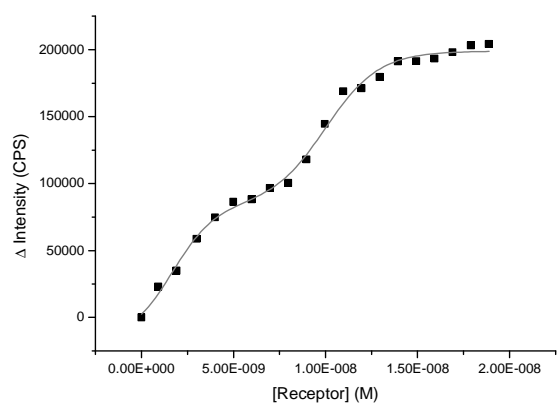


Figure S14. Non-linear curve fit for **Zn₂2 + Cu₄** (1 mol% each) in DOPC-vesicles.

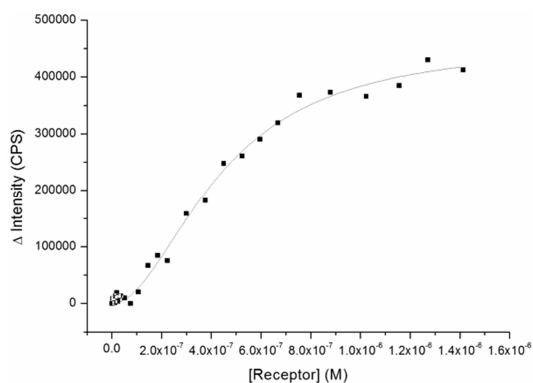


Figure S15. Non-linear curve fit for **Zn₂⁺** (1 mol% each) in DSPC-vesicles.

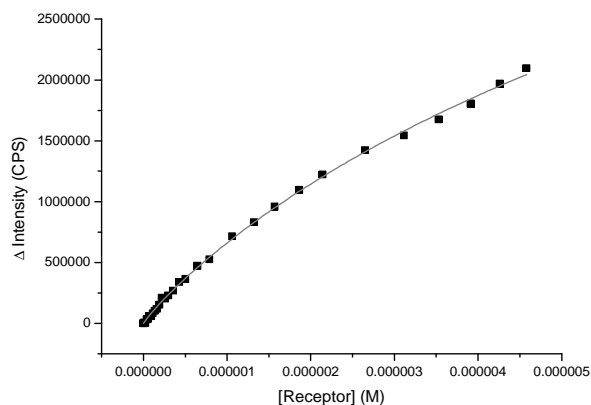


Figure S16. Non-linear curve fit for **Cu₄⁺** (1 mol% each) in DSPC-vesicles.

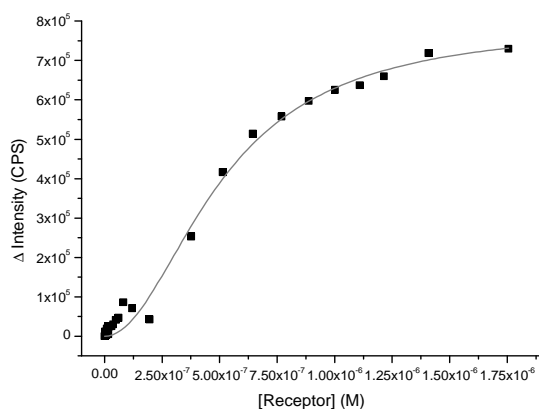


Figure S17. Non-linear curve fit for **Zn₂⁺ + Cu₄⁺** (1 mol% each) in DSPC-vesicles.

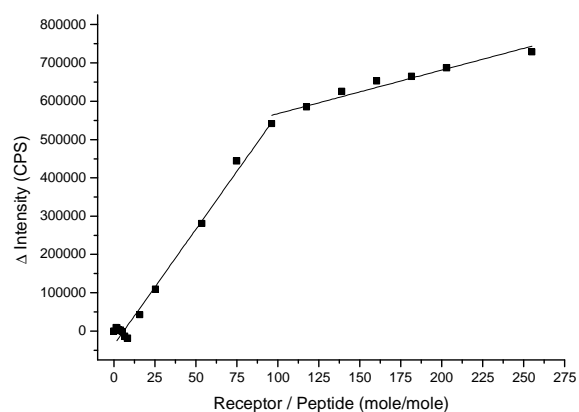


Figure S18. Job's Plot (limiting reagent method) of **P1** vs. DSPC-vesicles doped with **Zn₂⁺** + **Cu₄⁺** (1 mol% each).

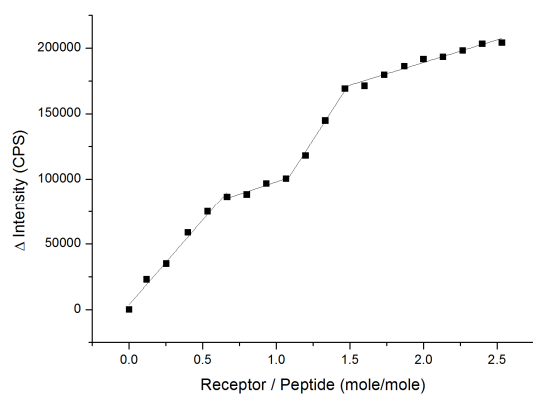


Figure S19. Job's Plot (limiting reagent method) of **P1** vs. DOPC-vesicles doped with **Zn₂⁺** + **Cu₄⁺** (1 mol% each)

Supporting experimental for Zn₂⁺/Cu₃⁺-vesicles vs. P2

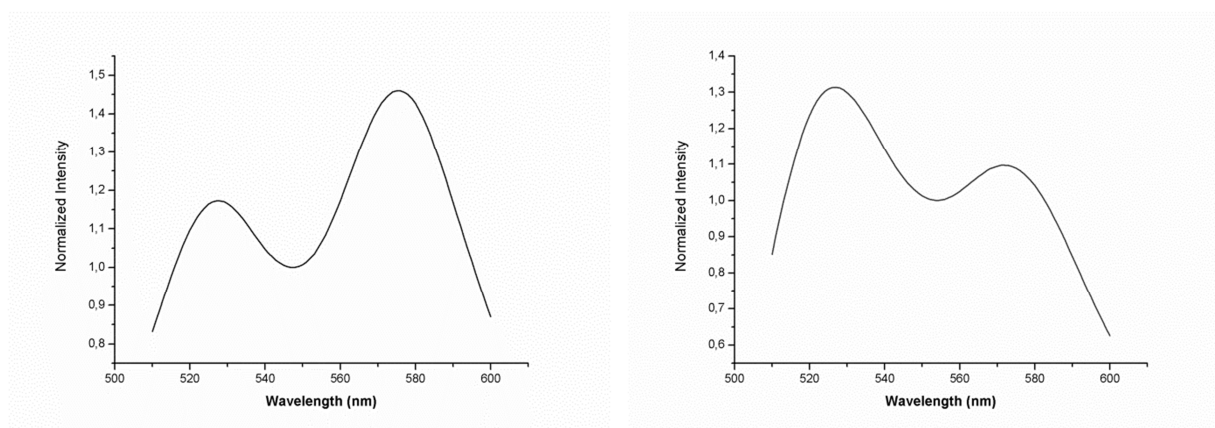


Figure S20. Fluorescence emission spectra of DSPC (left) and DOPC (right) vesicles equipped with **Cu₃⁺** and **Zn₂₁⁺** (0.5 mol% each).

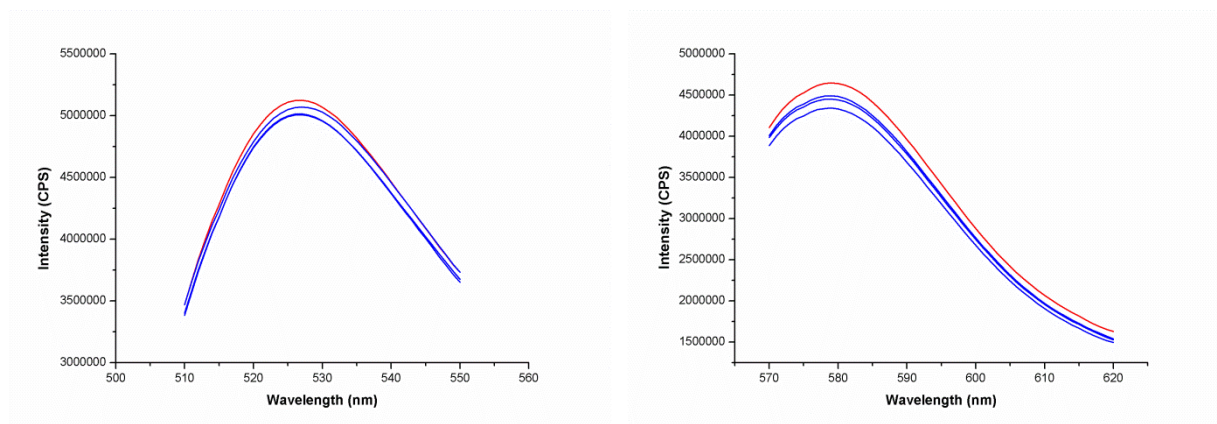


Figure S21. Raw emission spectra of DOPC vesicles functionalized with either 0.1 mol% of **Zn₂1** (left) or **Cu₃** (right) in the presence of increasing amounts of mono- or divalent peptide ligands (**P₀**, **P_H**, **P_P** or **P₂**, 0 – 100 eq.). Peptide binding towards these mono-receptor-vesicles does not produce a significant emission response.

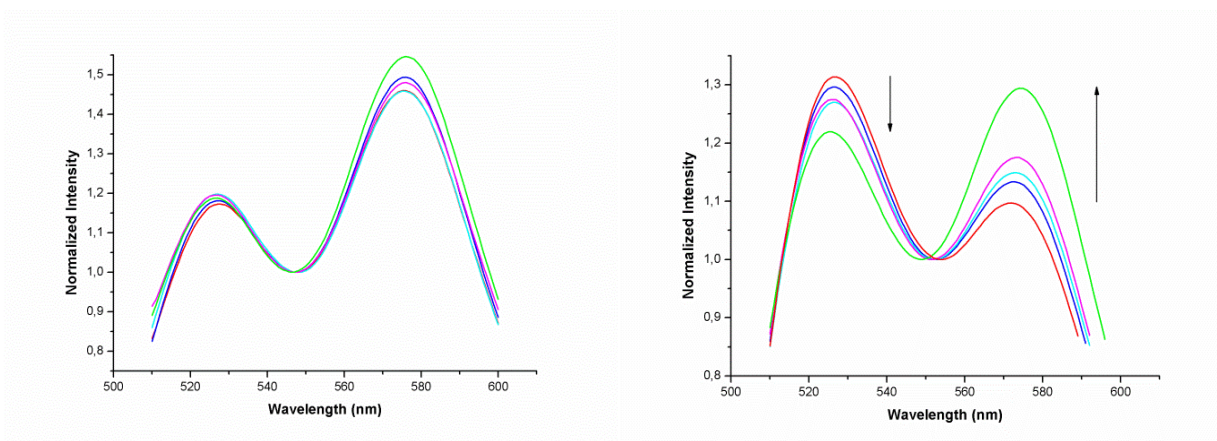


Figure S22. Emission spectra of DSPC vesicles (left) and DOPC vesicles (right) functionalized with 0.5 mol% **Cu₃** and **Zn₂1** each in the presence of increasing amounts of **P₂**.

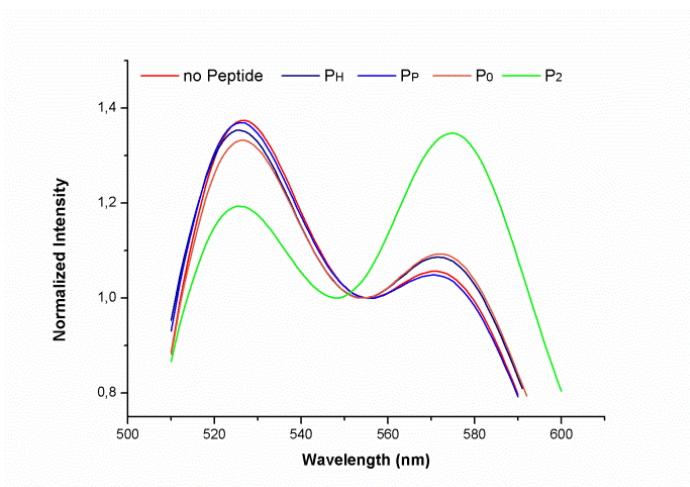


Figure S23. Emission spectra of DOPC vesicles (0.5 mol% **Cu₃** and **Zn₂1**) in the presence of equivalent amounts of the control peptides **P_H**, **P_P** and **P₀** compared to **P₂**.

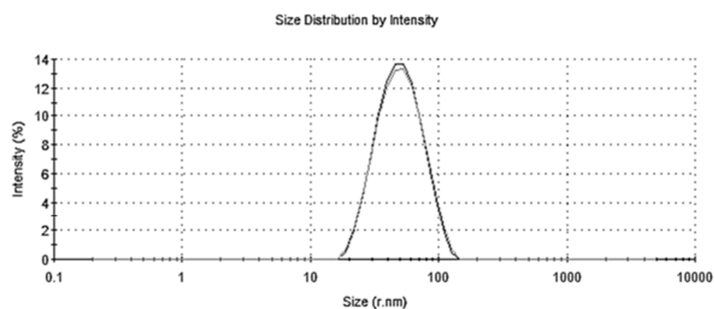


Figure S24. Observed particle size distribution for mixtures of DOPC/**Cu3**-vesicles (0.1 mol%) and DOPC/**Zn₂₁**-vesicles (0.1 mol%) before (black) and after (grey) treatment with **P2** showing no apparent crosslinking and increase in vesicle size.

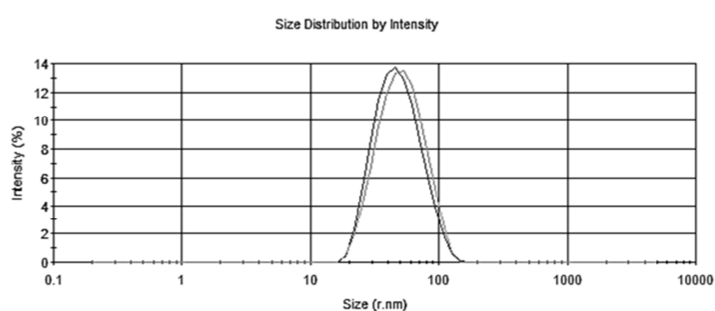


Figure S25. Observed particle size distribution for DOPC vesicles functionalized with **Cu3** and **Zn₂₁** (0.1 mol% each) before (black) and after (grey) treatment with **P2** showing no apparent crosslinking and increase in vesicle size.

References

1. B. Alberts, A. Johnson and J. Lewis, *Molecular Biology of the Cell. 4th edition*, Garland Science, New York, 2002.
2. M. Luckey, *Membrane Structural Biology*, Cambridge Univ. Press, 2008.
3. S. Singer, *Science*, 1992, **255**, 1671-1677.
4. A. Grakoui, S. K. Bromley, C. Sumen, M. M. Davis, A. S. Shaw, P. M. Allen and M. L. Dustin, *Science*, 1999, **285**, 221-227.
5. M. Renner, C. G. Specht and A. Triller, *Curr. Opin. Neurobiol.*, 2008, **18**, 532-540.
6. P. Tolar, J. Hanna, P. D. Krueger and S. K. Pierce, *Immunity*, 2009, **30**, 44-55.
7. S. Tomas and L. Milanesi, *Nat. Chem.*, 2010, **2**, 1077-1083.
8. X. Wang, R. J. Mart and S. J. Webb, *Org. Biomol. Chem.*, 2007, **5**, 2498-2505.
9. T. Schrader, M. Maue and M. Ellermann, *J. Recept. Signal Transduct. Res.*, 2006, **26**, 473-485.
10. K. Bernitzki and T. Schrader, *Angew. Chem. Int. Ed.*, 2009, **48**, 8001-8005.

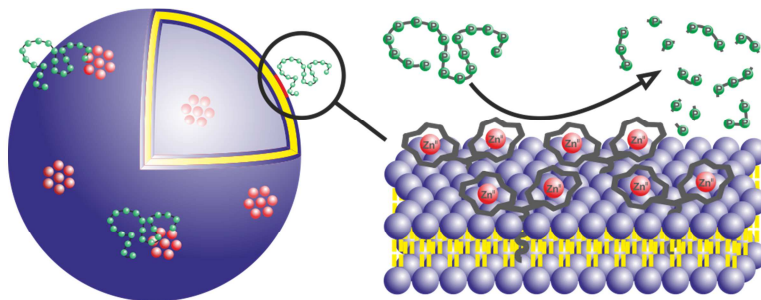
11. A. I. Elegbede, M. K. Haldar, S. Manokaran, J. Kooren, B. C. Roy, S. Mallik and D. K. Srivastava, *Chem. Commun.*, 2007, 3377–3379.
12. A. Perl, A. Gomez-Casado, D. Thompson, H. H. Dam, P. Jonkheijm, D. N. Reinhoudt and J. Huskens, *Nat. Chem.*, 2011, **3**, 317-322.
13. P. Scrimin and P. Tecilla, *Curr. Opin. Chem. Biol.*, 1999, **3**, 730-735.
14. P. Tecilla, F. Mancin, P. Scrimin and U. Tonellato, *Coord. Chem. Rev.*, 2009, **253**, 2150-2165.
15. J. Voskuhl and B. J. Ravoo, *Chem. Soc. Rev.*, 2009, **38**.
16. B. Gruber, E. Kataev, J. Aschenbrenner, S. Stadlbauer and B. König, *J. Am. Chem. Soc.*, 2011, **133**, 20704-20707.
17. D. A. Jose, S. Stadlbauer and B. König, *Chem. Eur. J.*, 2009, **15**, 7404-7412.
18. E. Mahon, T. Aastrup and M. Barboiu, *Chem. Commun.*, 2010, **46**, 2441-2443.
19. L. Chen, S. Xu and J. Li, *Chem. Soc. Rev.*, 2011, **40**, 2922-2942.
20. M. Komiyama, T. Takeuchi, T. Mukawa and H. Asanuma, *Molecular Imprinting*, Wiley-VCH, 2004.
21. J. T. Groves, *Angew. Chem.*, 2005, **117**, 3590-3605.
22. S. Shinkai and M. Takeuchi, *Biosens. Bioelectron.*, 2004, **20**, 1250-1259.
23. N. W. Turner, B. E. Wright, V. Hlady and D. W. Britt, *J. Colloid Interface Sci.*, 2007, **308**, 71-80.
24. B. Gruber, S. Stadlbauer, A. Späth, S. Weiss, M. Kalinina and B. König, *Angew. Chem. Int. Ed.*, 2010, **49**, 7125-7128.
25. B. Gruber, S. Stadlbauer, K. Woinaroschy and B. König, *Org. Biomol. Chem.*, 2010, **8**, 3704-3714.
26. A. Grauer, A. Riechers, S. Ritter and B. König, *Chem. Eur. J.*, 2008, **14**, 8922-8927.
27. For phase transition temperatures and other physical properties of lipids see also LIPIDAT database (<http://www.lipidat.tcd.ie/homeLIPIDAT.asp>)
28. S.-i. Tamaru and I. Hamachi, ed. R. Vilar, Springer Berlin / Heidelberg, 2008, pp. 95-125.
29. The Zn-DPA complex will coordinate to the serine phosphate moiety, while complex Cu⁴ coordinates the imidazole moiety of histidine.
30. L. M. Loura and M. J. Prieto, *Frontiers in Physiology*, 2011, **2**.
31. Integrated DNA Technologies - Technical Bulletins, Fluorescence Resonance Energy Transfer, 2000, www.idtdna.com
32. In the absence of the target analyte peptide no FRET-emission is detected, as the average distance of the two chromophores in the fluid membrane is too large (Figure S20).
33. As indicated by these measurements vesicle preparation and purification results in up to 25% loss of embedded amphiphiles. All apparent binding constants reported in here however were not corrected regarding this decreased receptor concentration. As a result all log K-values are considered "minimum" affinities.

34. S. Hünig, G. Märkl and J. Sauer, *Einführung in die apparativen Methoden in der Organischen Chemie, 2nd Edition*, Würzburg / Regensburg, 1994.
35. A. Ojida, K. Honda, D. Shinmi, S. Kiyonaka, Y. Mori and I. Hamachi, *J. Am. Chem. Soc.*, 2006, **128**, 10452-10459.
36. M. E. Jung and T. I. Lazarova, *The Journal of Organic Chemistry*, 1997, **62**, 1553-1555.
37. R. C. MacDonald, R. I. MacDonald, B. P. M. Menco, K. Takeshita, N. K. Subbarao and L.-r. Hu, *Biochim. Biophys. Acta*, 1991, **1061**, 297-303.
38. A. J. Jin, D. Huster, K. Gawrisch and R. Nossal, *Eur. Biophys. J.*, 1999, **28**, 187-199.
39. J. F. Nagle and S. Tristram-Nagle, *Biochim. Biophys. Acta*, 2000, **1469**, 159-195.
40. P. Balgavy, M. Dubnickova, N. Kucerka, M. A. Kiselev, S. P. Yaradaikin and D. Uhrikova, *Biochim. Biophys. Acta*, 2001, **1512**, 40-52.
41. D. W. Fry, J. C. White and I. D. Goldman, *Anal. Biochem.*, 1978, **90**, 809-815.

CHAPTER 5

VESICLES AND MICELLES FROM AMPHIPHILIC Zn(II)-CYCLEN COMPLEXES AS HIGHLY POTENT PROMOTERS OF HYDROLYTIC DNA CLEAVAGE

Phosphate esters are essential to any living organism and their specific hydrolysis plays an important role in many metabolic processes. As phosphodiester bonds can be extraordinary



stable, as in DNA, great effort has been put into mimicking the active sites of hydrolytic enzymes which can easily cleave these linkages and were often found to contain one or more coordinated metal ions. With this in mind, we report micellar and vesicular Zn(II)-cyclen complexes which considerably promote the hydrolytic cleavage of native DNA and the activated model substrate bis(4-nitrophenyl)phosphate (BNPP). They are formed by self-assembly from amphiphilic derivatives of previously employed complexes in aqueous solution and therefore allow a simple and rapid connection of multiple active metal sites without great synthetic effort. Considering the hydrolytic cleavage of BNPP at 25 °C and pH 8, the micellar and vesicular metal catalysts show an increase of second-order rate constants (k_2) by 4 – 7 orders of magnitude compared to the unimolecular complexes under identical conditions. At neutral pH, they produce the highest k_2 values reported so far. For pBR322 plasmid DNA, both a conversion of the supercoiled to the relaxed and linear form, and also a further degradation into smaller fragments by double strand cleavages could be observed after incubation with the vesicular Zn(II)-complexes. Finally, even the cleavage of nonactivated single-stranded oligonucleotides could be considerably promoted compared to background reaction.

This chapter has been published:

B. Gruber, E. Kataev, J. Aschenbrenner, S. Stadlbauer and B. König, *J. Am. Chem. Soc.* **2011**, *133*, 20704-20707.

Author contributions:

BG designed and performed BNPP-, pBR322- and TaqMan®probe-assays and wrote the manuscript; EK performed BNPP-assays and contributed to manuscript writing; JA carried out BNPP-, pBR322- and TaqMan®probe-assays in the course of her teacher's thesis (Zulassungsarbeit); SS synthesized compound Zn1; BK supervised the project and is corresponding author.

Introduction

Phosphate esters are ubiquitously found in nature and essential to any living being as DNA with its phosphodiester backbone contains the genetic code of an organism. Therefore these biomolecules need to possess a sufficient stability under physiological conditions to prevent premature degradation or accidental altering - DNA has an estimated half-life of 30 million years concerning the spontaneous hydrolysis of a single phosphodiester bond.¹

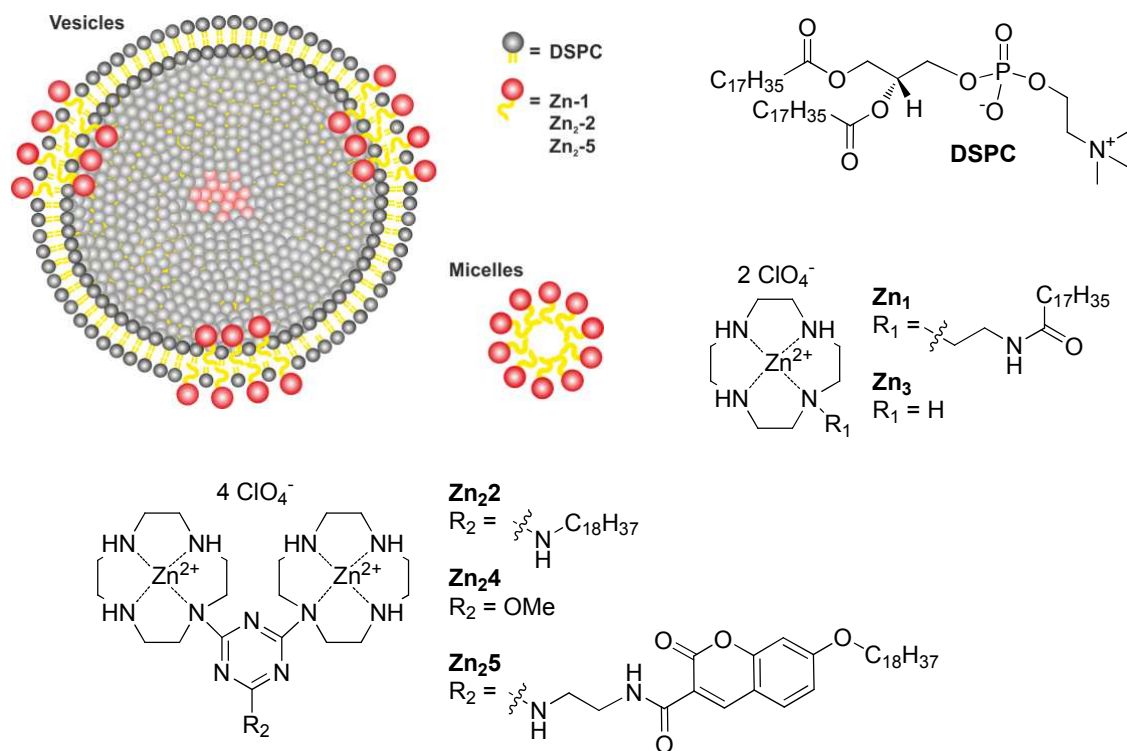
Nevertheless the specific hydrolysis of such very stable phosphodiester bonds plays an important role in metabolic and regulatory processes² and is easily performed by specific enzymes, which often contain metal ions in their active sites.^{3, 4} Understanding and mimicking these enzymes still represents a challenge for chemists. A variety of different synthetic catalysts for hydrolysis of DNA and corresponding model substrates have been reported, usually based on lanthanide^{5, 6} or transition metal ions like Cu(II), Ni(II), Co(II) and Zn(II).⁷⁻¹⁰ Although Zn(II) ions were occasionally reported to be less efficient, they are the choice of hydrolytic enzymes. Therefore, the design of zinc-based catalysts for phosphodiester hydrolysis is a favorable biomimetic strategy.^{11, 12} Covalent connection of two or more Zn(II)-catalytic centers by a defined spacer has allowed to achieve higher catalytic rates for the cleavage of non-activated phosphate ester bonds, than those observed only for a single Zn(II)-center.¹¹ Combination of catalytic centers through non-covalent interactions in a metallomicelle¹³⁻¹⁶ as well as immobilization on polymer supports^{17, 18} or on nanoparticles¹⁹ are other successful strategies to increase hydrolytic activity.^{20, 21}

Results and Discussion

We report here self-assembled catalytic systems, which are able to promote the hydrolysis of both native DNA and activated model substrates. The catalysts are based on amphiphilic derivatives of the Zn(II)-complex of 1,4,7,10-tetraazacyclododecane, which was previously found to promote the hydrolytic cleavage of phosphodiester substrates.²² In buffered aqueous solution the amphiphilic catalysts Zn1 and Zn2 spontaneously assemble either into homomicelles or into vesicular membranes if mixed with a suitable lipid component like 1,2-distearoyl-*sn*-glycero-3-phosphocholine (DSPC; Scheme 1).

Syntheses and preparation procedures have been previously described by us^{23, 24} or are given in the Supporting Information (SI). A series of mono- and bis-cyclen-based zinc complexes (Zn1 - Zn5) have been tested for the hydrolysis of the simple DNA model substrate bis-(4-nitrophenyl) phosphate (BNPP) in the pH range from 7 to 9 by following the absorption (Abs) increase of released nitrophenolate (NP) at 408 nm.²² We have employed our amphiphilic catalyst derivatives as micellar and vesicular solutions by adding them to 1 - 10 mM solutions of BNPP and recorded kinetics using an initial slopes method in TRIS buffer

(50 mM) at a slightly basic pH of 8.0, as these are common conditions for DNA hydrolysis experiments and allow a comparison of rate constants with reported values and in HEPES buffer (25 mM) at neutral pH (7.4), which renders the hydrolysis conditions more challenging.



Scheme 1. (Amphiphilic) Zn(II)-complexes and vesicular/micellar catalyst systems.

While at pH 8 Zn₂4 represents one of the most active Zn(II) complexes for this reaction,¹⁶ we observed that hydrolytic rates are exceeded by more than four orders of magnitude using Zn₂2 micelles (at 2.3 mM BNPP and 0.045 mM Zn₂2; Table 1)²⁵. The rate constant for Zn₁-micelles under these conditions is one order of magnitude lower. However, compared to Zn₃ as reference the micellar system outperforms the unimolecular catalyst by seven orders of magnitude at identical experimental conditions. At pH 7.4 Zn₁-micelles give about the same rate constants as at pH 8 whereas the rate constant of Zn₂2-micelles drops by about one order of magnitude. As a result both micellar catalysts give similar k_2 -values under these conditions and still show a remarkable promotion of BNPP hydrolysis, whereas the unimolecular complexes Zn₃ and Zn₂4 are not able to produce significant amounts of NP here.

After observing the remarkable rate increases for the micellar catalysts we used the amphiphilic zinc complexes in vesicular catalysts optimizing a number of parameters: We prepared vesicles in sizes ranging from about 60-150 nm and compared their rate constants which turned out to be all in the same order of magnitude however the maximum activity was obtained at about 100 nm (see SI, Table S3 and Figure S12). As a result we used these

for all further experiments. Next we varied particle composition in terms of Zn(II)-content of the DSPC vesicle membrane. The peak activity here was found at loading levels of 10 mol% Zn₂ as shown by pseudo-first order rate constants k_{obs} in Table S2. Higher amounts of metal complexes lead to increasing particle destabilization (indicated by DLS, size exclusion experiments and shifted emission wavelengths, cf. Figure S4) and reduced catalytic efficiency. Generally best results were achieved at BNPP concentrations of 2.3 mM and 0.02 equivalents of Zn(II) (see also Figures S7 and S8). At these conditions the vesicular catalysts derived from Zn1 and Zn₂ yielded second order rate constants in the same order of magnitude as the Zn1- and Zn₂-micelles (Table 1).

Entry	Catalyst	T (° C)	pH	k_2 (M ⁻¹ s ⁻¹)	k_{rel}	Ref
1	OH ⁻	35	7	2.4×10^{-5}	1	20a
2	Zn1-vesicles (DSPC / Zn1 9:1)	25	8	1.5	n.d.	a)
3	Zn1-vesicles (DSPC / Zn1 9:1)	25	7.4	1.8	75000	a)
4	Zn ₂ -vesicles (DSPC / Zn ₂ 9:1)	25	8	24	n.d.	a)
5	Zn ₂ -vesicles (DSPC / Zn ₂ 9:1)	25	7.4	9.4	391667	a)
6	Zn1-micelles ^{a)}	25	8	7.9	n.d.	a)
7	Zn1-micelles ^{a)}	25	7.4	7.4	308333	a)
8	Zn ₂ -micelles ^{a)}	25	8	68	n.d.	a)
9	Zn ₂ -micelles ^{a)}	25	7.4	7.9	329167	a)
10	Zn3	25	8	6.3×10^{-7}	n.d.	11
11	Zn3	25	7.4	- ^{b)}	- ^{b)}	a)
12	Zn ₂ 4	25	8	1.3×10^{-3}	n.d.	11
13	Zn ₂ 4	25	7.4	- ^{b)}	- ^{b)}	a)
14	Zn(II)-micelles	35	10	4.3×10^{-4}	n.d.	7a
15	Zn(II)-MPGNs	40	7	1.5	62500	9
16	Ce(IV)-micelles	37	7	0.6	25000	20b
17	Ce(IV)-MPGNs	40	7	0.93	38750	20b

Table 1. Second order rate constants (k_2) for BNPP hydrolysis at neutral pH and 25 °C unless otherwise stated and second order rate constants relative to the hydroxide promoted reaction (k_{rel}). ^{a)} This work; ^{b)} Below detection limit.

All kinetic data showed excellent reproducibility (cf. Figure S16) and control experiments with pure DSPC vesicles containing no metal complexes and buffer solution were performed to determine background hydrolysis. No significant amounts of the hydrolysis product nitrophenolate could be detected here (Figure S15).

We explain the dramatically increased reaction rates of our self-assembled catalyst systems by the high local concentration of coordinated Zn(II) ions either in the metallomicelles or in

tightly packed domains of metal complexes embedded in the bilayer membranes²⁶ and the decreased polarity²⁷ at the vesicle bilayer-water interface, which can be compared to MeOH/CHCl₃-mixtures (SI, Figure S5) and therefore facilitates a nucleophilic attack of the phosphodiester substrate compared to bulk water. Despite the high reaction rates however no complete conversion of the BNPP substrate could be achieved by micelles or vesicles as indicated by the saturation Abs values and the produced NP equivalents (see also SI). Although this was not observed in the previous studies with Zn₃ and Zn₂4 product inhibition might explain limited turnovers as much lower amounts of Zn²⁺ (0.02 eq.) were used for micellar and vesicular catalysis compared to the unimolecular complexes which were usually employed stoichiometrically.²² A high excess of BNPP and NP(P) might replace counterions (like reactive OH⁻) in the surrounding layer of the densely packed Zn²⁺ aggregates and therefore reduce their catalytic activity or even lead to particle destabilization due to charge neutralization (cf. Figure S9).

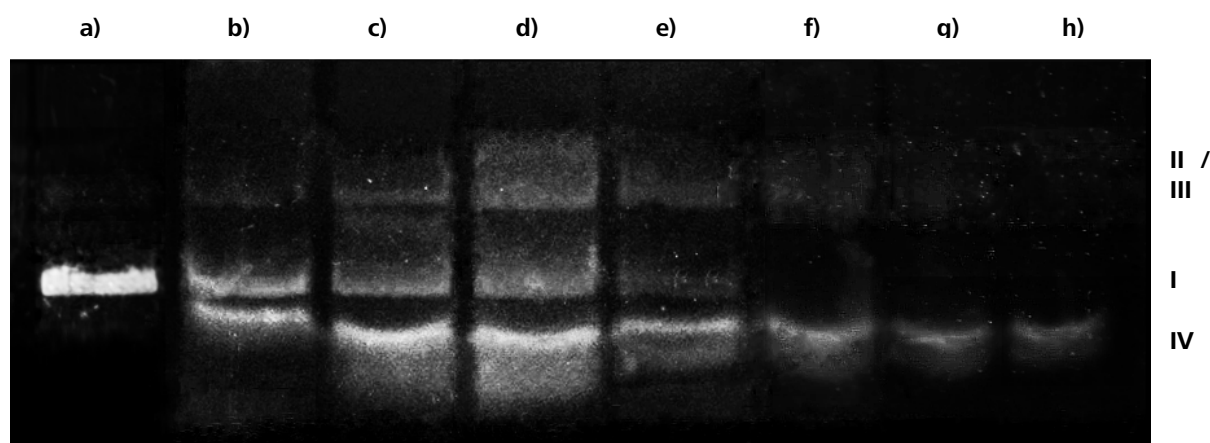


Figure 1. Agarose gel (0.7%) electrophoresis of pBR322 (100 ng per lane) vs. Zn₂-vesicles (1 x 10⁻⁴ M) incubated at 40 °C at pH 7.4 for (a) 0 h (b) 4 h (c) 11 h (d) 24 h (e) 33 h (f) 38 h (g) 42 h (h) 48 h.

The high hydrolysis rates observed with the activated phosphate diester BNPB encouraged us to expand the study to the hydrolysis of less activated oligonucleotides. pBR322 plasmid DNA is a widely used test substrate for artificial hydrolases. The dsDNA is transformed by strand cleavage from its initial supercoiled strained form (I) into its relaxed circular form (II) and further on to its open linear form (III). All forms are distinguishable by agarose gel electrophoresis.^{28, 29} Supercoiled pBR322 (100 ng) with a size of 4.3 kb was incubated with Zn₂-vesicles (1 x 10⁻⁴ Zn(II)) at pH 7.4 and 40 °C for different periods of time before the reactions were stopped with an excess of SDS and EDTA. The obtained samples were then separated on agarose mini gels (0.7% w/w) and stained with ethidium bromide. As shown in Figure 1, the supercoiled DNA form (I) is completely degraded with increasing incubation times of up to 38 h. However it is not only transformed to forms II/III, but also to smaller DNA fragments (IV) with a size of approximately 2.0 kb³⁰ corresponding to about half the size of the plasmid. The band of these fragments appears on the gel even before the bands of form II/III indicating that double-strand cleavages take place. The cleavage is not selective

and all bands broaden with progressing incubation times; after 24 h all four forms are present. The bands become subsequently weaker with time and convert into a smear around band IV. Such degradation is remarkable under these conditions and usually only reported for oxidative degradation conditions.³¹ Control experiments using vesicles without Zn₂ and only buffer solution showed that the supercoiled DNA remained stable under the otherwise unchanged experimental conditions. Additionally, separate samples of the vesicular catalysts were applied to the gels without DNA to exclude the occurrence of fluorescent bands by vesicle-ethidium bromide interactions (Figure S18).

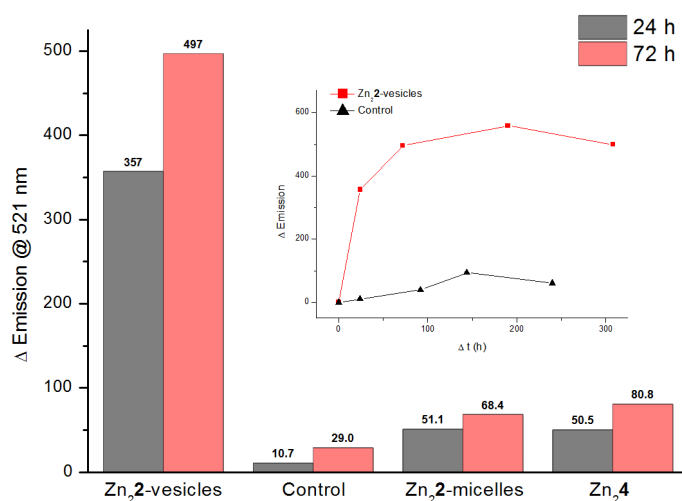


Figure 2. Emission increase of TaqMan® probe (1×10^{-8} M) incubated with Zn₄, Zn₂-vesicles and -micelles (1×10^{-5} M Zn(II)) and buffer only at 40 °C and pH 8.0 for 24 and 72 h. Inset: Kinetics for Zn₂-vesicles and background hydrolysis for comparison.

After observing high hydrolysis rates for BNPP and on strained plasmide dsDNA we tested our catalytic systems on a single-stranded oligonucleotide as a more challenging substrate. We chose the commercially available TaqMan® probe consisting of a 24mer oligonucleotide with the random sequence CAAGTTTGACCAAGTCACAACGGC and a 5' fluorescence label (FAM; $\lambda_{\text{exc}} = 495$ nm, $\lambda_{\text{em}} = 520$ nm) and 3' quencher (BHQ-1 $\lambda_{\text{max}} = 534$ nm). The intact probe shows only very weak fluorescence intensity, but upon its cleavage at an arbitrary site the effect of the quencher on the fluorophore diminishes and an increasing emission intensity can be monitored. For our hydrolysis assay this probe (10^{-8} M) was incubated with Zn₂-micelles and -vesicles at 40 °C for increasing periods of time. The reactions were stopped by addition of SDS and EDTA and fluorescence emission intensities at 520 nm were recorded and plotted against incubation time as shown in Figure 2 (inset). In contrast to the results for BNPP the vesicular catalysts of Zn₂ clearly outperformed the micellar catalyst, which gave only a small enhancement over background hydrolysis similar to the monomeric water-soluble complex Zn₂3 illustrated by the comparison of a FAM emission increase after 24 and 72 h. According to the saturation fluorescence of the vesicular kinetics it was assumed that about 75%³² of the probe molecules have been cleaved at least at a single site which is

remarkable for a stable non-activated phosphodiester substrate. As control the kinetics were again repeated with pure DSPC vesicles and buffer solution which resulted in no fluorescence increase compared to background reaction.

The better performance of vesicles compared to micelles in the catalysis of polyphosphates may be explained by multivalence effects resulting in a higher substrate affinity of the vesicular catalyst. This hypothesis is supported by the much higher affinity of fructose-1,6-bisphosphate, used as a non-hydrolysable model substrate, to coumarin-labeled amphiphilic Zn(II)-complex Zn_25 (10^{-5} M in HEPES) if embedded in DSPC vesicles (10 mol% Zn_25) compared to homomicelles. Its attached fluorescence label previously allowed the direct observation of phosphate ion binding to the zinc complex in a vesicular environment by emission quenching²³ and is assumed to respond in a similar way if assembled in micelles (see SI, Figure S20 left). Emission titrations with fructose-1,6-bisphosphate revealed a binding constant towards the vesicles in the micromolar range,²³ while no significant zinc-phosphate coordination could be detected in micelles under these conditions (Figure S20 right).

Micellar and vesicular catalysts that promote the hydrolysis of phosphate esters were self-assembled from amphiphilic Zn(II)-cyclen complexes and commercial lipids. The approach avoids laborious synthesis to covalently connect multiple catalytic centers or attaching them to polymers or nanoparticles. Vesicles with embedded domains of dinuclear Zn(II) complexes showed a remarkable promotion of phosphodiester cleavage reactions. Although substrate conversion is limited here due to considerable product inhibition the highest so far reported activities for Zn(II) based catalysts in terms of second order rate constants for the hydrolysis of BNPP at neutral pH and 25 °C were observed, exceeding even those of lanthanide complexes.^{33, 34} pBR322 plasmid DNA is readily degraded by double strand cleavage, which is difficult to achieve with non-enzymatic catalysts.¹¹ The catalytic vesicles also considerably enhance the cleavage of a non-activated single-strand oligonucleotide compared to background reaction control.

Conclusion

In conclusion, vesicles with embedded metal complexes as catalytic active sites show a remarkable catalytic performance in phosphodiester hydrolysis although turnover numbers need to be improved to enable an effective applicability of these systems. Their preparation however is easy and very versatile which greatly facilitates further performance tuning in future studies. In particular the hydrolysis of non-activated oligophosphates is promoted, which might be due to the presence of dense clusters of bis-Zn(II) cyclen complexes as catalytic centers on the vesicle surface. Mechanistic details will also be investigated further. Combining such catalytically active sites with binding sites for sequence recognition by co-

embedding might pave the way to functionalized vesicles, which are able to discriminate in their hydrolysis between different substrates or target specific DNA sequences mimicking the properties of hydrolytic enzymes more closely.

Experimental Part and Supporting Information

Methods and Material

General

Phospholipids were purchased from Avanti Polar Lipids Inc., pBR322 DNA and the 1 kb DNA Ladder molecular weight standard from New England Biolabs Inc. and the TaqMan® probe from BioCat. Commercially available starting materials and solvents of standard quality were used without any further purification if not stated otherwise. Optional purification steps were performed according to accepted general procedures.³⁵ Thin layer chromatography (TLC) analyses were performed on silica gel 60 F-254 with a 0.2 mm layer thickness with detection via UV light at 254 nm / 326 nm or through staining with ninhydrin in EtOH. Column chromatography was performed on silica gel (70–230 mesh) from Merck. Melting Points were determined on Büchi SMP or a Lambda Photometrics OptiMelt MPA 100. Recorded with a Bio-Rad FTS 2000 MX FT-IR and Bio-Rad FT-IR FTS 155. Varian CH-5 (EI), Finnigan MAT 95 (CI; FAB and FD), Finnigan MAT TSQ 7000 (ESI). Xenon served as ionisation gas for FAB. Elemental analyses were carried out by the centre for chemical analysis of the Faculty of Chemistry and Pharmacy at the University of Regensburg.

NMR Spectra

Bruker Avance 600 (1H: 600.1 MHz, 13C: 150.1 MHz, T = 300 K), Bruker Avance 400 (1H: 400.1 MHz, 13C: 100.6 MHz, T = 300 K), Bruker Avance 300 (1H: 300.1 MHz, 13C: 75.5 MHz, T = 300 K). The chemical shifts are reported in δ [ppm] relative to external standards (solvent residual peak). The spectra were analyzed by first order, the coupling constants are given in Hertz [Hz]. Characterization of the signals: s = singlet, d = doublet, t = triplet, q = quartet, m = multiplet, bs = broad singlet, psq = pseudo quintet, dd = double doublet, dt = double triplet, ddd = double double doublet. Integration is determined as the relative number of atoms. Assignment of signals in 13C-spectra was determined with DEPT-technique (pulse angle: 135 °) and given as (+) for CH₃ or CH, (-) for CH₂ and (C_q) for quaternary C_q. Error of reported values: chemical shift: 0.01 ppm for 1H-NMR, 0.1 ppm for 13C-NMR and 0.1 Hz for coupling constants. The solvent used is reported for each spectrum.

Absorption and Emission Spectroscopy

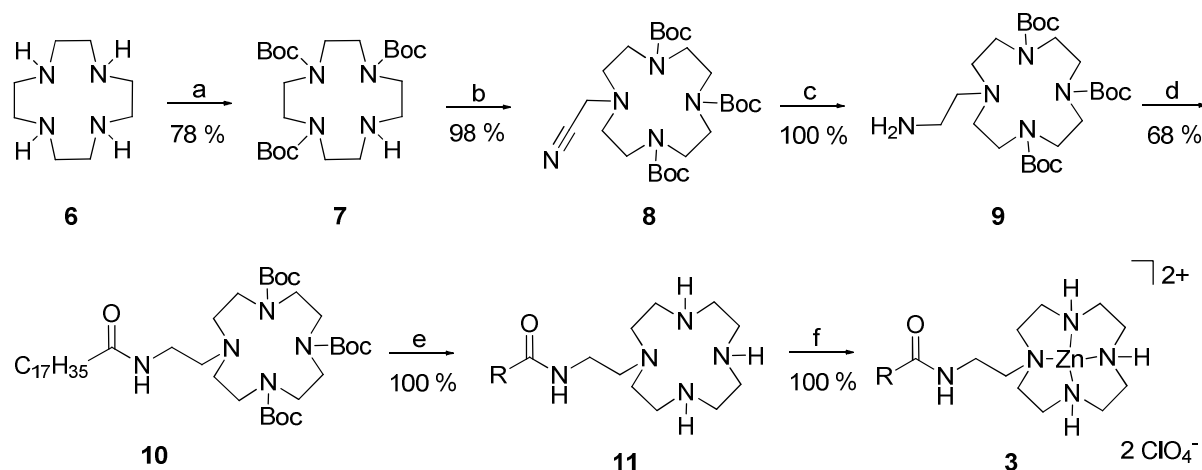
Fluorescence spectra were recorded on a 'Cary Eclipse' fluorescence spectrophotometer and absorption spectra on a "Cary BIO 50" UV/VIS/NIR spectrometer from Varian. All measurements were performed in 1 cm quartz cuvettes (Hellma) and UV-grade solvents (Baker or Merck) at 25 °C.

Dynamic Light Scattering

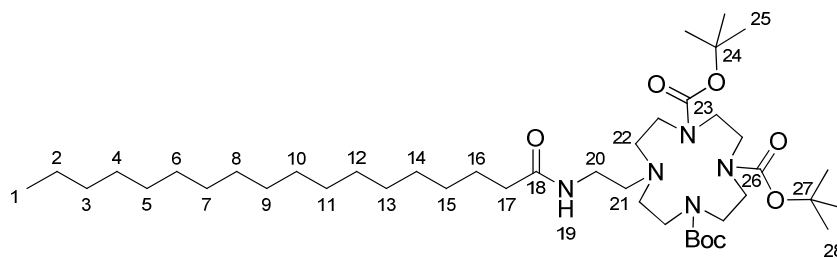
PCS measurements were performed on a Malvern Zetasizer Nano ZS at 25 °C using 1 cm disposable polystyrene cuvettes and automatically optimized settings.

Synthesis of amphiphilic mononuclear Zn(II)-cyclen

The protected mono-cyclen amine **9** was prepared according to literature known procedures³⁶ and allowed to form the amide with stearic acid using TBTU and HOBt as activation reagents in a dry DMF / THF solvent mixture. Cleavage of the Boc-groups by HCl saturated ether, subsequent deprotonation by basic anion exchanger resin and complex formation by treatment with one equivalent Zn(ClO₄)₂ gave the amphiphilic mononuclear Zn(II)-cyclen **Zn1**.

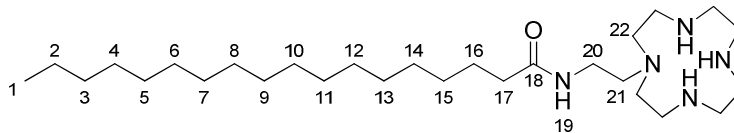


Scheme S1. Synthesis of **Zn1**: (a) Boc₂O, DCM, RT, 3 h; (b) bromoacetonitrile, K₂CO₃, MeCN, 80 °C, 20 h; (c) H₂/Raney Ni, EtOH/NH₃, RT, 20 bar, 48 h; (d) stearic acid, TBTU, HOBt, DIPEA, DMF / THF, 40 °C, 3 h; (e) HCl / ether, DCM o/n, basic ion exchanger resin; (f) Zn(ClO₄)₂, MeOH, 65 °C, 19 h.



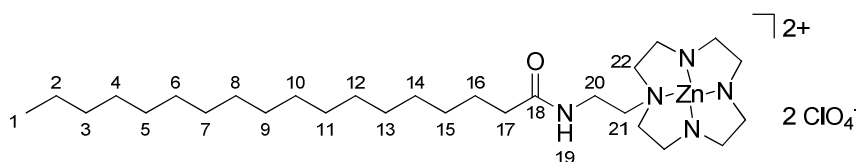
10-(2-Octadecanoylamino-ethyl)-1,4,7,10 tetraaza-cyclododecane-1,4,7-tricarboxylic acid tri-tert-butyl ester (**10**)

Stearic acid (170 mg, 0.60 mmol), DIPEA (412 μ L, 2.39 mmol), TBTU (211 mg, 0.66 mmol), and HOBt (101 mg, 0.66 mmol) were dissolved under nitrogen atmosphere in dry DMF (4 mL) under ice cooling and stirred for 1 h. Subsequently amine **9** (308 mg, 0.60 mmol) dissolved in DMF was added. The reaction was allowed to warm to room temperature and was 3 h at 40 °C. The reaction progress was monitored by TLC (EE). After completion of the reaction the solvent was removed and the crude product was purified by flash column chromatography on flash silica gel (EE; R_f = 0.45) yielding compound **10** (320 mg, 0.41 mmol, 68%) as a colourless oil. **¹H-NMR** (400 MHz; CDCl₃): δ (ppm) = 0.86 (t, 3J = 7.0 Hz, 3 H, HSQC, COSY: C¹H₃), 1.18-1.31 (m, 28 H, HSQC, COSY: C²H₂-C¹⁵H₂), 1.43 (s, 9 H, HSQC: C²⁸H₃), 1.45 (s, 18 H, HSQC: C²⁵H₃), 1.54-1.66 (m, 2 H, HSQC, COSY: C¹⁶H₂), *conformational isomers*: 2.16^a, 2.29^b (t, $^3J^a$ = 8.0 Hz, $^3J^b$ = 7.6 Hz, 2 H, HSQC, COSY: C¹⁷H₂), 2.63 (bs, 6 H, HSQC, COSY: C²²H₂; HSQC, COSY: C²¹H₂), 3.24-3.59 (m, 14 H, HSQC, COSY: C²²H₂; HSQC, COSY: C²⁰H₂), 6.28 (bs, 1 H, HSQC: NH¹⁹). – **¹³C-NMR** (100 MHz; CDCl₃): δ (ppm) = 14.1 (+, 1 C, HSQC, COSY: C¹H₃), *assignment*: 22.6 (–, 1 C), 29.30 (–, 1 C), 29.37 (–, 1 C), 29.50 (–, 1 C), 29.60 (–, 2 C), 29.62 (–, 1 C), 29.65 (–, 6 C), 31.9 (–, 1 C), HSQC, COSY: C²H₂-C¹⁵H₂), 25.7 (–, 1 C), HSQC, COSY: C²H₂-C¹⁵H₂), 28.5 (+, 6 C, HSQC, COSY: C¹⁶H₂), 28.6 (+, 3 C, HSQC: C²⁸H₃), *conformational isomers*: 33.9^b, 36.5^a (–, 1 C, HSQC, COSY: C¹⁷H₂), 36.5 (–, 1 C, HSQC, COSY: C²¹H₂), 48.1 (–, 4 C, HSQC, COSY: C¹⁶H₂), 49.9 (–, 2 C, HSQC, COSY: C¹⁶H₂), 52.7 (–, 1 C, HSQC, COSY: C²⁰H₂), 55.0 (–, 1 C, HSQC, COSY: C¹⁶H₂), 55.6 (–, 1 C, HSQC, COSY: C¹⁶H₂), 79.6, 79.8 (C_q, 3 C, HSQC, HMBC: C²⁴, C²⁷), 155.4 (C_q, 1 C, HSQC, HMBC: C²⁶), 156.2 (C_q, 2 C, HSQC, HMBC: C²³), *conformational isomers*: 173.5^a, 175.9^b (C_q, 1 C, HSQC, HMBC: C¹⁸). – **IR** (ATR) [cm⁻¹]: $\tilde{\nu}$ = 2922, 2850, 1689, 1460, 1416, 1365, 1248, 1156, 1019, 772. – **MS** (ESI(+), EE/MeOH + 10 mmol/L NH₄Ac): m/z (%) = 782.7 (100) [MH⁺]. – **HRMS** Calcd for C₄₃H₈₃N₅O₇ 779.6136; Found: 779.6123. – **MF**: C₄₃H₈₃N₅O₇ – **FW**: 782.16 g/mol



Octadecanoic acid [2-(1,4,7,10 tetraaza-cyclododec-1-yl)-ethyl]-amide (**11**)

Compound **10** (246 mg, 0.31 mmol) was dissolved in dichloromethane (4 mL) and cooled to 0 °C. Subsequently 6.3 mL HCl / ether were added and the solution was stirred for 20 h at room temperature. The solvent was removed in vacuum yielding the protonated hydrochloride of compound **10** quantitative as a colourless solid. To obtain the free base of compound **10** a strong basic ion exchange resin was swollen for 15 min in water/MeOH (8:2) and washed neutral with water. A column was charged with resin (3.5 ml, 40.0 mmol hydroxy equivalents at a given capacity of 0.9 mmol/mL). The hydrochloride salt was dissolved in a mixture of MeOH/water (8:2), put onto the column and eluted with the same solvent mixture. The elution of the product was controlled by pH indicator paper (pH > 10) and was completed when pH again was neutral. The eluate was concentrated and lyophilized to yield quantitatively 149 mg (0.31 mmol) of free base **10**, as colourless hygroscopic solid. **MP**: 148 – 150 °C. – **¹H-NMR** (300 MHz; CDCl₃): δ (ppm) = 0.84 (t, ³J = 6.7 Hz, 3 H, C¹H₃), 1.22 (m, 28 H, C²H₂-C¹⁵H₂), 1.59 (m, 2 H, C¹⁶H₂), 2.17 (t, ³J = 7.4 Hz, 2 H, C¹⁷H₂), 2.36-3.67 (m, 20 H, C²⁰H₂, C²¹H₂, C²²H₂), 6.78 (bs, 1 H, NH¹⁹). – **¹³C-NMR** (75 MHz; CDCl₃): δ (ppm) = 14.1 (+, 1 C, CH₃), 22.7, 25.8, 29.35, 29.49, 29.56, 29.66, 29.70, 31.9 (–, 14 C, CH₂), 36.7 (–, 1 C, CH₂), 37.5 (–, 1 C, CH₂), 45.4 (–, 2 C, CH₂), 46.1 (–, 2 C, CH₂), 47.2 (–, 2 C, CH₂), 51.5 (–, 2 C, CH₂), 53.8 (–, 2 C, CH₂), 173.6 (C_q, 1 C, RCONHR'). – **IR** (ATR) [cm⁻¹]: $\tilde{\nu}$ = 2916, 2850, 1644, 1546, 1466, 1350, 1276, 812, 718. – **MS** (ESI(+), EE/MeOH + 10 mmol/L NH₄Ac): m/z (%) = 482.4 (100) [MH⁺], 262.1 (50) [M + 2 H⁺ + MeCN]²⁺, 241.1 (50) [M + 2 H⁺]²⁺. – **HRMS** Calcd for C₂₈H₅₉N₅O 482.4798; Found: 482.4785. – **MF**: C₂₈H₅₉N₅O – **FW**: 481.82 g/mol



Amphiphilic mononuclear Zn(II)-cyclen (**Zn1**)

Compound **11** (50 mg, 0.10 mmol) was dissolved in 1 mL MeOH and heated to 65 °C to get a clear solution. Subsequently zinc(II)-perchlorate (44 mg, 117 μmol) dissolved in 1 ml MeOH was added slowly to the stirred reaction mixture. The reaction mixture was stirred for additional 19 h at 65 °C. The solvent was removed in vacuum and the residue was redissolved in water and lyophilized to yield 77 mg (0.10 mmol, 100%) of **Zn1** as a lightly

brownish solid. **MP**: 161 °C. – **¹H-NMR** (600 MHz; CDCl₃ / CD₃OD 1:1): δ (ppm) = 0.58 (t, ³J = 7.1 Hz, 3 H, HSQC, COSY: C¹H₃), 0.93-1.06 (m, 28 H, HSQC, COSY: C²H₂-C¹⁵H₂), 1.26-1.36 (m, 2 H, HSQC, COSY: C¹⁶H₂), 2.03 (t, ³J = 7.8 Hz, 2 H, HSQC, COSY: C¹⁷H₂), 2.45-2.58 (m, 8 H, HSQC, COSY: cyclen-CH₂), 2.59-2.73 (m, 8 H, HSQC, COSY: cyclen-CH₂), 2.75-2.87 (m, 2 H, HSQC, COSY: C²⁰H₂), 3.15 (t, ³J = 5.0 Hz, 2 H, HSQC, COSY: C²¹H₂), 3.65 (bs, 1 H, HSQC: NH), 4.24 (bs, 2 H, HSQC: NH). – **¹³C-NMR** (150 MHz; CDCl₃): δ (ppm) = 13.2 (+, 1 C, HSQC, COSY: C¹H₃), 22.1, 28.65, 28.73, 28.94, 29.08, 31.3(–, 14 C, HSQC, COSY: C²H₂-C¹⁵H₂), 25.0 (–, 1 C, HSQC, COSY: C¹⁶H₂), 35.6 (–, 1 C, HSQC, COSY: C¹⁷H₂), 36.4 (–, 1 C, HSQC, COSY: C²¹H₂), 42.0 (–, 1 C, HSQC, COSY: cyclen-CH₂), 43.4 (–, 2 C, HSQC, COSY: cyclen-CH₂), 44.0 (–, 1 C, HSQC, COSY: C²⁰H₂), 44.1 (–, 1 C, HSQC, COSY: cyclen-CH₂), 50.9 (–, 2 C, HSQC, COSY: cyclen-CH₂), 51.0 (–, 1 C, HSQC, COSY: cyclen-CH₂), 53.7 (–, 1 C, HSQC, COSY: cyclen-CH₂), 178.2 (C_q, 1 C, C¹⁸). – **IR** (ATR) [cm⁻¹]: $\tilde{\nu}$ = 2917, 2850, 1647, 1625, 1467, 1076, 720, 622. – **MS** (ESI(+), MeOH + 10 mmol/L NH₄Ac): m/z (%) = 544.4 (100) [M²⁺ – H⁺]⁺. – **HRMS** Calcd for C₂₈H₅₈N₅O [M²⁺ – H⁺]⁺ 544.3933; Found: 544.3921. – **MF**: [C₂₈H₅₉N₅OZn] (ClO₄)₂. – **FW**: 746.09 g/mol

Micellar catalysts

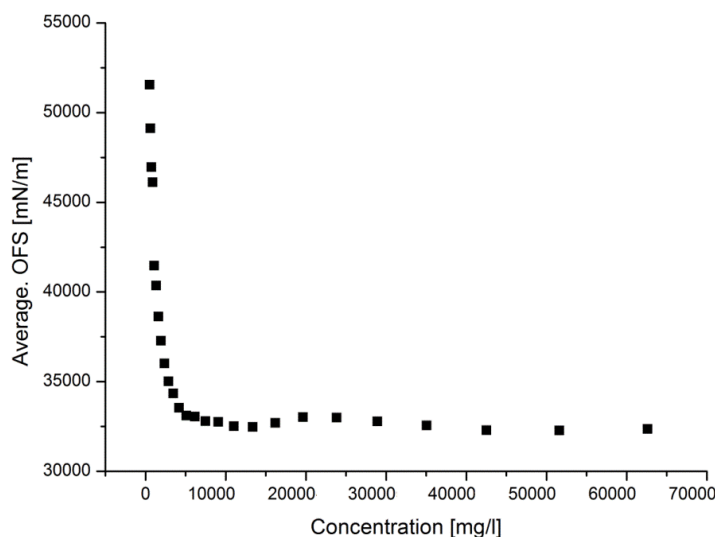


Figure S1. Typical surface tension isotherm for Zn(II)-complexes in aqueous solution (here Zn₂₅).

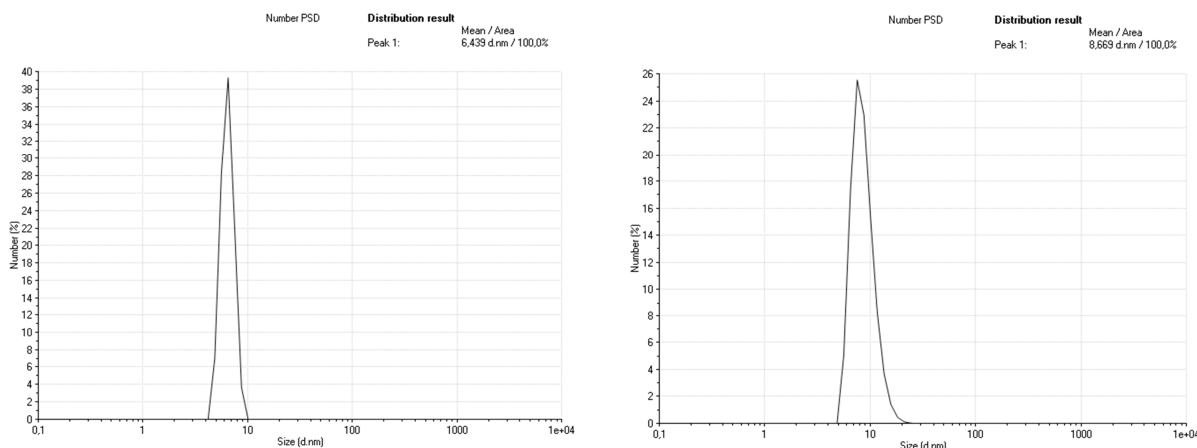


Figure S2. Size distribution data (mean diameters in nm) for micellar (10^{-3} M) Zn₂₂ (left) and Zn₂₅ (right). The radius of the main population is in good agreement with the length of the monomeric amphiphiles (~3 nm for Zn₂₂ and ~4 nm for Zn₂₅).

Vesicular catalysts

Preparation

In small glass reaction vessels 1 - 5 μ mol of phospholipid(s) were dissolved in chloroform and optionally 1-25 mol% of dissolved amphiphilic metal complexes (Zn₁, Zn₂₂, Zn₂₅) or dye (12) were added and mixed. The solvent was completely removed at 75°C under reduced pressure and an appropriate amount of buffer (25 mM HEPES, pH 7.4 or 50 mM TRIS, pH 8.0) was added to obtain lipid concentrations of 1 - 2 mM. Heating to 75 °C and vigorous shaking for 5 - 15 minutes yielded a turbid multi-lamellar vesicle suspension. Small uni-lamellar dispersions were obtained by extrusion through polycarbonate membranes with a defined pore size (50 - 800 nm) by using a LiposoFast liposome extruder from Avestin.³⁷ Vesicle size distributions were determined using Dynamic light scattering (DLS). The standard size distribution of species obtained after extrusion through 100 nm membranes is shown in Figure S3.

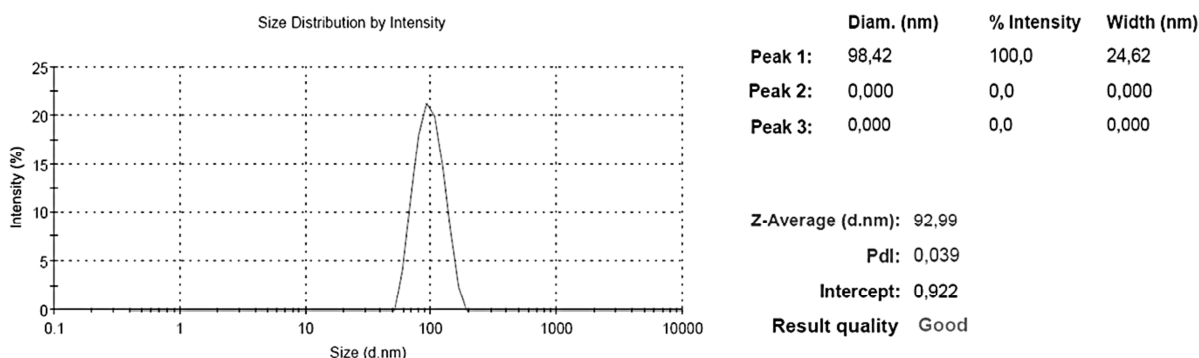


Figure S3. Typical DLS data for vesicles extruded through 100 nm membranes.

Catalyst concentration

For all vesicular catalysts the receptor concentration refers to the outer surface exposed binding sites, as only these should be reactive, with the assumption that embedded compounds distribute equally in both layers of the vesicle membrane.³⁸ The ratio of active Zn-containing catalytic sites on outer and inner surface were assumed to be 1:1³⁹ with the assumption that the bilayer thickness for the prepared vesicles amounts to 5 nm.^{40, 41}

Size exclusion chromatography (SEC)

In order to remove low molecular weight solutes vesicles can be purified by size exclusion chromatography via small spin columns.⁴² For this Sephadex LH-20 SEC medium was swollen in buffer solution prior to use. 5 mL bed volume per mL vesicle suspension was transferred into a small plastic syringe with filter support and removed plunger and the solvent removed by centrifugation (Eppendorf bench top centrifuge, 15 s at 4400 rpm). Vesicle solutions were added onto the column and recovered by subsequent centrifugation.

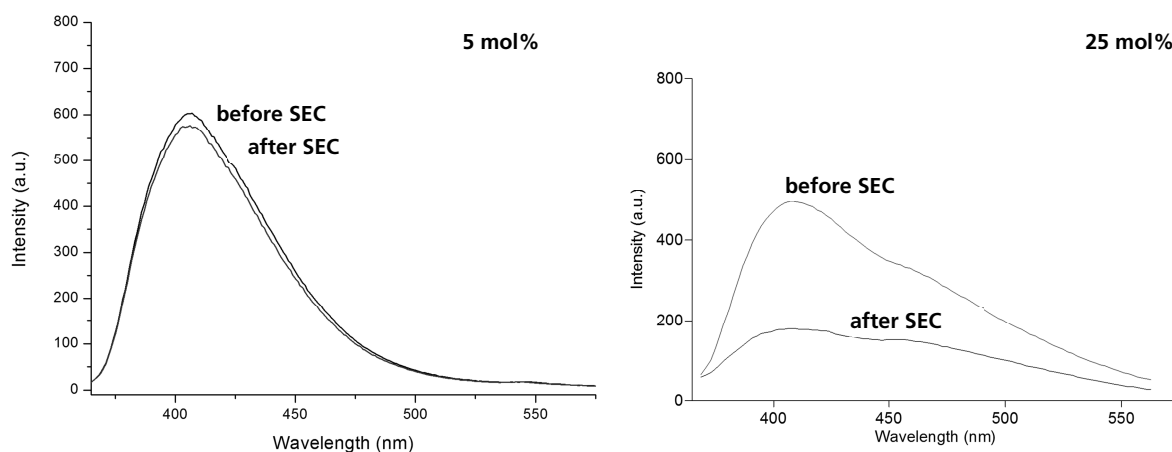


Figure S4. Fluorescence emission spectra of Zn₂₅-vesicles before and after SEC column: At low loading levels (5 mol%) of Zn₂₅ the metal complexes are nearly quantitatively embedded in the vesicle membranes and as a result passed through the separation medium (left). High loading levels (25 mol%) however result in residual lower molecular Zn₂₅ which is removed during SEC as indicated by the decreased emission (right).

Investigation of the polarity of a vesicle-water interface

The amphiphilic dansyl dye **12** was prepared according to a literature known procedure⁴³ and imbedded in DSPC vesicles. The fluorescence of the vesicles and solutions of the dye in different solvents were measured and compared to determine the relative polarity of the vesicle bilayer-water interface.

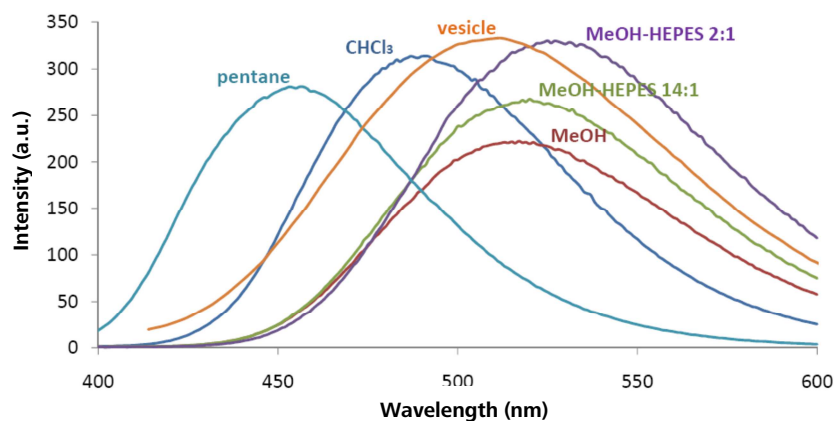


Figure S5. Polarity-sensitive dansyl dye **12** and its emission spectra in vesicular solution and different (organic) solvents.

To assure that compound **12** is actually located in close proximity to the polar lipid headgroups and not “buried” inside the hydrophobic core of the membrane we have also prepared vesicles from lipids with modified headgroups: zwitterionic 1,2-distearoyl-*sn*-glycero-3-phosphocholine (DSPC), cationic 1,2-stearoyl-3-trimethylammonium-propane (DSTAP) and anionic 1,2-distearoyl-*sn*-glycero-3-phosphoethanolamine-N-[methoxy(polyethylene glycol)-350] (DSPEG). As shown in Figure S6 these headgroup modifications directly affect the emission properties of the dansyl dye. As a result it can be assumed that **12** is really located at the vesicle membrane-water interface similarly to the metal complexes used for the hydrolysis studies.

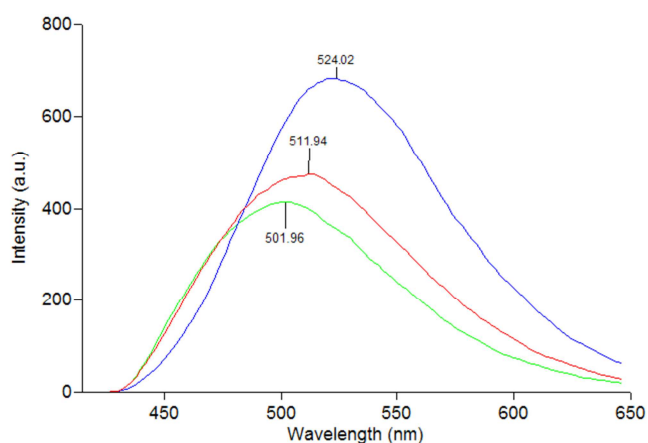


Figure S6. Emission properties of dansyl dye **12** (5 mol%) embedded in DSPC- (red), DSTAP- (green) and DSPEG-vesicles (blue trace). Changing the charged lipid headgroups results in a blue- (DSTAP) or red-shift (DSPEG) of the emission maximum by 10 - 12 nm.

BNPP kinetics

Reaction conditions

Rate constants were determined using 2.3 mM BNPP solutions and a total Zn(II)-concentration of 4.5×10^{-5} M (0.02 eq). The measurements were performed in 25 mM HEPES buffer (pH 7.4) or in 50mM TRIS buffer (pH 8.0) at 25 °C. Kinetic data was corrected for spontaneous hydrolysis (background reaction) and evaluated with OriginLab Origin and Microsoft Excel software. All observed rate constants were determined by initial slopes method.²²

Optimization of substrate and catalyst concentrations

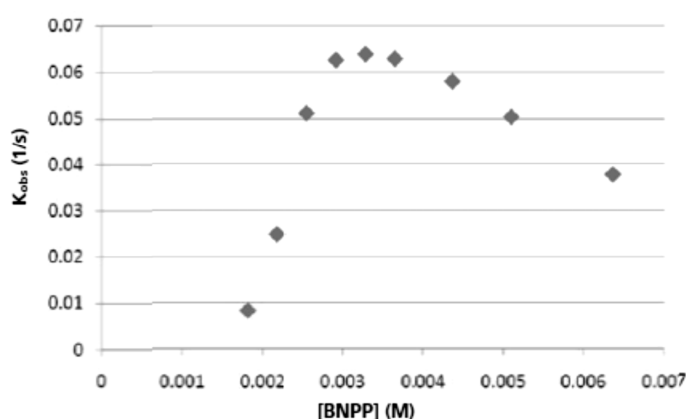


Figure S7. Optimizing conditions for BNPP hydrolysis: BNPP concentration vs. pseudo-first order rate constants.

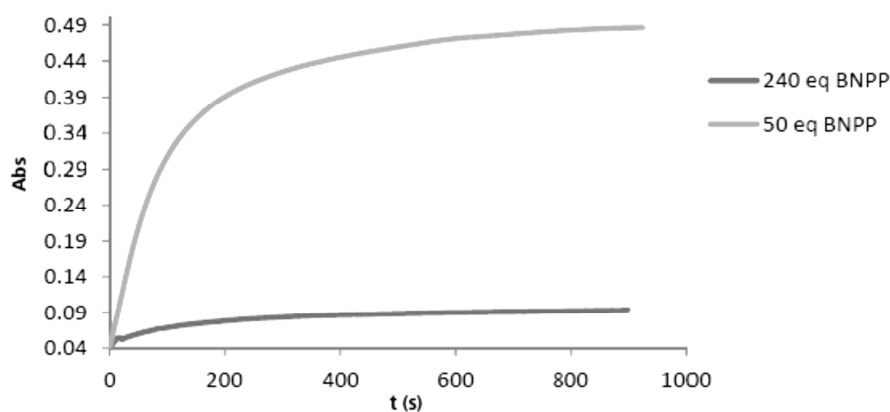


Figure S8. Kinetic traces showing highest NP production for 20 - 50 eq. of BNPP (in relation to $Zn_{(2)}$ complexes).

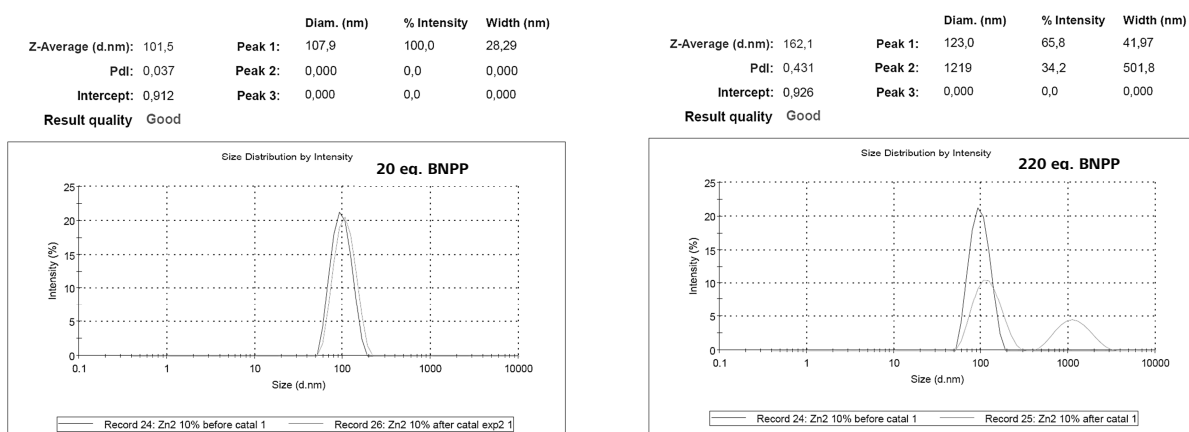


Figure S9. DLS data: Vesicles are stable during hydrolytic reactions for 20 eq. of BNPP (left), high amounts of BNPP (> 200 eq.) however cause vesicle destabilization and aggregation (right).

Catalytic activity of vesicles with different loading levels of Zn₂2

mol% of Zn ^{II}	[Zn ^{II}] (M)	k _{obs} (s ⁻¹)	STDV (s ⁻¹) ^{a)}	k _{obs} (s ⁻¹ M ⁻¹)	Eq. of NP ^{b)}
1%	4.59E-06	- ^{c)}			
2.5%	1.15E-05	0.001665	0.0001	145	0.27
5%	2.30E-05	0.000683	0.00006	30	1.61
10%	4.58E-05	0.00351	0.0007	77	1.28
15%	6.87E-05	0.002625	0.00005	38	0.15
20%	9.16E-05	0.0026325	0.00017	29	0.44

Table S10. Comparison of vesicular catalysts containing different amounts of Zn₂2 amphiphiles (in mol% of total vesicular lipid) by initial nitrophenolate production. ^{a)} Standard deviation calculated from three identical experiments; ^{b)} After 200 seconds; ^{c)} Below detection limit.

Catalytic activity of vesicles with different size

Several Zn₂2 / DSPC-vesicles (ratio 1:9) of different sizes were tested for their promotion of BNPP hydrolysis. The reaction conditions here were chosen as following: [BNPP] = 2.3 mM, [Zn₂2] = 4.5 × 10⁻⁵ M, 25mM HEPES buffer at pH 7.4, 25°C.

Vesicle diameter (nm)	k _{obs} (s ⁻¹ M ⁻¹)	Eq. of NP
61	17.0(1.5)	1.48
93	76.8(6.80)	2.56
128	42.4(4.83)	0.86
156	64.6(5.44)	0.24

Table S1. Rate constants (and initial nitrophenolate production after 200 seconds) obtained for vesicles of different size.

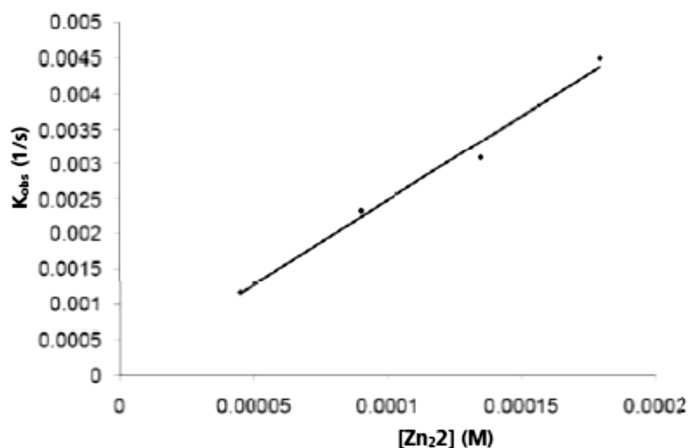
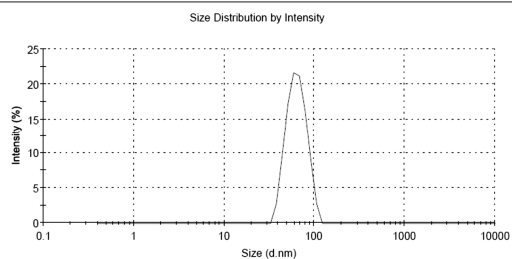


Figure S11. Observed rate constants of BNPP hydrolysis by Zn₂2-vesicles (Zn₂2:DSPC is 1:9): k_{obs} (s^{-1}) vs. [Zn₂2] in 50mM TRIS buffer, pH 8.0, 25°C.

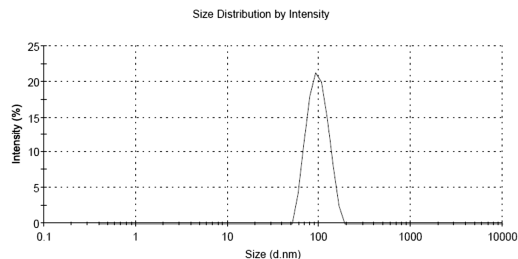
61 nm vesicles

	Diam. (nm)	% Intensity	Width (nm)
Z-Average (d.nm): 60.77	Peak 1: 64.80	100.0	15.73
Pdl: 0.058	Peak 2: 0.000	0.0	0.000
Intercept: 0.910	Peak 3: 0.000	0.0	0.000
Result quality	Refer to quality report		



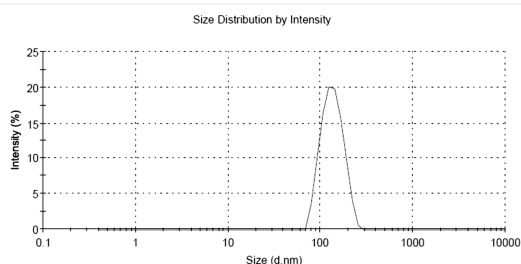
93 nm vesicles

	Diam. (nm)	% Intensity	Width (nm)
Z-Average (d.nm): 92.99	Peak 1: 98.42	100.0	24.62
Pdl: 0.039	Peak 2: 0.000	0.0	0.000
Intercept: 0.922	Peak 3: 0.000	0.0	0.000
Result quality	Good		



128 nm vesicles

	Diam. (nm)	% Intensity	Width (nm)
Z-Average (d.nm): 127.7	Peak 1: 136.8	100.0	35.95
Pdl: 0.062	Peak 2: 0.000	0.0	0.000
Intercept: 0.916	Peak 3: 0.000	0.0	0.000
Result quality	Good		



156 nm vesicles

	Diam. (nm)	% Intensity	Width (nm)
Z-Average (d.nm): 155.9	Peak 1: 176.1	100.0	61.33
Pdl: 0.111	Peak 2: 0.000	0.0	0.000
Intercept: 0.909	Peak 3: 0.000	0.0	0.000
Result quality	Good		

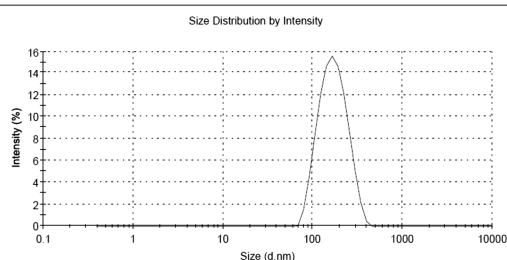


Figure S12. DLS data of vesicles used for size-dependency measurements.

Kinetic data for vesicles

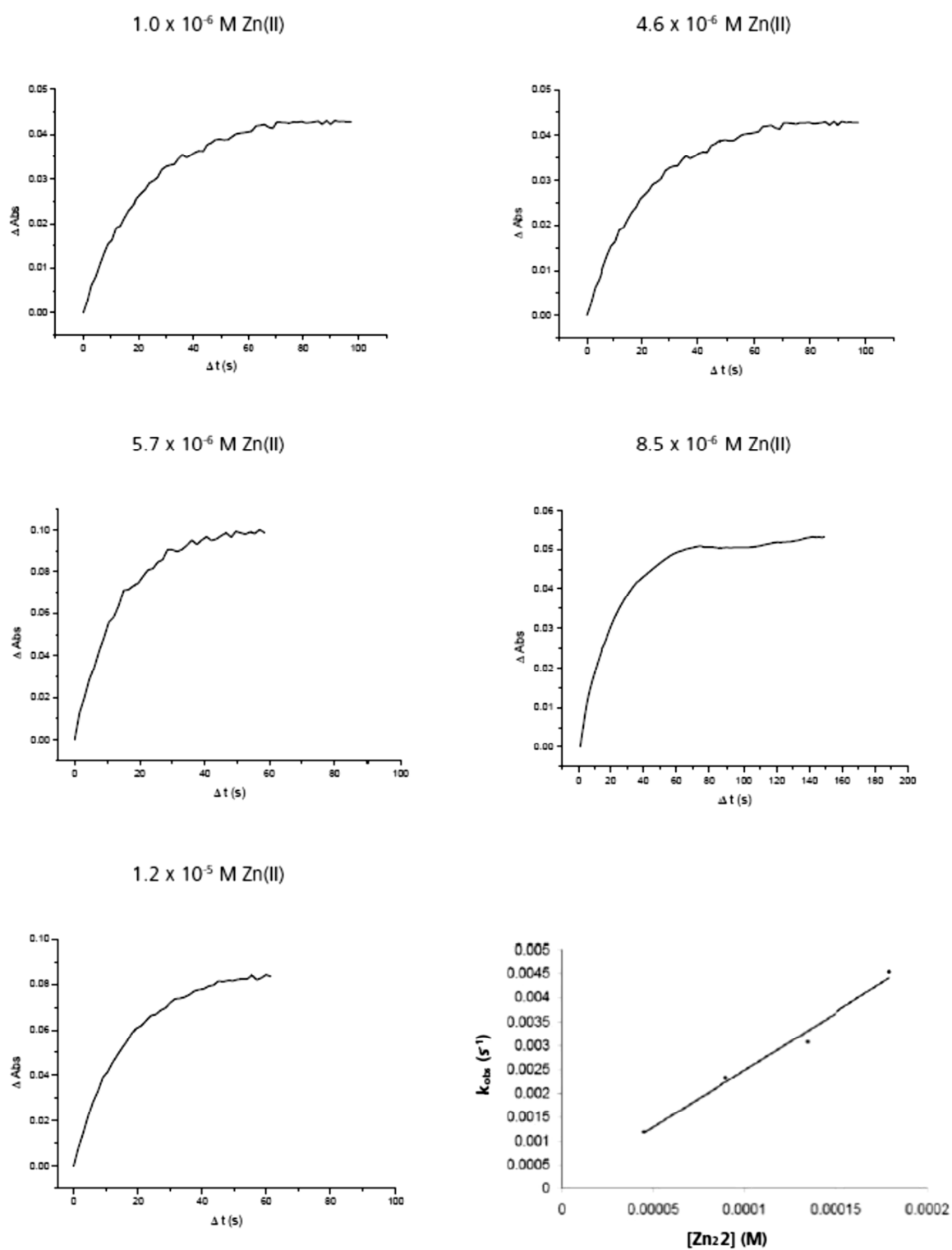


Figure S13. Changes in the absorption at 408 nm (accumulation of p-nitro-phenylphosphate) during the hydrolysis catalyzed by Zn $_2$ -vesicles (10 mol%) in 50 mM TRIS buffer at pH 8.0.

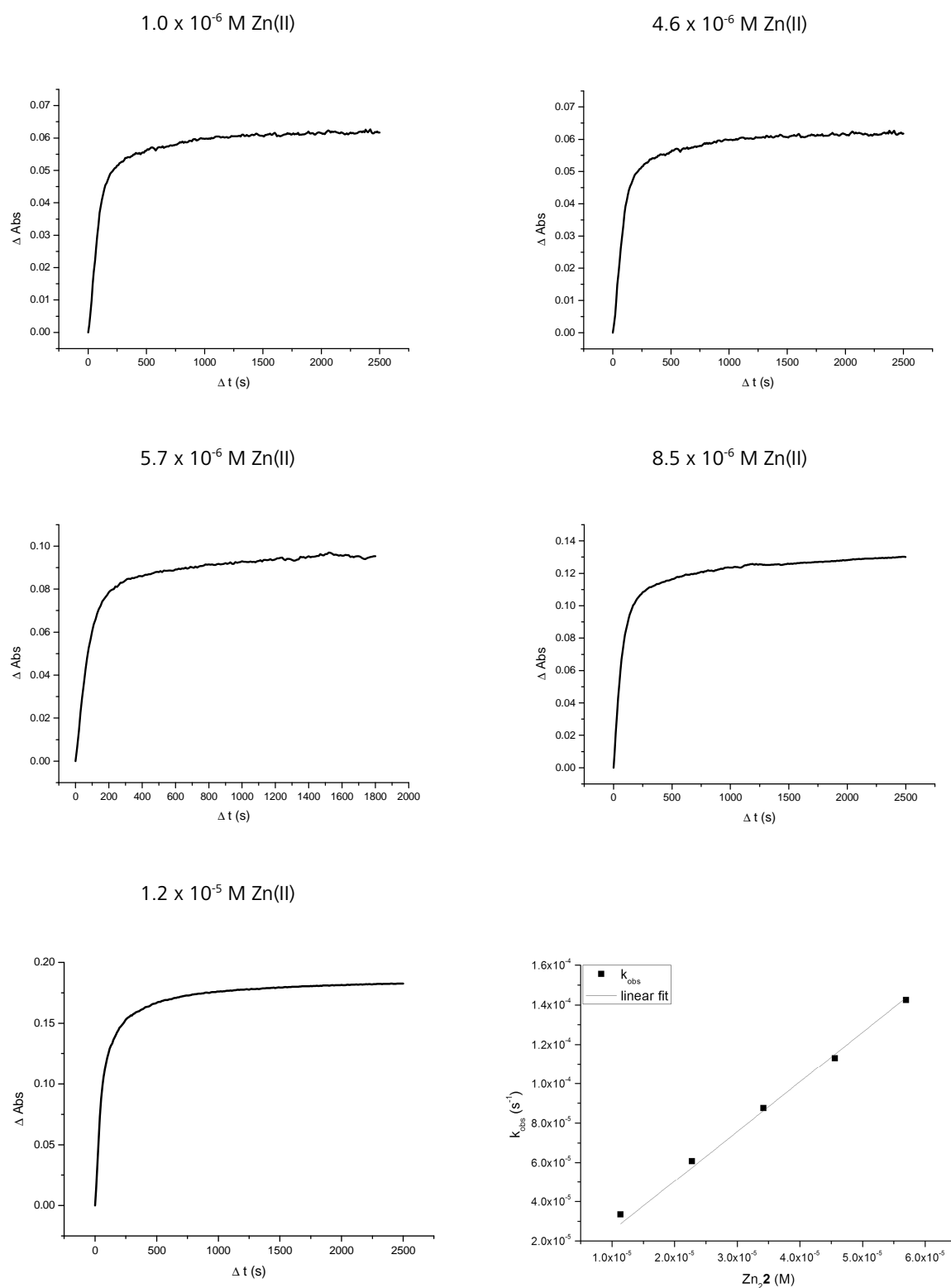


Figure S14. Changes in the absorption at 408 nm (accumulation of p-nitro-phenylphosphate) during the hydrolysis catalyzed by Zn $_2$ -vesicles (10 mol%) in 25 mM HEPES at pH 7.4.

Control experiments

All kinetics were corrected for spontaneous background hydrolysis (buffer addition only) under the experimental conditions. Control experiments also included the addition of vesicles not containing any Zn(II)-complexes to assure that these do not promote the cleavage of BNPP. Both background hydrolysis and control vesicles however do not produce a significant signal under the experimental conditions (Figure S15).

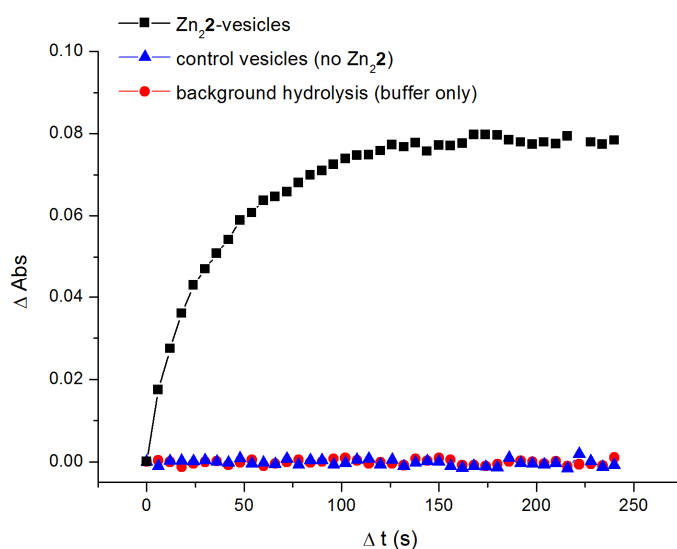


Figure S15. BNPP hydrolysis with Zn₂2-vesicles and control experiments.

All kinetic measurements used for evaluation were repeated at least twice and found to show excellent reproducibility. Figure S16 exemplarily shows one kinetic curve with error bars (standard deviation) from three independent experiments.

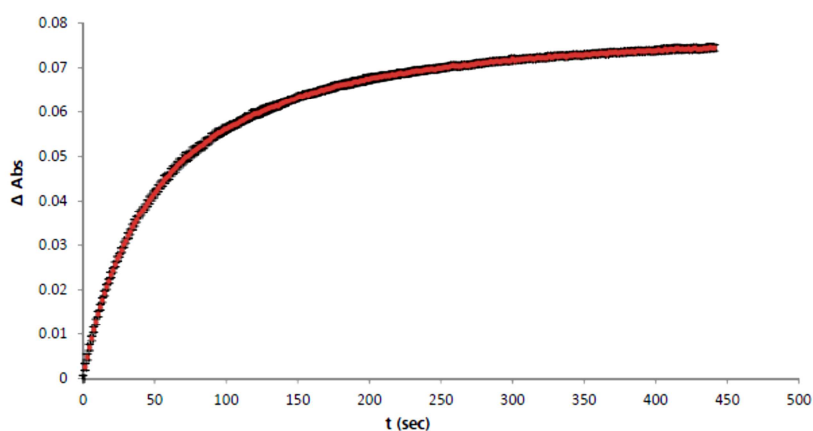


Figure S16. Average kinetic curve (red markers) for BNPP hydrolysis at pH 8.0 with standard deviation (black bars) derived from three independent measurements.

Kinetic data for micelles

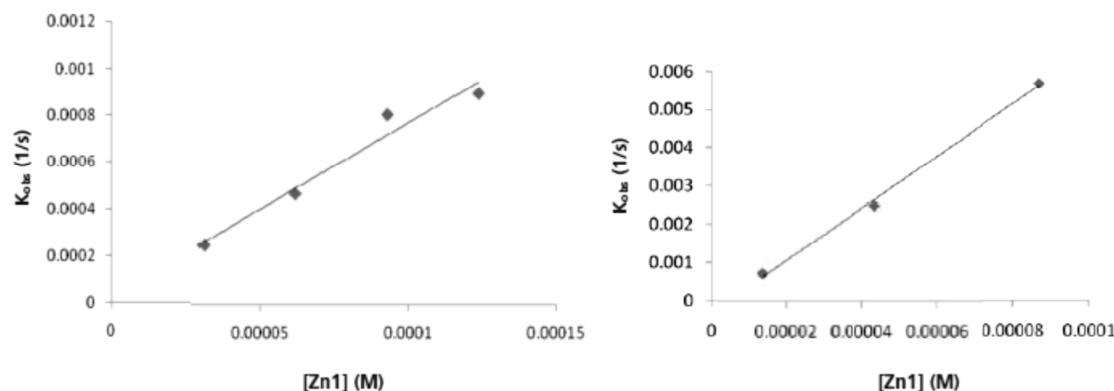


Figure S17. Observed rate constants for BNPP hydrolysis. (Left) Zn1-micelles: k_{obs} (s^{-1}) vs. $[\text{Zn1}]$ in 25mM HEPES buffer, pH 7.4, 25°C; (Right) Zn2-micelles: k_{obs} (s^{-1}) vs. $[\text{Zn2}]$ in 50mM TRIS buffer, pH 8.0, 25°C.

Hydrolysis of pBR322 plasmide dsDNA

All samples were incubated at 40 °C under stirring in 25 mM HEPES buffer (pH 7.4) and for workup treated with an excess of EDTA and SDS. The samples were mixed with bromophenol blue and glycerin and applied on agarose mini gels (0.7% w/w). Electrophoresis was performed in TAE buffer (pH 8.3, 55 V, 1.5 h) and bands stained with ethidium bromide and visualized under UV light.

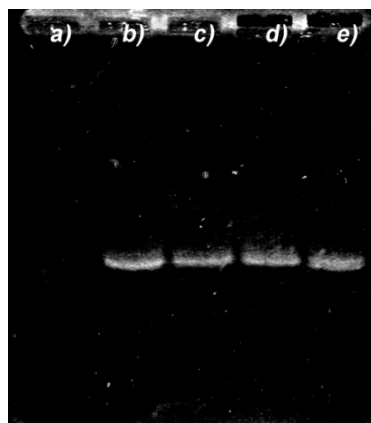


Figure S18. Control experiments for electrophoresis: Ethidium bromide staining of 0.7% (w/w) agarose gel with (a) Zn2-vesicles in absence of pBR322; (b) 75 ng pBR322; (c) 75 ng pBR322 incubated at 40 °C for 20 h; (d) 75 ng pBR322 + Zn4 incubated at 40 °C for 20 h; (e) 75 ng pBR322 + control vesicles incubated at 40 °C for 20 h.

Hydrolysis of TaqMan® probe

All samples were incubated at 40 °C under stirring in 50 mM TRIS buffer (pH 8.0) and for workup treated with an excess of EDTA and SDS. Samples were diluted (10^{-8} M DLO) and emission spectra recorded ($\lambda_{\text{exc}} = 495$ nm, $\lambda_{\text{em}} = 520$ nm) and plotted against incubation time.

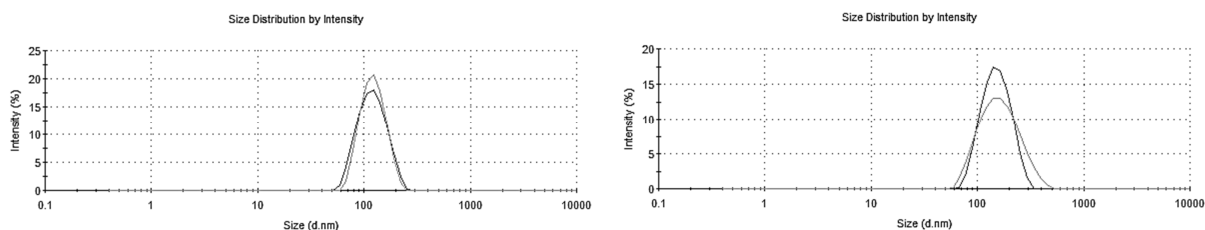


Figure S19. Vesicles were found to show no considerable aggregation in the presence of pBR322 (left) and TaqMan® probe (right) under the conditions used for the hydrolysis studies.

Multivalence effect of vesicles vs. micelles for polyphosphate substrates

We previously reported high affinity constants of vesicular Zn₂5 towards phosphate anions like pyrophosphate (PP_i) and fructose-1,6-diphosphate.²³ The binding especially of highly charged phosphate anions like (PP_i) results in a considerable emission quenching of the fluorescent complexes here. We propose a similar mechanism for the Zn₂5-micelles and exemplarily demonstrated this by a titration with sodium pyrophosphate (PP_i) which is known to have a very high affinity towards Zn₂5. PP_i also binds to the Zn₂5-micelles as indicated by the considerable emission quenching (Figure S20 left). The addition of equal amounts of Fructose-6-diphosphate however was found to produce only a very small change in fluorescence intensity (Figure S20 right) so that only a very weak binding can be assumed here. As a result the vesicles exhibit a much higher affinity towards this non-hydrolysable model substrate than the micelles which might explain their superior performance in the hydrolysis of oligophosphates.

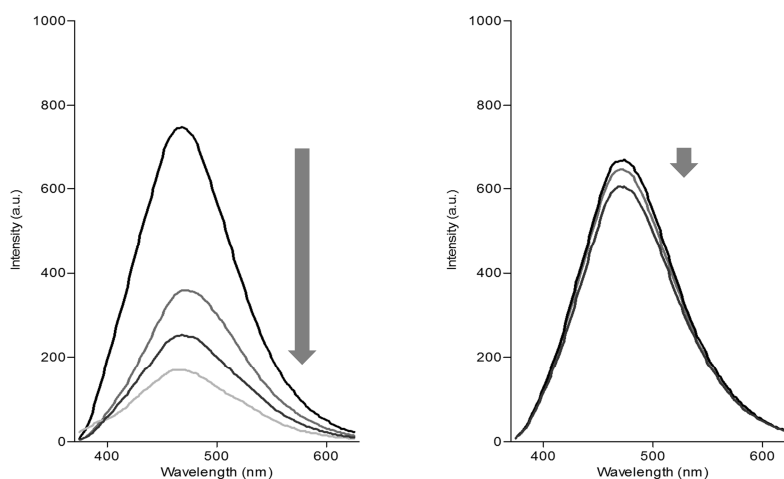


Figure S20. Emission titration of Zn₂5-micelles with sodium pyrophosphate (PP_i) (left) and fructose-1,6-diphosphate (right).

References

1. M. I. Fekry and K. S. Gates, *Nat. Chem. Biol.*, 2009, **5**, 710-711.
2. A. Sreedhara and J. A. Cowan, *J. Biol. Inorg. Chem.*, 2001, **6**, 337-347.
3. M. Livieri, F. Mancin, G. Saielli, J. Chin and U. Tonellato, *Chem. Eur. J.*, 2007, **13**, 2246-2256.
4. C. Jik, *Curr. Opin. Chem. Biol.*, 1997, **1**, 514-521.
5. P. Gomez-Tagle and A. K. Yatsimirsky, *Inorg. Chem.*, 2001, **40**, 3786-3796.
6. M. Komiyama, N. Takeda and H. Shigekawa, *Chem. Comm.*, 1999, 1443-1451.
7. T. Koike and E. Kimura, *J. Am. Chem. Soc.*, 1991, **113**, 8935-8941.
8. M. Zulkefeli, A. Suzuki, M. Shiro, Y. Hisamatsu, E. Kimura and S. Aoki, *Inorg. Chem.*, 2011.
9. C. Vichard and T. A. Kaden, *Inorg. Chim. Acta*, 2002, **337**, 173-180.
10. G.-m. Yang, J. Li, Y.-w. Ren, H. Guo, M.-y. Duan, F.-x. Zhang and X. Zhang, *Transition Met. Chem.*, 2009, **34**, 191-196.
11. F. Mancin and P. Tecilla, *New J. Chem.*, 2007, **31**, 800-817.
12. T. Niittymaki and H. Lonnberg, *Org. Biomol. Chem.*, 2006, **4**, 15-25.
13. E. Kimura, H. Hashimoto and T. Koike, *J. Am. Chem. Soc.*, 1996, **118**, 10963-10970.
14. F. M. Menger, L. H. Can, E. Johnson and D. H. Dursttt, *J. Am. Chem. Soc.*, 1987, **109**, 2800-2803.
15. F. B. Jiang, L. Y. Huang, X. G. Meng, J. Du, X. Q. Yu, Y. F. Zhao and X. C. Zeng, *J. Colloid Interface Sci.*, 2006, **303**, 236-242.
16. P. Tecilla, F. Mancin, P. Scrimin and U. Tonellato, *Coord. Chem. Rev.*, 2009, **253**, 2150-2165.
17. V. Singh, M. Zharnikov, A. Gulino and T. Gupta, *J. Mater. Chem.*, 2011, **21**, 10602-10618.
18. T. Walenzyk and B. König, *Inorg. Chim. Acta*, 2005, **358**, 2269-2274.
19. R. Bonomi, F. Selvestrel, V. Lombardo, C. Sissi, S. Polizzi, F. Mancin, U. Tonellato and P. Scrimin, *J. Am. Chem. Soc.*, 2008, **130**, 15744-15745.
20. F. Manea, L. Pasquato, L. J. Prins and P. Scrimin, *Nucleic Acids Symp. Ser.*, 2007, **51**, 67-68.
21. N. J. Buurma, *Annual Reports Section "B" (Organic Chemistry)*, 2011.
22. M. Subat, K. Woinaroschy, C. Gerstl, B. Sarkar, W. Kaim and B. König, *Inorg. Chem.*, 2008, **47**, 4661-4668.
23. B. Gruber, S. Stadlbauer, K. Woinaroschy and B. König, *Org. Biomol. Chem.*, 2010, **8**, 3704-3714.
24. D. S. Turygin, M. Subat, O. A. Raitman, V. V. Arslanov, B. König and M. A. Kalinina, *Angew. Chem. Int. Ed.*, 2006, **45**, 5340-5344.
25. CMC was determined to be less than 1.5×10^{-4} M (see Figure 3 in the SI).

26. B. Gruber, S. Stadlbauer, A. Späth, S. Weiss, M. Kalinina and B. König, *Angew. Chem. Int. Ed.*, 2010, **49**, 7125-7128.
27. H. Saito, T. Araiso, H. Shirahama and T. Koyama, *J. Biochem.*, 1991, **109**, 559-565.
28. C. X. Yuan, Y. B. Wei and P. Yang, *Chin. J. Chem.*, 2006, **24**, 1006-1012.
29. L. Tjioe, A. Meininger, T. Joshi, L. Spiccia and B. Graham, *Inorg. Chem.*, 2011, **50**, 4327-4339.
30. According to 1 kb DNA Ladder molecular weight standard.
31. Y. M. Zhao, J. H. Zhu, W. J. He, Z. Yang, Y. G. Zhu, Y. Z. Li, J. F. Zhang and Z. J. Guo, *Chem. Eur. J.*, 2006, **12**, 6621-6629.
32. Estimated from a standard curve of free FAM measured under similar conditions.
33. A. K. Yatsimirsky, *Coord. Chem. Rev.*, 2005, **249**, 1997-2011.
34. R. Bonomi, P. Scrimin and F. Mancin, *Org. Biomol. Chem.*, 2010, **8**, 2622-2626.
35. S. Hünig, G. Märkl and J. Sauer, *Einführung in die apparativen Methoden in der Organischen Chemie, 2nd Edition*, Würzburg / Regensburg, 1994.
36. R. Reichenbach-Klinke, M. Kruppa and B. König, *J. Am. Chem. Soc.*, 2002, **124**, 12999-13007.
37. R. C. MacDonald, R. I. MacDonald, B. P. M. Menco, K. Takeshita, N. K. Subbarao and L.-r. Hu, *Biochim. Biophys. Acta*, 1991, **1061**, 297-303.
38. A. I. Elegbede, M. K. Haldar, S. Manokaran, J. Kooren, B. C. Roy, S. Mallik and D. K. Srivastava, *Chem. Commun.*, 2007, 3377-3379.
39. A. J. Jin, D. Huster, K. Gawrisch and R. Nossal, *Eur. Biophys. J.*, 1999, **28**, 187-199.
40. J. F. Nagle and S. Tristram-Nagle, *Biochim. Biophys. Acta*, 2000, **1469**, 159-195.
41. P. Balgavy, M. Dubnickova, N. Kucerka, M. A. Kiselev, S. P. Yaradaikin and D. Uhrikova, *Biochim. Biophys. Acta*, 2001, **1512**, 40-52.
42. D. W. Fry, J. C. White and I. D. Goldman, *Anal. Biochem.*, 1978, **90**, 809-815.
43. Y. Kitano, Y. Nogata, K. Matsumura, E. Yoshimura, K. Chiba, M. Tada and I. Sakaguchi, *Tetrahedron*, 2005, **61**, 9969-9973.

SUMMARY

This work describes the functionalization of biomimetic vesicle membranes by the incorporation of various synthetic amphiphiles. The presented approach enables rapid and simple development of bio-inspired nanomaterials for applications in biomolecule sensing and catalysis.

Chapter 1 introduces the general concept of functional synthetic vesicle membranes and provides a brief overview about significant developments in this area.

Chapter 2 describes synthesis and membrane-embedding of amphiphilic non-fluorescent and fluorescent Zn(II)-cyclen complexes for the recognition of phosphate anions. The obtained functionalized vesicles were characterized and finally employed for optical sensing and differentiation of phosphorylated proteins.

Chapter 3 presents a novel approach for the design of modular chemosensors for small biomolecules. For this amphiphilic binding sites based on transition metal complexes and crown ethers as well as amphiphilic fluorescent dyes were synthesized and co-embedded in DSPC vesicle membranes. Initially formed dye-receptor clusters within the lipid bilayers are assumed to rearrange upon receptor-ligand interactions and as a result produce an emission response. Ligand selectivities and optical properties can be easily adjusted by simply changing the vesicle's amphiphilic building blocks.

In Chapter 4 fluid vesicle membranes are used for the dynamic recognition of multivalent ligands via receptor-recruiting. Two amphiphilic receptors with attached FRET-pair labels were prepared and embedded in DOPC vesicles. While energy transfer is low in the initial state of the particles a unique FRET signature is observed by the presence of a peptide ligand which binds to both receptor sites and brings the two fluorescence labels into close proximity.

Chapter 5 finally demonstrates the use of metal complex-functionalized vesicles (and also micelles) as self-assembled catalyst systems. For the transition metal-mediated hydrolysis of phosphate esters it was shown that vesicular metal complexes based on Zn(II)-cyclen provide considerably enhanced reactivity towards the simple model substrate BNPP as well as stable substrates like plasmid DNA and single-stranded oligonucleotides compared to the analogous complexes in homogeneous aqueous solution.

ZUSAMMENFASSUNG

In der vorliegenden Arbeit wurden selbstorganisierte, biomimetische Vesikelmembranen durch den Einbau neuer, synthetischer Amphiphile funktionalisiert. Diese Methode ermöglicht die schnelle und einfache Herstellung funktioneller Nanomaterialien für diverse Anwendungsgebiete wie z.B. Chemosensorik und Katalyse.

Kapitel 1 stellt allgemeine Konzepte funktionaler, synthetischer Vesikel vor und gibt einen kurzen Überblick über relevante Arbeiten auf diesem Gebiet.

Kapitel 2 beschreibt die Synthese nicht-fluoreszenter und fluoreszenter, amphiphiler Metallkomplexe basierend auf Zn(II)-cyclen und ihren Einbau in DSPC-Vesikelmembranen. Die erhaltenen Partikel wurden physikochemisch charakterisiert und auf ihre Eigenschaften bezüglich der molekularen Erkennung von biologisch relevanten Phosphatanionen untersucht. Optimierte lumineszente Rezeptorvesikel konnten schließlich für den optischen Nachweis und zur Unterscheidung von phosphorylierten und nicht phosphorylierten Proteinen eingesetzt werden.

In Kapitel 3 wird ein neuartiger Ansatz zur Herstellung modularer Chemosensoren vorgestellt. Anstatt synthetische Rezeptoren als Bindungsstellen und Farbstoffe als Reportergruppen kovalent zu verknüpfen, wurden die einzelnen Komponenten in selbstorganisierte Vesikelmembranen eingebettet. Die Gegenwart entsprechender Liganden erzeugt eine Reorganisation membraninterner Rezeptor-Farbstoff-Cluster und somit eine Änderung der Emissionseigenschaften. Ligand-Selektivität und optische Antwort der Partikel können dabei schnell und einfach durch Austausch der Rezeptor- und Farbstoff-Bausteine variiert werden.

Kapitel 4 demonstriert die Erkennung multivalenter Liganden mittels dynamischer Rekrutierung von Bindungsstellen in fluiden Membranen. Dazu wurden zwei amphiphile Rezeptoren mit FRET-komplementären Fluoreszenzlabeln synthetisiert und in DOPC-Membranen eingelagert. Im ursprünglichen Zustand der Partikel kann dabei, durch einen relativ großen mittleren Abstand, nur ein geringer Energietransfer beobachtet werden. Die Anwesenheit von Peptidliganden, die an beide Rezeptoreinheiten binden und somit die Farbstoffe in räumliche Nähe bringen, erzeugt jedoch eine spezifische FRET-Signatur.

In Kapitel 5 wird ein Anwendungsbeispiel für den Einsatz funktionalisierter Vesikel als selbstorganisierte Katalysatorsysteme aufgezeigt. Für die Übergangsmetallkomplex-vermittelte Hydrolyse von Phosphatestern konnte gezeigt werden, dass vesikuläre (sowie mizellare) Katalysatoren erheblich gesteigerte Reaktionsgeschwindigkeiten für den Umsatz des Modellsubstrats BNPP zeigen und selbst stabile Substrate wie Plasmid-DNA und Oligonukleotide umgesetzt werden können.

ABBREVIATIONS

AES	Atomic emission spectroscopy
AFM	Atomic force microscopy
Aq	Aqueous
Ar	Aryl
Asp	Aspartic acid
ATP	Adenosine triphosphate
Bipy	Bipyridine
BNPP	Bis(para-nitrophenyl)phosphate
Boc	<i>tert</i> -Butyloxycarbonyl
BSA	Bovine serum albumin
c	Concentration
C(M)S	Coumarin-methyl-sulfonate
calcd	Calculated
cAMP	Cyclic adenosine monophosphate
Cbz	Benzyloxycarbonyl
CF	Carboxyfluorescein
CI	Chemical Ionisation
COSY	Correlated spectroscopy
cyclen	1,4,7,10-tetraazacyclododecane
d	Day(s)
DAD	Diode array detector
DCC	Dicyclohexylcarbodiimide
DCM	Dichloromethane
DEA	Diethylamine
DET	Diethylenetriammonium
DIPEA	Diisopropylethylamine
DLS	Dynamic light scattering
DMAP	4-(dimethylamino)-pyridine
DMF	Dimethylformamide
DMPC	1,3-Bis(sn-3-phosphatidyl)-sn-glycero-2-phosphocholine
DMSO	Dimethylsulfoxide
DOPC	1,3-bis(sn-3-phosphatidyl)-sn-glycero-2-phosphocholine
DP	Di-picolyl
Dpa	Di-(2-picolyl)amine
DPPC	1,3-bis(sn-3-phosphatidyl)-sn-glycero-2-phosphocholine
DSC	Differential scanning calorimetry

DSPC	1,2-distearoyl-sn-glycero-3-phosphocholine
EA	Ethylacetate
EDC	<i>N</i> -(3-Dimethylamino-propyl)- <i>N'</i> -ethylcarbo-diimide
EI-MS	Electron-impact ionization mass spectrometry
eq	Equivalents
ES-MS	Electrospray ionization mass spectrometry
Et	Ethyl
EtOAc	Ethylacetate
EtOH	Ethanol
FAB	Fast-Atom-Bombardment
FAM	Carboxyfluorescein
FRET	Fluorescence resonance energy transfer
Glu	Glutamic acid
GTP	Guanosine-5'-triphosphate
h	Hour
HBTU	2-(1 <i>H</i> -Benzotriazole-1-yl)-1,1,3,3-tetramethyl-uronium hexafluorophosphate
hCA	Human carbonic anhydrase
HEPES	<i>N</i> -2-Hydroxy-ethylpiperazine- <i>N'</i> -2-ethansulfonic acid
His	Histidine
HOBt	Hydroxybenzotriazole
HPLC	High pressure liquid
HRMS	High resolution mass spectrometry
HSQC	Heteronuclear single quantum coherence
ICP	Inductively coupled plasma
IDA	Iminodiacetic acid
IR	Infrared
ITC	Isothermal titration calorimetry
J	Coupling Constant
LB	Langmuir Blodgett
Me	Methyl
MeCN	Acetonitrile
MeOH	Methanol
MF	Molecular formula
min	Minutes
MLV	Multilamellar vesicles
MP	Melting point
MW	Molecular weight
NEt ₃	Triethylamine

NMR	Nuclear magnetic resonance
NOESY	Nuclear overhauser enhancement spectroscopy
NTA	Nitrilotriacetic acid
o/n	Over night
PCS	Photon correlation spectroscopy
PE	Petrol Ether (Hexanes)
PEG	Polyethylene glycol
Ph	Phenyl
PMT	Photo multiplier tube
POPC	1-palmitoyl-2-oleoyl-sn-glycero-3-phosphocholine
PP _i	Pyrophosphate
pSer	Phosphorylated serine
R _f	Retention factor
ROESY	Rotating frame NOE spectroscopy
rpm	Rounds per minute
RT	Room temperature
SAM	Self assembled monolayer
SEC	Size exclusion chromatography
SUV	Small unilamellar vesicles
TAMRA	Tetramethylrhodamine
TBTU	O-(benzotriazol-1-yl)- <i>N,N,N',N'</i> -tetramethyluronium tetrafluoroborate
TEM	Transmission electron microscopy
Terpy	Terpyridine
TFA	Trifluoroacetic acid
THF	Tetrahydrofuran
TLC	Thin layer chromatography
TMR	Tetramethylrhodamine
TRIS	Tris(hydroxymethyl)-aminomethane
UV	Ultraviolet
Vis	Visible
x	Mole Fraction

CURRICULUM VITAE**Personal data**

Name	Benjamin Gruber
Date of birth	21. 04. 1984
Place of birth	Berchtesgaden
Nationality	German

Education

10 / 2008 – 07 / 2012	PhD Thesis <i>“Functional Lipid Membranes: Bio-inspired Nanomaterials for Sensing and Catalysis”</i> Group of Prof. Dr. Burkhard König, Institute of Organic Chemistry, University of Regensburg
01 / 2008 – 09 / 2008	Diploma Thesis <i>“Liposome-immobilized bis-Zn(II)-cyclen - Uses in phosphate recognition and catalytic phosphodiester hydrolysis”</i> Group of Prof. Dr. Burkhard König, Institute of Organic Chemistry, University of Regensburg
10 / 2003 – 12 / 2007	Studies of Chemistry University of Regensburg
09 / 1995 – 06 / 2003	Abitur (A-Levels) Rottmayr-Gymnasium Laufen

Internships

03 / 2007 – 04 / 2007	Research training in biochemistry Faculty of Biology and Preclinical Medicine, University of Regensburg
02 / 2006 & 09 / 2005	Practical training in technical chemistry Karl-Winnacker-Institute, DECHEMA e.V., Frankfurt/Main

Research & teaching experience

10 / 2008 –**Scientific Co-worker**

Research:

- Synthesis and characterization of functional amphiphiles (with focus on transition metal complexes and fluorescent dyes)
- Development of supramolecular sensors and catalysts based on artificial responsive membranes

Teaching:

- Supervision of practical lab courses in organic chemistry
- Supervision of Bachelor-, Master- and Diploma theses

Awards & scholarships

09 / 2012

„New Journal of Chemistry“ poster prize of the Suprachem2012 conference in Strasbourg

06 / 2011

„365 Orte im Land der Ideen“ - Award for the research project „Künstliche Antikörper dank Nanosensoren“

02 / 2011 – 05 / 2009

Travel grants from GDCh, Volkswagen-Stiftung, Liebig-Vereinigung, Freunde der Universität Regensburg e.V.

Memberships

01 / 2009 –

Gesellschaft Deutscher Chemiker (GDCh)

01 / 2009 –

Verband angestellter Akademiker und leitender Angestellter der chemischen Industrie e.V. (VAA)

Publications

- B. Gruber, B. König, *Chem. Eur. J.* **2012**, DOI: 10.1002/chem.201202982 (Concept Article).
- B. Gruber, S. Balk, S. Stadlbauer, B. König, *Angew. Chem. Int. Ed.* **2012**, DOI 10.1002/anie.201205701; *Angew. Chem.* **2012**, DOI 10.1002/ange.201205701 (Hot paper).
- B. Gruber, E. Kataev, J. Aschenbrenner, S. Stadlbauer, B. König, *J. Am. Chem. Soc.* **2011**, *133*, 20704-20707.
- B. Gruber, S. Stadlbauer, A. Späth, S. Weiss, M. Kalinina, B. König, *Angew. Chem. Int. Ed.* **2010**, *49*, 7125-7128; *Angew. Chem.* **2010**, *122*, 7280-7284.
- B. Gruber, S. Stadlbauer, K. Woinaroschy, B. König, *Org. Biomol. Chem.* **2010**, *8*, 3704-3714.

Scientific presentations

- B. Gruber, B. König, *ORCHEM 2012*, Weimar, 09 / **2012**, Poster.
- B. Gruber, B. König, *6th International Symposium "Supramolecular Systems in Chemistry and Biology"*, Strasbourg (F), 09 / **2012**, Poster.
- B. Gruber, B. König, *4th EuCheMS Chemistry Congress*, Prague (CZ), 08 / **2012**, Poster.
- B. Gruber, B. König, *Suprachem - 4th International Summer School*, Regensburg, 09 / **2011**, Oral.
- B. Gruber, B. König, *Mini-Symposium Sensorik*, Regensburg, 06 / **2011**, Oral.
- B. Gruber, B. König, *OC meets solution chemistry*, Regensburg, 03 / **2011**, Oral.
- B. Gruber, E. Kataev, J. Aschenbrenner, S. Stadlbauer, B. König, *Symposium in Supramolecular Chemistry*, Duisburg-Essen, 02 / **2011**, Poster.
- B. Gruber, B. König, *X-mas Colloquium of the Institute of Organic Chemistry*, Regensburg, 12 / **2010**, Oral.
- B. Gruber, B. König, *Supramolecular Chemistry – Quo Vadis?*, Taormina (I), 10 / **2010**, Oral.
- B. Gruber, S. Stadlbauer, B. König, *3rd EuCheMS Chemistry Congress*, Nürnberg, 08 / **2010**, Poster.
- B. Gruber, S. Stadlbauer, B. König, *GDCh Wissenschaftsforum 2009*, Frankfurt / Main, 09 / **2009**, Poster.
- B. Gruber, S. Stadlbauer, B. König, *Suprachem - 5th International Symposium*, Kiev (UA), 05 / **2009**, Poster.

ACKNOWLEDGEMENTS

I would like to show my gratitude to Prof. Dr. Burkhard König for the opportunity to do my Diploma and PhD theses in his group, the freedom to develop ideas and of course his ever-present motivation and financial support. Also I am indebted to Prof. Dr. Kirsten Zeitler, Prof. Dr. Henri Brunner and Prof. Dr. Jörg Daub for refereeing/chairing my defense, to Prof. Dr. Maria Kalinina for her advice regarding the co-embedding project and to the DFG, GDCk and all other funding organizations for financial support and numerous travel grants.

And to make this short: A BIG THANK YOU to all past & present friends & fellows for the support (of any kind whatsoever) and the great time in Regensburg - **UR** the best!

Amongst the "Königs" I first have to mention my lab mates of the last few years Dr. Andi Grauer, Dr. Alex Riechers, Dr. Flo Schmidt, Stefan "(B)alki" Balk and Tobias "Fliesn" Lang for the good lab atmosphere, professional advice, latest gossip or just wasting time... Also the other members of the "Hammer & Vesikel"-subgroup (formerly known as MolRec) Dr. Evgeny Kataev, Andi Müller, Thomas Zanni and the next generation of "PhotoCat-renegades" Malte "Alte(r)" Hansen and Stefan Troppmann for the enjoyable collaboration. Special thanks go to Dr. Stefan "Done" Stadlbauer for being a guide during my Diploma time and his great synthetic effort. Thanks also to the other "seniors" Dr. Danny Engel (formerly known as Vomasta), Dr. Michi Egger and Dr. Harry Schmaderer for the warm welcome in the group and the cold Falki. And to today's most persistent "Feierabendbier"-partner ("Holz-")Michl Dobmeier and **ALL** the others who ever joined our meetings in the **Café König** with one or more hot (or cold) beverage - no matter at which time of day (or night). Big thanks also to my fellows and "travel-mates" Dr. Robbl "Sha-La-"Lechner, Dr.s Caro Fischer & Rub, "Diplomant" Josef Herrmann, Sanne Kümmel, Susa Schmidbauer, Andi "The Biertrinker" Hohenbeatner and Dr. "Colombiana" Cristian Ochoa-Puentes for some legendary "scientific away games", "food festivals", "international evenings" and other events. Further thanks to ("schwarze Na-")Tascha Kuzmanovic for PhD-song inspiration and "Wheel-Master" Tobi Troppmann. And of course my numerous student co-workers who contributed a lot of (more or less) meaningful data to this work (especially Jana Aschenbrenner). Not to forget our "secret sovereign" Mrs. Liebl and all our technicians and permanent (by busy) staff...

Thanks also to all the other groups and friends for their scientific and not-so-scientific support - especially the (former) AK-Reiser-crowd (feat. Dr. Flo "Coach" Sahr, Dr. "Salat" Alex Schätz, "Quetschn"-Michl Schwarz and many others...) and my "refuge" the Fraunhofer EMFT group! For the great time I'm particularly grateful to "families" Stich (Dr. Matthias & Becky), "Harrarara" (Dr. Klaus & Dr. Agnes), Schmidt (Dr. Flo & Dr. Jenny), Hager (Dr. Markus & Judith) and "Bachelor" (Roland & Julia).

Last but by no means least my **BIGGEST** thanks goes to my bride-to-be Anna for her true love, backup and absolute support and of course to my family - without the never-ending encouragement of my parents Helga and Walter you would not be reading this right now...

Thanks...

...also for not being mad at me if I forgot to mention your name here - cheer up: you just saved a tree ;)